The role of hillslope position in controlling carbon flux from peatlands

BOOTHROYD, IAN,MICHAEL

The role of hillslope position in controlling carbon flux from peatlands

Ian Michael Boothroyd

Department of Earth Sciences

Durham University

One volume

Thesis submitted in accordance with the regulations for the degree of Doctor of Philosophy in Durham University, Department of Earth Sciences, 2014

Cotton Grass

Hand-maiden, humble courtiers,

yes-men in silver wigs,

they stoop at the path's edge,

bend low to the emperor's feet,

to the military parade

of boots and sticks

Then it's back to work,

to the acid acres,

to wade barefoot through waterlogged peat,

trawling the mist,

carding the air for threads of sheep-wool

snagged on the breeze,

letting time blaze through their

ageless hair like the wind.

Simon Armitage, 2010.

Ian Michael Boothroyd

The role of hillslope position in controlling carbon flux from peatlands

Abstract

Peatlands are important terrestrial carbon stores, both in the United Kingdom and globally. The cool and wet climate of the UK allows blanket bog peatlands to form in upland regions, with peat deposits covering the landscape across entire hillslopes. Blanket bogs are important sinks and sources of CO_2 and dissolved organic carbon (DOC). Many factors affect the carbon cycle of peatlands, including climate, hydrology, vegetation, land management and topography. Although hillslope position can influence the hydrology of peatlands, the effect it has on the production and transport of different carbon species is poorly understood.

This thesis investigates the impact hillslope position has upon the hydrology and carbon release pathways of blanket bogs in upland regions. Hydrology, CO_2 fluxes and DOC concentrations were studied at two hillslopes in the Peak District, Derbyshire, across four hillslope positions: top-slope, upper mid-slope, lower mid-slope and bottom-slope.

Results show that slope position was the dominant control affecting water table variation. Although slope position did influence variation in CO_2 fluxes, its impact was small compared to other factors, including small-scale heterogeneity and microtopographic variation. Slope position was an important control influencing variation in DOC concentrations. Dissolved organic carbon concentrations decreased down-slope as high water tables and water movement flushed DOC from the peat subsurface. Model results indicate that slope position is an important factor that should be included in carbon budget models but further work is required to further improve understanding of hillslope processes.

Declaration and Copyright

I confirm that no part of the material presented in this thesis has previously been submitted by me or any other person for a degree in this or any other university. Where relevant, material from the work of others has been acknowledged.

Signed:

Date:

Acknowledgements

I would like to start by offering sincere thanks to my supervisor, Professor Fred Worrall, for all his advice and support whilst writing this thesis and during my time at Durham University. His patience and encouragement have been greatly appreciated. Thanks also go to my second supervisor, Dr Tim Allott, for the advice he has provided during the course of my PhD.

Many thanks go to my friends and colleagues in my research group. I have greatly enjoyed working with you. In particular, I am grateful to Simon Dixon who has helped me so much with field work, lab work and all other kinds of support during my PhD, as well as being an awesome house mate. Suzane Qassim, Zhuoli Zhang, Cat Moody, Helen Foster, Gareth Clay, Kate Turner and Madeleine Bell - thank you all for your friendship, encouragement, fielding an endless number of inane questions and providing so many laughs.

Thanks to all my friends in the Department of Earth Sciences who have made life so much fun in Durham. My sometime house mates, Ben Franklin, Isobel Yeo and Sarah Porter; my bay buddies Iona Macintosh, Rachel Bullock and Sian Evans for all their banter; Dave Ashby, Claire Nattrass, BJ, Pete Tollan, Mark Brodie et al.; and my football friends. Thank you all.

Thanks to Moors for the Future Partnership for allowing use of the LiDAR data used throughout this thesis. Professor Martin Evans was also a great help in providing the University of Manchester weather station data used in this thesis Joanne Peterkin's help with lab work was very much appreciated as well.

Finally, I'd like to thank my family for all their love, support and encouragement over the past few years. This thesis would not have been possible without it.

Table of Contents

Abstract i

Declaration and Copyright ii

Acknowledgements iii

Table of Contents iv

List of Figures x

List of Tables xvii

Chapter 1 Introduction 1

1.1 Peatland formation 1

1.2 Peatland hydrology 2

1.3 Peatlands and the carbon cycle 6

1.3.1 Carbon storage 6

1.3.2 Carbon balance 6

1.3.3 Dissolved organic carbon 8

1.3.4 Land-atmosphere carbon dioxide flux 12

1.4 Hillslope 16

1.5 Thesis aims and hypotheses 19

1.6 Thesis outline 20

Chapter 2 The impact of hillslope position on carbon flux 22

2.1 Introduction 22

2.2 Aims and objectives 23

2.3 Materials and methods 23

2.3.1 Study sites 23

2.3.1.1 Featherbed Moss 25

2.3.1.2 Alport Low 26

2.3.2 Experimental design 30

2.3.2.1 Factorial design 30

2.3.2.2 Vegetation survey 32

2.3.2.3 Experimental plots 32

2.3.3 Field monitoring 33

2.3.3.1 Gaseous CO_2 flux 33

2.3.3.2 Water table depth & water collection 38

2.3.4 Water chemistry analysis 38
2.3.4.1 Basic water chemistry measurements 39
2.3.4.2 Dissolved organic carbon 39
2.3.4.3 Anion concentrations 40
2.3.5 Analysis of LiDAR terrain parameters 41
2.3.6 Statistical analysis 42
2.3.6.1 Analysis of variance and covariance 43
2.3.6.2 Multiple linear regression 46
2.3.6.3 Runoff occurrence 46
2.4 Results 48
2.4.1 Hydrology 50
2.4.1.1 Water table depth 50
2.4.1.2 Runoff occurrence 56
2.4.2 Gaseous fluxes 56
2.4.2.1 R_{eco} 56
2.4.2.2 P_G 63
2.4.2.3 NEE 68
2.4.3 DOC 72
2.4.3.1 DOC in soil pore water 72
2.4.3.2 DOC in runoff water 79
2.4.4 Water chemistry 81
2.4.4.1 Soil pore water chemistry 81
2.4.4.2 Runoff water chemistry 91
2.5 Discussion 99
2.5.1 Limitations 99
2.5.2 Hydrology 100
2.5.3 CO_2 flux 104
2.5.4 DOC 109
2.6 Conclusions 112
Chapter 3 The effect of organic matter composition on carbon flux 115
3.1 Introduction 115
3.2 Aims and objectives 118
3.3 Materials and methods 119
3.3.1 Soil and vegetation 119

3.3.2 Elemental analysis 120
3.3.3 Energy content (gross heat value) 121
3.3.4 Thermogravimetric analysis 122
3.3.5 Statistical analysis 123
3.3.5.1 Analysis of variance and covariance 123
3.3.5.2 Principal components analysis 124
3.3.5.3 Impact upon hydrology and carbon flux 125
3.4 Results 125
3.4.1 Bulk density 130
3.4.2 Elemental composition 132
3.4.3 Atomic ratios 142
3.4.4 Carbon oxidation state & oxidative ratio 150
3.4.5 Energy content 155
3.4.6 Thermogravimetric analysis 158
3.4.7 Multivariate analysis 165
3.4.8 Impact of organic matter on hydrology & carbon 170
3.5 Discussion 173
3.5.1 Limitations 173
3.5.2 Bulk density 174
3.5.3 Organic matter composition and energy content 176
3.5.4 Thermogravimetric analysis 180
3.5.5 Multivariate analysis 182
3.5.6 Organic matter and carbon cycling 182
3.6 Conclusions 184
Chapter 4 Carbon flux of a hillslope transect 186
4.1 Introduction 186
4.2 Aims and objectives 187
4.3 Materials and methods 187
4.3.1 Experimental design 187
4.3.2 Field monitoring 190
4.3.2.1 Gaseous CO_2 flux 190
4.3.2.2 Water table depth & water collection 190
4.3.2.3 Basic water chemistry measurements 191
4.3.2.4 Dissolved organic carbon 191

4.3.2.5 Anion concentrations 192
4.3.3 Statistical analysis 192
4.3.3.1 Analysis of variance and covariance 192
4.3.3.2 Multiple linear regression 193
4.3.3.3 Runoff occurrence 193
4.4 Results 194
4.4.1 Hydrology 195
4.4.1.1 Water table depth 195
4.4.1.2 Runoff occurrence 198
4.4.2 Gaseous fluxes 200
4.4.2.1 Ecosystem respiration 202
4.4.2.2 Gross photosynthesis 205
4.4.2.3 Net ecosystem exchange 208
4.4.2.4 CO_2 flux and study year 211
4.4.3 Dissolved organic carbon 214
4.4.3.1 Soil pore water 215
4.4.3.2 Runoff water 220
4.4.3.3 Water type 220
4.4.3.4 Process blanks 222
4.5 Discussion 223
4.5.1 Limitations 223
4.5.2 Hydrology 224
4.5.3 CO_2 flux 225
4.5.4 DOC 228
4.6 Conclusions 230
Chapter 5 Hillslope hydrology and water chemistry 232
5.1 Introduction 232
5.2 Aims and objectives 235
5.3 Materials and methods 236
5.3.1 Experimental design 236
5.3.1.1 Annual datasets 236
5.3.1.2 Tracer study 237
5.3.2 Laboratory analysis 239
5.3.3 Statistical analysis 239

5.3.3.1 Principal components analysis 240
5.3.3.2 Analysis of variance / covariance 240
5.3.3.3 Runoff and 10 cm water occurrence 241
5.4 Results 242
5.4.1 2010 – 2011 dataset 242
5.4.2 2011 – 2012 dataset 256
5.4.2.1 10 cm water occurrence 256
5.4.2.2 2011 – 2012 multivariate analysis 257
5.4.3 Tracer experiment 270
5.4.3.1 Bromide concentrations 270
5.4.3.2 Runoff and 10 cm water occurrence 274
5.5 Discussion 274
5.5.1 Limitations 274
5.5.2 Water chemistry and flowpaths 276
5.5.3 Tracer study 281
5.6 Conclusions 283
Chapter 6 Modelling the effects of hillslope position 286
6.1 Introduction 286
6.2 Aims and objectives 291
6.3 Methods 291
6.3.1 Model set-up 291
6.3.2 Correction factors 293
6.4 Results 297
6.5 Discussion 300
6.5.1 Limitations 300
6.5.2 Carbon species and slope position 301
6.5.3 Carbon balance 305
6.5.4 Model applicability 306
6.6 Conclusions 307
Chapter 7 Conclusions 309
7.1 Introduction 309
7.2 Thesis objectives 310
7.3 Principal findings and conclusions 311
7.4 Limitations of the dataset 313

7.5 Recommendations for future work 314
Appendices 318
Appendix A 318
Appendix B 319
Appendix C 319
Appendix D 320
Appendix E 320
References 322

List of Figures

Figure 1.1 Conceptual model of hillslope positions 19

Figure 2.1 Map of study sites in Peak District, Derbyshire 24

Figure 2.2 Hummock plot (L) and Eriophorum spp. (R) plots on Alport Low top-slope 28

Figure 2.3 Nested sub-slope design: TS = top-slope; UM = upper mid-slope; LM = lower mid-slope; BS = bottom-slope 31

Figure 2.4 Experimental plot set-up: A = infra-red gas analyser; B = chamber; C = gas collar; D = dipwell; E = surface water runoff trap 33

Figure 2.5 Boxplot of median WTD by slope 51

Figure 2.6 WTD ANOVA main effects & interaction plot: significant differences denoted where letters are not shared between slope positions 53

Figure 2.7 WTD ANCOVA main effects & interaction plot: significant differences denoted where letters are not shared between slope positions 54

Figure 2.8 Boxplot of median R_{eco} by slope 57

Figure 2.9 LnR_{eco} ANOVA main effects plot: significant differences denoted where letters are not shared by slope positions 59

Figure 2.10 Relative R_{eco} ANOVA main effects and interactions plot: significant differences denoted where letters are not shared between slope positions 61

Figure 2.11 Boxplot of median P_G by slope 64

Figure 2.12 LnP_G ANOVA main effects plot: significant differences denoted where letters are not shared between slope positions 65

Figure 2.13 Relative P_G ANOVA main effects plot: significant differences denoted where letters are not shared between slope positions 66

Figure 2.14 Boxplot of median NEE by slope 68

Figure 2.15 NEE ANOVA main effects plot: significant differences denoted where letters are not shared between slope positions 69
Figure 2.16 Boxplot of soil pore water median DOC concentration by slope 73
Figure 2.17 Soil pore water DOC ANOVA main effects & interaction plot: significant differences denoted where letters are not shared between slope positions 74
Figure 2.18 Soil pore water DOC ANCOVA main effects plot: significant differences denoted where letters are not shared between slope positions 76
Figure 2.19 Relative soil pore water DOC ANOVA main effects & interaction plot: significant differences denoted where letters are not shared between slope positions 77
Figure 2.20 Boxplot of median runoff water DOC concentration by slope 80
Figure 2.21 Soil pore water pH ANOVA main effects plot: significant differences denoted where letters are not shared between slope positions 83
Figure 2.22 Soil pore water LnConductivity ANOVA main effects plot: significant differences denoted where letters are not shared between slope positions 84
Figure 2.23 Soil pore water LnConductivity ANCOVA main effects plot: significant differences denoted where letters are not shared between slope positions 85
Figure 2.24 Soil pore water Abs_{400} ANOVA main effects & interaction plot: significant differences denoted where letters are not shared between slope positions 87
Figure 2.25 Soil pore water Abs_{400} ANCOVA main effects & interaction plot: significant differences denoted where letters are not shared between slope positions 88
Figure 2.26 Soil pore water E4:E6 ANOVA main effects plot: significant differences denoted where letters are not shared between slope positions 90
Figure 2.27 Soil pore water E4:E6 ANCOVA main effects plot: significant differences denoted where letters are not shared between slope positions 90
Figure 2.28 Runoff water pH ANOVA main effects & interaction plot: significant differences denoted where letters are not shared between slope positions 91

Figure 2.29 Runoff water conductivity ANOVA main effects & interaction plot: significant differences denoted where letters are not shared between slope positions 93
Figure 2.30 Runoff water Abs_{400} ANOVA main effects & interaction plot: significant differences denoted where letters are not shared between slope positions 94
Figure 2.31 Runoff water specific absorbance ANOVA main effects: significant differences denoted where letters are not shared between slope positions 96
Figure 2.32 Runoff water E4:E6 ANOVA main effects and interaction plot: significant differences denoted where letters are not shared between slope positions 98
Figure 2.33 Runoff water E4:E6 ANCOVA main effects: significant differences denoted where letters are not shared between slope positions 99
Figure 2.34 Soil pipe near Alport Low bottom-slope 104
Figure 3.1 Mean bulk density with depth ± standard error 130
Figure 3.2 $Ln\rho_{bd}$ ANOVA main effects & interaction plot: significant differences denoted where letters are not shared between slope positions 132
Figure 3.3 Mean CHNO content with depth ± standard error 133
Figure 3.4 Carbon ANOVA main effects & interaction plot by slope: significant differences denoted where letters are not shared between slope positions 135
Figure 3.5 Carbon ANOVA main effects plot by substrate: significant differences denoted where letters are not shared between substrates; NSM = Non-Sphagnum moss spp..... 136
Figure 3.6 Soil nitrogen ANOVA main effects plot by slope: significant differences denoted where letters are not shared between slope positions 137
Figure 3.7 Substrate nitrogen ANOVA main effects by slope: significant differences denoted where letters are not shared between slope positions 138
Figure 3.8 Substrate nitrogen ANOVA main effects plot by substrate: significant differences denoted where letters are not shared between substrates; NSM = Non-Sphagnum moss..... 138

Figure 3.9 Hydrogen ANOVA main effects by substrate: significant differences denoted where letters are not shared between substrates: NSM = Non-sphagnum moss spp. 140
Figure 3.10 Oxygen ANOVA main effects plot by slope: significant differences denoted where letters are not shared between slope positions 141
Figure 3.11 Oxygen ANOVA main effects by substrate: significant differences denoted where letters are not shared between substrates: NSM = Non-Sphagnum moss spp. 142
Figure 3.12 Mean atomic ratios with depth ± standard error 143
Figure 3.13 C:N ANOVA main effects by slope: significant differences denoted where letters are not shared between slope positions 145
Figure 3.14 C:N ANOVA main effects plot by substrate: significant differences denoted where letters are not shared between substrates; NSM = Non-Sphagnum moss spp. 146
Figure 3.15 H:C ANOVA main effects plot by slope: significant differences denoted where letters are not shared between slope positions 147
Figure 3.16 H:C ANOVA main effects plot by substrate: significant differences denoted where letters are not shared by substrates; NSM = Non-Sphagnum moss spp. 148
Figure 3.17 O:C ANOVA main effects plot by slope: significant differences denoted where letters are not shared between slope positions 149
Figure 3.18 O:C ANOVA main effects by substrate: significant differences denoted where letters are not shared between substrates: NSM = Non-Sphagnum moss spp. 150
Figure 3.19 Mean carbon oxidation state (C_{OX}) and oxidative ratio (OR) with depth ± standard error 151
Figure 3.20 C_{OX} ANOVA main effects & interaction plot: significant differences denoted where letters are not shared between slope positions 152
Figure 3.21 C_{OX} ANOVA main effects plot by substrate: significant differences denoted where letters are not shared between substrates; NSM = Non-Sphagnum moss spp. 153

Figure 3.22 OR ANOVA main effects & Interaction plot by slope: significant differences denoted where letters are not shared between slope positions 154
Figure 3.23 OR ANOVA main effects plot by substrate: significant differences denoted where letters are not shared between substrates; NSM = Non-Sphagnum moss spp. 155
Figure 3.24 Mean energy content with depth ± standard error 156
Figure 3.25 Energy content ANOVA main effects plot: significant differences denoted where letters are not shared between slope positions 157
Figure 3.26 Energy content ANOVA main effects plot by substrate: significant differences denoted where letters are not shared between substrates: NSM = Non-Sphagnum moss 158
Figure 3.27 TG and DTG curves for cellulose, humic acid, lignin, soil and vegetation: NSM = Non-Sphagnum moss spp. 159
Figure 3.28 Scatterplot of TG weight loss PC1 & PC2; NSM = Non-Sphagnum moss spp. 160
Figure 3.29 Scatterplot of TG weight loss PC2 & PC3: NSM = Non-Sphagnum moss spp.; prefix EM = end-member; A – C = labels 162
Figure 3.30 TG PC2 & PC3 ANOVA main effects plot by slope: significant differences denoted where letters are not shared between slope positions 163
Figure 3.31 TG1 PC2 & PC3 ANOVA main effects plot by site 164
Figure 3.32 Scatterplot of Multivariate PC1 & PC2: NSM = Non-Sphagnum moss spp.; prefix EM = end-member; A-C = labels 166
Figure 3.33 Scatterplot of Multivariate PC1 & PC3: NSM = Non-Sphagnum moss spp. 167
Figure 3.34 Scatterplot of Multivariate PC2 & PC3: NSM = Non-Sphagnum moss spp. 167
Figure 3.35 Multivariate PC2 & PC4 ANOVA main effects plots by slope: significant differences denoted where letters are not shared between slope positions 169
Figure 3.36 WTD ANOVA main effects & interactions plot: significant differences denoted where letters are not shared between slope positions 171
Figure 4.1 Map of Alport Low slope transect 188

Figure 4.2 WTD ANOVA main effects plot 196

Figure 4.3 LnR_{eco} ANOVA main effects plot (values unlogged) 202

Figure 4.4 LnR_{eco} ANCOVA main effects plot (values unlogged) 204

Figure 4.5 LnP_G ANOVA main effects plot (values unlogged) 206

Figure 4.6 LnP_G ANCOVA main effects plot (values unlogged) 207

Figure 4.7 NEE ANOVA main effects plot 209

Figure 4.8 NEE ANCOVA main effects plot 211

Figure 4.9 Study year LnR_{eco} and LnP_G ANOVA main effects plot (values unlogged): significant differences denoted where letters are not shared between slope positions 213

Figure 4.10 Study year LnP_G and NEE ANOVA main effects plots (P_G values unlogged) 213

Figure 4.11 Soil pore water DOC ANOVA main effects plot 216

Figure 4.12 Soil pore water DOC ANCOVA main effects plot 218

Figure 4.13 Water type DOC ANOVA / ANCOVA main effects plot 221

Figure 5.1 Map of Alport Low slope transect and bromide tracer application location 238

Figure 5.2 Loading plot of 2010 – 2011 PC1 & PC2 248

Figure 5.3 Scatterplot of 2010 -2011 PC1 & PC2: SPW = soil pore water; RO = runoff water; prefix EM = end-member; prefix R =region; A – E = labels 249

Figure 5.4 Scatterplot of 2010 – 2011 PC1 & PC3; SPW = soil pore water; RO = runoff water; prefix EM = end-member; prefix R =region; A – C = labels 250

Figure 5.5 2010 – 2011 site-slope-water type interaction mean PC1 score ± standard error: AL = Alport Low; FM = Featherbed Moss; SPW = soil pore water; RO = runoff water 252

Figure 5.6 2010 – 2011 PC1 ANOVA main effects & interactions plot: significant differences denoted where letters are not shared between slope positions 253

Figure 5.7 2010 – 2011 PC1 ANOVA main effects & interactions plot 254

Figure 5.8 Scatter plot of 2010 – 2011 PC1 & PC2 runoff water samples: A = Alport Low; F = Featherbed Moss; E = Eriophorum spp. plots; H = Hummock plots 255

Figure 5.9 Loading plot of 2011 – 2012 PC1 & PC2 263

Figure 5.10 Scatterplot of 2011 – 2012 PC1 & PC2; SPW = soil pore water; RO = runoff water; 10 cm = 10 cm water; prefix EM = end-member; prefix R =region; A – D = labels 264

Figure 5.11 Scatterplot of 2011 – 2012 PC1 & PC5; SPW = soil pore water; RO = runoff water; 10 cm = 10 cm water; prefix EM = end-member; prefix R =region; A – E = labels 266

Figure 5.12 2011 – 2012 water type PC1 ANOVA main effects; significant differences denoted where letters are not shared between water types 267

Figure 5.13 2011 – 2012 PC1 ANOVA main effects plot by slope; SPW = soil pore water; 10 cm = 10 cm water 269

Figure 5.14 Mean Br^- concentrations ± standard error; tracer applied between slope positions 3 & 4 272

Figure 6.1 Map of study sites in Peak District, Derbyshire, with PD control 294

Figure 6.2 Modelled carbon export values for gaseous, fluvial and complete carbon budgets: error bars = ± 6% error 298

List of Tables

Table 2.1 Average values of site parameters for Featherbed Moss and Alport Low; NB missing peat depth measurements due to time constraints 25

Table 2.2 Featherbed Moss site details 26

Table 2.3 Alport Low site details: NB missing peat depth measurements due to time constraints 29

Table 2.4 DOC calibration R^2 and detection limits: *denotes deletion of a 0 mg C l^{-1} standard; LCL = lower confidence limit; UCL = upper confidence limit 40

Table 2.5 Terrain indices adapted from table 2 Wilson (2012) 42

Table 2.6 Covariates used in ANCOVA: %E = % Eriophorum spp. dominance; TPs = terrain parameters (slope angle, wetness index and altitude) 44

Table 2.7 Percentage data removed from each variable used in ANOVA/ANCOVA: SPW = soil pore water; RO = runoff water 48

Table 2.8 Percentage data removed from each variable used in MLR by slope position: * = unlogged P_G used in NEE MLR 49

Table 2.9 Descriptive statistics for response variables: SE = standard error 51

Table 2.10 WTD ANOVA / ANCOVA: ω^2 = % variance 52

Table 2.11 WTD MLR: Sin M and Cos M = sin and cos values by month; SE = standard error 55

Table 2.12 Chi-squared results for runoff (RO) occurrence by slope 56

Table 2.13 CO_2 flux ANOVA / ANCOVA: ω^2 = % variance 58

Table 2.14 LnR_{eco} Kruskal-Wallis results 59

Table 2.15 Relative CO_2 flux ANOVA: ω^2 = % variance 61

Table 2.16 Relative R_{eco} Kruskal-Wallis results 61

Table 2.17 LnR_{eco} MLR: Sin M & Cos M = sin & cos by month; 1/T = temperature coefficient; SE = standard error 63

Table 2.18 Relative P_G Kruskal-Wallis results 66

Table 2.19 LnP_G MLR: Sin M & Cos M = sin & cos by month; SE = standard error 67

Table 2.20 NEE Kruskal-Wallis results 70

Table 2.21 NEE MLR: Sin M & Cos M = sin & cos by month; SE = standard error 71

Table 2.22 Soil pore water (SPW) and runoff (RO) water DOC ANOVA / ANCOVA: ω^2 = % variance 74

Table 2.23 Relative Soil pore water (SPW) DOC ANOVA: ω^2 = % variance 77

Table 2.24 Soil pore water DOC MLR: Sin M & Cos M = sin & cos by month: SE = standard error 78

Table 2.25 Soil pore water chemistry descriptive statistics: SE = standard error 81

Table 2.26 Soil pore water pH & conductivity ANOVA / ANCOVA: ω^2 = % variance 82

Table 2.27 Soil pore water Abs_{400}, specific absorbance & E4:E6 ANOVA / ANCOVA: ω^2 = % variance 86

Table 2.28 Soil pore water LnSpecific absorbance Kruskal-Wallis results 89

Table 2.29 Runoff water chemistry descriptive statistics: SE = standard error 92

Table 2.30 Runoff water pH & conductivity ANOVA: ω^2 = % variance 92

Table 2.31 Runoff water pH Kruskal-Wallis results 93

Table 2.32 Runoff water Abs_{400}, specific absorbance & E4:E6 ANOVA / ANCOVA: ω^2 = % variance 95

Table 2.33 Runoff water LnAbs_{400} Kruskal-Wallis results 96

Table 2.34 Runoff water E4:E6 Kruskal-Wallis results 98

Table 2.35 Proportion of observed runoff between study sites 102

Table 2.36 Summary table of significance of slope position, denoted by 'X' 114

Table 3.1 Percentage of data removed from each dataset 126

Table 3.2 Reference material CHNO content ± standard error (SE) 127

Table 3.3 Reference material atomic ratios, C_{OX}, and OR 127

Table 3.4 Reference material energy content ± standard error (SE) 127

Table 3.5 Descriptive statistics for response variables by slope across entire one metre core: SE = standard error 128

Table 3.6 Descriptive statistics for response variables by substrate: SE = standard error 129

Table 3.7 $Ln\rho_{bd}$ ANOVA: ω^2 = % variance 131

Table 3.8 CHNO soil and substrate ANOVA: ω^2 = % variance 134

Table 3.9 Atomic ratio soil and substrate ANOVA: ω^2 = % variance 144

Table 3.10 C:N Kruskal-Wallis results 145

Table 3.11 C_{OX} and OR soil and substrate ANOVA: ω^2 = % variance 152

Table 3.12 Energy content ANOVA: ω^2 = % variance 156

Table 3.13 The first seven principal components of weight loss by temperature range 161

Table 3.14 TG ANOVA: ω^2 = % variance 163

Table 3.15 TG PC3 Kruskal-Wallis results 164

Table 3.16 The first four principal components of multivariate analysis 165

Table 3.17 Multivariate ANOVA: ω^2 = % variance 168

Table 3.18 Multivariate PC2 Kruskal-Wallis results 169

Table 3.19 TG PC2 & PC3 MLR: SE = standard error 170

Table 3.20 Organic matter ANOVA: ρ_{BD} = bulk density; WI = wetness index; ω^2 = % variance 171

Table 3.21 Organic matter MLR: Sin M & Cos M = sin and cos by month; SE = standard error 172

Table 4.1 Alport Low transect site details 189

Table 4.2 Percentage data removed from each variable dataset: SPW = soil pore water; RO = runoff water; and water type = combined SPW, RO and stream water 194

Table 4.3 WTD (mm) descriptive statistics according to slope position and month: SE = standard error 195

Table 4.4 WTD ANOVA / ANCOVA; ω^2 = % variance 196

Table 4.5 Significant differences for WTD 197

Table 4.6 WTD MLR: R^2 = 67.50%; SE = standard error 198

Table 4.7 Chi-squared results for runoff (RO) occurrence by slope 199

Table 4.8 Monthly rainfall for study years 2010 – 2011 & 2011 – 2012: Starting month = first month of sampling; NB data gaps present (see N for comparisons); Two data points removed as outliers: 23.23 mm from 14/7/2010 & 22.23 mm from 12/8/2012 199

Table 4.9 Descriptive statistics for response variables by slope; SE = standard error..... 200

Table 4.10 Descriptive statistics for response variables by month; SE = standard error 201

Table 4.11 CO_2 flux ANOVA / ANCOVA; ω^2 = % variance 203

Table 4.12 Significant differences for LnR_{eco} 203

Table 4.13 LnR_{eco} MLR; Sin M & Cos M = sin and cos by month; 1/T = temperature coefficient; SE = standard error 205

Table 4.14 Significant differences for LnP_G 206

Table 4.15 LnP_G MLR: R^2 = 55.90%; Sin M & Cos M = sin & cos by month; 1/T = temperature coefficient; SE = standard error 208

Table 4.16 Significant differences for NEE 210

Table 4.17 NEE MLR: R^2 = 38.30%; Sin M & Cos M = sin & cos by month; SE = standard error 211

Table 4.18 CO_2 flux ANOVA for study year; ω^2 = % variance 212

Table 4.19 DOC descriptive statistics for response variables by slope: SE = standard error.... 214

Table 4.20 DOC descriptive statistics for response variables by month: SE = standard error.. 215

Table 4.21 Soil pore water (SPW) and runoff (RO) water DOC ANOVA / ANCOVA: ω^2 = % variance..... 217

Table 4.22 Significant differences for soil pore water DOC 217

Table 4.23 Soil pore water DOC MLR: R^2 = 47.50%; Sin M = sin by month; SE = standard error 219

Table 4.24 Water type DOC ANOVA / ANCOVA; ω^2 = % variance..... 221

Table 4.25 Process blank descriptive statistics for response variables; Abs_{400} = absorbance at 400 nm; SE = standard error 222

Table 5.1 Descriptive statistics for 2010 – 2011 anion concentrations (detection limit <<0.05 mg l^{-1}): SPW = soil pore water; RO = runoff water; SE = standard error 243

Table 5.2 River Etherow precipitation data 07/06/2010 – 04/01/2012: SE = standard error .. 244

Table 5.3 Percentage data removed from 2010 – 2011 water chemistry variables: SPW = soil pore water; RO = runoff water; Abs_{400} = absorbance at 400 nm 244

Table 5.4 2010 – 2011 PCA cell occupancy: all slope positions had six sample plots except Alport Low top-slope and bottom-slope that had 12; June was sampled in 2010 and 2011 on Alport Low; SPW = soil pore water; RO = runoff water 246

Table 5.5 First four principal components of 2010 – 2011 dataset 247

Table 5.6 2010 – 2011 PC1 ANOVA: ω^2 = percentage variance 251

Table 5.7 Kruskal-Wallis results of 2010 – 2011 PC1 dataset 256

Table 5.8 April – August 2012 Chi-squared results for 10 cm water occurrence by slope; 257

Table 5.9 Descriptive statistics for 2011 – 2012 water chemistry: SPW = soil pore water; RO = runoff water; 10 cm = 10 cm water; SE = standard error 259

Table 5.10 Percentage data removed from 2011 – 2012 water chemistry variables: SPW = soil pore water; RO = runoff water; Abs_{400} = absorbance at 400 nm 260

Table 5.11 2011 – 2012 PCA cell occupancy: three sample plots for SPW & RO water & two for 10 cm water per slope position; SPW = soil pore water; RO = runoff water; 10 cm = 10 cm water 262

Table 5.12 The first five principal components of 2011 – 2012 dataset 263

Table 5.13 2011 – 2012 PC1 ANOVA; ω^2 = percentage variance; % Erio spp. = percentage Eriophorum spp. 267

Table 5.14 Significant differences 2011 – 2012 PC1 ANOVA / ANCOVA models 268

Table 5.15 Chi-squared results for runoff (RO) water and 10 cm water (10 cm) occurrence by slope 274

Table 6.1 Relative correction factors input in Durham Carbon Model 295

Table 6.2 Relative WTD ANOVA: ω^2 = percentage variance 296

Chapter 1 Introduction

1.1 Peatland formation

Peatlands are formed from the accumulation of partially decomposed organic material, whereby primary productivity of plants exceeds the loss of organic material by decomposition and respiration processes (Moore, 1989). However, the accumulation of organic material is controlled by low rates of decomposition rather than high levels of productivity (Moore, 1989). This process occurs in wetland environments, where water tables are predominantly close to the surface, limiting aerobic microbial activity. There are several peatland types, predominantly distinguished between ombrotrophic bogs that receive water inputs from precipitation only and are typically oligotrophic with low nutrient status, and fens that also receive water from telluric groundwater sources and thus have a higher solute content from the interaction of water with external mineral layers (Bragg, 2002).

Ombrotrophic bogs can typically be divided into blanket bogs and raised bogs, though Charman (2002) also refers to intermediate blanket-raised bogs where two raised bogs coalesce to form a single expanse of ombrotrophic peat. Raised bogs form where the water balance is positive, with precipitation exceeding evapotranspiration and peat accumulates in a convex profile as a dome (Charman, 2002). Blanket bogs cover the landscape, including slopes, and require cool and wet conditions, with bog formation suggested to need an annual 1000 mm rainfall, minimum of 160 days of >1 mm rainfall, a mean temperature of <15 °C for the warmest month and little seasonal fluctuation in temperature (Lindsay et al., 1988). Initial blanket bog development can either be from the infilling of small pools or primary peat production on top of moist soils, which develops outward across the landscape by paludification or upslope waterlogging (Graniero and Price, 1999). Because blanket bog forms in hyper-oceanic climates (Charman, 2002), it can also develop in upland regions of the UK,

Ireland and northwestern seaboard of Europe (Moore and Bellamy, 1974). In upland regions, blanket peat forms from paludification due to impermeable soils and high precipitation maintaining a permanently wet environment, which must also be cool in temperature (Heathwaite, 1993). Convergent slope profiles and low slope angles can be important for maintaining high water tables and anaerobic conditions that lead to peat development but it is possible for peat to form on steeper slopes (Graniero and Price, 1999). Indeed, Moore and Bellamy (1974) observed that blanket bogs have occurred on slopes up to 18 – 25°. Price (1992) highlighted the influence that maritime climates can have upon blanket bog development, affecting the water balance with greater inputs from fog and reduced evaporative losses leading to higher water tables.

1.2 Peatland hydrology

Ingram (1978) introduced the terms acrotelm and catotelm to distinguish the upper and lower peat layers in the diplotelmic peat model. The acrotelm is the upper layer, defined as the zone in which the water table fluctuates, experiences variable moisture content and possesses high hydraulic conductivity (Ingram, 1978). As such, the acrotelm experiences oxygenation during periods of water table decline, has peat-forming aerobic bacteria and other microorganisms and a live matrix of growing plant material (Ingram, 1978). Beneath the acrotelm is the catotelm, which by contrast, does not have variable water content, has a small hydraulic conductivity, is not subject to air entry and peat-forming aerobic microorganisms are absent. As such, there is a smaller range or less abrupt variation in the physical and biological properties of the catotelm (Ingram, 1978). The term haplotelmic was applied by Ingram (1978) to the situation where the acrotelm was absent and only catotelm persists; this situation could arise through natural erosion or human intervention. Haplotelmic peat may exhibit some of the properties of an acrotelm, such as in function but not physical structure; the topmost peat

layer is catotelmic peat exposed to the surface, peat forming vegetation is absent and bulk density profiles change (Lindsay, 2010).

Despite the long-term use of the diplotelmic, acrotelm-catotelm model to define peatland morphology and hydrology, some studies have questioned whether the concept is still appropriate and applicable. Holden and Burt (2003) argued that while the acrotelm-catotelm model was applicable to raised mires, it did not accurately reflect the more complex hydrology of blanket bogs. Holden and Burt (2003) observed that while most lateral water movement was observed in the upper peat layers at Moor House in the North Pennines and low hydraulic conductivities were observed at relatively shallow depths leading to the dominance of saturation-excess overland flow, preferential flow routes such as macropores and soil pipes provided a significant percentage of streamflow. For Cottage Hill Sike, a blanket peat catchment at Moor House, soil pipes have been estimated to contribute 13.7% of annual streamflow (Smart et al., 2013), demonstrating that preferential flow routes can bypass the assumed hydrological function inferred by the acrotelm-catotelm model (Holden et al., 2012). Morris and Waddington (2011) further refuted the ubiquity of the diplotelmic model, observing that during modelled simulations of residence time distributions for a raised bog, three different hydraulic conductivity profiles and residence time distributions would have been considered identical under the diplotelmic model owing to identical water table positions.

Lindsay (2010) questioned the validity of Clymo's (1992) acrotelm-catotelm model based upon bulk density. The model of Clymo (1992) suggested that bulk density was variable in the acrotelm, but from six centimetres depth showed a progressive increase in density until reaching the catotelm boundary, wherein there was little subsequent variation in bulk density. A standard bulk density value of 0.03 g cm^{-3} in the acrotelm was lower than for the catotelm, 0.12 g cm^{-3}. However, Lindsay (2010) noted that the standard acrotelm-catotelm model did not

apply to the bulk density profile of many peatlands, with haplotelmic peat often showing a decrease in bulk density with depth. Thus, the acrotelm-catotelm model both hydrologically and physically does not apply to all peatlands and can be dependent upon local conditions that have affected the condition of the peat.

Despite the acrotelm-catotelm model not being appropriate to all peatlands, it nonetheless informs understanding of the hydrological function of blanket bogs. Evans et al. (1999) identified five mechanisms by which runoff is generated from blanket peat catchments: infiltration-excess overland flow; saturation-excess overland flow; rapid acrotelm (unsaturated zone) flow generated by percolation-excess flow at the boundary between the acrotelm and a saturated catotelm; and rapid acrotelm flow generated by percolation-excess flow at the boundary between the acrotelm and catotelm where the upper layers of the catotelm are unsaturated.

Evans et al. (1999) observed water tables within five centimetres of the surface 83% of the time at Moor House in the North Pennines, which led to rapid runoff generation in response to rainfall events. Such observations on runoff response have been attributed to low hydraulic conductivities at depth in the catotelm leading to higher water tables near the surface. Given the relationship between water table depth (WTD) and surface runoff response, stream discharge is flashy during rainfall events on blanket peatlands (Price, 1992). Mean storm peak lag times at Trout Beck in the North Pennines has been shown to be rapid, at 2.7 hours and 72% of precipitation produced as runoff (Holden and Burt, 2003). However, the hydrological function of peatlands varies with the condition of the peatland. Intact peatlands have been shown to experience water table drawdown events during periodic dry spells, with water tables predominantly close to the surface (Allott et al., 2009). However, eroded peatlands often have low water tables, and therefore experience short-term wet-up events whereby the water table rises towards the surface during rainfall events but also experiences a

rapid decline following cessation of rainfall (Allott et al., 2009, Daniels et al., 2008a). The hydrological function of a peatland therefore varies depending upon whether it is intact or has undergone a form of disturbance, whether through natural erosion (Daniels et al., 2008a) or management intervention (Holden et al., 2011, Clay et al., 2009a).

Water table depth is important to the hydrological function and runoff response of peatlands, but an important control upon WTD and surface runoff generation is hillslope position. In the Peak District, Allott et al. (2009) assessed variation in water table with slope, demonstrating that while eroded slopes experience water table drawdown, intact slopes have WTDs similar to intact plateau and flat sites, typically <150 mm from the surface. Holden and Burt (2003) analysed the effect of slope position upon runoff generation in peatlands, finding that while saturation-excess overland flow was produced across all slope positions, it was more prolonged on foot-slopes compared to top-slopes and mid-slopes, while mid-slopes produced more subsurface runoff. Consequently, the lowest part of the slope had the highest frequency and longest duration of saturation conditions, with the mid-slope having fewer months when saturation-excess overland flow occurred (Holden, 2009). Slope position also affects the occurrence of sub-surface preferential flow routes due to changes in soil structure across the slope (Holden, 2005a). Thus hillslopes can have an important impact upon peatland hydrology through the transfer of water from shedding to accumulation areas. Model results have also suggested that hillslopes dominate the hydrological response on a catchment scale through controlling flow paths (Lane and Milledge, 2013). Although some research has been conducted to assess hillslope hydrology in blanket peats, more work needs to be done to further characterise hillslope hydrology and improve understanding of hydrological processes on a slope scale, particularly across slopes of differing geomorphology.

1.3 Peatlands and the carbon cycle

1.3.1 Carbon storage

Peatlands are one of the most important terrestrial carbon stocks due to the accumulation of organic material over time. An estimated 446 Gt C is stored across a global peatland area of 3 813 553 km^2 (Joosten, 2009). This global estimate is in relatively good agreement with the estimated 500 ± 100 Gt C stored in northern peatlands derived from a synthesis of literature (Yu, 2012). The United Kingdom (UK) is estimated to store 1.745 Gt C in peat soils (Joosten, 2009), whilst it has been suggested that across Europe, the UK holds 14.8% of the land surface area with more than 25% organic carbon (Montanarella et al., 2006). In the UK, blanket bogs represent the largest peatland area, an estimated 92% (Lindsay, 1995, Clark et al., 2010c) and are typically found in upland environments, where cooler temperatures and high levels of rainfall favour peatland formation. However, there are large uncertainties involved in estimating peatland carbon stocks. Uncertainties include the values used as estimates of percentage carbon, mean peat depth and bulk density, along with errors introduced from extrapolation and underrepresentation of the world's largest peatland areas (Yu, 2012).

1.3.2 Carbon balance

There are multiple species and pathways by which carbon is cycled in peatlands. Precipitation inputs include dissolved and particulate inorganic carbon (DIC, PIC) and dissolved and particulate organic carbon (DOC, POC). Gaseous fluxes include the emission and oxidation of methane (CH_4) and the sequestration and efflux of carbon dioxide (CO_2). Fluvial fluxes include DIC, DOC, dissolved CO_2, CH_4 and POC. Carbon dioxide flux, in the form of net ecosystem exchange (NEE), is typically the largest carbon flux. Average fluxes relative to NEE

include: DOC export (24%), CO_2 evasion (12%), POC export (4%), precipitation DOC (1%) CO_2 (1%) and DIC export (1%), with all other fluxes <1% (Dinsmore et al., 2010). Worrall et al. (2003b) suggested that Moor House National Nature Reserve, a peatland in northern England, was a net sink of carbon, with the net uptake of CO_2 at 54% of total carbon turnover while the fluvial transport of POC and DOC were the largest exports of carbon from the catchment.

The carbon budget model of Worrall et al. (2003b) has undergone continued development as the Durham Carbon Model (DCM). An updated model with improved modelling techniques suggested Moor House was in fact a carbon source and indicated POC was the largest fluvial flux, while the greatest change in flux over the study period was that associated with increasing DOC (Worrall et al., 2007b). Worrall et al. (2009a) found that the largest component of the carbon budget at Moor House was primary productivity, with net ecosystem respiration (R_{eco}) and the loss of DOC the next most significant components of the carbon budget. The model of Worrall et al. (2009a) was based upon direct monitoring of carbon fluxes and suggested that Moor House was a net carbon sink and highlighted the importance of continual model development through improved understanding of carbon cycling which will consequently lead to more accurate carbon budget models. As such, it is important to improve carbon budget models to reduce uncertainty and error. Increased understanding of peatland function and carbon cycling is an important aspect of this and the DCM has continued to evolve, incorporating additional factors that influence the carbon budget, such as land management. Examples include drainage (Rowson et al., 2010), burning and grazing on peatland catchments (Clay et al., 2010b) and vegetation management (Dixon, 2012).

Several carbon budgets have been constructed for peatlands. Dinsmore et al. (2010) found that for a lowland ombrotrophic bog in Scotland, net ecosystem exchange (NEE - the sum of primary productivity and R_{eco}) was the largest carbon flux at -136 and -93.5 g C m^{-2} yr^{-1}

for 2007 and 2008 respectively (a negative sign convention is used to represent a carbon sink in this thesis, with regards to the atmospheric pool). Similarly, at Mer Bleue in Canada, an estimated carbon sink of -60 g C m^{-2} yr^{-1} was largely derived from the balance between gross photosynthesis (P_G) (-530 g C m^{-2} yr^{-1}) and R_{eco} (460 g C m^{-2} yr^{-1}), with losses from DOC, DIC and CH_4 amounting to as little as 10 g C m^{-2} yr^{-1} (Moore et al., 2002). However, a multi-annual study at Mer Bleue between 1998 – 2004 demonstrated the importance of DOC to the carbon budget as it amounted to 37% of mean NEE (Roulet et al., 2007). The influence of DOC to the total carbon budget has been further exemplified elsewhere; Dinsmore et al. (2010) found downstream export of DOC was the second most important flux after NEE at 18.6 ± 16.0 and 32.2 ± 18.7 g C m^{-2} yr^{-1} for 2007 and 2008; an average 24% loss of carbon from the NEE uptake. Over a five year study period, DOC export (19.3 ± 4.59 g C m^{-2} yr^{-1}) was shown to equate to 54.3% of total aquatic carbon losses (Dinsmore et al., 2013). Koehler et al. (2011) also found DOC flux to be the second largest component of the carbon budget, equating to an average 29% of the NEE mean. However, in eroded catchments such as in the South Pennines, POC flux can be an important component of the carbon budget as well (Billett et al., 2010). Nevertheless, across multiple studies and nations, the gaseous flux of CO_2 via P_G and R_{eco} and fluvial flux of DOC represent the most important pathways that comprise the carbon budget of ombrotrophic peatlands (Billett et al., 2010). As such, DOC and gaseous CO_2 fluxes shall be discussed in further detail below.

1.3.3 Dissolved organic carbon

There are multiple controls on DOC flux, both biotic and abiotic. It is important to develop as thorough an understanding of these as possible in order to create accurate carbon budget models. There has been an upward trend in DOC concentrations in UK upland peatland streams: a 65% increase in DOC concentration was observed over a 12 year period (Freeman et

al., 2001a), whilst Worrall et al. (2004), stated there was a 77% increase in DOC across 198 catchments.

Many factors can affect DOC concentration and flux. Freeman et al. (2001b) observed that the increased presence of phenol oxidase caused a 27% reduction in phenolic compounds that inhibit hydrolase enzymes from decomposing organic matter. Consequently, it was argued that water table drawdown in peatlands would provide aerobic conditions to allow phenol oxidase to reduce the concentration of phenolic compounds, thus leading to greater hydrolase enzyme activity and ultimately higher levels of DOC production. However, although this process has been suggested to cause an enzyme-latch (Freeman et al., 2001b) that continues DOC production after water tables return to previous high levels creating anaerobic conditions, this process is de-coupled from CO_2 respiration (Worrall et al., 2005).

Rising temperatures have been shown to enhance DOC concentration (Freeman et al., 2001a, Clark et al., 2005) and is linked to increased biological activity (Dinsmore et al., 2013). Interaction effects between temperature and water table depth (WTD) can affect the temperature sensitivity of DOC production (Clark et al., 2009). Despite this, it has been argued that any increase in DOC export as a result of enhanced production from rising temperatures could be negated and the export of DOC lowered as warming increases evapotranspiration, causing a reduction in discharge rates and consequently greater DOC retention (Pastor et al., 2003).

Water table drawdown can enhance DOC production (Mitchell and McDonald, 1995, Wallage et al., 2006) but may cause suppression of DOC solubility when oxidation of sulphur to SO_4^{2-} occurs (Clark et al., 2005, Daniels et al., 2008b), which is related to acidity and acid neutralising capacity (Clark et al., 2012). Clark et al. (2012) performed laboratory experiments to determine the relationship between WTD, DOC production and SO_4^{2-} oxidation. It was suggested that while water table drawdown enhances biological activity with a concomitant

increase in organic matter decomposition and therefore DOC production, the oxidation of reduced sulphur can also lead to increased soil water acidity that suppresses DOC solubility, meaning organic carbon was produced but retained in the solid phase until water tables recovered sufficiently to reduce SO_4^{2-}. During a manipulation experiment investigating the effects of acidity upon DOC mobility, Evans et al. (2012) observed a decrease in DOC when peat and organo-mineral soils were treated with an acid solution, while alkaline manipulations raised pH levels and increased DOC concentration. However, the impact of further additions in the acid treatment was limited for acidic soils compared to the observed increase in DOC following treatment with alkaline solutions; the opposite was true for soils with a higher starting pH level.

The impact of water table drawdown upon DOC solubility can also have an important effect across large spatial scales; gullying can also affect DOC concentration as enhanced water table drawdown in gully edge locations can increase oxidation of sulphur to SO_4^{2-} (Daniels et al., 2008b). Increased SO_4^{2-} content in catchments with a high density of gullying resulted in lower concentrations of DOC compared to catchments with a low density of gullying (Daniels et al., 2008b). Land management can also affect DOC production and transport. Dissolved organic carbon export was shown to be significant from urban and grazed land on mineral and organo-mineral soils, but not arable land (Worrall et al., 2012b), while moorland burning has been suggested to affect DOC concentration through alterations of hydrology enhancing aerobic decomposition and carbon loss (Yallop and Clutterbuck, 2009) and DOC composition through mobilisation of older carbon stores with hydrological change(Clutterbuck and Yallop, 2010). However, the effect of moorland burning may not be apparent over long time periods if the degree of burning has not changed over time (Chapman et al., 2012). Peat drainage has also been shown to influence the production and export of DOC, with enhanced drainage suggested to increase DOC production and therefore drain blocking has the effect of lowering DOC concentration (Wallage et al., 2006, Höll et al., 2009). Others have argued that

management intervention techniques do not decrease productivity but rather the yield of DOC (Gibson et al., 2009), while DOC concentrations can increase post blocking due to accumulation of dissolved organic matter at depth as DOC export decreases (Glatzel et al., 2003).

It is evident that landscape scale features such as drainage ditches and erosion gullies can affect the production and cycling of DOC. However, an aspect that has been overlooked with regards to DOC dynamics in peatland systems is the potential impact that hillslope position may have. Hillslope position could have an important influence upon DOC in peatlands for a number of reasons. Hillslope position is an influential control upon WTD, which as discussed above, affects DOC concentrations through increasing or decreasing the rate of oxidation of organic matter. Furthermore, variation in WTD can affect flowpath (Holden and Burt, 2003), meaning that hillslope position could influence the transport of DOC from shedding to accumulation areas at the base of the hillslope.

Preferential flow routes could also affect the transfer of carbon across the hillslope. Soil pipe networks have been recognised as conduits for carbon export, including DOC (Holden et al., 2012), which can be dominated by near-surface, young, carbon sources (Billett et al., 2012). Soil pipe density has been shown to vary with hillslope position, with a greater frequency of soil pipes occurring on top-slope and foot-slope locations where soil structural properties may be more heterogeneous (Holden, 2005a). Thus, hillslope position could affect DOC production and transport, not only due to potential controls on WTD, but also runoff generation and transport through preferential flow routes. It has been argued that understanding of the effect water movement has upon DOC retention and release is limited (Limpens et al., 2008, Holden, 2005b) and topographic variation could be amongst the unknown controls (Clark et al., 2010b). As such, investigating whether hillslope position affects carbon cycling could be an important avenue of research to improve understanding of carbon

cycling in peatlands. Furthermore, understanding of DOC dynamics has been improved by assessing the role of hillslope for non-peat soils (McGlynn and McDonnell, 2003, Creed et al., 2013), with changes in DOC concentration between upland hillslope areas and flatter riparian zones observed (Morel et al., 2009, Mei et al., 2012). Slope position can also influence other biogeochemical cycles, such as the transport of nitrates (Castellano et al., 2013). However, little work has been conducted to assess the exact role of hillslope in peatland catchments, which could be expected to behave differently.

1.3.4 Land-atmosphere carbon dioxide flux

Several environmental (hydro-climatic) factors influence rates of R_{eco} and P_G. Temperature is one of the most important, with both soil and air temperature shown to increase rates of R_{eco} and P_G. Lloyd and Taylor (1994) used an Arrhenius relationship between temperature and soil respiration, while an exponential relationship was found by Lafleur et al. (2005) between R_{eco} and air temperature and near-surface soil temperature at Mer Bleue in Canada. Dorrepaal et al. (2009) suggested a 1 °C temperature increase accelerated R_{eco} by 60% in spring and 52% in summer. Pelletier et al. (2011) noted that microtopographic variation in NEE was because differences in P_G and R_{eco} were related to changes in air and soil temperature, as well as WTD. Furthermore, the effect of temperature and WTD upon CO_2 flux is often interrelated. Silvola et al. (1996a) observed a change in the relationship between WTD and Q_{10} response function, a measure of temperature sensitivity that models the change in respiration over a 10°C change in temperature. While both increasing temperature and increased WTDs (due to increased aerobic respiration) enhanced CO_2 flux, water tables closer to the surface (i.e. a higher soil moisture content) increased the temperature sensitivity of CO_2 fluxes (Silvola et al., 1996a).

Despite the observed increase in CO_2 flux with lowering of the water table, the relationship between water table and CO_2 flux is not consistent. Tuittila et al. (2004) noted that while water level controlled both R_{eco} and P_G, beyond 30 cm depth moisture levels became limiting, in agreement with Silvola et al. (1996a). Indeed, while Lafleur et al. (2005) found a relationship between R_{eco} and temperature, none was found with WTD for a number of reasons, including a lack of sensitivity to variation in moisture content as water tables were deep. Tuittila et al. (2004) suggested that at a cut-away peatland where *Sphagnum* was reintroduced, maximum rates of P_G were achieved at a WTD of -12 cm; moisture stress limited P_G with further decreases in WTD and reduced oxygen levels limited P_G at shallower WTDs. Regardless of the varying impact of WTD upon CO_2 flux, water table drawdown can nonetheless have a significant impact upon carbon accumulation and the overall carbon balance of a peatland. Alm et al. (1999) suggested a ratio of 4:1 moist to dry summers was necessary to maintain a carbon sink, with dry conditions shown to both increase rates of respiration and decrease P_G, leading to reduced levels of carbon accumulation and potentially net carbon release (Bubier et al., 2003).

Photosynthetically active radiation (PAR) is another important control upon the rate of P_G and NEE. Light saturation in *Eriophorum angustifolium* and *Eriophorum vaginatum* has been shown to occur between 500 – 700 µmol m^{-2} s^{-1} (Gebauer et al., 1998). Across a range of microforms with different vascular and *Sphagnum moss spp*. carbon dioxide uptake was observed by Pelletier et al. (2011) to saturate at ~1000 µmol m^{-2} s^{-1}. Nieveen et al. (1998) found for NEE that assimilation increased at a linear rate with increasing light intensity at low light levels, with the response curve for net ecosystem exchange and solar irradiation shaped by a rectangular hyperbola, which was also observed by Bubier et al. (2003). However, P_G at maximum available light (PAR >1000 µmol m^{-2} s^{-1}) did not vary between ericaceous shrub and herbaceous plant species, nor did P_G vary significantly among sites (Bubier et al., 2003). Despite lack of variation in P_G, NEE did vary at high PAR levels across the site for beaver ponds,

poor fen and bog hummock and hollows – though bog microforms were not significantly different from one another (Bubier et al., 2003). The response between NEE and PAR can nonetheless vary among different microforms, with inter-annual variation between the response of microforms also observed (Pelletier et al., 2011).

Ecosystem respiration, P_G and NEE vary both diurnally and seasonally as well. Nieveen et al. (1998) observed changing diurnal patterns in NEE between winter and summer months, with a relatively flat diurnal cycle of CO_2 efflux during winter but a switch to net CO_2 uptake between ~0600 – 1900 in summer. Despite this, no clear trend was found between 0700 – 1600 (Nieveen et al., 1998). Over a six year study period, Roulet et al. (2007) observed NEE to switch from a winter efflux of CO_2 to sequestration in April, while the switch back to a net source occurred in September or October. At a poor fen in Sweden, Nilsson et al. (2008) noted the shift to a CO_2 sink occurred in April and May for 2004 and 2005 respectively, while the return to a CO_2 source took place during September. Considerable inter-annual variation is also possible with NEE (Roulet et al., 2007, Koehler et al., 2011), with Shurpali et al. (1995) noting a change between a net source and sink between dry and wet years. The dry year, which experienced moisture stress, reduced levels of CO_2 uptake but enhanced CO_2 release due to water table drawdown from increased soil aeration (Shurpali et al., 1995).

Given the influence of water table upon CO_2 flux, the effects of land management are often associated with changes in WTD. Martikainen et al. (1995) showed that drainage increased CO_2 emissions from both fen and bog peatlands, though CH_4 emissions were reduced. Drainage has also been shown to alter vegetation communities, with *Eriophorum spp*. and *Sphagnum* shown to reduce in abundance down-slope of drainage ditches that lower the water table (Stewart and Lance, 1991). Other land management strategies can affect the carbon balance of peatlands as well. It has been suggested that grazing and burning promote greater levels of photosynthesis and reduce rates of R_{eco} in young vegetation compared to

older, degenerate, vegetation (Clay et al., 2010b). However, any reduction in carbon emissions on burnt plots is mitigated by carbon release during the combustion process (Clay et al., 2010b).

Variation in vegetation can affect rates of CO_2 flux from peatlands. Bortoluzzi et al. (2006) found that *Sphagnum* dominated plots had greater fluxes via R_{eco} and P_G than *Eriophorum* dominated plots, though *Eriophorum* had a greater flux of CH_4. The higher CH_4 flux from *Eriophorum* was likely due to large air spaces (lacunae) allowing transport of CH_4 to the surface in waterlogged conditions (Thomas et al., 1996, Marinier et al., 2004). Despite the observation of greater CO_2 fluxes from *Sphagnum* than *Eriophorum*, the lacunar system has also been noted to increase productivity and sequestration of CO_2 (Komulainen et al., 1999), with efficient carbon binding leading to carbon accumulation (Alm et al., 1997).

Topographic variation has also been shown to influence CO_2 flux. Ecosystem respiration, P_G and NEE have been shown to vary across topographic micro-forms of different vegetation (Alm et al., 1997, Pelletier et al., 2011, Wu et al., 2011), which can respond differently to temperature and moisture variation (Sommerkorn, 2008). It has been argued by Laine et al. (2006) that it is important to understand spatial variation in NEE and multi-scale assessment is important. Furthermore, large scale features such as gullies can influence CO_2 flux and while such effects may be associated with vegetation change (McNamara et al., 2008, Clay et al., 2012), eroded gullies can influence landscape scale carbon budgets (Evans and Lindsay, 2010b). The study of Evans and Lindsay (2010b) was limited by not incorporating fluxes observed through field monitoring and it is important to be able to relate direct observations in the field to larger scale variation. Indeed it has been argued that although automated measurements of CO_2 flux can provide good temporal resolution, manual measurements are important when capturing the spatial variation associated with

heterogeneous wetlands (Burrows et al., 2005) and can be used to incorporate different landscape elements (Schrier-Uijl et al., 2010).

Despite recognition of the importance of assessing multi-scale variation in CO_2 flux, little is known about how hillslope position affects rates of R_{eco} and P_G from peatlands. Carbon dioxide flux could vary with slope position given the importance of topographic variation, as discussed above. Furthermore, given that slope position could be an important control upon DOC cycling, this may have an impact upon respiration rates. Hillslope position has been shown to affect DOC transport and create hotspots of soil CO_2 efflux for forested landscapes (Creed et al., 2013) and it is possible that in peatland environments, CO_2 flux varies with slope position because of the transport of substrates along the slope. As such, hillslope position needs to be investigated to determine whether slope-scale measurements influence variation in CO_2 fluxes.

1.4 Hillslope

An area of peatland science that has been little studied, certainly in relation to carbon cycling, is the hillslope, perhaps because so many of the world's peatlands are raised bogs rather than blanket bogs. Hillslope could be an important feature that controls the hydrology and carbon flux of peatlands. As discussed above, WTD and runoff generation has been shown to vary with slope position, while DOC production and transport could be affected by slope position as well. Moreover, it is important to assess multi-scale variation in CO_2 fluxes, yet slope-scale has not yet been considered as a component affecting CO_2 fluxes and needs to be investigated.

As a landscape scale feature, there are several interpretations of how to represent different hillslope shapes and positions as unique and discrete landform elements. Several

methods of distinguishing landscape and hillslope units are based upon profile and plan curvature, considering the hillslope as a three-dimensional unit given the impact convergent or divergent slopes can have upon flowpaths and ultimately soil formation (Huggett, 1975, Pennock et al., 1987). Huggett (1975) described four combinations of flow patterns across hillslopes based upon Troeh (1964): convex slope and concave contour leading to convergent lateral flux and divergent vertical flux; concave slope and contour leading to convergent lateral and vertical flux; convex slope and contour leading to divergent lateral and vertical flux; and concave slope and convex contour leading to divergent lateral flux but convergent vertical flux. On Quantock Hill in Somerset, England, a Brown-Earth soil hillslope, Anderson and Burt (1978) also recognised the importance of topography in controlling flow direction. Convergent flow and saturation-excess overland flow predominated from convergent hollows (Anderson and Burt, 1978).

Pennock's (1987) landform classification identified seven landform elements, based upon an initial five from Ruhe (1960): divergent shoulders; convergent shoulders; divergent backslopes; convergent backslopes; divergent footslopes; convergent footslopes; and level. A gradient of 3° was arbitrarily chosen to separate backslope and level elements. Thus Ruhe (1960) and Pennock (1987) classified the hillslope based upon discrete hillslope positions whilst recognising the importance of profile curvature, particularly upon soil moisture content, with an expected moisture content of shoulders<backslopes<footslopes (Pennock et al., 1987).

Several studies have derived hillslope and landform elements using digital elevation models (DEMs). Irvin et al. (1997) used the classification of Ruhe and Walker (1968) of: flat summit; convex shoulder; linear backslope; concave footslope; and flat, alluvial toeslope as a starting point to assess the landscape of Pleasant Valley, Wisconsin, through fuzzy and ISODATA classifications. It was suggested that dividing the landscape into different units could be useful in delineating soil units and reducing intensive fieldwork sampling (Irvin et al., 1997).

Indeed, Park and van de Giesen (2004) modelled soil moisture properties within different landscape units and reduced Conacher and Dalrymple's (1977) nine landscape catena units to six soil landscape units of: interfluve; shoulder; backslope; footslope; toeslope; and channel.

Hillslope position can therefore affect flowpaths and subsequently soil moisture, which can have an impact upon soil formation. Furthermore, hydrology and biogeochemical cycles are linked, for instance with hillslope affecting the nitrogen cycle by influencing zones where denitrification takes place (Burt and Pinay, 2005). Despite the importance of hillslope position to hydrology and biogeochemistry, little research has been done to consider the impact of hillslope position upon carbon cycling in peatlands, yet It is important to understand how CO_2 flux and DOC vary across different spatial scales and hillslope may therefore be important.

The purpose of this thesis, therefore, is to investigate the affect that hillslope position has upon peatland hydrology and carbon cycling. This study adopts the approach of assessing the hillslope applied by Holden and Burt (2003) and Holden (2005a) who separated the hillslope into discrete topographic positions of top-slope, mid-slope and foot-slope, acknowledging the importance of distinguishing slope gradient and slope morphology. This allows a simplification of the hillslope to ascertain any differences in hydrology and carbon cycling that may occur due to hillslope position. As outlined in Chapter 2 (section 2.3.2.1) the mid-slope was further sub-divided into upper and lower sections to allow more detailed assessment of variation across the entire hillslope. As such, four hillslope positions are used in this thesis, herein referred to as: top-slope; upper mid-slope; lower mid-slope; and bottom-slope (Figure 1.1). The division between upper and lower mid-slope was done *in situ* when installing equipment and thus represents a desire to capture more spatial variation rather than representing change associated with a quantifiable property such as a reduction in a given slope angle.

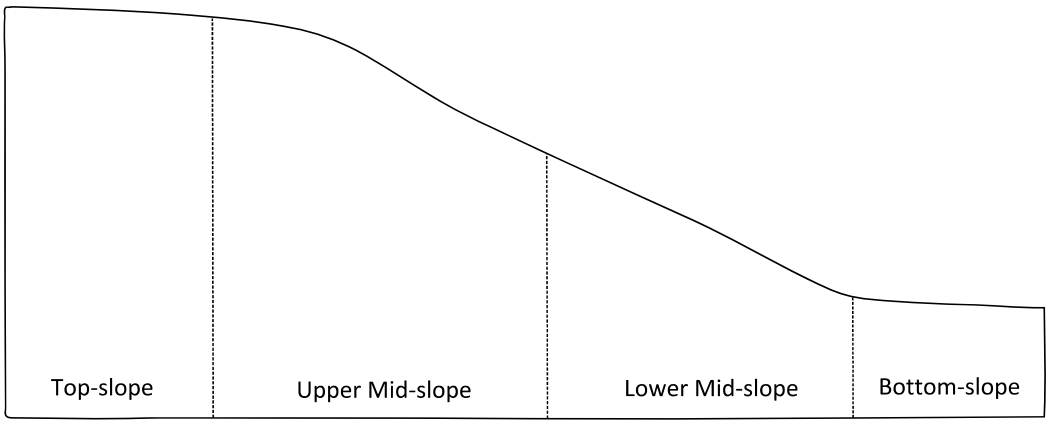

Figure 1.1 Conceptual model of hillslope positions

1.5 Thesis aims and hypotheses

The purpose of this thesis is to establish whether hillslope position significantly affects the gaseous and fluvial carbon pathways of peatland systems and put results into a conceptual and process-based context. The hypotheses of this thesis can be summarised as:

- Hillslope position significantly affects the hydrology and carbon flux of peatlands.
- Variation in hydrology can be explained by the physical composition of peat soil, while variation in CO_2 fluxes and DOC are due to changes in organic matter, with labile carbon sources enhancing productivity.
- Trends in hillslope hydrology and carbon flux are consistent along the hillslope, with bottom-slope fluxes replicable to the riparian zone.
- Tracers can be used to identify water movement across the hillslope, with greater water movement and mixing of water sources on the bottom-slope.
- Hillslope position is an important parameter that affects the output of carbon budget models.

1.6 Thesis outline

The thesis is divided into the following chapters:

- Chapter 2 investigates the role that hillslope position has upon peatland hydrology and carbon flux. Water table depth, CO_2 fluxes and DOC concentrations are monitored in a one-year fieldwork campaign across two hillslopes in the Peak District, Derbyshire, UK. All subsequent chapters are constructed based upon the results of this chapter and as such relate back to its findings and conclusions. Chapter 2 serves as the methods chapter for field monitoring and water chemistry analysis and is applicable to Chapter 4 and Chapter 5 as well.
- Chapter 3 is a laboratory study into the physical and chemical composition of peat, vegetation and litter. Multiple soil cores up to one metre in depth from the surface were collected along with vegetation samples. The purpose was to establish whether soil organic matter composition, as well as that of vegetation and litter, varied with hillslope position. Furthermore, physical and compositional variables were incorporated into the statistical models for WTD, CO_2 fluxes and DOC developed in Chapter 2 to ascertain if they provided an explanation to the hillslope trends identified in that chapter.
- Chapter 4 is a second one-year field monitoring campaign of WTD and carbon fluxes, but changes the focus from discrete hillslope positions to a slope transect that continues monitoring to the riparian zone and stream. The purpose was to investigate whether the trends associated with hillslope position in chapter 2 were consistent across each slope position and could be observed to change with progression along the slope. It was also designed to explore the importance of spatial heterogeneity, inter-annual variation and develop a more detailed understanding of the hydrology of the hillslope.

- Chapter 5 explores changes in water chemistry along the hillslope by incorporating multiple water sources into a multivariate study of the composition of water and its relationship to hillslope position. It assesses the transport and mixing of water across the hillslope, identifying unique end-members and compositional trends. A tracer study is used to explicitly monitor the movement of water down-slope to the riparian zone and identify how flowpath changes with hillslope position.
- Chapter 6 incorporates the relative proportions of WTD, R_{eco}, P_G and DOC for each hillslope position into a carbon budget model. The relative proportions are based upon the results of Chapter 2. The impact of hillslope position upon carbon budget models is assessed.
- Chapter 7 synthesises the findings of each chapter into an overall conclusion of the thesis. Avenues for further research are recommended.

Chapter 2 The impact of hillslope position on carbon flux

2.1 Introduction

Chapter 1 outlined a synthesis of the literature of the trends associated with the hydrology and carbon cycling of peatlands and the factors that influence variation in them. This synthesis showed that despite hillslope position being *a priori* important factor that would affect peatland hydrology through influencing water table depth (WTD) and runoff generation, there was a lack of research investigating the potential impact of hillslope position upon the carbon flux of upland peatlands. Hillslope position could be important particularly to peatlands in the British Isles, where blanket peat covers the landscape and can develop on hillslopes. The purpose of this chapter is to investigate whether hillslope position is an important factor controlling carbon flux from peatlands by monitoring CO_2 fluxes and dissolved organic carbon (DOC) concentrations. This chapter shall also explore the relationship between hillslope position and hydrology. The results and conclusions of this chapter are important in directing the research of subsequent chapters.

2.2 Aims and objectives

The broad aim of this chapter is to establish what influence slope position has upon the hydrology and carbon cycling of peatlands. A number of objectives shall address this aim:

- Determine the effect of hillslope position on the hydrological response of peatlands by assessing variation in WTD and surface water runoff response.
- Determine whether CO_2 flux varies with slope position by monitoring ecosystem respiration (R_{eco}), gross photosynthesis (P_G) and net ecosystem exchange (NEE) across the hillslope.
- Determine how concentrations of DOC change with slope position in soil pore water and surface runoff water.
- Establish whether any relationship found between slope position and WTD, CO_2 flux and DOC is independent of other factors that may explain variation attributed to the hillslope.

2.3 Materials and methods

2.3.1 Study sites

Two sites were used to conduct fieldwork for this chapter: Featherbed Moss and Alport Low in the Peak District National Park, Derbyshire (Figure 2.1). The Peak District was initially selected as a locality for the study owing to its large area of blanket peat. The two study sites were initially identified as ideal hillslope areas using Environment Agency (provided by Moors for the Future Partnership) two-metre ground resolution LiDAR data (with 25 cm vertical accuracy) of Bleaklow and Kinder Scout, areas of the Peak District, flown in December 2002 and May 2005 (Evans and Lindsay, 2010a). An on-site inspection confirmed the suitability of Featherbed Moss and Alport Low for use in the study prior to installation of study plots.

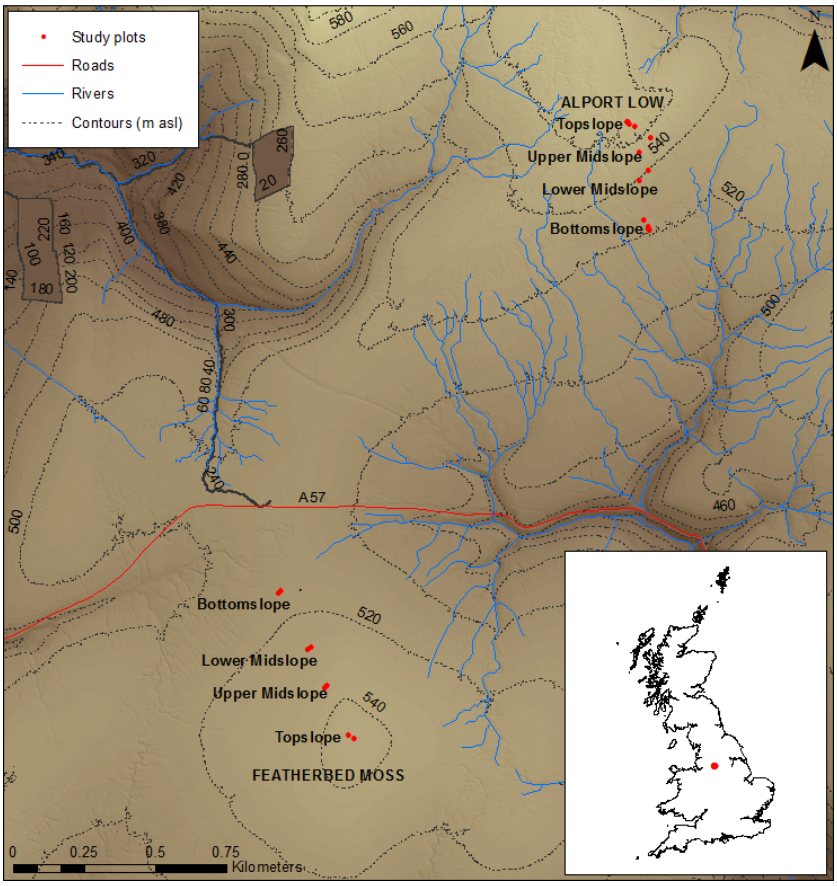

Figure 2.1 Map of study sites in Peak District, Derbyshire

Featherbed Moss and Alport Low were selected as replicate slopes, though it was not possible to control aspect. Table 2.1 shows the summary of site parameters for both study sites. Featherbed Moss had low slope angles of <5° across all slope positions, while Alport Low had steeper mid-slopes. Each study site is discussed separately in more detail below.

Table 2.1 Average values of site parameters for Featherbed Moss and Alport Low; NB missing peat depth measurements due to time constraints

Site	Slope	*Eriophorum* dominance (%)	Peat depth (m)	Altitude (m)	Aspect (°)	Slope angle (°)	Wetness index
Featherbed Moss	Top-slope	94	-2.04	543.7	102.0	1.1	6.1
	Upper mid-slope	96	-1.71	535.1	298.5	4.0	7.1
	Lower mid-slope	85	-2.16	525.9	328.8	3.5	7.8
	Bottom-slope	95	-2.62	515.2	297.5	3.6	7.5
Alport Low	Top-slope (Hummock)	31		564.0	169.8	4.2	4.6
	Top-slope (*Eriophorum*)	94		563.2	158.9	5.3	4.7
	Upper mid-slope	33	-1.34	556.5	138.5	9.1	6.4
	Lower mid-slope	65	-1.34	538.3	145.8	10.4	6.3
	Bottom-slope (*Eriophorum*)	98	-2.70	521.9	141.7	3.4	5.4
	Bottom-slope (Hummock)	70	-2.77	521.0	161.4	2.9	6.5

2.3.1.1 Featherbed Moss

Featherbed Moss is situated south of the A57 Snake Pass road (Figure 2.1). Extensive areas of Featherbed Moss are eroded, with peat haggs immediately south of the A57 and dense gullying to the North East, around Thomason's Hollow (Tallis, 1973). Featherbed Moss drains into two stream networks, the River Ashop and Shelf Brook, and is underlain by soft Pendle or Shale Grits (Tallis, 1973). The area used for this study is the intact blanket peat found on the plateau at Featherbed Top, down to the bottom-slope to the North West. The slope positions used in the study have an altitudinal range of 544 – 515 m and are dominated by *Eriophorum vaginatum* and *Eriophorum angustifolium* (Table 2.2). The top-slope site is a flat plateau and although slope angle increases further down-slope, it remains gently sloping, with a maximum slope angle of 4.2°. Peat depth decreases from the top-slope to a minimum on the upper mid-slope of 1.60 m. Peat depth subsequently increases further down-slope, typically more than two metres on the lower mid-slope and 2.47 m or above at the bottom-slope plots. Peat depth can be indicative of water table depth and affect surface water generation (Wilson

et al., 2010). Previous research on Featherbed has suggested a median water table depth on the top-slope plateau of 134.75 mm (Allott et al., 2009).

Table 2.2 Featherbed Moss site details

Slope position	Plot	*Eriophorum* dominance (%)	Peat depth (m)	Altitude (m)	Aspect (°)	Slope angle (°)	Wetness index
Top-slope	1	96	-1.88				
	2	96	-1.91	543.7	152.2	1.0	6.5
	3	100	-1.87				
	4	88	-2.27				
	5	88	-2.00	543.7	51.8	1.1	5.6
	6	96	-2.31				
Upper Mid-slope	1	100	-1.64				
	2	100	-1.63	535.0	294.6	4.2	6.9
	3	84	-1.60				
	4	100	-1.75				
	5	92	-1.87	535.1	302.3	3.8	7.2
	6	100	-1.74				
Lower Mid-slope	1	96	-2.26				
	2	88	-2.20	525.8	331.0	3.4	7.6
	3	100	-2.26				
	4	100	-2.21				
	5	28	-2.12	525.9	326.6	3.6	7.9
	6	96	-1.91				
Bottom-slope	1	100	-2.63				
	2	72	-2.79	514.9	291.5	3.8	7.7
	3	100	-2.70				
	4	96	-2.47				
	5	100	-2.60	515.4	303.5	3.3	7.3
	6	100	-2.55				

2.3.1.2 Alport Low

The second study site, Alport Low, is situated to the north of the A57, heading towards Bleaklow plateau (Figure 2.1). Alport Low is underlain by the Millstone Grit Series, with thin periglacial deposits overlying the bedrock (Evans and Lindsay, 2010a). Alport Low is steeper

sloping than Featherbed Moss, with slope angles exceeding 10° on mid-slope sections (Table 2.3) and has suffered from more extensive erosion than Featherbed Moss. The top-slope site displays type I gullying (Bower, 1961), with a dendritic network of branching gullies associated with low slope angles. On the steeper mid-slopes, this gives way to type II gullying of individual linear gullies. This affected the distribution of the study plots. Whereas on Featherbed Moss the nested sub-slope plots (section 2.3.2) were relatively close to each other, on the mid-slope of Alport Low the sub-slope plots were separated onto interfluves either side of a gully. As such, the slope positions do not follow a linear alignment down the slope as they do on Featherbed Moss. Gullies divert flow away from the local area, causing drainage and an increase in the depth of the water table. The immediate water table drawdown zone as a result of gully erosion is within two metres of the gully edge, although it has also been shown that across the Peak District, eroded sites typically display lower water tables beyond the gully edge zone compared to intact sites (Allott et al., 2009). All plots on Alport Low were consequently installed on interfluves more than two metres away from gully edges, to avoid possible water table drawdown as a result of gully edge effects.

Vegetation was more varied on Alport Low than Featherbed Moss and to account for this, specific *Eriophorum spp*. plots were installed at the top-slope and bottom-slope, where *Eriophorum spp.* were more dominant. Plots were installed alongside top-slope and bottom-slope plots placed on hummocks which had a greater mixture of vegetation (Figure 2.2). Table 2.3 shows the percentage of *Eriophorum spp.* dominance, recorded from a vegetation survey at the end of the first year of data gathering, in August 2011. The specific *Eriophorum* sites had very high *Eriophorum spp.* dominance, typically 96% or more, other than plot five on the top-slope, which was surrounded by bare peat in a bog pool of surrounding water. Such percentages of *Eriophorum spp.* dominance were similar to those recorded on the study plots Featherbed Moss (Table 2.2), whilst the hummock sites were more varied, with higher levels of *Vaccinium myrtillus* causing a lower percentage of *Eriophorum spp.* coverage, particularly on

the top-slope hummock plots. Vegetation also varied on the mid-slopes, with the sub-slope plots 1-3 on the upper mid-slope dominated by non-*Sphagnum* moss, whilst plots 4-6 also had more *Vaccinium* as the dominant vegetation. The vegetation survey for plot five was lost and the survey for plot six was used as a proxy, owing to their observed similarity.

Figure 2.2 Hummock plot (L) and Eriophorum spp. (R) plots on Alport Low top-slope

Table 2.3 Alport Low site details: NB missing peat depth measurements due to time constraints

Slope position	Plot	*Eriophorum* dominance (%)	Peat depth (m)	Altitude (m)	Aspect (°)	Slope angle (°)	Wetness index
Top-slope (Hummock)	1	48					
	2	36		564.1	151.0	4.1	4.0
	3	68					
	4	12					
	5	8		563.9	188.6	4.3	5.1
	6	12					
Top-slope (*Eriophorum*)	1	100					
	2	100		563.7	166.9	4.4	4.8
	3	100					
	4	100					
	5	68		562.6	150.9	6.1	4.5
	6	96					
Upper Mid-slope	1	0	-1.25				
	2	0	-1.44	557.5	131.3	7.4	7.1
	3	40	-1.29				
	4	64	-1.28				
	5	48	-1.37	555.4	145.7	10.8	5.6
	6	48	-1.42				
Lower Mid-slope	1	80					
	2	100		538.8	148.5	10.1	6.4
	3	100					
	4	64	-1.30				
	5	16	-1.49	537.8	143.1	10.6	6.1
	6	28	-1.23				
Bottom-slope (*Eriophorum*)	1	100	-2.55				
	2	96	-2.56	522.8	136.7	4.3	5.4
	3	96	-2.63				
	4	96	-2.67				
	5	100	-2.82	521.0	146.7	2.5	5.3
	6	100	-2.96				
Bottom-slope (Hummock)	1	72	-2.78				
	2	88	-2.68	521.2	175.6	3.1	5.7
	3	52	-2.56				
	4	96	-2.96				
	5	32	-2.89	520.7	147.1	2.7	7.2
	6	80	-2.75				

2.3.2 Experimental design

2.3.2.1 Factorial design

A factorial design was employed for the study in order to examine the impact of slope position on carbon fluxes above and beyond effects due to site, seasonal cycle and measurement error. To control for the effect of study site (i.e. Featherbed Moss and Alport Low), month of sampling and slope position were replicated across the two study sites. The site factor, therefore, has two levels (Featherbed Moss and Alport Low). The seasonal cycle has 12 levels, one representing each month, and henceforward referred to as the month factor. The slope position factor has four levels and is described in detail below.

Slope position was divided into top-slope, mid-slope and bottom-slope. The mid-slope was further subdivided into upper and lower mid-slope sections so as to increase monitoring on the slope and capture a better resolution of slope angle and altitudinal variation. Each slope position had six study plots, which were subdivided into two groups of three. This created a further sub-slope category in the factorial design, nested within slope position (Figure 2.3). The aim of this was to capture better spatial resolution within the slope positions, given the heterogeneous nature of peatlands and the variation in conditions at a plot scale. The sub-slopes were separated with an arbitrary designation of ‘A’ and ‘B’. On Alport Low, the top-slope and bottom-slope had two further sub-slope designations of ‘C’ and ‘D’ to account for the extra plots distinguishing *Eriophorum* and hummocks.

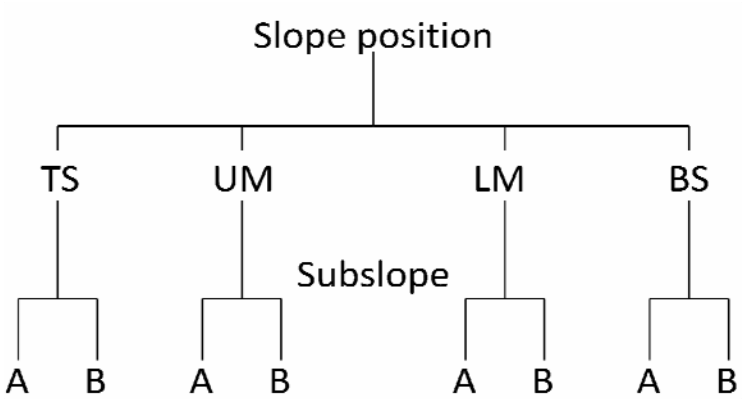

Figure 2.3 Nested sub-slope design: TS = top-slope; UM = upper mid-slope; LM = lower mid-slope; BS = bottom-slope

It was intended that vegetation should be a factor accounted for in the experiment. As discussed above (section 2.3.1) Featherbed Moss and Alport Low did not share the same vegetation community composition. Featherbed Moss was uniformly dominated by *Eriophorum spp*. across the entire slope, whereas the increased slope angle and erosion on Alport Low meant that different vegetation microforms were dominant at different slope positions and between nested sub-slopes, such as between different gully interfluves on the upper mid-slope. Plots were positioned to account for this variation. Alport Low had more hummock forms with shrub vegetation along the slope and it was a broad aim that the plots along the Alport slope should reflect this. Specific *Eriophorum* plots were installed on the top-slope and bottom-slope alongside the hummock plots as vegetation at these slope positions most closely resembled that on Featherbed Moss.

2.3.2.2 Vegetation survey

Vegetation surveys were conducted between July and August 2011 when one year's data sampling on the study sites was complete. Quadrats were placed on each study plot (described below), with the gas collar in the centre of the quadrat. Dominant vegetation was recorded in each grid square (5x5 10 cm quadrat), whilst other species present were recorded as subdominant. Vegetation is used as a covariate in statistical analysis (section 2.3.6), accounted for as percentage dominance of *Eriophorum spp*.

2.3.2.3 Experimental plots

Study plots consisted of a uPVC gas collar 15 cm in diameter inserted less than five centimetres into the ground so as to minimise damage to the rhizosphere, a one metre uPVC dipwell inserted more than 75cm into the ground and a surface runoff trap (Figure 2.4). Later in the study further dipwells were added to some plots (see section 2.3.3.2). For the dipwells, holes were drilled into the dipwells every 10 cm to allow the inflow of water from surrounding peat and the water level in the dipwell to equilibrate with the surrounding peat, thus allowing an accurate measurement of WTD. Dipwells were open-ended and used to collect soil pore water. Runoff traps were closed with bungs at both ends to prevent inflow of soil pore water and precipitation. Holes were drilled in the runoff traps, which were inserted into the ground parallel to the hillslope until the holes sat flush with the ground surface to allow the inflow of water from across the ground surface. Chapter 5 discusses the water chemistry of soil pore water and surface runoff water and addresses issues regarding how distinct they are from one another and what they represent in terms of flowpaths.

Study plots were installed on Alport Low in May 2010 and a month later on Featherbed Moss owing to access restrictions during the nesting season. Plots were left for a minimum of

one month following installation to allow equilibration of the water table in the dipwells and for vegetation to recover from disturbance by installation of the gas collars. As such, sampling began on Alport Low in June 2010 and on Featherbed Moss in July 2010 and continued each month until June 2011 on both sites, when 12 months of data had been collected on Featherbed Moss.

Figure 2.4 Experimental plot set-up: A = infra-red gas analyser; B = chamber; C = gas collar; D = dipwell; E = surface water runoff trap

2.3.3 Field monitoring

2.3.3.1 Gaseous CO_2 flux

Carbon dioxide flux was measured using an infra-red gas analyser (IRGA – Figure 2.4). A dynamic closed-chamber method was used, a technique that is widely employed (Larsen et al., 2007, Ojanen et al., 2010, Pelletier et al., 2011) and allows detailed *in situ* measurement of CO_2 fluxes across small spatial scales. An EGM-4 IRGA (PP systems, Hitchin, UK) was attached

to an acrylic CPY-2 (PP Systems, Hitchin, UK) closed-canopy chamber. Prior to analysis, the IRGA conducted an internal calibration (repeated every 10 measurements) and the chamber was flushed between each measurement using an internal pump to return CO_2 levels in the detector loop and chamber to ambient concentrations. After flushing, the chamber was placed on the gas collar with a tight seal. Following a five second equilibration period, CO_2 concentration was recorded every 4 – 5 seconds for a period of 124 seconds. Ecosystem respiration (the combined total of autotrophic and heterotrophic respiration) was measured by placing an opaque shroud over the chamber to block any photosynthetically active radiation (PAR), thus preventing photosynthesis from occurring. Net ecosystem exchange (the overall balance between the simultaneous processes of P_G and R_{eco}) was recorded after R_{eco}, with air temperature and PAR measured concurrently with CO_2 concentration by probes inside the chamber.

Carbon dioxide concentration (ppmv) was converted into a flux of g CO_2 m^{-2} h^{-1} based upon the linear change in CO_2 concentration over time, using an automated spreadsheet, which was allowed to remove up to 25% of the data when necessary to improve the fit of the regression. This data removal was sometimes necessary if equilibration inside the chamber took longer than the equilibration period, causing a poor fit at the start of the measurement period. The conversion method was based upon the ideal gas law, from which the weight of CO_2 was calculated as outlined in equation 2.1 below:

$$G = 1 \times 10^6 [CO_2] V \left(\frac{p}{nRT}\right) m_r \quad (2.1)$$

Where: G = the mass of gas (g); $[CO_2]$ = the concentration of CO_2 (ppmv); V = the volume of the chamber (l); p = pressure (atm); n = the number of moles; R = the universal gas constant (l atm mol^{-1} K^{-1}); T = temperature (K); and m_r = the relative atomic mass (g mol^{-1}) of CO_2. The

mass of CO_2 was then converted into a flux based upon the change in CO_2 over time, having accounted for surface area.

Gross photosynthesis was derived by subtracting R_{eco} from the NEE flux, as it was not possible to directly monitor photosynthesis due to the simultaneous process of respiration. A negative sign convention was used to indicate sequestration of CO_2 from the atmosphere, indicating uptake of CO_2, with positive values indicating efflux of CO_2 to the atmosphere.

The relationship between plant productivity and respiration is well established. Raich and Schlesinger (1992) suggested that net primary productivity was correlated with soil respiration across multiple biomes, as heterotrophic respiration is driven by mineralisation of labile material produced during photosynthesis. This relationship is widely accepted (Janssens et al., 2001, Yuan et al., 2011, Caprez et al., 2012) and the inclusion of a dependency on gross primary productivity when modelling R_{eco} has been shown to improve the predictive capability of the model (Larsen et al., 2007, Migliavacca et al., 2011). However, the relationship between R_{eco} and P_G can be subject to self-correlation, as is the case with some of the studies listed above (Larsen et al., 2007). This is due to the partitioning of NEE to derive R_{eco} with P_G being estimated as the residual of NEE – R_{eco}. When using P_G to predict variation in R_{eco}, it has been argued that a shared component between the response and predictor datasets, in this case the R_{eco} term, leads to self-correlation (Vickers et al., 2009). This can lead to the identification of potentially spurious relationships (i.e. type I errors) between the two variables that do not exist in reality (Kenney, 1982).

So far in the literature discussions of self-correlation in CO_2 fluxes concern the partitioning of NEE into R_{eco} and P_G from eddy-covariance CO_2 flux data (Vickers et al., 2009, Lasslop et al., 2010a), with night time measurements of NEE (when no photosynthesis takes place) used to parameterise models of R_{eco}, which can then be used to derive P_G. It has been contended though that R_{eco} is not correlating to itself, but rather it is the error in the

estimation of R_{eco} that causes the issue (Lasslop et al., 2010a). Lasslop et al. (2010a) argue that because R_{eco} has been removed from NEE, it is not actually a component of P_G, but the error from the measurement of R_{eco} is nonetheless transferred into the estimate of P_G. As such it is proposed in Eq. (4) from Lasslop et al. (2010a) that the true value of estimated P_G is based on:

$$PG_{est} = Reco_{est} - NEE_{obs} = PG_{true} + \varepsilon Reco + \varepsilon NEE \quad (2.2)$$

Where: 'true' = the actual value of P_G based on estimated and observed ('est' and 'obs') R_{eco} and NEE and estimated P_G also includes the error terms for both R_{eco} and NEE, denoted by 'ε' (Lasslop et al., 2010a). Consequently, the overall potential for self-correlation has been overstated by Vickers et al. (2009), who mistakenly argue that there is no real relationship between R_{eco} and NEE.

Lasslop et al. (2010a) suggest that self-correlation can be minimised by using only night time data to derive R_{eco} and only daytime data for P_G to create quasi-independent datasets. This approach has been used in the literature to minimise the influence of self-correlation (Lasslop et al., 2010b, Migliavacca et al., 2011, Yuan et al., 2011). Furthermore, Migliavacca et al. (2011) found no significant differences between self-correlation corrected R_{eco}-P_G models and uncorrected models, indicating results were similar and the relationship between R_{eco} and P_G was the same regardless of self-correlation.

It was not possible to apply such correction methods using the dataset gathered in this thesis because CO_2 flux measurements in this study were not based on continuous readings throughout day and night, but on spot sample based chamber techniques. However, it must be noted that the advantage of chamber techniques is that R_{eco} is not derived from NEE, as it is with eddy-covariance techniques. Instead, R_{eco} is measured separately from NEE, but using the same method on the same collar. As such, R_{eco} and NEE can be considered to be quasi-independent of each other. As only the transferred error causes self-correlation, this can be

further minimised. Systematic error when measuring R_{eco} and NEE should be similar, as they are measured with the same protocols, so the error transferred from R_{eco} to P_G is most likely due to random error. Therefore, to minimise the impact of self-correlation the magnitude of the random error of R_{eco} relative to its true magnitude needs to be minimised.

This thesis employs measures to minimise the potential for errors in CO_2 flux datasets, in part by checking and removing if still incorrect, measured values which defy the micrometeorological sign convention employed reporting CO_2 fluxes in this thesis. Furthermore, given that self-correlation is associated with error, the larger R_{eco} and P_G values are likely to have a greater degree of error. As such, the removal of outlying values as detailed in section 2.3.6 acts as a further constraint on self-correlation. While data is being gathered all fluxes are measured using a standardised protocol on a regularly serviced IRGA which periodically self-calibrates. These measures together should minimise the potential for error within the dataset.

Nonetheless, it must be acknowledged that the degree to which self-correlation influences the relationship between R_{eco} and P_G cannot be estimated. Despite this, it has been argued that such correlations are legitimate when: "1) they satisfy the assumptions of the correlation analysis, 2) the variables are meaningful, that is, they represent concepts of interest and not just a component of them, and 3) the variables do not share a large error term" (Prairie and Bird, 1989). The relationship between rates of respiration and photosynthesis has been identified using non-chamber based methods, such as isotope pulse labelling techniques (Fenner et al., 2004, Crow and Wieder, 2005, Ward et al., 2009), whilst other studies have assessed the relationship between soil organic matter quality (Leifeld et al., 2012, Hardie et al., 2011), litter quality (Ward et al., 2010) and net primary production (Raich and Schlesinger, 1992, Bond-Lamberty et al., 2004) to rates of soil respiration. As such, given the measures outlined above to minimise errors and the physical interpretability of the

relationship between R_{eco} and P_G, this thesis shall use P_G as a covariate to explain variation in R_{eco}, as well as NEE. Given the steps taken to minimise errors in this dataset it seems likely the magnitude of any potential self-correlation will be small with respect to the expected magnitude of the real association between R_{eco} / NEE and P_G.

2.3.3.2 Water table depth & water collection

Whilst measuring carbon dioxide flux, WTD was measured simultaneously by inserting a conductivity probe into a dipwell until contact with the water surface was made. The value was corrected each month (in case of shrink/ swell) for the height of the dipwell that remained above the surface. The dipwell for Featherbed Moss lower mid-slope plot 1 was replaced in February 2011 as the dipwell had sunk below the ground surface. Soil pore water samples were collected from dipwells once all CO_2 flux measurements had been completed for a given plot, so as not to lower the water table during flux measurement. The time interval between completion of CO_2 flux measurements and soil pore water sampling was less than five minutes. Surface runoff water was collected from the runoff traps, which were emptied each month.

2.3.4 Water chemistry analysis

Prior to analysis, water samples were filtered at ≤0.45 µm to remove particulate matter using cellulose-acetate syringe-filters.

2.3.4.1 Basic water chemistry measurements

Electrode methods were used to analyse pH (HI-9025, Hanna Instruments) and electrical conductivity (HI-9033). UV-visible absorbance measurements were made using a Jenway 6505 UV/Vis. Spectrophotometer at 400, 465 and 665 nm wavelengths. Measurements made at 400 nm (Abs_{400}) were used to derive a basic colour reading for water samples, whilst measurements at 465 and 665 nm determined the E4:E6 ratio. The E4:E6 ratio can be used to infer information regarding the composition of DOC present in the sample, by inferring the degree of humification of the sample. More mature humic acids are indicated by lower E4:E6 ratios, with high ratios indicative of fulvic acids (Thurman, 1985). Specific absorbance was established by dividing Abs_{400} by DOC concentration.

2.3.4.2 Dissolved organic carbon

Dissolved organic carbon concentration was determined using a colourimetric method (Bartlett and Ross, 1988). Mn(III) is reduced by organic carbon present in water samples when concentrated sulphuric acid is added (Bartlett and Ross, 1988), leading to a loss of colour which is observed by measuring absorbance at 495 nm. A suite of oxalic acid standards (0, 7.5, 15, 30, 60 mg C l^{-1}) were used to determine a calibration curve of organic carbon against absorbance at 495 nm, whilst calibration blanks were run approximately every 12 samples. Because the method has an upper detection limit of 60 mg C l^{-1}, samples were typically diluted four times owing to the high colour levels of soil pore water samples. The precision of the 0 mg C l^{-1} standards was occasionally poor, with absorbance values sometimes close to those of the 7.5 mg C l^{-1} standard. Because two standards at each concentration were analysed, the 0 mg C l^{-1} standard with an absorbance in the range of the 7.5 mg C l^{-1} standards was removed from the calibration (as it had deviated from the line defined by the other standards). Deletion of a single 0 mg C l^{-1} standard was done on four occasions (Table 2.4).

The accuracy of the calibration reduced as it approached the intercept, meaning that concentrations approaching 0 mg C l^{-1} may not have been accurate as they were below the limit of detection. Detection limits were determined for DOC analysis based upon the last recorded absorbance value where the lower confidence limit of a given DOC concentration was still positive. Absorbance values that caused a negative DOC value on the lower confidence limit were rejected and no DOC data recorded (Table 2.4).

*Table 2.4 DOC calibration R^2 and detection limits: *denotes deletion of a 0 mg C l^{-1} standard; LCL = lower confidence limit; UCL = upper confidence limit*

Date	R^2	Abs Limit	DOC mg C l^{-1} Limit	LCL	UCL
June 2010	99.7	0.265	1.147	0.180	2.749
09/08/2010	99.3	0.271	2.174	0.172	2.174
07/09/2010	99.3	0.251	2.204	0.136	4.272
06/10/2010*	99.7	0.268	1.643	0.011	3.275
03/11/2010*	99.0	0.249	2.840	0.112	5.567
25/11/2010	99.3	0.249	2.112	0.130	4.093
13/01/2011	99.6	0.251	1.475	0.010	2.940
15/02/2011	99.7	0.257	1.466	0.208	2.723
02/03/2011*	99.9	0.279	1.156	0.084	2.228
22/03/2011	99.5	0.240	1.956	0.203	3.709
18/04/2011	99.0	0.259	2.436	0.071	4.802
03/06/2011*	99.5	0.245	1.916	0.019	3.813
13/06/2011	98.1	0.232	3.480	0.240	6.720
Mean	**99.4**	**0.255**	**2.000**	**0.121**	**3.774**

2.3.4.3 Anion concentrations

Anion concentrations of F^-, Br^-, NO_3^-, PO_4^{3-}, Cl^- and SO_4^{2-} were measured using ion chromatography. A Metrohm 761 Compact IC connected to an 813 Compact Auto-sampler was used. Samples were calibrated against standards of 1.25, 2.5, 5 and 10 mg l^{-1} using linear calibration curves, with blanks run prior to and following the standards. Further blanks were

run between each slope position (approximately every 12 samples). A flat baseline was maintained with an eluent solution of sodium carbonate and sodium hydrogen carbonate, using a suppressor module. The IC column was maintained by periodically running a cleaning solution that was 10 x the concentration of the eluent.

2.3.5 Analysis of LiDAR terrain parameters

The LiDAR data of Bleaklow and Kinder Scout was used to derive terrain parameters including slope angle, aspect, altitude and wetness index for the two study sites. Terrain Analysis System (TAS), an open-source GIS package (Lindsay, 2005), was used to ascertain the terrain indices listed above. The LiDAR data had undergone object removal by the Environment Agency (Evans and Lindsay, 2010a), whilst pre-processing was carried out prior to analysis of the LiDAR digital elevation model (DEM), using the Impact Reduction Approach recommended by Lindsay and Creed (2005) to remove artefact depressions in the data. Slope and aspect were measured in degrees, whilst wetness index (equation 2.3) was used as a measure for the propensity to saturation across the hillslope, accounting for topographic setting using slope and specific catchment area contributing water supply to a given cell. The wetness index was calculated as:

$$WI = \ln \frac{As}{\tan S} \tag{2.3}$$

Where: *As* = specific catchment area; and *S* = slope. Three flow algorithms available in TAS were tested: D8, FD8 and FD8-Quinn. The FD8 flow algorithm was ultimately selected for use as the D8 flow algorithm is a single flow direction algorithm, whilst the FD8 flow algorithm does allow for dispersal of flow in multiple directions, which can be more appropriate on hillslopes. There was little difference between FD8 and FD8-Quinn. A *p* value (which determines the degree of divergence) of 1.1 was used for the FD8 flow algorithm, as

recommended by Freeman (1991). The terrain parameters were determined for each nested sub-slope (section 2.3.2.1) using an average value from the cell containing the location of the sub-slope and the surrounding cells (9 cells including the central sub-slope cell). Terrain parameters can be used to account for the effect of various factors (Table 2.5) that could influence WTD, rates of CO_2 flux and DOC concentration.

Table 2.5 Terrain indices adapted from table 2 Wilson (2012)

Parameters	Type	Significance
Elevation	Local	Climate, vegetation, potential energy
Slope	Local	Precipitation, overland/subsurface flow velocity and runoff rate, soil water content
Aspect	Local	Flow direction, solar insolation, evapotranspiration, flora and fauna distribution and abundance
Wetness index	Regional	Spatial distributions and extent of zones of saturation (i.e. variable source areas) for runoff generation as a function of upslope contributing area, soil transmissivity and slope

2.3.6 Statistical analysis

Prior to statistical analysis, each dataset was checked for outlying values and a number of statistical tests performed to test the required assumptions in the dataset that analysis of variance (ANOVA) required. Values beyond three standard deviations of the mean were removed as they represented extreme outlying values. This was a conservative approach that removed only a small percentage of data and improved dataset distribution. Details of the percentage data removed for each ANOVA dataset is provided in section 2.4. For R_{eco}, negative data points (representing a CO_2 sink) were removed; similarly positive P_G values indicating a source of CO_2 were removed. Values below the limit of detection for soil pore water and runoff water DOC concentrations were also removed.

2.3.6.1 Analysis of variance and covariance

It is an assumption of ANOVA that the datasets used are normally distributed, however the test is robust with some departure from normality (Rutherford, 2001, Schmider et al., 2010). The Anderson-Darling test was used to determine the distribution of each dataset; if there was a non-normal distribution, the data was natural-log transformed. Levene's test was performed to test the assumption of homogeneity of variances (equal distribution of error between factor levels), on both untransformed and log transformed data. Most variables passed Levene's test, but even when log transformed, many datasets were non-normal. As ANOVA is robust against the assumptions of normality (Rutherford, 2001, Schmider et al., 2010), statistical analyses were conducted on the untransformed or transformed datasets that had the lowest Anderson-Darling statistics (i.e. were closest to a normal distribution); this was done to minimise the departure from normality, as recommended by Rutherford (2001). As a further check against the assumptions of normality, the nonparametric Kruskal-Wallis test was conducted alongside ANOVA to test for significant factors.

The lowest Anderson-Darling statistic was used as the selection criteria for the inclusion of covariates. The only datasets which were not log transformed were WTD, NEE, pH and NO_3^-; this was because WTD and NEE contained values above and below zero, pH is already a logarithm and as discussed below, NO_3^- concentrations were unlogged to allow a larger *N* (as zero values are removed by logging) for analysis of covariance (ANCOVA).

Analysis of variance was undertaken using a General Linear Modelling approach. Backwards modelling was applied, incorporating all relevant factors (and covariates in ANCOVA) and dropping out insignificant variables one-by-one until a model with only significant variables was constructed for backwards modelling. For ANCOVA, forwards modelling of covariates from the accepted ANOVA modelling was also applied. The most physically interpretable model was then used. The factorial research design (section 2.3.2.1)

allowed testing of significant differences for site, slope, sub-slope, month and interaction effects between factors. This approach meant that the impact of slope position could be tested having accounted for the influence of other factors in the model.

Analysis of variance identified whether a factor had a significant influence upon a dependent variable; ANCOVA was used to explain why there may be an effect by accounting for the influence of covariates (e.g. air temperature) on the dependent variable. Tukey's *post hoc* pairwise comparisons was used to identify the locations of the significant differences identified between factor levels (e.g. with slope position, whether top-slope, upper mid-slope, lower mid-slope and bottom-slope were significantly different from each other). The list of covariates used for a given response variable is provided in Table 2.6. For ANCOVA on DOC concentration, only anions that could have an effect upon DOC concentration and were non-zero mg l^{-1} more than fifty per cent of the time were included. However, if there was a large percentage of 0 mg l^{-1} data included, as with NO_3^- concentrations, the untransformed data was used regardless of its distribution to allow analysis of a larger number of samples overall.

Table 2.6 Covariates used in ANCOVA: %E = % Eriophorum spp. dominance; TPs = terrain parameters (slope angle, wetness index and altitude)

WTD	R_{eco}	NEE	P_G	DOC	Runoff DOC	Water chemistry
% E	% E	% E	% E	% E	% E	% E
AT	WTD	WTD	WTD	WTD	pH	WTD
TPs	AT	AT	AT	AT	Conductivity	AT
	P_G	P_G	PAR	pH	E4:E6	TPs
	TPs	PAR	TPs	Conductivity	Cl^-	
		TPs		E4:E6	SO_4^{2-}	
				Cl^-	NO_3^-	
				SO_4^{2-}	TPs	
				NO_3^-		
				TPs		

Analysis of variance was also applied to datasets of relative R_{eco}, P_G and DOC to determine how the magnitude of the response variable at a given hillslope position varied relative to the top-slope. On a monthly basis, individual plot measurements were indexed to the average value of the site (Featherbed Moss or Alport Low) top-slope plots for each response variable to more easily visualise relative differences between slope positions. On Alport Low, in order to maximise comparability, the top-slope *Eriophorum spp*. plots' average was used as the basis to determine the relative value of the response variable at the bottom-slope *Eriophorum spp*. plots. Covariates were not included in the analysis given the top-slope average (one) did not vary in relation to a given covariate. NEE and WTD were excluded from relative datasets as they had both positive and negative values and the effect size would have a large degree of variation.

For ANOVA and ANCOVA analysis, the proportion of variation in the response variable that is explained by a given factor or covariate can be determined by using the generalised omega squared statistic (ω^2). The method of calculation employed in this thesis is that of Olejnik and Algina (2003), as outlined below:

$$\omega^2 = \frac{(Seq\ SS_a - df_a \times AdjMS_{error})}{(Seq\ SS_{tot} + AdjMS_{error})} \quad (2.4)$$

Where: $Seq\ SS_a$ = the sequential sum of squares for a given factor or covariate; df_a = the degree of freedom for the given factor or covariate; $AdjMS_{error}$ = the adjusted mean square error; and $Seq\ SS_{tot}$ = the sequential sum of squares total. This calculates the proportion of variance explained by each factor and covariate but it is a different statistic and method to the coefficient of determination (R^2) that states the total variation explained in a model. As such, R^2 and ω^2 values will not be exactly the same.

2.3.6.2 Multiple linear regression

Multiple linear regressions (MLR) were performed to determine how models predicting variation in a given response (dependent) variable changed with hillslope position. Modelling was performed on amalgamated datasets and on separate datasets for each slope position. The inclusion of independent predictive variables (covariates – Table 2.6) in the models was guided by results from ANCOVA. Seasonality, which was treated as a factor in ANOVA models, was incorporated into the MLR framework as sin and cos functions (Eq.2.5), varying with month:

$$sin\left(\frac{\pi m}{6}\right) and \cos\left(\frac{\pi m}{6}\right) \quad (2.5)$$

Where: m = the month number (January = 1 to December = 12). The reciprocal of air temperature (1/T – K) was incorporated into the model, as the gradient of the linear relationship with $\ln(R_{eco})$ can be used to account for that flux's activation energy (Lloyd and Taylor, 1994). A backwards and forwards modelling approach was applied, as with ANCOVA, to select the most appropriate model. As with ANOVA and ANCOVA, datasets were checked for outlying values and non-normal distributions.

2.3.6.3 Runoff occurrence

The frequency of runoff occurrence was assessed using the χ^2 test, adopting the approach of Fleiss et al. (2003), which was used by Clay et al. (2009a). Runoff was observed to have occurred when a sufficient volume of sample to conduct water chemistry analyses was collected in the runoff traps. A ratio could then be determined for each slope position based on the number of times runoff was observed against the total possible number of times it could have occurred. As such, values for each slope position were corrected for instances

when it was not possible to collect a sample. For example, sheep were often grazing around the bottom-slope plots on Alport Low and would remove bungs from the top of the runoff traps. It was not possible to determine whether water in the runoff traps was the result of surface runoff or precipitation inputs. Consequently such samples were excluded from the analysis and were not analysed for water chemistry either.

The test statistic was generated from the difference between the proportion of runoff observed for each slope position and the proportion of runoff observed across all hillslope positions combined. The test statistic was calculated as:

$$\chi^2 = \frac{1}{\bar{p}\,\bar{q}} \sum_{i=1}^{m} n_i.(p_i - \bar{p})^2 \quad (2.6)$$

Where: $\bar{p}$ = the overall proportion of runoff; $\bar{q}$ = 1 - $\bar{p}$; n_i = the number of possible observations; and p_i = the proportion of observed runoff (with characteristic) for a given slope position. Using the method of Fleiss et al. (2003), *post hoc* testing was applied to determine which slope positions (if any) lead to a significant difference observed in the proportion of runoff frequency.

2.4 Results

Table 2.7 shows the percentage of data as outlying values removed from the ANOVA and ANCOVA datasets. Individual results for ANOVA and ANCOVA state whether datasets were untransformed or log transformed. The maximum number of data points removed was 15, for soil pore water pH, which amounted to 2.09% of the data.

Table 2.7 Percentage data removed from each variable used in ANOVA/ANCOVA: SPW = soil pore water; RO = runoff water

Variable	Dataset	N	N removed	% removed
WTD	WTD	711	4	0.56
LnR_{eco}	CO_2 flux	645	1	0.16
LnP_G	CO_2 flux	593	5	0.84
NEE	CO_2 flux	667	10	1.50
Air temperature	Environmental	679	0	0.00
1/T	Environmental	679	9	1.33
PAR	Environmental	640	1	0.16
DOC	SPW	688	5	0.73
	RO	518	9	1.74
Abs_{400}	SPW	716	2	0.28
	RO	578	1	0.17
Specific absorbance	SPW	688	4	0.58
	RO	516	0	0.00
E4:E6	SPW	709	9	1.27
	RO	529	10	1.89
pH	SPW	716	15	2.09
	RO	552	0	0.00
Conductivity	SPW	715	7	0.98
	RO	532	2	0.38
Cl^-	SPW	704	2	0.28
	RO	539	9	1.67
SO_4^{2-}	SPW	689	9	1.31
	RO	528	4	0.76
NO_3^-	SPW	704	12	1.70
	RO	539	8	1.48

*Table 2.8 Percentage data removed from each variable used in MLR by slope position: * = unlogged P_G used in NEE MLR*

Slope	Variable	N	N removed	% removed	Variable	N	N removed	% removed	Variable	N	N removed	% removed
Top-slope	WTD	216	0	0.00	AT	213	0	0.00	pH	224	3	1.34
Upper mid-slope		140	0	0.00		129	0	0.00		140	3	2.14
Lower mid-slope		142	0	0.00		135	0	0.00		145	4	2.76
Bottom-slope		213	3	1.41		202	0	0.00		207	6	2.90
Top-slope	LnR_{eco}	200	0	0.00	1/T	213	0	0.00	LnConductivity	224	0	0.00
Upper mid-slope		123	1	0.81		129	0	0.00		139	2	1.44
Lower mid-slope		127	0	0.00		135	0	0.00		145	2	1.38
Bottom-slope		195	1	0.51		202	0	0.00		207	3	1.45
Top-slope	LnP_G	184	1	0.54	LnPAR	194	0	0.00	NO_3^-	225	6	2.67
Upper mid-slope		116	2	1.72		122	1	0.82		139	4	2.88
Lower mid-slope		120	8	6.67		131	1	0.76		140	2	1.43
Bottom-slope		173	4	2.31		193	0	0.00		200	4	2.00
Top-slope	PG*	184	3	1.63	DOC	222	4	1.80				
Upper mid-slope		116	2	1.72		137	0	0.00				
Lower mid-slope		120	5	4.17		140	0	0.00				
Bottom-slope		174	2	1.15		189	1	0.53				
Top-slope	NEE	207	4	1.93	LnE4:E6	222	1	0.00				
Upper mid-slope		128	2	1.56		138	1	0.00				
Lower mid-slope		135	4	2.96		144	2	1.39				
Bottom-slope		197	2	1.02		205	5	2.44				

Table 2.8 shows the percentage of data removed from datasets for individual slope positions used in MLR. The maximum number of data points removed was eight, meaning 6.67% of lower mid-slope LnP_G data was removed. Lower mid-slope unlogged P_G (used for the NEE regression, section 2.4.2.3) had the next highest percentage of data removed (4.17%), while all other datasets had <3% of data removed as outlying values.

As stated in section 2.3.6.1, the non-parametric Kruskal-Wallis test was used to identify whether slope position was significant when the dataset of a response variable failed the assumption of normality. Kruskal-Wallis results are only reported when they disagree with ANOVA results.

2.4.1 Hydrology

2.4.1.1 Water table depth

Raw WTD data indicated that the upper and lower mid-slope experienced water table drawdown relative to the top-slope and bottom-slope, which both had median WTDs <50 mm from the surface (Figure 2.5). At some point during the year of analysis, all hillslope positions had WTDs saturated above the surface (Table 2.9), whilst the maximum observed WTD on the upper and lower mid-slope (-840 mm and -706 mm respectively) was considerably greater than those observed at the top-slope (-489 mm) and bottom-slope (-363 mm).

Table 2.9 Descriptive statistics for response variables: SE = standard error

Variable	Slope	N	Mean	SE Mean	Maximum	Minimum
WTD (mm)	Top-slope	216	-106	9	-489	65
	Upper Mid-slope	140	-300	20	-840	25
	Lower Mid-slope	142	-220	20	-706	31
	Bottom-slope	213	-56	5	-363	80
R_{eco} (g CO_2 m^2 h^{-1})	Top-slope	200	0.19	0.01	1.367	0.010
	Upper Mid-slope	123	0.23	0.02	0.748	0.011
	Lower Mid-slope	127	0.23	0.02	1.075	0.017
	Bottom-slope	195	0.20	0.01	1.454	0.006
NEE (g CO_2 m^{-2} h^{-1})	Top-slope	207	-0.09	0.02	0.699	-0.852
	Upper Mid-slope	128	-0.09	0.02	0.495	-0.975
	Lower Mid-slope	135	-0.13	0.03	0.434	-1.883
	Bottom-slope	197	-0.16	0.02	0.800	-1.886
P_G (g CO_2 m^{-2} h^{-1})	Top-slope	184	-0.31	0.03	-1.917	-0.002
	Upper Mid-slope	116	-0.35	0.03	-1.630	-0.004
	Lower Mid-slope	120	-0.38	0.04	-2.343	-0.004
	Bottom-slope	174	-0.41	0.03	-2.579	0.000
Soil pore water DOC (mg C l^{-1})	Top-slope	222	105	4	278.0	4.6
	Upper Mid-slope	137	107	6	275.3	8.3
	Lower Mid-slope	140	87	5	260.7	7.7
	Bottom-slope	189	73	3	217.7	4.6
Runoff water DOC (mg C l^{-1})	Top-slope	159	83	5	272.8	5.9
	Upper Mid-slope	91	89	6	266.5	6.8
	Lower Mid-slope	104	80	6	275.9	3.5
	Bottom-slope	164	77	4	262.6	5.1

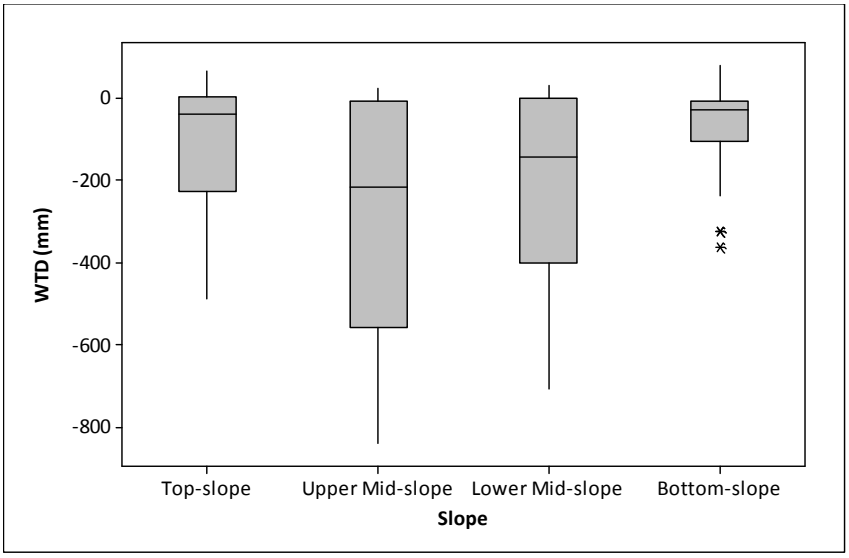

Figure 2.5 Boxplot of median WTD by slope

Results from ANOVA (R^2 = 88.79%, Table 2.10) indicated that site, slope position, sub-slope and month were all significant factors explaining variation in WTD. The ANOVA error terms is not shown; although it includes measurement error, it also includes unexplained factors and interactions. Because the coefficient of determination is high in the WTD ANOVA the error term in this instance is low due to the high amount of variance explained by factors in the model, and is most likely caused by measurement error.

Table 2.10 WTD ANOVA / ANCOVA: ω^2 = % variance

WTD ANOVA			WTD ANCOVA		
Factor	**P**	**ω^2**	**Factor / covariate**	**P**	**ω^2**
Site	<0.0001	22.68%	Slope angle	<0.0001	52.55%
Slope	<0.0001	30.32%	Wetness index	<0.0001	0.24%
Sub-slope	<0.0001	3.92%	Site	<0.0001	2.09%
Month	<0.0001	5.11%	Slope	<0.0001	6.34%
Site*Slope	<0.0001	26.52%	Sub-slope	<0.0001	7.34%
Site*Month	0.010	0.22%	Month	<0.0001	4.99%
			Site*Slope	<0.0001	15.56%
			Site*Month	0.007	0.23%
N 707		**R^2 88.79%**	**N 707**		**R^2 89.35%**

Slope position explained the most variation (p <0.0001 ω^2 = 30.32%) and the main effects plot (Figure 2.6) indicated that mean WTD for top-slope, upper mid-slope, lower mid-slope and bottom-slope was -144, -303, -208 and -46 mm respectively. *Post hoc* testing revealed that all hillslope positions had a significantly different WTD from one another. Site (p <0.0001) explained 22.68% of variation in WTD, which was significantly deeper on Alport Low than Featherbed Moss. Consequently, there was a significant interaction between site and slope (Figure 2.6), revealing a more complex dynamic between hillslope position and WTD than was apparent solely from the main effects output. On Featherbed Moss, mean WTD was deepest on the top-slope (-162 mm), but was generally close to the surface across all hillslope

positions. Alport Low experienced drawdown patterns more akin to those of the main effects output, albeit with greater variation. WTD on the upper mid-slope (-558 mm) and lower mid-slope (-400 mm) was deeper than the main effects mean but was broadly similar on the top and bottom-slope. Month ($p < 0.0001$, $\omega^2 = 5.11\%$) indicated a significant drawdown was observed in April and June.

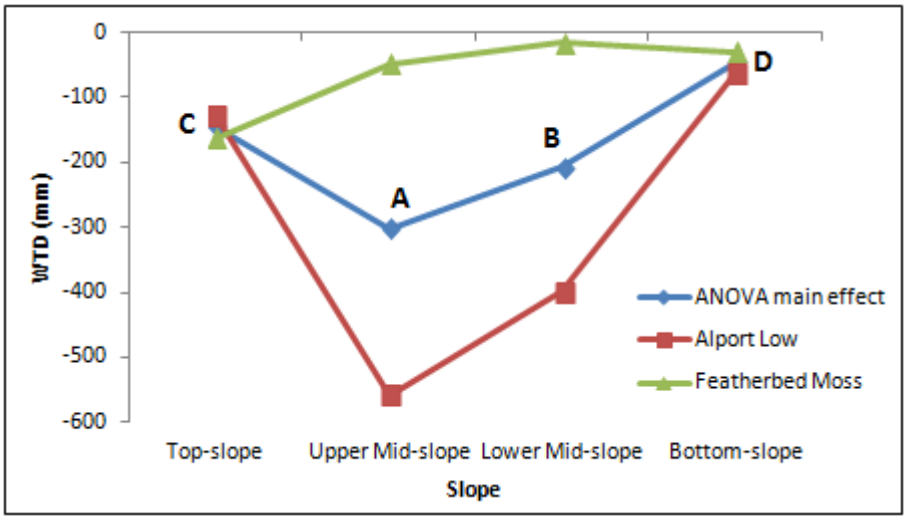

Figure 2.6 WTD ANOVA main effects & interaction plot: significant differences denoted where letters are not shared between slope positions

The ANCOVA model did not increase the predictive ability of the model a great deal ($R^2 = 89.35\%$, Table 2.10), but covariates did account for some of the variation in WTD caused by the ANOVA factors. Slope angle ($p < 0.0001$ $\omega^2 = 52.55\%$) and wetness index ($p < 0.0001$ $\omega^2 = 0.24\%$) were significant, with slope angle of particular importance. Figure 2.7 showed an increase of 150 mm in WTD at the top-slope relative to the ANOVA main effects model. There was a smaller increase towards the surface on the bottom-slope. The top-slope and bottom-

slope were no longer significantly different having accounted for the influence of slope angle and wetness index.

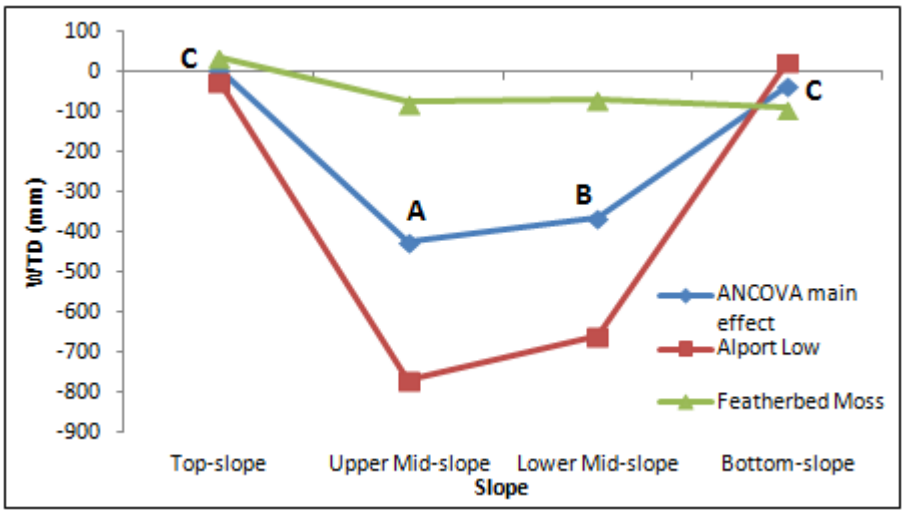

Figure 2.7 WTD ANCOVA main effects & interaction plot: significant differences denoted where letters are not shared between slope positions

Multiple linear regression modelling was used to see whether the covariates varied with hillslope position. Table 2.11 showed that for the entire dataset there was a seasonal cycle to WTD, represented by the sin and cos monthly values. Slope had a negative correlation to WTD; an increase in slope angle increased WTD. No significant relationship with wetness index was found, in contrast to the ANCOVA model, suggesting a weak relationship between WTD and wetness index in this dataset. Slope angle was significant on the top-slope and bottom-slope, yet had a positive correlation with WTD. The lack of variation in slope angle on the top-slope and bottom-slope (Table 2.2 and Table 2.3) caused an unrealistic relationship between slope angle and WTD. Wetness index could be more appropriate on flatter slopes where the propensity of saturation based upon not only slope angle but also source area is

accounted for. Given the weak relationship between WTD and wetness index though, this is speculative and cannot be confirmed.

Analysis of the residuals for the two mid-slopes indicated two distinct patterns – one for Featherbed Moss, the other for Alport Low. This reflected the importance of accounting for differences with study site when modelling WTD. Slope angle had a significant negative relationship on the upper-midslope with WTD, whilst larger wetness index values had a positive effect upon WTD. Slope angle was not significant on the lower midslope; instead wetness index explained the differences in WTD.

Table 2.11 WTD MLR: Sin M and Cos M = sin and cos values by month; SE = standard error

Slope	Predictor	Coeff	SE Coeff	P value
All data	Constant	90	10	<0.0001
	Sin M	-18	7	0.013
	Cos M	39	7	<0.0001
R^2 = 54.8%	Slope angle	-51	2	<0.0001
Top-slope	Constant	-800	100	<0.0001
	Cos M	40	10	<0.0001
	Slope angle	31	8	<0.0001
R^2 = 20.2%	Wetness index	110	17	<0.0001
Upper mid-slope	Constant	3700	200	<0.0001
	Cos M	36	10	<0.0001
	Slope angle	-161	5	<0.0001
R^2 = 91.7%	Wetness index	-430	20	<0.0001
Lower mid-slope	Constant	-2030	80	<0.0001
	Sin M	-40	10	0.004
	Cos M	30	10	0.023
R^2 = 80.7%	Wetness index	260	10	<0.0001
Bottomslope	Constant	-190	30	<0.0001
	Sin M	-21	5	<0.0001
	Cos M	45	5	<0.0001
	Slope angle	20	6	0.001
R^2 = 36.5%	Wetness index	12	4	0.001

2.4.1.2 Runoff occurrence

Runoff was assessed using the χ^2 test (Table 2.12). The largest proportion of observed runoff was on the lower mid-slope at 0.921. The proportion of runoff was similar on the top-slope (0.841) and bottom-slope (0.864), but the upper mid-slope was lower (0.708). The difference in runoff proportion across the hillslope was significant (χ^2 25.97, p <0.0001). *Post-hoc* testing indicated that the upper and lower mid-slopes were significantly different in their runoff frequency, though the greater proportion of observed runoff on the lower mid-slope was not significantly different from the top-slope or bottom-slope.

Table 2.12 Chi-squared results for runoff (RO) occurrence by slope

Slope	Expected RO	Observed RO	RO Proportion
Top-slope	220	185	0.841
Upper Mid-slope	144	102	0.708
Lower Mid-slope	140	129	0.921
Bottom-slope	214	185	0.864
TOTAL	718	601	0.837
χ2 = 25.97			**P <0.0001**

2.4.2 Gaseous fluxes

2.4.2.1 R_{eco}

The lowest median rate of R_{eco} (Figure 2.8) was at the top-slope (0.133 g CO_2 m^{-2} h^{-1}), with the highest rate on the lower mid-slope (0.174 g CO_2 m^{-2} h^{-1}). This was corroborated by the mean values, which similarly show the highest rates of R_{eco} on the mid-slope positions (Table 2.9). The maximum rate of R_{eco} recorded was on the bottom-slope in June 2010 (1.454 g CO_2 m^{-2} h^{-1}).

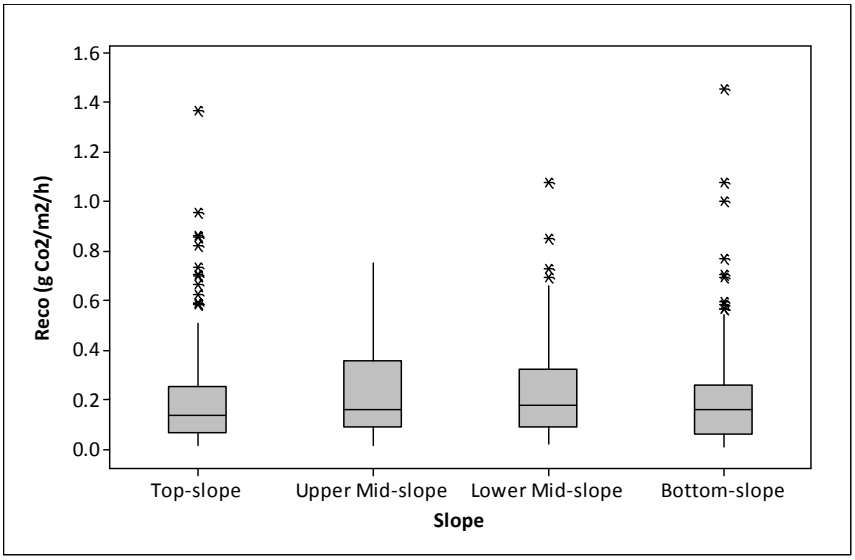

Figure 2.8 Boxplot of median R_{eco} by slope

ANOVA (Table 2.13) indicated month ($p < 0.0001$, $\omega^2 = 44.28\%$) was the largest control on the rate of R_{eco}. There was a strong seasonal cycle, with significantly higher rates of R_{eco} typically occurring between May – September, while winter months had much lower rates of R_{eco}. Sub-slope ($p < 0.0001$, $\omega^2 = 5.74\%$) was significant, as was slope ($p = 0.004$, $\omega^2 = 1.25\%$). A further 1.51% was explained by the interaction between slope and month ($p = 0.016$). The main effects plot (Figure 2.9) indicated R_{eco} was significantly lower on the bottom-slope (0.113 g CO_2 m^{-2} h^{-1}) relative to the upper mid-slope (0.145 g CO_2 m^{-2} h^{-1}) and lower mid-slope (0.142 g CO_2 m^{-2} h^{-1}). There were no significant differences between Alport Low and Featherbed Moss. Given that sub-slope had a higher ω^2 than slope it suggested slope position was not as important as local scale heterogeneity.

Results from Kruskal-Wallis (Table 2.14) suggested that slope was significant ($p = 0.038$) but although the z statistic indicated that both top-slope and bottom-slope had lower rates of R_{eco} than the median value, R_{eco} was lowest on the top-slope. It must be noted that the Kruskal-Wallis test is limited compared to ANOVA, given that the effects caused by other

significant factors cannot be accounted for when deriving the overall influence caused by slope position. It could be that the heterogeneity across peatlands, to some degree assessed using sub-slope in the ANOVA model, explained the differences between the two techniques.

Table 2.13 CO_2 flux ANOVA / ANCOVA: ω^2 = % variance

LnR_{eco} ANOVA			**LnR_{eco} ANCOVA**		
Factor	**P**	**ω^2**	**Factor / Covariate**	**P**	**ω^2**
Slope	0.004	1.25%	WTD	0.001	6.13%
Sub-slope	<0.0001	5.74%	LnP_G	<0.0001	43.24%
Month	<0.0001	44.28%	Wetness index	<0.0001	0.28%
Slope*Month	0.016	1.51%	Slope	0.008	0.03%
			Sub-slope	<0.0001	2.57%
			Month	<0.0001	13.54%
N 644		**R^2 52.82%**	**N 565**		**R^2 65.83%**
LnP_G ANOVA			**LnP_G ANCOVA**		
Factor	**P**	**ω^2**	**Factor / Covariate**	**P**	**ω^2**
Slope	0.013	1.36%	WTD	0.005	3.59%
Month	<0.0001	39.90%	1/T	<0.0001	32.12%
			LnPAR	<0.0001	4.37%
			Altitude	0.014	0.32%
			Month	<0.0001	11.62
N 588		**R^2 41.30%**	**N 547**		**R^2 52.06%**
NEE ANOVA			**NEE ANCOVA**		
Factor	**P**	**ω^2**	**Factor / Covariate**	**P**	**ω^2**
Slope	0.007	1.29%	*% Eriophorum spp.*	<0.0001	1.61%
Month	<0.0001	17.46%	LnP_G	<0.0001	45.02%
			LnPAR	<0.0001	1.85%
			Slope angle	0.001	0.67%
			Month	<0.0001	5.37%
N 657		**R^2 18.78%**	**N 553**		**R^2 54.55%**

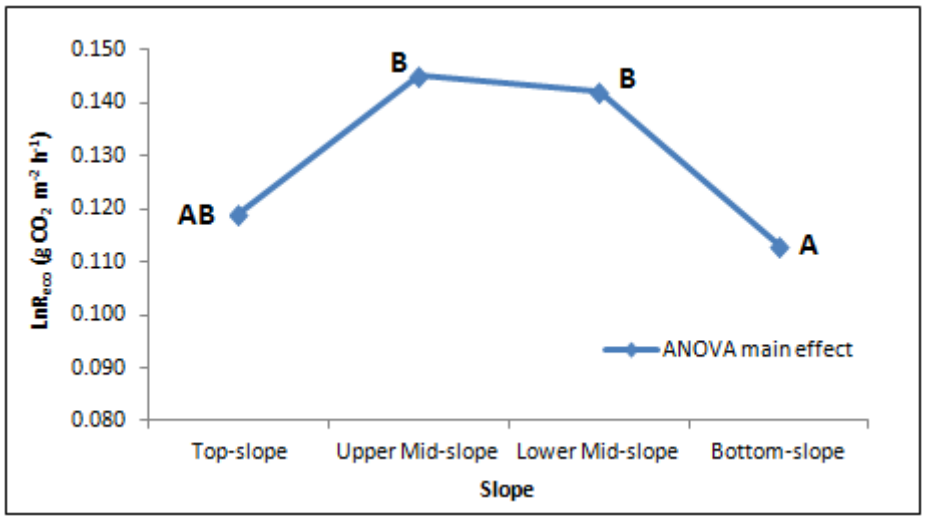

Figure 2.9 LnR$_{eco}$ ANOVA main effects plot: significant differences denoted where letters are not shared by slope positions

Table 2.14 LnR$_{eco}$ Kruskal-Wallis results

Slope	N	Median	Ave Rank	Z
Top-slope	200	-2.017	298.7	-2.18
Upper Mid-slope	123	-1.845	347.8	1.68
Lower Mid-slope	127	-1.749	348.4	1.75
Bottom-slope	194	-1.864	314.0	-0.76
Overall	644		322.5	
H = 8.41		**DF = 3**		**P = 0.038**

ANCOVA analysis (Table 2.13) improved the predictive capability of the model (R^2 = 65.83%), with WTD (p = 0.001, ω^2 = 6.13%), P_G (p <0.0001, ω^2 = 43.24%) and wetness index (p <0.0001, ω^2 = 0.28%) significant covariates. WTD had a negative correlation to R_{eco}, suggesting that as the water table gets deeper, the rate of R_{eco} increases. Wetness index had a minimal effect upon R_{eco}. Gross photosynthesis was the most important covariate and inclusion of it in the model accounted for the influence of temperature due to co-linearity.

Month ($p < 0.0001$, $\omega^2 = 13.54\%$) was significant, though some of the significant differences in R_{eco} between months in the ANOVA model were accounted for by covariates. Sub-slope ($p < 0.0001$, $\omega^2 = 2.57\%$), as with the ANOVA model, explained more variation than slope ($p = 0.008$, $\omega^2 = 0.03\%$), which was almost fully explained by the covariates. Regression analysis could therefore explain how the response of R_{eco} to the covariates differs across the slope.

ANOVA of relative (to the top-slope) R_{eco} (Table 2.15, $R^2 = 49.93\%$), indicated relative R_{eco} was significantly higher across all other slope positions than the top-slope. No significant difference was found between top-slope and bottom-slope from R_{eco} ANOVA, but bottom-slope relative R_{eco} had a mean from the main effects (Figure 2.10) of 1.45 - indicating that R_{eco} was 45% higher than on the top-slope. The upper mid-slope had the highest ratio (1.59), with the lower mid-slope (1.51) also higher than the bottom-slope. The mid-slopes were not significantly different from the bottom-slope, in contrast to the ANOVA results and the relative data better reflected the results of the Kruskal-Wallis test (Table 2.14). Site ($p = 0.001$, $\omega^2 = 4.61\%$) was found to be significant with the relative data, in contrast to R_{eco} itself, as relative R_{eco} was greater on Featherbed Moss. The interaction between site and slope ($p = 0.012$, $\omega^2 = 1.34\%$) explained more variation in relative R_{eco} than slope itself ($p = 0.001$, $\omega^2 = 0.84\%$), with a large increase in relative R_{eco} on the upper mid-slope of both study sites, but little difference between the Alport Low top-slope and lower mid-slope. Relative R_{eco} was significantly higher in August than all other months, though much of the data on Alport Low was missing for this month due to equipment failure. No significant slope effect was found for relative R_{eco} data by the Kruskal-Wallis test (Table 2.16).

Table 2.15 Relative CO_2 flux ANOVA: ω^2 = % variance

Ratio R_{eco}			Ratio P_G		
Factor	**P**	**ω^2**	**Factor**	**P**	**ω^2**
Site	0.001	4.61%	Site	0.007	1.39%
Slope	0.001	0.84%	Slope	0.005	2.31%
Sub-slope	<0.0001	3.57%	Sub-slope	0.003	1.62%
Month	<0.0001	20.76%	Month	<0.0001	6.40%
Site*Slope	0.012	1.34%	Site*Month	<0.0001	6.86%
Site*Month	<0.0001	12.75%	Slope*Month	<0.0001	7.13%
Slope*Month	<0.0001	6.00%			
N 635		**R^2 49.93%**	**N 581**		**R^2 25.74%**

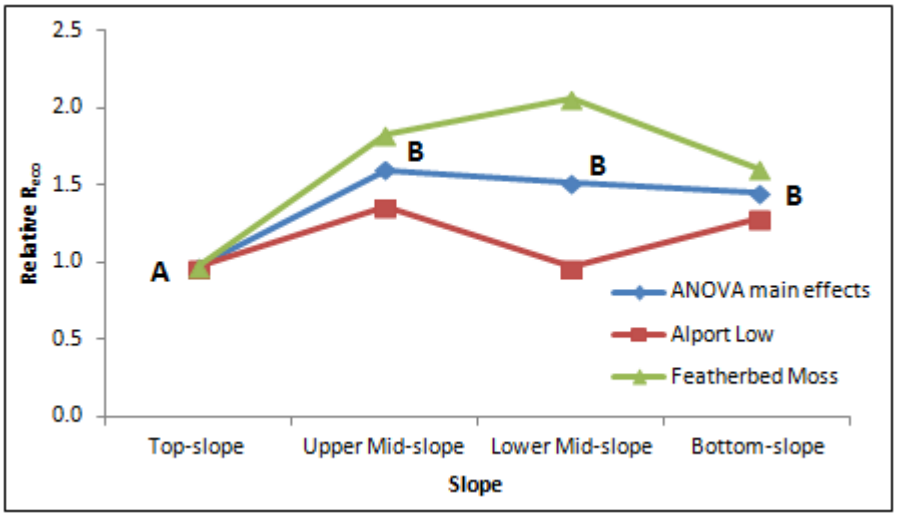

Figure 2.10 Relative R_{eco} ANOVA main effects and interactions plot: significant differences denoted where letters are not shared between slope positions

Table 2.16 Relative R_{eco} Kruskal-Wallis results

Slope	N	Median	Ave Rank	Z
Top-slope	195	0.92	307.6	-0.95
Upper Mid-slope	123	1.04	332.6	0.98
Lower Mid-slope	125	1.00	325.4	0.50
Bottom-slope	192	0.97	314.4	-0.33
Overall	635		318.0	
H = 1.69		**DF = 3**		**P = 0.064**

Regression analysis (Table 2.17) of all data from 2010 - 11 revealed that water table had a negative relationship with R_{eco}. Wetness index had a positive relationship with R_{eco}, though its overall influence in the ANCOVA model was limited. Gross photosynthesis had a positive correlation to R_{eco} and was the only constant predictor across all hillslope positions, aside from the seasonal cycle explaining seasonal variation. On the lower mid-slope (R^2 = 56.0%), all the variation that could be explained by the independent variables was accounted for by seasonal variation and P_G. Ecosystem respiration was not sensitive to changes in water table on the mid-slopes, where the largest variation in WTD was observed between the two study sites; WTD was only significant on the top-slope. On the upper mid-slope and bottom-slope 1/T was significant, indicating sensitivity to temperature beyond that explained by colinearity between temperature and P_G. As such the differences between the upper mid-slope and bottom-slope were not caused by temperature effects, though this may be the case with the lower mid-slope. The bottom-slope was sensitive to variations in wetness index, but the response was different from that of the upper mid-slope, which had a negative correlation to wetness index.

Table 2.17 LnR_{eco} MLR: Sin M & Cos M = sin & cos by month; 1/T = temperature coefficient; SE = standard error

Slope	Predictor	Coef	SE Coef	P
All data	Constant	-1.9	0.2	<0.0001
	Sin M	-0.14	0.04	<0.0001
	Cos M	-0.48	0.05	<0.0001
	WTD	-0.0006	0.0001	<0.0001
	LnP_G	0.35	0.02	<0.0001
R^2 = 57.8%	Wetness index	0.06	0.02	0.016
Top-slope	Constant	-1.7	0.1	<0.0001
	Cos M	-0.42	0.08	<0.0001
	WTD	-0.0020	0.0004	<0.0001
R^2 = 58.5%	LnP_G	0.35	0.04	<0.0001
Upper Mid-slope	Constant	9	4	0.011
	Sin M	-0.23	0.07	0.010
	Cos M	-0.4	0.1	0.001
	1/T	-3000	1000	0.008
	LnP_G	0.21	0.06	<0.0001
R^2 = 64.7%	Wetness index	-0.16	0.07	0.044
Lower Mid-slope	Constant	-1.4	0.1	<0.0001
	Sin M	-0.29	0.08	<0.0001
	Cos M	-0.51	0.09	0.000
R^2 = 56.0%	LnP_G	0.37	0.06	0.000
Bottom-slope	Constant	6	3	0.111
	Sin M	-0.27	0.06	<0.0001
	Cos M	-0.3	0.1	0.017
	1/T	-2000	1000	0.029
	LnP_G	0.35	0.05	<0.0001
R^2 = 65.4%	Wetness index	0.09	0.04	0.039

2.4.2.2 P_G

Figure 2.11 shows the median rates of P_G, with the largest on the bottom-slope (-0.312 g CO_2 m^{-2} h^{-1}). The upper mid-slope had a median P_G of -0.260 g CO_2 m^{-2} h^{-1} and lower mid-slope -0.234 g CO_2 m^{-2} h^{-1}. The median P_G for the topslope was considerably lower at -0.181 g CO_2 m^{-2} h^{-1}. Despite this, the mean P_G on the top-slope value (-0.31 ± 0.03 g CO_2 m^{-2} h^{-1}, Table 2.9) was within the standard error of the upper mid-slope (-0.35 ± 0.03 g CO_2 m^{-2} h^{-1}). The

maximum rate of P_G recorded across the year of study was on the bottom-slope (-2.579 g CO_2 m^{-2} h^{-1}).

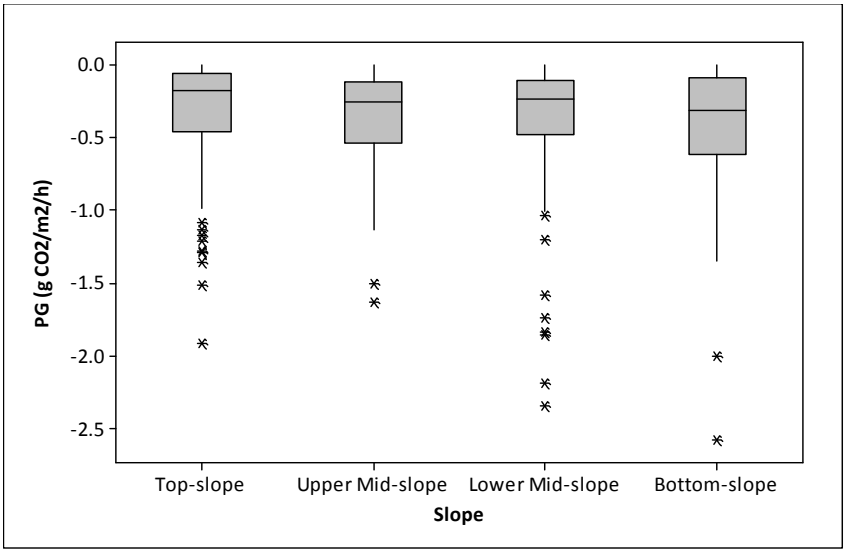

Figure 2.11 Boxplot of median P_G by slope

The ANOVA model (Table 2.13) explained 41.30% of variation in P_G, though only slope ($p = 0.013$, $\omega^2 = 1.36\%$) and month ($p < 0.0001$, $\omega^2 = 39.9\%$) were significant. The main driver, as with R_{eco}, was the seasonal pattern. Gross photosynthesis was significantly higher in spring, summer and autumn months, though May, June and July had significantly higher rates of P_G to all other months than between themselves. Though only a small amount of variation was accounted for by slope, it was nonetheless significant. The relationship between slope and P_G reflected the raw data, to the extent that the top-slope (-0.125 g CO_2 m^{-2} h^{-1} – Figure 2.12) had a significantly lower rate of P_G than the bottom-slope (-0.169 g CO_2 m^{-2} h^{-1}). Both mid-slope positions had the same mean rate of P_G (-0.165 g CO_2 m^{-2} h^{-1}) and were not significantly different from either the top or bottom-slope.

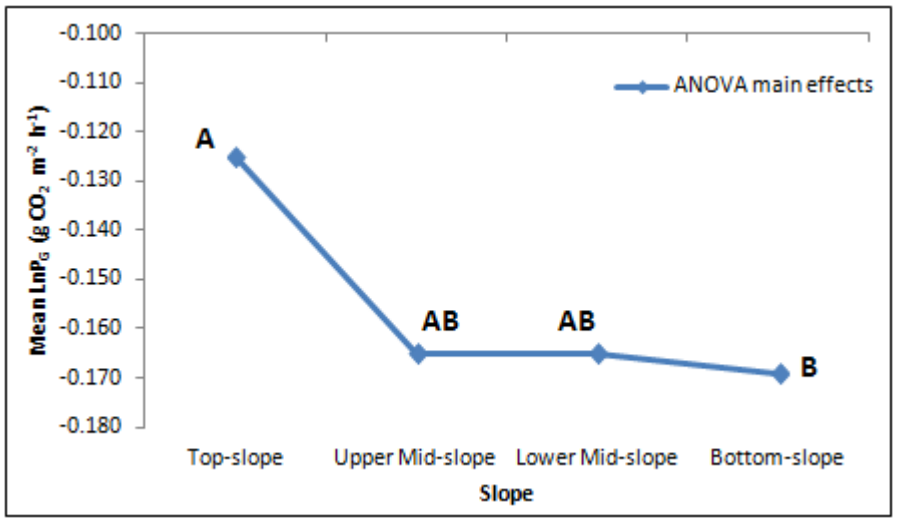

Figure 2.12 LnP_G ANOVA main effects plot: significant differences denoted where letters are not shared between slope positions

ANCOVA (R^2 = 52.06%) revealed that 1/T (p <0.0001, ω^2 = 32.12%) and month (p <0.0001, ω^2 = 11.62%) were the most important variables explaining variation in P_G. In the ANCOVA model, rates of P_G were significantly lower in February and March relative to other months (March – December for February; May – October for March) but April had lower rates of P_G than July and October and December had significantly lower rates of P_G than October. As such, many of the significant differences between months in the ANOVA model were explained by inclusion of 1/T and PAR (p <0.0001, ω^2 = 4.37%) in the model. WTD (p = 0.005, ω^2 = 3.59%) was also significant, with a negative relationship indicating that as WTD gets closer to the surface, rates of P_G decrease (LnP_G had a positive sign convention in the model). Altitude was negatively correlated to P_G (p <0.0001, ω^2 = 0.32%), but was of limited importance. Slope was not significant; variation across the slope was explained by WTD, temperature and PAR.

ANOVA of relative P_G (R^2 = 25.74%, Table 2.15) found site, slope, sub-slope and month factors to be significant with significant interactions between site and month and slope and

month. Relative P_G was significantly lower on the top-slope (1.14, Figure 2.13) compared to the upper mid-slope (1.94) and bottom-slope (1.78). The significant difference between the top and bottom-slope was in agreement with the ANOVA P_G model, though the top-slope and upper mid-slope were not significantly different in the ANOVA model. As with the relative R_{eco} data, Featherbed Moss (1.97) had a higher ratio than Alport Low (1.35). However, Kruskal-Wallis of ratio P_G, as with ratio R_{eco}, suggested that slope was not significant (Table 2.18).

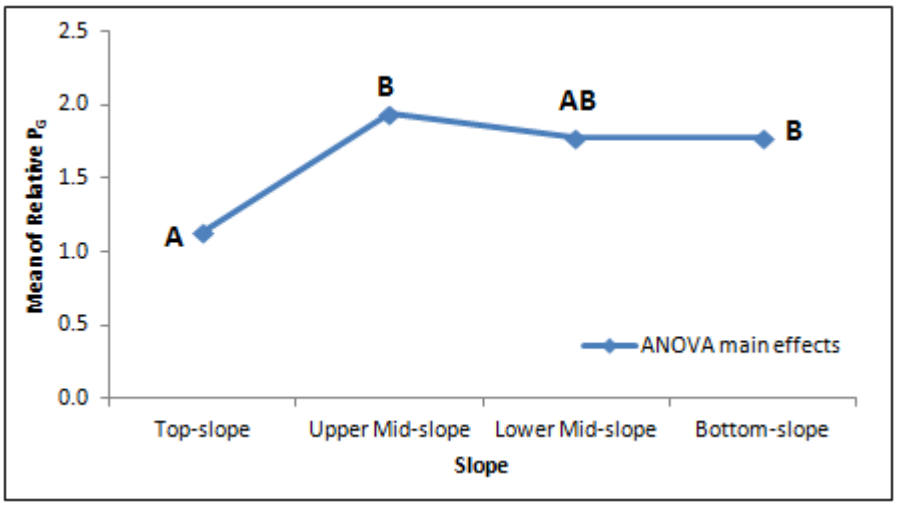

Figure 2.13 Relative P_G ANOVA main effects plot: significant differences denoted where letters are not shared between slope positions

Table 2.18 Relative P_G Kruskal-Wallis results

Slope	N	Median	Ave Rank	Z
Top-slope	182	0.95	265.50	-2.48
Upper Mid-slope	114	1.04	310.50	1.38
Lower Mid-slope	114	0.88	293.20	0.16
Bottom-slope	171	0.98	303.70	1.18
Overall	581		291.00	
H = 6.74		**DF = 3**		**P = 0.080**

Table 2.19 LnP_G MLR: Sin M & Cos M = sin & cos by month; SE = standard error

Slope	Predictor	Coef	SE Coef	P
All data	Constant	11	4	0.003
	Sin M	-0.49	0.06	<0.0001
	Cos M	-0.4	0.1	<0.0001
	WTD	-0.0007	0.0002	<0.0001
	1/T	-3300	900	<0.0001
	LnPAR	0.43	0.05	<0.0001
R^2 = 49.1%	Altitude	-0.006	0.002	0.012
Top-slope	Constant	18	4	<0.0001
	Sin M	-0.5	0.1	<0.0001
	WTD	-0.0016	0.0005	0.004
	1/T	-6000	1000	<0.0001
R^2 = 49.5%	LnPAR	0.41	0.08	<0.0001
Upper Mid-slope	Constant	9	5	0.063
	Sin M	-0.4	0.1	<0.0001
	WTD	0.0006	0.0003	0.048
	1/T	-4000	1000	0.002
R^2 47.3%	LnPAR	0.5	0.1	<0.0001
Lower Mid-slope	Constant	22	12	0.065
	Sin M	-0.5	0.1	<0.0001
	Cos M	-0.5	0.1	<0.0001
	WTD	-0.0021	0.0006	0.001
	LnPAR	0.42	0.09	<0.0001
R^2 = 43.4%	Altitude	-0.05	0.02	0.028
Bottom-slope	Constant	38	12	0.002
	Sin M	-0.6	0.1	<0.0001
	Cos M	-0.8	0.1	<0.0001
	LnPAR	0.55	0.08	<0.0001
R^2 = 60.4%	Altitude	-0.08	0.02	0.001

Regression analysis (Table 2.19) confirmed the importance of seasonality (sin M, cos M), WTD, temperature (1/T), PAR and altitude in controlling rates of P_G across the entire dataset (all data). However, altitude was not a significant covariate explaining variation in P_G at the top-slope or upper mid-slope. Covariates also differed for the lower mid-slope, with altitude significant but not 1/T. This was the case for the bottom-slope as well, for which WTD was also not significant. The lower rates of P_G on the top-slope could be due to temperature

and WTD controls, for which the bottom-slope was insensitive and P_G was instead controlled by seasonal change, PAR and altitude.

2.4.2.3 NEE

Median NEE values showed all hillslope positions to be net sinks of CO_2 during daylight hours between June 2010 and June 2011 (Figure 2.14). The largest NEE sink was at the bottom-slope (-0.084 g CO_2 m^{-2} h^{-1}), whilst the smallest was at the top-slope (-0.042 g CO_2 m^{-2} h^{-1}), though each slope position was at times a source of CO_2. The size of the NEE sink increased down-slope.

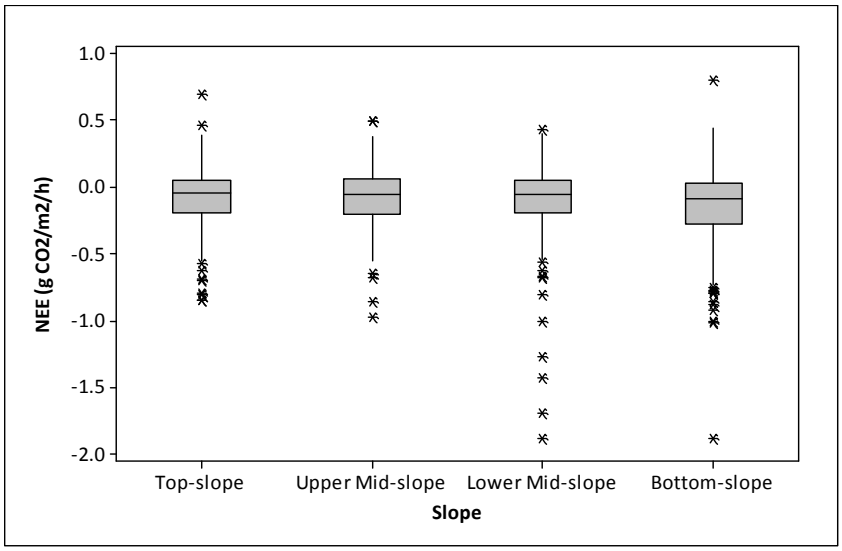

Figure 2.14 Boxplot of median NEE by slope

ANOVA showed a significant difference in NEE between the bottom-slope and all other hillslope positions. Mean NEE values from the ANOVA main effects (Figure 2.15) were -0.078, -0.068, -0.064 and -0.133 g CO_2 m^2 h^{-1} respectively for the top-slope, upper mid-slope, lower

mid-slope and bottom-slope. Given that the bottom-slope had significantly lower rates of R_{eco} than the mid-slope sites and a significantly higher rate of P_G than the top-slope, the overall pattern shown by NEE was unsurprising.

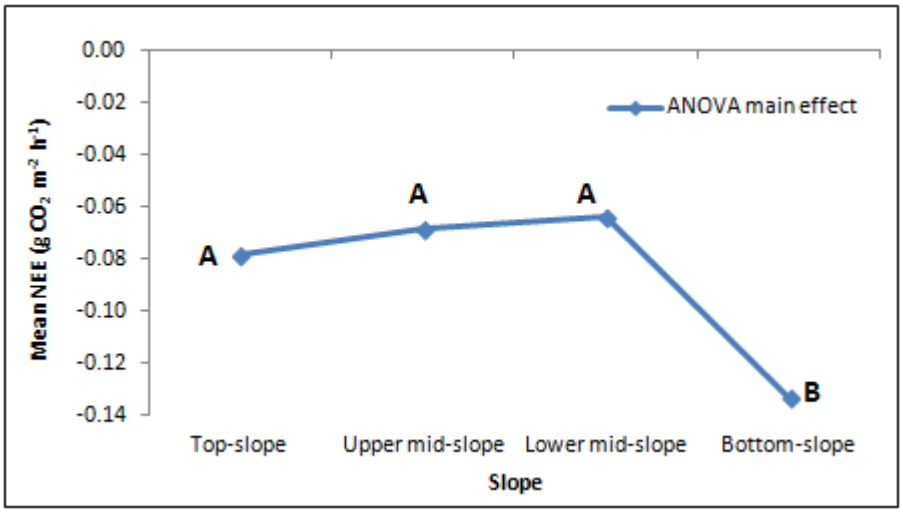

Figure 2.15 NEE ANOVA main effects plot: significant differences denoted where letters are not shared between slope positions

Though slope was significant ($p = 0.007$, $\omega^2 = 1.29\%$, Table 2.13), the most important factor predicting variation in NEE was month ($p < 0.0001$, $\omega^2 = 17.46\%$), as with R_{eco} and P_G. January, February, August and December were all classified as months when NEE was a source of CO_2 to the atmosphere. It was unsurprising for the winter months, when temperatures were low and rates of P_G reduced by senescence of vegetation. During sampling in August, conditions were poor on Alport Low, with thick fog, rain and low temperatures. The data showed that even during summer months, weather conditions could cause a net efflux of CO_2 to the atmosphere. In general though, between April and October, NEE was significantly different from December – February, reflecting the difference between times of a net CO_2 sink

and source. The ANOVA model only explained 18.78% of variance in NEE, meaning the error term was larger than for R_{eco} and P_G ANOVA models, which had larger coefficients of determination. The NEE error term included unexplained factors and interactions. Although median values from Kruskal-Wallis (Table 2.20) showed a decrease in NEE down-slope (i.e. greater CO_2 sink), it was not significant (p = 0.069).

Table 2.20 NEE Kruskal-Wallis results

Slope	N	Median	Ave Rank	Z
Top-slope	207	-0.042	340.0	1.00
Upper Mid-slope	127	-0.054	335.7	0.44
Lower Mid-slope	130	-0.057	349.3	1.36
Bottom-slope	193	-0.082	299.2	-2.60
Overall	657		329.0	
H = 7.11		**DF = 3**		**P = 0.069**

ANCOVA analysis (Table 2.13) showed that P_G (p <0.0001, ω^2 = 45.02%) and month (p <0.0001, ω^2 = 5.37%) explained most variation in NEE, whilst the percentage of *Eriophorum spp.* (p <0.0001, ω^2 = 1.61%), PAR (p <0.0001, ω^2 = 1.85%) and slope angle (p = 0.001, ω^2 = 0.67%) were also significant. The covariates accounted for the lower NEE values for spring – autumn months in the ANOVA model, and as such NEE was actually a significantly greater CO_2 sink during winter months in the ANCOVA model. Slope was no longer significant with the covariates included in the NEE model.

The residuals of MLR indicated a low level of accuracy at high and low values when the covariates from the ANCOVA model were used. To remove this, P_G data without log-transformation was used instead. Regression analysis for the entire dataset (all data, Table 2.21, R^2 = 74.5%) found a positive correlation with P_G and a negative correlation with PAR and percentage *Eriophorum spp*. As would be expected, low levels of P_G (negative values close to zero) moved the direction of NEE towards a source. Likewise, higher levels of PAR decreased

NEE, therefore increasing the potential for a CO_2 sink. Vegetation communities with a higher percentage of *Eriophorum spp*. also increased the CO_2 sink. Unlike the ANCOVA model, a significant relationship with temperature was found. However, the effect of temperature was to increase NEE (i.e. towards a source of CO_2), which agreed with the relationship between temperature and R_{eco} rather than P_G.

Table 2.21 NEE MLR: Sin M & Cos M = sin & cos by month; SE = standard error

Slope	Predictor	Coef	SE Coef	P
All data	Constant	0.39	0.03	<0.0001
	Sin M	-0.023	0.007	0.002
	Cos M	-0.06	0.01	<0.0001
	% *Eriophorum spp*.	-0.0012	0.0002	<0.0001
	Air Temp	0.008	0.001	<0.0001
	P_G	0.68	0.02	<0.0001
R^2 = 74.5%	LnPAR	-0.051	0.006	<0.0001
Top-slope	Constant	0.43	0.05	<0.0001
	Cos M	-0.09	0.01	<0.0001
	% *Eriophorum spp*.	-0.0016	0.0002	<0.0001
	P_G	0.58	0.04	<0.0001
R^2 = 72.5%	LnPAR	-0.046	0.008	<0.0001
Upper Mid-slope	Constant	0.30	0.07	<0.0001
	Sin M	-0.03	0.01	0.017
	Cos M	-0.09	0.02	<0.0001
	Air Temp	0.012	0.003	<0.0001
	P_G	0.76	0.05	<0.0001
	LnPAR	-0.06	0.01	<0.0001
R^2 = 76.4%	Slope angle	0.016	0.003	<0.0001
Lower Mid-slope	Constant	0.46	0.06	<0.0001
	Cos M	-0.12	0.02	<0.0001
	% *Eriophorum spp*.	-0.0010	0.0003	0.004
	P_G	0.68	0.05	<0.0001
R^2 =74.0%	LnPAR	-0.05	0.01	<0.0001
Bottom-slope	Constant	0.26	0.06	<0.0001
	Air Temp	0.015	0.002	<0.0001
	P_G	0.68	0.04	<0.0001
R^2 = 76.0%	LnPAR	-0.06	0.01	<0.0001

ANOVA indicated that NEE was significantly more negative at the bottom-slope compared all other hillslope positions. Air temperature, P_G and PAR were all significant in explaining variation in NEE, and there was no seasonal pattern beyond that associated with the covariates on the bottom-slope. This was not the case for other slope positions, which had a seasonal sensitivity beyond that caused by P_G, temperature or PAR. Percentage *Eriophorum spp*. was significant on the lower mid-slope and top-slope and as such vegetation was more important than on the bottom-slope. The coefficient of P_G was the same for the lower mid-slope (0.68 ± 0.05 Δg CO_2 m^{-2} h^{-2}) and bottom-slope (0.68 ± 0.04 Δg CO_2 m^{-2} h^{-2}), but differed for the top-slope (0.58 ± 0.04 Δg CO_2 m^{-2} h^{-2}), which was outside the standard error of the bottom-slope. This implied that differences in the amount of P_G may have been the cause of variation in NEE at the top and bottom-slope. This result was consistent with results from ANOVA analysis of P_G (Figure 2.12). Slope angle was important in the upper mid-slope regression, indicating that as slope angle increased, so did NEE.

2.4.3 DOC

2.4.3.1 DOC in soil pore water

DOC concentration in soil pore water varied with hillslope position (Figure 2.16). Median DOC concentration was >90 mg C l^{-1} for both the top-slope and upper mid-slope, whilst there was a decrease to ~75 mg l^{-1} on the lower mid-slope and bottom-slope. The maximum observed concentration of DOC (Table 2.9) was 278.0 mg C l^{-1} on the top-slope, whilst the minimum (when not removed as below the limit of detection) was 4.6 mg C l^{-1}, on both the top-slope and bottom-slope.

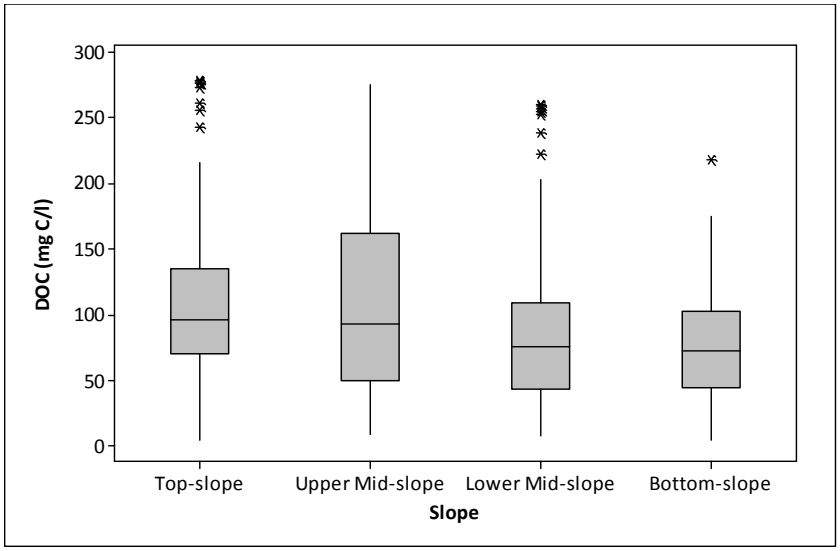

Figure 2.16 Boxplot of soil pore water median DOC concentration by slope

Site, slope, sub-slope, month and interactions between site and slope, site and month and slope and month were all significant in the ANOVA model (R^2 = 50.63%, Table 2.22). Slope ($p < 0.0001$, ω^2 = 6.51%) was the second most important factor after month ($p < 0.0001$, ω^2 = 23.61%). The effect of slope was further noted with the significant interaction between site and slope ($p < 0.0001$, ω^2 = 5.96%) and slope and month ($p < 0.0001$, ω^2 = 5.51%). The top-slope (105.2 mg C l^{-1} – Figure 2.17) and upper mid-slope (104.9 mg C l^{-1}) had significantly higher concentrations of DOC than the lower mid-slope (86.1 mg C l^{-1}), which also had a significantly higher DOC concentration than the bottom-slope (70.1 mg C l^{-1}). As such the ANOVA main effects indicated DOC concentration significantly decreased down-slope, but study site also had a significant impact upon DOC concentrations.

Table 2.22 Soil pore water (SPW) and runoff (RO) water DOC ANOVA / ANCOVA: ω^2 = % variance

SPW DOC ANOVA			SPW DOC ANCOVA		
Factor	**P**	**ω^2**	**Factor / covariate**	**P**	**ω^2**
Site	<0.0001	4.31%	WTD	<0.0001	17.30%
Slope	<0.0001	6.51%	pH	0.001	1.37%
Sub-slope	<0.0001	0.48%	LnConductivity	<0.0001	0.21%
Month	<0.0001	23.61%	LnE4:E6	0.004	0.04%
Site*Slope	<0.0001	5.96%	NO_3^-	<0.0001	9.61%
Site*Month	<0.0001	4.23%	Slope	<0.0001	5.06%
Slope*Month	<0.0001	5.51%	Month	<0.0001	15.52%
			Slope*Month	<0.0001	3.01%
N 683		**R^2 50.63%**	**N 598**		**R^2 52.16%**
RO DOC ANOVA			**RO DOC ANCOVA**		
Factor	**P**	**$\omega^2$2**	**Factor / covariate**	**P**	**ω^2**
Month	<0.0001	24.81%	LnConductivity	0.001	11.67%
			E4:E6	<0.0001	6.73%
			$LnSO_4^{2-}$	0.016	1.62%
			Month	<0.0001	22.57%
N 509		**R^2 24.85%**	**N 394**		**R^2 42.65%**

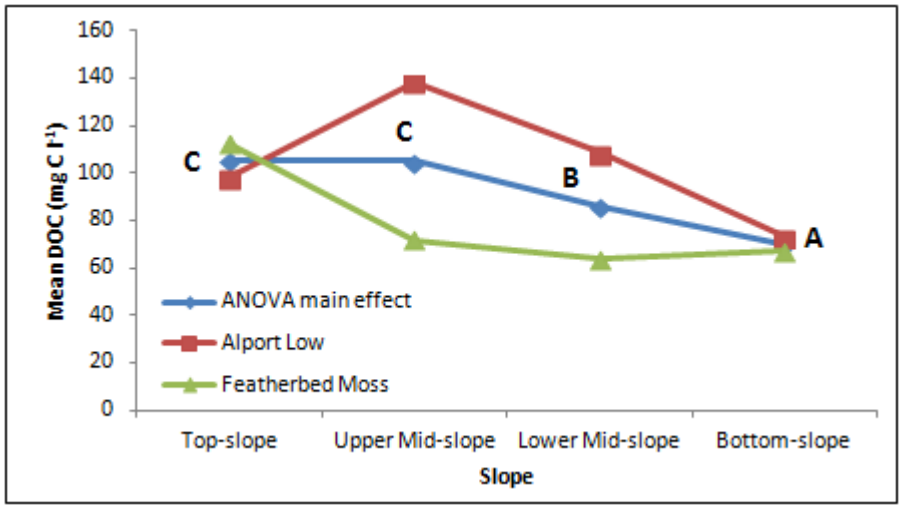

Figure 2.17 Soil pore water DOC ANOVA main effects & interaction plot: significant differences denoted where letters are not shared between slope positions

Mean DOC concentration was significantly higher on Alport Low (104.5 mg C l^{-1}) than on Featherbed Moss (78.6 mg C l^{-1}) and the differences between the two study sites was

notable with the interaction between site and slope. Whereas DOC concentration decreased between the top-slope and lower-midslope on Featherbed Moss (Figure 2.17), it increased between the top-slope and upper mid-slope on Alport Low and was still higher on the lower mid-slope than the top-slope. Nonetheless, both study sites had a large decrease in DOC concentration between the top-slope and bottom-slope.

DOC concentration was lower in December – March and May than between June – November. There appeared to be two distinct phases characterising seasonal change in DOC concentration. Between June and October, DOC concentrations increased to a maximum of 135.2 mg C l^{-1} (mean value from ANOVA main effect) and thereon decreased to 53.8 mg l^{-1} in December. This pattern was repeated between January 2011 and April 2011, when DOC concentration increased, before declining in May. Though this pattern was uniform across the top-slope, upper mid-slope and lower mid-slope, the bottom-slope did not reflect this. DOC increased between April and May 2011 and although it decreased at the bottom-slope between November and December, it was to a much smaller extent than other hillslope positions. The interaction of slope and month indicated that DOC on the upper mid-slope decreased by 98.8 mg C l^{-1} but only 6.4 mg C l^{-1}on the bottom-slope.

The top-slope had a significantly greater DOC concentration than all other hillslope positions in the ANCOVA model (R^2 = 52.16 %, Table 2.22).WTD ($p < 0.0001$, ω^2 = 17.30%) was the single most important covariate and its inclusion in the model accounted for the influence of study site and sub-slope. Furthermore, it suggested that the high DOC concentrations on the Alport Low upper mid-slope were caused by the deeper water tables. Accounting for this, the upper mid-slope was no longer significantly different from the lower mid-slope and bottom-slope. The mean main effects DOC concentrations (Figure 2.18) were 103.9, 82.5, 77.5 and 85.3 mg C l^{-1} for the top-slope, upper mid-slope, lower mid-slope and bottom-slope respectively. While there was a minor decrease in mean DOC for the top-slope relative to the ANOVA model, there was a particularly large decrease in DOC for the upper mid-slope, whilst

DOC concentration increased on the bottom-slope, reflecting the importance of hydrology to DOC. Indeed, pH ($p = 0.001$, $\omega^2 = 1.37\%$) and conductivity ($p < 0.0001$, $\omega^2 = 0.21\%$) were significant, though only to a small degree in the case of conductivity. The presence of nitrate was also significant ($p < 0.0001$, 9.61%).

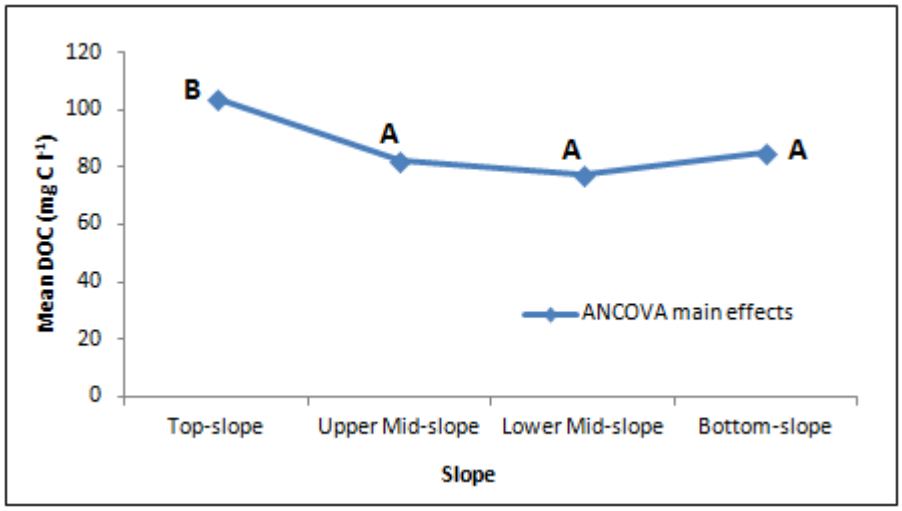

Figure 2.18 Soil pore water DOC ANCOVA main effects plot: significant differences denoted where letters are not shared between slope positions

ANOVA of relative (to the top-slope) DOC ($R^2 = 25.11\%$, Table 2.23) showed significant differences between site, slope, month and interactions. *Post hoc* significant differences between slope positions reflected those of the DOC ANOVA model. The lower mid-slope ratio of 0.85 was significantly lower than the top-slope and upper mid-slope, whilst the ratio of DOC on the bottom-slope was even lower at 0.71 (Figure 2.19). The differences between study sites were again apparent, with a ratio of 1.31 on the upper mid-slope on Alport Low, versus 0.69 on Featherbed Moss. The large decrease observed in the DOC ANOVA model between November and December on the upper mid-slope was reflected in the relative data, dropping

from 1.31 in November to just 0.66 in December. The bottom-slope (1.14 in December) increased relative to the top-slope.

Table 2.23 Relative Soil pore water (SPW) DOC ANOVA: ω^2 = % variance

SPW Relative DOC ANOVA		
Factor	**P**	**ω^2**
Site	<0.0001	5.25%
Slope	<0.0001	6.06%
Month	0.040	1.29%
Site*Slope	<0.0001	4.87%
Site*Month	<0.0001	1.77%
Slope*Month	<0.0001	5.84%
N 683		**R^2 25.11%**

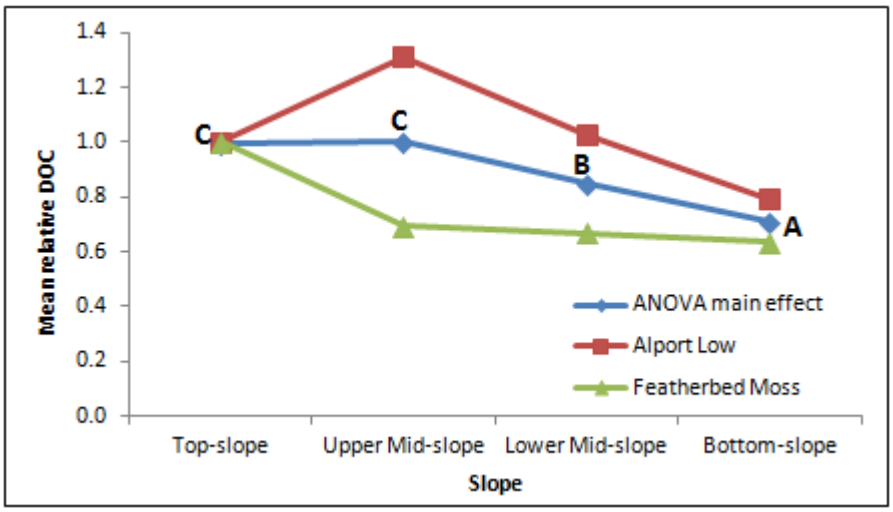

Figure 2.19 Relative soil pore water DOC ANOVA main effects & interaction plot: significant differences denoted where letters are not shared between slope positions

Table 2.24 Soil pore water DOC MLR: Sin M & Cos M = sin & cos by month: SE = standard error

Slope	Predictor	Coef	SE Coef	P
All data	Constant	-110	50	0.016
	Sin M	-27	3	<0.0001
	WTD	-0.14	0.01	<0.0001
	pH	17	7	0.014
	LnConductivity	43	7	<0.0001
	LnE4:E6	-17	6	0.005
R^2 = 36.7%	NO_3^-	-13	1	<0.0001
Top-slope	Constant	140	20	<0.0001
	Sin M	-29	4	<0.0001
	Cos M	-14	4	0.001
	WTD	-0.15	0.02	<0.0001
	LnE4:E6	-20	9	0.020
R^2 = 35.0%	NO_3^-	-9	3	0.001
Upper Mid-slope	Constant	-300	100	0.033
	Sin M	-15	7	0.036
	WTD	-0.16	0.02	<0.0001
	pH	50	20	0.011
	LnConductivity	40	20	0.048
R^2 = 49.3%	NO_3^-	-13	2	<0.0001
Lower Mid-slope	Constant	-20	50	0.661
	Sin M	-26	6	<0.0001
	WTD	-0.16	0.02	<0.0001
	LnConductivity	50	10	0.001
	LnE4:E6	-40	10	0.001
R^2 = 50.8%	NO_3^-	-22	5	<0.0001
Bottom-slope	Constant	-30	40	0.399
	Sin M	-32	3	<0.0001
	WTD	-0.17	0.04	<0.0001
	Air Temp	1.4	0.4	0.003
R^2 = 40.0%	pH	20	10	0.042

Regression analysis (Table 2.24) confirmed the significant covariates used in ANCOVA as having a significant correlation with DOC for the entire dataset. The relationship between DOC and predictors varied with hillslope position though. pH and conductivity were not significant on the top-slope. Water table depth, E4:E6 and NO_3^- had a negative correlation to DOC. pH and conductivity were significant on the upper mid-slope and conductivity on the lower mid-slope, indicating a positive correlation with DOC. Nitrate was not significant at the

bottom-slope, but temperature had a positive correlation with DOC, despite not being significant in the ANCOVA. The influence of temperature upon DOC was consequently only apparent at a more localised scale and, even so, was insignificant for most slope positions. The negative correlation between DOC and E4:E6 would suggest that as E4:E6 increased, DOC decreased; indicating a switch to fulvic acids was associated with lower DOC concentrations. Further analysis of E4:E6 would be required to establish the exact differences with slope.

2.4.3.2 DOC in runoff water

Median values of DOC (Figure 2.20) collected from surface water runoff traps suggested there was little difference in DOC concentration with slope position, though the upper mid-slope (77.7 mg C l^{-1}) was marginally higher than the other slope positions, which ranged from 67.1 – 71.8 mg C l^{-1}. DOC concentrations were generally much lower in runoff water than soil pore water, though the maximum observed concentration of 275.9 mg C l^{-1} on the lower mid-slope in June 2010 was similar to the maximum observed from soil pore water (Table 2.9).

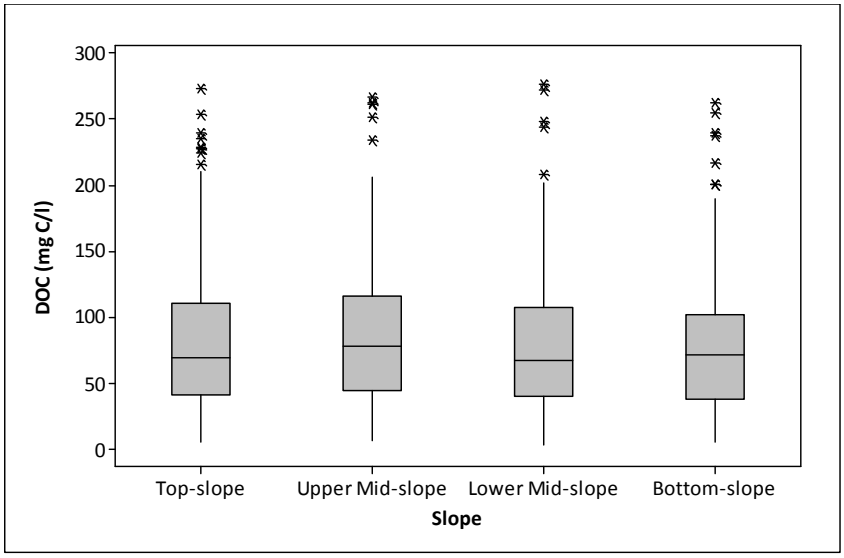

Figure 2.20 Boxplot of median runoff water DOC concentration by slope

Month ($p < 0.0001$, $\omega^2 = 24.81\%$) was the only significant factor in the ANOVA model ($R^2 = 24.85\%$, Table 2.22); no slope effect was found with runoff water DOC. July (114.8 mg C l^{-1}) had the highest DOC concentration, with the lowest occurring in December (34.6 mg C l^{-1}). In general, runoff water DOC increased from winter lows to maxima in the summer, with concentrations in June and July significantly higher than winter and spring months, though this was also the case for September and October. As only one factor was significant, there was more unexplained variance in the error term than for the soil pore water ANOVA model. ANCOVA analysis ($R^2 = 42.65\%$, Table 2.22) indicated that conductivity, E4:E6, SO_4^{2-} and month were significant covariates. Conductivity was positively correlated with DOC as was SO_4^{2-} concentration. The positive correlation between DOC and E4:E6 was the reverse of that for soil pore water.

2.4.4 Water chemistry

2.4.4.1 Soil pore water chemistry

Descriptive statistics for the major water chemistry parameters analysed are provided in Table 2.25.

Table 2.25 Soil pore water chemistry descriptive statistics: SE = standard error

Variable	Slope	N	Mean	SE Mean	Maximum	Minimum
pH	Top-slope	224	3.86	0.03	5.96	3.30
	Upper Mid-slope	140	3.84	0.03	5.55	3.26
	Lower Mid-slope	145	3.92	0.03	5.71	3.39
	Bottom-slope	207	3.92	0.02	5.62	3.46
Conductivity ($\mu s\ cm^{-1}$)	Top-slope	224	53	1	108.4	20.1
	Upper Mid-slope	139	52	1	143.0	17.6
	Lower Mid-slope	145	45	2	251.0	11.6
	Bottom-slope	207	42.6	0.8	74.1	12.0
Abs_{400}	Top-slope	225	0.199	0.007	0.522	0.020
	Upper Mid-slope	140	0.173	0.009	0.557	0.031
	Lower Mid-slope	144	0.159	0.008	0.542	0.023
	Bottom-slope	207	0.127	0.004	0.355	0.020
E4:E6	Top-slope	222	7.3	0.2	19.25	2.33
	Upper Mid-slope	138	7.8	0.2	22.00	3.09
	Lower Mid-slope	144	7.2	0.3	27.00	2.60
	Bottom-slope	205	7.9	0.3	29.50	2.67
Specific Absorbance	Top-slope	222	0.0023	0.0001	0.0144	0.0004
	Upper Mid-slope	137	0.0023	0.0002	0.0135	0.0004
	Lower Mid-slope	140	0.0025	0.0001	0.0102	0.0004
	Bottom-slope	189	0.0026	0.0002	0.0130	0.0004

Mean pH (Table 2.25), varied from 3.84 ± 0.03 (upper mid-slope) to 3.92 (± 0.03 lower mid-slope, ± 0.02 bottom-slope), with a range of 3.26 – 5.96. Results of ANOVA (R^2 = 29.79%, Table 2.26) found a significant slope effect ($p < 0.0001$, ω^2 = 1.20%), though compared with local scale heterogeneity represented by sub-slope ($p < 0.0001$, ω^2 = 8.03%) and seasonal change ($p < 0.0001$, ω^2 = 17.55%), slope was the weakest explanatory variable. Nonetheless,

slope (Figure 2.21) was significant, with pH on the top-slope (pH = 3.78) lower than the lower mid-slope (pH 3.88) and bottom-slope (pH = 3.90). The upper mid-slope (pH = 3.81) also had a lower pH than the bottom-slope. Water table improved the model fit in the ANCOVA model (R^2 = 30.7%) and had a negative correlation to pH. However, it did not change the relationship between slope and pH, with the significant differences remaining the same as the ANOVA model.

Table 2.26 Soil pore water pH & conductivity ANOVA / ANCOVA: ω^2 = % variance

pH ANOVA			**pH ANCOVA**		
Factor	**P**	**ω^2**	**Factor / Covariate**	**P**	**ω^2**
Slope	<0.0001	1.20%	WTD	0.048	1.28%
Sub-slope	<0.0001	8.03%	Slope	<0.0001	0.90%
Month	<0.0001	17.55%	Sub-slope	<0.0001	7.60%
Slope*Month	0.002	2.98%	Month	<0.0001	18.04%
			Slope*Month	0.002	3.22%
N 701		**R^2 29.79%**	**N 662**		**R^2 30.7%**
LnConductivity ANOVA			**LnConductivity ANCOVA**		
Factor	**P**	**ω^2**	**Factor**	**P**	**ω^2**
Slope	<0.0001	6.99%	% *Eriophorum spp*.	0.001	13.25%
Sub-slope	<0.0001	11.73%	Slope angle	0.001	1.36%
Month	<0.0001	33.19%	Wetness index	<0.0001	0.77%
Slope*Month	0.002	3.47%	Altitude	<0.0001	3.49%
			Slope	0.028	1.08%
			Sub-slope	<0.0001	1.87%
			Month	<0.0001	33.49%
			Slope*Month	<0.0001	3.72%
N 708		**R^2 55.41%**	**N 708**		**R^2 59.05%**

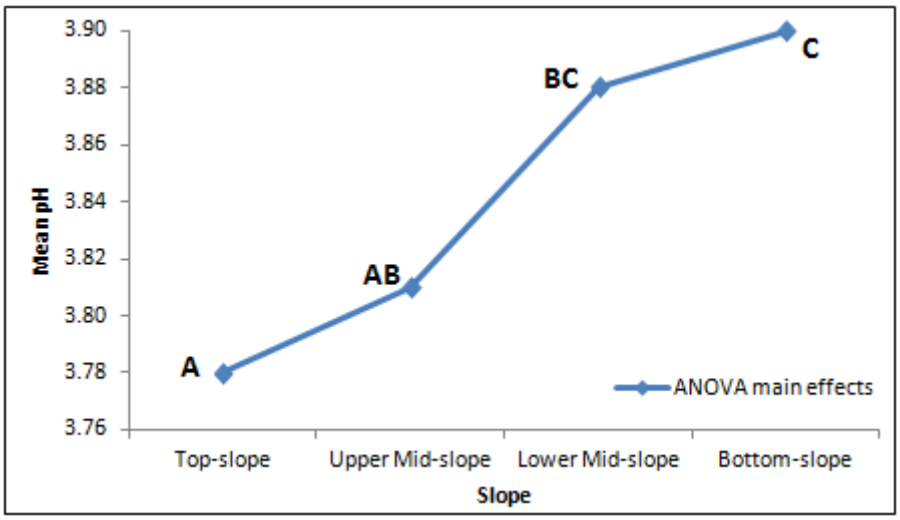

Figure 2.21 Soil pore water pH ANOVA main effects plot: significant differences denoted where letters are not shared between slope positions

Conductivity (Table 2.25) decreased from the top-slope (53 ± 1 µs cm^{-1}) to the bottom-slope (42.6 ± 0.8 µs cm^{-1}), with a range of 11.6 – 251.0 µs cm^{-1}. Analysis of variance (R^2 = 55.41%, Table 2.26) revealed that slope (p <0.0001, ω^2 = 6.99%), sub-slope (p <0.0001, ω^2 = 11.73%), month (p <0.0001, ω^2 = 33.19%) and an interaction between slope and month (p <0.0001, ω^2 = 3.47%) were significant. Both seasonal change and local scale variation with sub-slope were more important than slope, but there was still a strong trend associated with slope. Figure 2.22 shows conductivity on the top-slope (51.9 µs cm^{-1}) and upper mid-slope (48.9 µs cm^{-1}) was significantly higher than the lower mid-slope (42.2 µs cm^{-1}) and bottom-slope (42.1 µs cm^{-1}), generally the opposite trend to pH which increased down-slope. Peaks in conductivity occurred in December (54.5 µs cm^{-1}) and May (60.0 µs cm^{-1}), months when DOC concentration showed distinct drops.

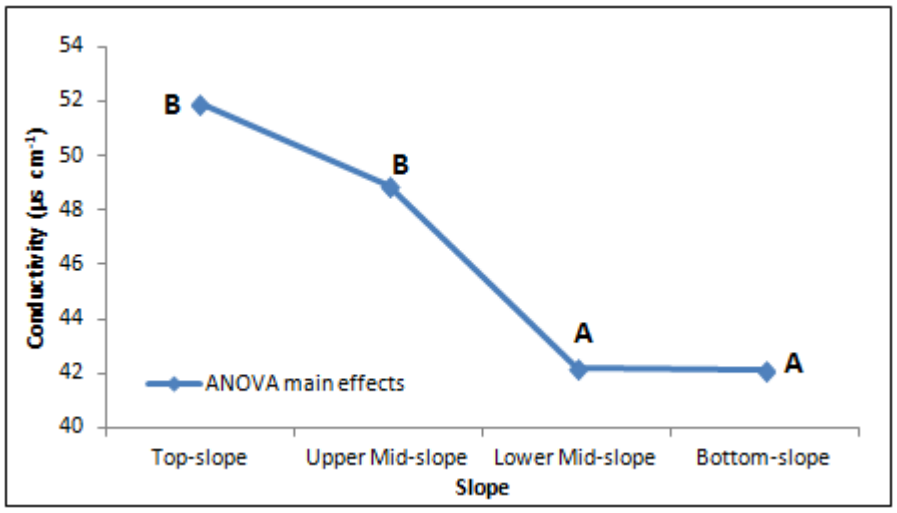

Figure 2.22 Soil pore water LnConductivity ANOVA main effects plot: significant differences denoted where letters are not shared between slope positions

Inclusion of covariates reduced the effect of sub-slope. Percentage *Eriophorum spp*. ($p = 0.001$, $\omega^2 = 13.25\%$) and slope angle ($p = 0.001$, $\omega^2 = 1.36\%$) were negatively correlated with conductivity, whilst wetness index ($p < 0.0001$, $\omega^2 = 0.77\%$) and altitude ($p < 0.0001$, $\omega^2 = 3.49\%$) were positively correlated. Although this changed the mean values from the ANCOVA main effects plot (Figure 2.23) to the top-slope having the lowest conductivity (43.0 µs cm^{-1}) and bottom-slope the highest (50.1 µs cm^{-1}), the significant difference was in fact between the lower mid-slope and bottom-slope. The high levels of conductivity on the bottom-slope were reflected in the slope-month interaction, which was different from the ANOVA interaction in this regard, though the seasonal pattern was broadly the same as the ANOVA model.

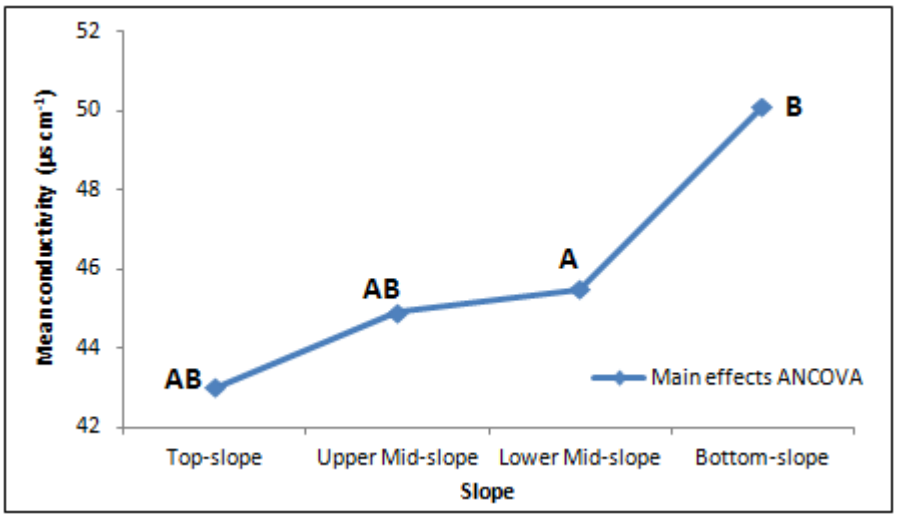

Figure 2.23 Soil pore water LnConductivity ANCOVA main effects plot: significant differences denoted where letters are not shared between slope positions

Abs_{400} (Table 2.25) progressively decreased down-slope from 0.199 ± 0.007 Abs_{400} on the top-slope to 0.127 ± 0.004 Abs_{400} at the bottom-slope. Analysis of variance (R^2 = 67.47%, Table 2.27) confirmed a significant relationship between Abs_{400} and slope position ($p < 0.0001$, ω^2 = 7.91%), which was the second most important factor after month. Abs_{400} on the top-slope (0.185 Abs_{400}, Figure 2.24) was significantly different from all other slope positions and although the mid-slopes were not significantly different from one another, there was a further decline in Abs_{400} between the mid-slope and bottom-slope (0.107 Abs_{400}). Abs_{400} was higher on Alport Low than Featherbed Moss, with an increase on the upper mid-slope relative to the top-slope reflecting the pattern observed with soil pore water DOC on Alport Low. In general, Abs_{400} was highest during summer and autumn, rapidly declining in December.

Table 2.27 Soil pore water Abs_{400}, specific absorbance & E4:E6 ANOVA / ANCOVA: ω^2 = % variance

$LnAbs_{400}$ ANOVA			**$LnAbs_{400}$ ANCOVA**		
Factor	**P**	**ω^2**	**Factor / Covariate**	**P**	**ω^2**
Site	<0.0001	2.02%	pH	<0.0001	0.28%
Slope	<0.0001	7.91%	LnConductivity	<0.0001	0.72%
Sub-slope	<0.0001	3.26%	$LnSO_4^{2-}$	<0.0001	5.15%
Month	<0.0001	46.09%	$LnCl^-$	<0.0001	21.38%
Site*Slope	<0.0001	3.37%	NO_3^-	<0.0001	14.25%
Site*Month	<0.0001	3.23%	Wetness index	0.025	1.89%
Slope*Month	0.001	1.56%	Site	<0.0001	0.00%
			Slope	<0.0001	4.25%
			Sub-slope	<0.0001	2.56%
			Month	<0.0001	20.54%
			Site*Slope	<0.0001	1.77%
			Site*Month	<0.0001	2.23%
			Slope*Month	0.001	1.20%
N 714		**R^2 67.47%**	**N 646**		**R^2 76.25%**
LnSpecific Absorbance ANOVA			**LnSpecific Absorbance ANCOVA**		
Factor	P	ω^2	**Factor / Covariate**	P	ω^2
Site	<0.0001	1.20%	WTD	<0.0001	1.34%
Slope	0.050	0.29%	LnConductivity	<0.0001	1.56%
Sub-slope	<0.0001	2.69%	$LnSO_4^{2-}$	<0.0001	2.62%
Month	<0.0001	6.60%	$LnCl^-$	<0.0001	3.50%
Site*Month	0.001	2.60%	NO_3^-	0.002	0.39%
			Month	<0.0001	8.49%
N 684		**R^2 13.39%**	**N 598**		**R^2 17.92%**
LnE4:E6 ANOVA			**LnE4:E6 ANCOVA**		
Factor	**P**	**ω^2**	**Factor / Covariate**	**P**	**ω^2**
Site	<0.0001	6.49%	LnConductivity	<0.0001	5.02%
Slope	0.022	1.02%	$LnSO_4^{2-}$	0.013	0.36%
Sub-slope	<0.0001	4.37%	$LnCl^-$	<0.0001	3.52%
Month	<0.0001	5.83%	Site	<0.0001	4.89%
Site*Month	<0.0001	2.24%	Slope	0.006	1.24%
Slope*Month	<0.0001	9.15%	Month	<0.0001	6.80%
			Site*Month	0.012	1.58%
N 700		**R^2 29.13%**	**N 655**		**R^2 23.44%**

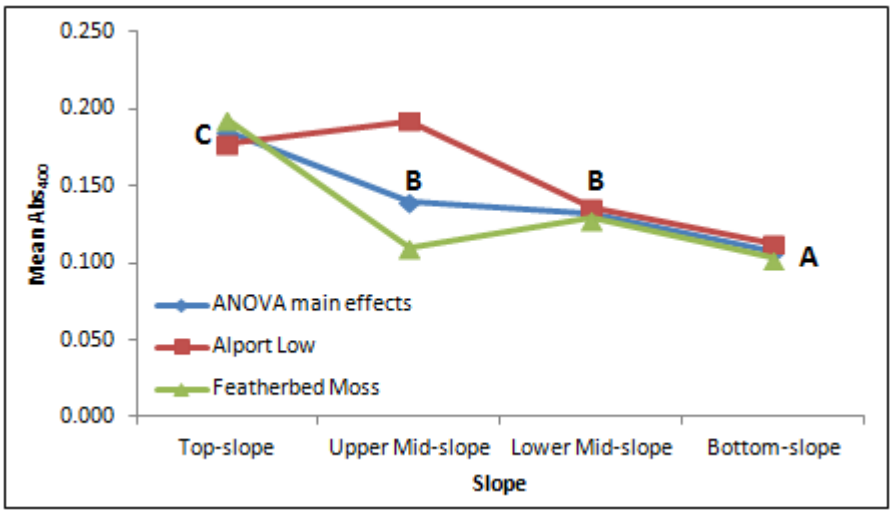

Figure 2.24 Soil pore water Abs_{400} ANOVA main effects & interaction plot: significant differences denoted where letters are not shared between slope positions

The general pattern in the ANCOVA model (Figure 2.25) was similar to that of the ANOVA model, with decreasing Abs_{400} down-slope, though the mid-slopes were significantly different from one another and the upper mid-slope on Alport Low no longer had higher Abs_{400} than the top-slope. Whereas the decline in DOC content on the Alport Low was explained by inclusion of WTD in the ANCOVA model, WTD was not significant in explaining variation in Abs_{400}. Rather pH ($p < 0.0001$, $\omega^2 = 0.28\%$) conductivity ($p < 0.0001$, $\omega^2 = 0.72\%$), SO_4^{2-} ($p < 0.0001$, $\omega^2 = 5.15\%$) Cl^- ($p < 0.0001$, $\omega^2 = 21.38\%$), NO_3^- ($p < 0.0001$, $\omega^2 = 14.25\%$) and wetness index ($p = 0.025$, $\omega^2 = 1.89\%$) were all significant.

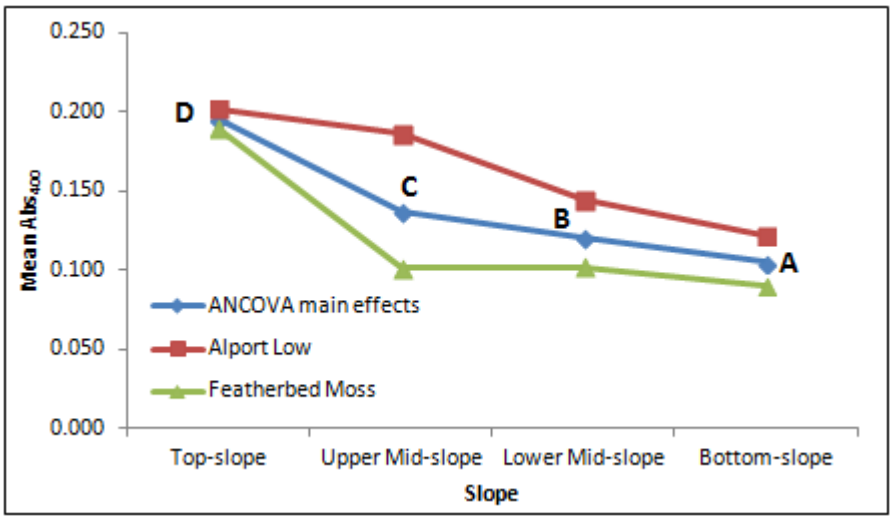

Figure 2.25 Soil pore water Abs_{400} ANCOVA main effects & interaction plot: significant differences denoted where letters are not shared between slope positions

Analysis of variance of specific absorbance (R^2 = 13.39%, Table 2.27) showed that although slope (p 0.050) was significant it only explained 0.29% of variation in specific absorbance and was not significant in the Kruskal-Wallis test (Table 2.28). Specific absorbance therefore was of limited use when applied to slope position. Featherbed Moss had a significantly higher specific absorbance than Alport Low, whilst December had significantly lower values than January – July. ANCOVA analysis improved the fit of the model (R^2 = 17.92%, Table 2.27) and only month remained a significant factor in the model. WTD was important, indicating higher water tables were associated with high specific absorbance, whilst conductivity was also positively correlated to specific absorbance. As with Abs_{400}, SO_4^{2-}, Cl^- and NO_3^- concentrations were significant. Despite the increase in variance explained by the ANCOVA model, the coefficient of determination was still low, with a lot of unexplained variance in the error term.

Table 2.28 Soil pore water LnSpecific absorbance Kruskal-Wallis results

Slope	N	Median	Ave Rank	Z
Top-slope	221	-6.246	356.3	1.26
Upper Mid-slope	136	-6.406	313.0	-1.94
Lower Mid-slope	140	-6.197	354.4	0.8
Bottom-slope	187	-6.331	338.7	-0.31
Overall	684		342.5	
H = 4.67		**DF = 3**		**P = 0.197**

Mean E4:E6 ratio (Table 2.25) was lowest on the lower mid-slope (7.2 ± 0.3) and highest on the bottom-slope (7.9 ± 0.3), though all slope positions had E4:E6 ratios close to the fulvic range of 8-10 (Thurman, 1985). Minimum E4:E6 (2.33, top-slope) was in the humic range, though the maximum value (29.50, bottom-slope) was higher than the fulvic range. ANOVA (R^2 = 29.13%) showed that site ($p < 0.0001$, ω^2 = 6.49%), slope ($p = 0.022$, ω^2 = 1.02%), sub-slope ($p < 0.0001$, ω^2 = 4.37%), month ($p < 0.0001$, ω^2 = 5.83%) and site-month ($p < 0.0001$, ω^2 = 2.24%) and slope-month ($p < 0.0001$, ω^2 = 9.15%) interactions were significant. E4:E6 (Figure 2.26) was significantly higher on the upper mid-slope (7.32) than the lower mid-slope (6.64), which potentially had more humic components than the upper mid-slope. Featherbed Moss had significantly lower E4:E6 ratios than Alport Low, whilst February had a significantly lower E4:E6 ratio than May, July – September and December.

The ANCOVA model (R^2 = 23.44%) did not improve predictive power compared to the ANOVA model, lowering the coefficient of determination due to the absence of the slope-month interaction. It was useful nonetheless though, with conductivity ($p < 0.0001$, ω^2 = 5.02%), SO_4^{2-} ($p = 0.013$, ω^2 = 0.36%) and Cl^- ($p < 0.0001$, ω^2 = 3.52%) significant covariates. The importance of these water quality parameters was the same as for the other DOC related variables of Abs_{400} and specific absorbance, with a positive correlation between E4:E6 and conductivity, whilst SO_4^{2-} and Cl^- decreased E4:E6. Inclusion of covariates changed the significant differences between slope positions (Figure 2.27) as E4:E6 on the bottom-slope (7.33) was significantly higher than the lower mid-slope (6.70) and top-slope (6.76).

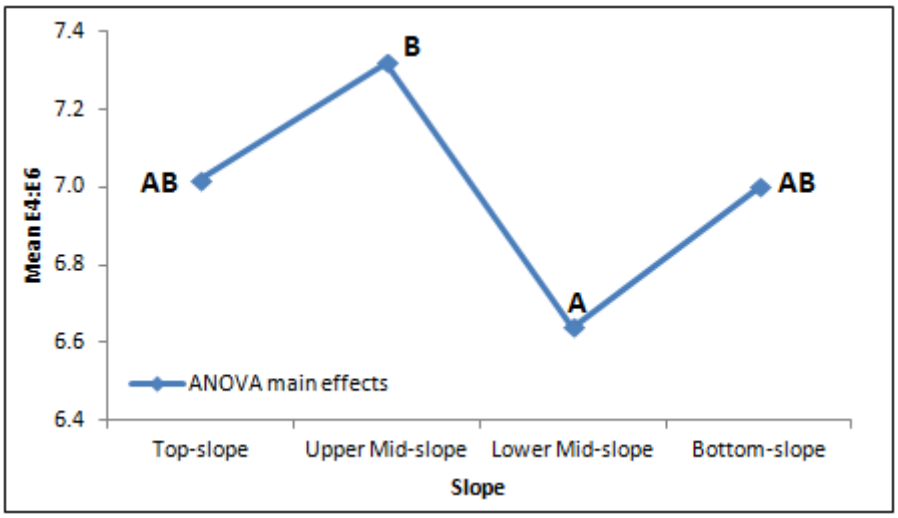

Figure 2.26 Soil pore water E4:E6 ANOVA main effects plot: significant differences denoted where letters are not shared between slope positions

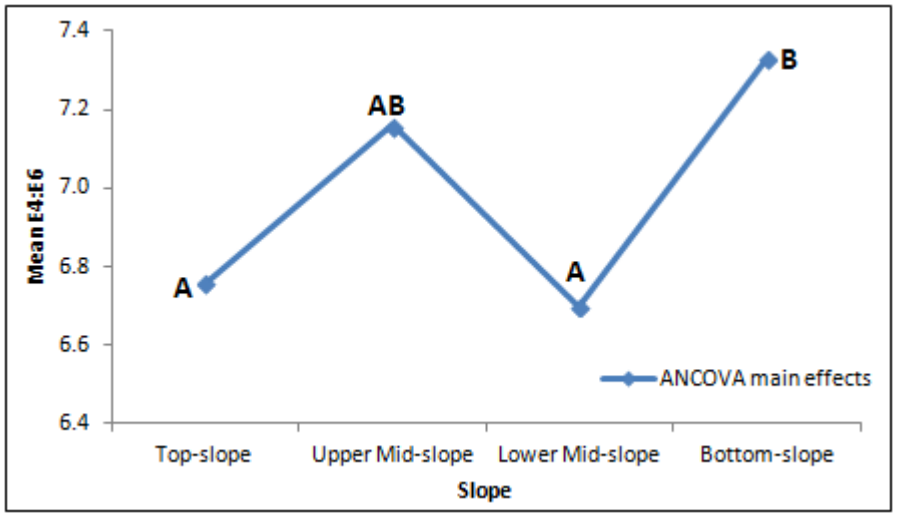

Figure 2.27 Soil pore water E4:E6 ANCOVA main effects plot: significant differences denoted where letters are not shared between slope positions

2.4.4.2 Runoff water chemistry

Table 2.29 shows the descriptive statistics for runoff water chemistry. pH was considerably higher across all hillslope positions compared to soil pore water (top-slope 5.77 ± 0.06, upper mid-slope 6.02 ± 0.07, lower mid-slope 5.6 ± 0.1, bottom-slope 5.89 ± 0.06). Minimum pH (3.63, lower mid-slope) did show that runoff water could have similar pH values to soil pore water though. Analysis of variance results (Figure 2.28) revealed the pH trend was not uniform across the two study sites. *Post hoc* testing indicated that the upper mid-slope (6.03) had a significantly higher pH than all other hillslope positions, whilst pH was also higher on Alport Low than Featherbed Moss. Aside from the top-slope on Alport Low (pH 5.97), pH was >6 for all other hillslope positions, whereas on Featherbed, pH was lower, declining to 4.68 on the lower mid-slope. Site ($p < 0.0001$, $\omega^2 = 22.45\%$, Table 2.30) was consequently the most important predictive variable, particularly with the interaction effects with slope and month as well. No covariates were significant and Kruskal-Wallis (Table 2.31) suggested slope was not significant.

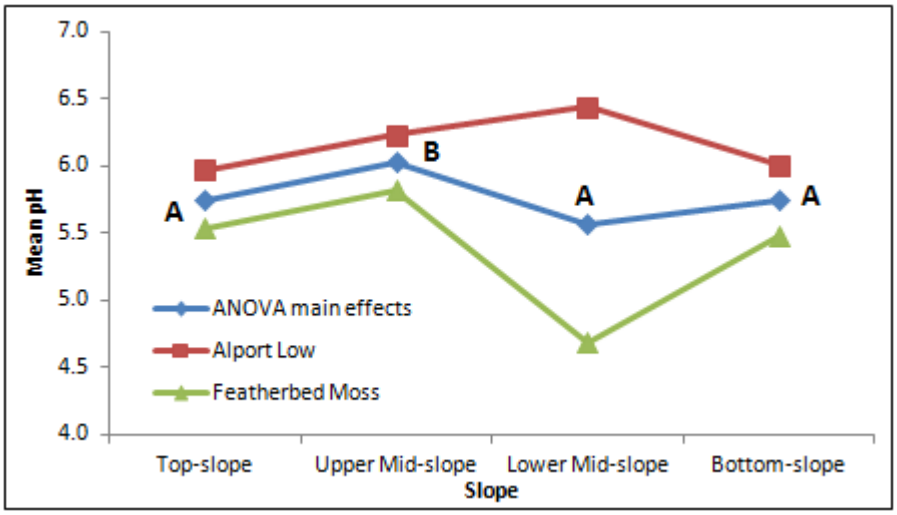

Figure 2.28 Runoff water pH ANOVA main effects & interaction plot: significant differences denoted where letters are not shared between slope positions

Table 2.29 Runoff water chemistry descriptive statistics: SE = standard error

Variable	Slope	N	Mean	SE Mean	Maximum	Minimum
pH	Top-slope	169	5.77	0.06	7.05	3.71
	Upper Mid-slope	91	6.02	0.07	6.94	3.77
	Lower Mid-slope	116	5.6	0.1	7.03	3.63
	Bottom-slope	176	5.89	0.06	6.98	3.83
Conductivity ($\mu s\ cm^{-1}$)	Top-slope	164	74	5	525.0	19.1
	Upper Mid-slope	85	86	7	299.0	15.2
	Lower Mid-slope	115	72	5	355.0	12.9
	Bottom-slope	168	70	3	241.0	13.9
Abs_{400}	Top-slope	177	0.089	0.008	0.906	0.007
	Upper Mid-slope	100	0.067	0.006	0.300	0.008
	Lower Mid-slope	123	0.070	0.006	0.329	0.005
	Bottom-slope	178	0.067	0.006	0.768	0.009
E4:E6	Top-slope	175	5.8	0.3	27.00	0.93
	Upper Mid-slope	93	5.7	0.3	19.00	1.00
	Lower Mid-slope	110	5.1	0.3	26.00	0.50
	Bottom-slope	151	6.0	0.3	19.00	0.50
Specific absorbance	Top-slope	158	0.0015	0.0001	0.0103	0.0001
	Upper Mid-slope	91	0.0010	0.0001	0.0040	0.0001
	Lower Mid-slope	104	0.0014	0.0002	0.0121	0.0001
	Bottom-slope	163	0.0012	0.0001	0.0090	0.0001

Table 2.30 Runoff water pH & conductivity ANOVA: ω^2 = % variance

pH ANOVA			LnConductivity ANOVA		
Factor	**P**	**ω^2**	**Factor**	**P**	**ω^2**
Site	<0.0001	22.45%	Site	<0.0001	16.23%
Slope	<0.0001	3.26%	Slope	<0.0001	3.74%
Sub-slope	<0.0001	5.53%	Sub-slope	<0.0001	2.72%
Month	<0.0001	7.49%	Month	<0.0001	16.51%
Site*Slope	<0.0001	8.65%	Site*Slope	<0.0001	2.83%
Site*Month	<0.0001	3.48%	Slope*Month	0.003	3.00%
N 552		**R^2 50.92%**	**N 530**		**R^2 44.5%**

Table 2.31 Runoff water pH Kruskal-Wallis results

Slope	N	Median	Ave Rank	Z
Top-slope	169	6.05	259.2	-1.70
Upper Mid-slope	91	6.15	301.5	1.63
Lower Mid-slope	116	6.06	258.7	-1.35
Bottom-slope	176	6.17	292.0	1.56
Overall	552		276.5	
H = 7.32		**DF = 3**		**P = 0.062**

As with pH, conductivity in runoff water was higher than soil pore water. Bottom-slope had the lowest mean (70 ± 3 µs cm^{-1} – Table 2.29), with the highest on the upper mid-slope (86 ± 7 µs cm^{-1}). Conductivity ranged between 12.9 – 525.0 µs cm^{-1}. ANOVA (Figure 2.29) showed that conductivity results reflected the pH ANOVA, with significantly higher conductivity on the upper mid-slope than other slope positions. As with pH, site ($p < 0.0001$, $\omega^2 = 16.23\%$, Table 2.30) was one of the most important variables, with conductivity higher on Alport Low. Month ($p < 0.0001$, $\omega^2 = 16.51\%$) was the most important factor, with a peak in conductivity occurring in June and a minimum in November. As with pH, no covariates were significant.

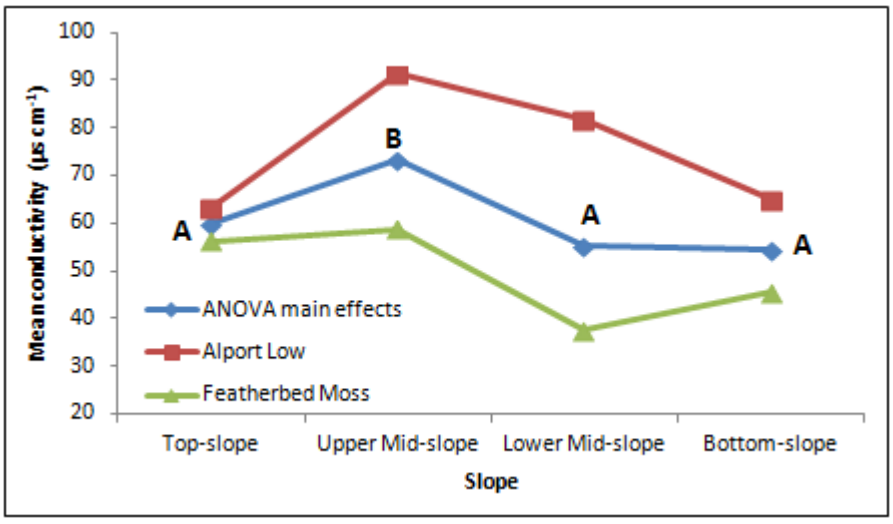

Figure 2.29 Runoff water conductivity ANOVA main effects & interaction plot: significant differences denoted where letters are not shared between slope positions

Abs_{400} (Table 2.29) on the top-slope (0.089 ± 0.008 Abs_{400}) was outside the standard error of the other hillslope positions, with a low on the upper mid-slope and bottom-slope (0.067 ± 0.006 Abs_{400}). Abs_{400} ranged between 0.005 – 0.906 but was lower than for soil pore water, again implying a difference in water chemistry between the two water source types. Abs_{400} (Figure 2.30) was significantly higher on the top-slope (0.058 Abs_{400}) than the lower mid-slope (0.044 Abs_{400}) and bottom-slope (0.046 Abs_{400}). Although this trend occurred on Alport Low, the lower mid-slope on Featherbed Moss had a higher mean Abs_{400} (0.083 Abs_{400}) than the top-slope (0.070 Abs_{400}). The most important factor (Table 2.32) was month ($p < 0.0001$, $\omega^2 = 31.54\%$). Abs_{400} was typically higher in summer months, peaking in July (0.125 Abs_{400}) and declining through autumn and winter to a minimum in January (0.022 Abs_{400}). Site ($p < 0.0001$, $\omega^2 = 10.08\%$) was more important than slope ($p = 0.006$, $\omega^2 = 2.95\%$), with Abs_{400} higher on Featherbed Moss.

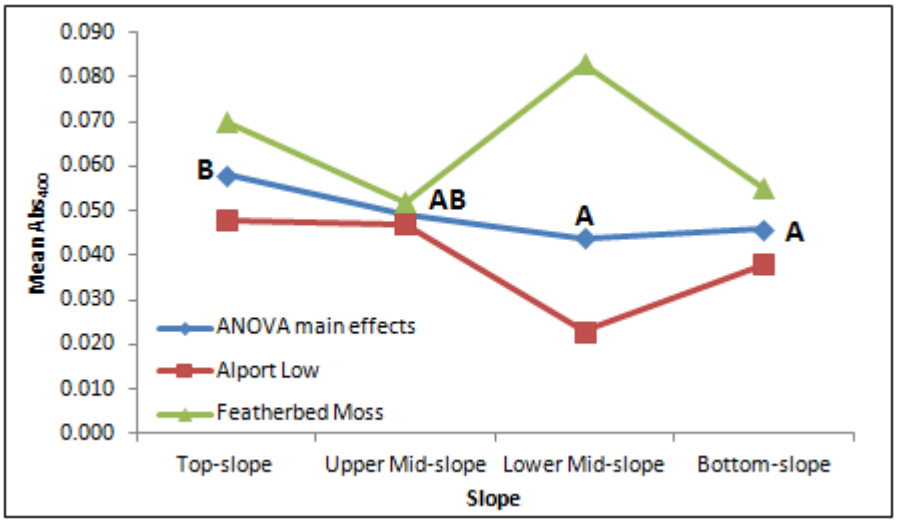

Figure 2.30 Runoff water Abs_{400} ANOVA main effects & interaction plot: significant differences denoted where letters are not shared between slope positions

ANCOVA ($R^2 = 72.44$ %, Table 2.32) improved on the ANOVA model by including pH ($p < 0.0001$, $\omega^2 = 28.86\%$) and E4:E6 ($p < 0.0001$, $\omega^2 = 17.05\%$) as covariates. pH was negatively

correlated with Abs_{400}, indicating that higher pH values were associated with lower levels of absorbance, in contrast to the positive correlation with pH for soil pore water. E4:E6 was positively correlated to Abs_{400}. Slope was of limited importance ($p = 0.007$, $\omega^2 = 0.68\%$). Kruskal-Wallis (Table 2.33) indicated that although Abs_{400} was higher on the top-slope, slope was not significant.

Table 2.32 Runoff water Abs_{400}, specific absorbance & E4:E6 ANOVA / ANCOVA: ω^2 = % variance

$LnAbs_{400}$ ANOVA			**$LnAbs_{400}$ ANCOVA**		
Factor	**P**	**ω^2**	**Factor / Covariate**	**P**	**ω^2**
Site	<0.0001	10.08%	pH	<0.0001	28.86%
Slope	0.006	2.95%	E4:E6	<0.0001	17.05%
Sub-slope	<0.0001	5.36%	$LnCl^-$	<0.0001	0.13%
Month	<0.0001	31.54%	Site	0.030	0.18%
Site*Slope	<0.0001	4.17%	Slope	0.007	0.68%
Site*Month	0.011	1.06%	Sub-slope	<0.0001	1.54%
			Month	<0.0001	23.95%
N 577		**R^2 55.20%**	**N 464**		**R^2 72.44%**
LnSpecific Absorbance ANOVA			**LnSpecific Absorbance ANCOVA**		
Factor	**P**	**ω^2**	**Factor / Covariate**	**P**	**ω^2**
Site	<0.0001	9.30%	pH	0.001	29.22%
Slope	0.002	3.63%	E4:E6	<0.0001	4.71%
Sub-slope	<0.0001	7.05%	$LnSO_4^{2-}$	<0.0001	5.50%
Month	<0.0001	4.39%	$LnCl^-$	<0.0001	2.05%
Site*Month	<0.0001	5.45%	NO_3^-	<0.0001	2.00%
N 516		**R^2 29.86%**	Slope angle	0.012	0.46%
			Month	<0.0001	3.73%
			N 400		**R^2 47.74%**
E4:E6 ANOVA			**E4:E6 ANCOVA**		
Factor	**P**	**ω^2**	**Factor / Covariate**	**P**	**ω^2**
Site	<0.0001	1.66%	% *Eriophorum spp*.	0.007	3.61%
Slope	0.002	1.85%	pH	<0.0001	5.39%
Month	<0.0001	8.68%	$LnSO_4^{2-}$	<0.0001	4.07%
Site*Slope	0.001	2.58%	Wetness index	0.015	0.92%
Slope*Month	0.003	4.36%	Slope	0.017	1.63%
			Month	<0.0001	8.65%
N 519		**R^2 19.15%**	**N 458**		**R^2 24.30%**

Table 2.33 Runoff water $LnAbs_{400}$ Kruskal-Wallis results

Slope	N	Median	Ave Rank	Z
Top-slope	176	-2.928	317.3	2.7
Upper Mid-slope	100	-3.101	281.0	-0.53
Lower Mid-slope	123	-3.194	271.6	-1.3
Bottom-slope	178	-3.135	277.6	-1.1
Overall	577		289.0	
H = 7.46		**DF = 3**		**P = 0.058**

Specific absorbance was lower in runoff water (Table 2.29) than soil pore water. The top-slope had the highest mean (0.0015 ± 0.0001) with the lowest on the upper mid-slope (0.0010 ± 0.0001). Specific absorbance ranged between 0.0001 – 0.0121. ANOVA revealed that site ($p < 0.0001$, $\omega^2 = 9.30\%$, Table 2.32), slope ($p = 0.002$, $\omega^2 = 3.63\%$), sub-slope ($p < 0.0001$, $\omega^2 = 7.05\%$), month ($p < 0.0001$, ω^2 4.39%) and a site-month ($p < 0.0001$, $\omega^2 = 5.45\%$) interaction were significant. Specific absorbance was higher on Featherbed Moss (0.0016) than Alport Low (0.0007). The monthly pattern indicated that specific absorbance was lower in May than January, July, August, November and December. Specific absorbance was higher on the top-slope (0.0011, Figure 2.31) than the upper mid-slope (0.0007).

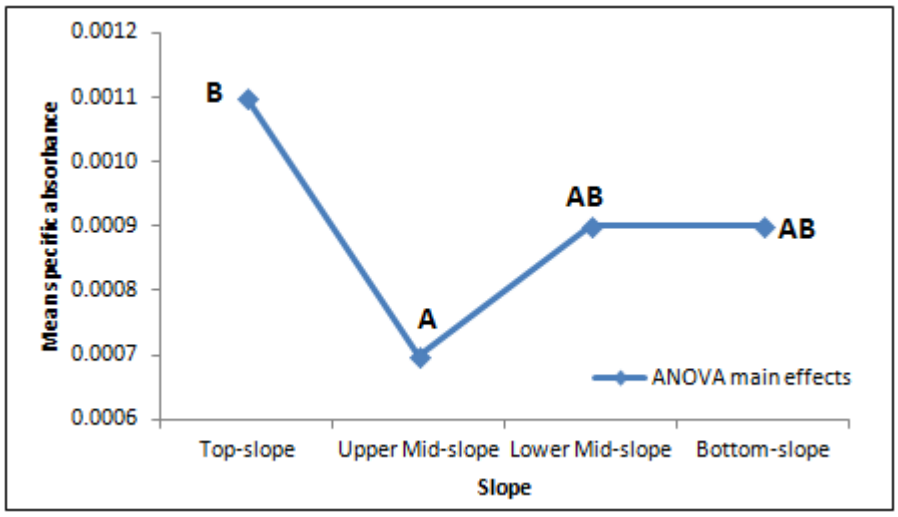

Figure 2.31 Runoff water specific absorbance ANOVA main effects: significant differences denoted where letters are not shared between slope positions

ANCOVA (Table 2.32) explained the influence of all factors other than month ($p < 0.0001$, $\omega^2 = 3.73\%$). pH ($p < 0.0001$, $\omega^2 = 29.22\%$) was the most important covariate in the model , though E4:E6 ($p < 0.0001$, $\omega^2 = 4.71\%$), SO_4^{2-} ($p < 0.0001$, $\omega^2 = 5.50\%$), Cl^- ($p < 0.0001$, $\omega^2 = 2.05\%$), NO_3^- ($p < 0.0001$, $\omega^2 = 2.00\%$) and slope angle (p 0.012, $\omega^2 = 0.46\%$) were all significant. Increasing slope angle was associated with a decrease in specific absorbance.

Despite the lower Abs_{400} and specific absorbance of runoff water, E4:E6 suggested it had more humic components than soil pore water given the lower mean E4:E6 ratios (Table 2.29). Site ($p < 0.0001$, $\omega^2 = 1.66\%$, Table 2.32), slope ($p = 0.002$, $\omega^2 = 1.85\%$), month ($p < 0.0001$, $\omega^2 = 8.68\%$), and interactions between site-slope ($p = 0.001$, $\omega^2 = 2.58\%$) and slope-month ($p = 0.003$, $\omega^2 = 4.36\%$) were significant. E4:E6 on the lower mid-slope (4.70, Figure 2.32) was significantly lower than all other slope positions, though this trend applied to Alport Low more than Featherbed Moss due to the importance of site and the site-slope interaction. The lower midslope E4:E6 ratio was much lower on Alport low (3.43), with little variation between the other hillslope positions. E4:E6 was lowest on the top-slope of Featherbed Moss (5.60) with a maximum of 6.07 on the bottom-slope, indicating much less variation than on Alport Low. Slope was not significant when assessed using Kruskal-Wallis (Table 2.34). Month was the single most important factor ($p < 0.0001$, 8.68%), with E4:E6 higher in July and August than winter months. The minimum was in January (4.54) and maximum was in August (7.32), suggesting humic compounds were flushed out in runoff water during winter.

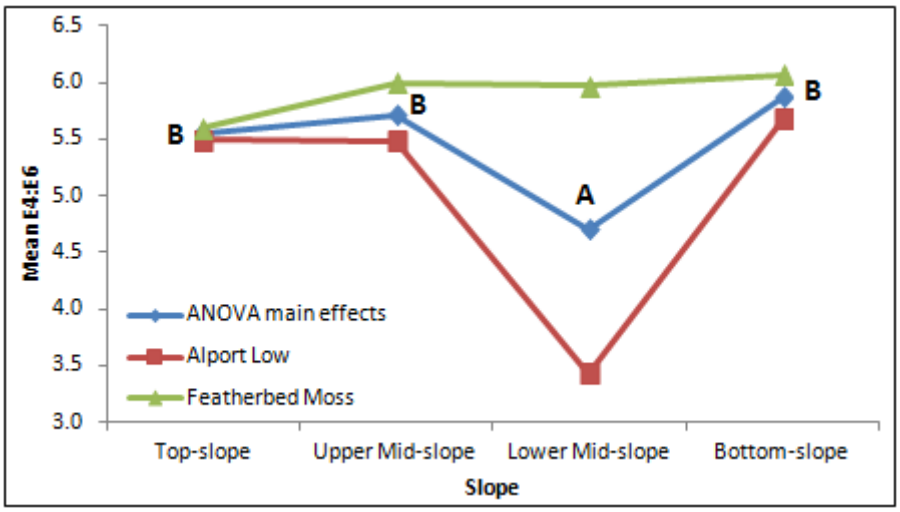

Figure 2.32 Runoff water E4:E6 ANOVA main effects and interaction plot: significant differences denoted where letters are not shared between slope positions

Table 2.34 Runoff water E4:E6 Kruskal-Wallis results

Slope	N	Median	Ave Rank	Z
Top-slope	171	5.45	261.2	0.13
Upper Mid-slope	92	5.42	265.4	0.38
Lower Mid-slope	108	4.69	227.9	-2.50
Bottom-slope	148	5.82	278.7	1.79
Overall	519		260.0	
H = 7.38		**DF = 3**		**P = 0.061**

Inclusion of covariates removed the effects associated with site and interactions. Percentage of *Eriophorum spp.* ($p = 0.007$, $\omega^2 = 3.61\%$, Table 2.32), pH ($p < 0.0001$, $\omega^2 = 5.39\%$), SO_4^{2-} ($p < 0.0001$, $\omega^2 = 4.07\%$) and wetness index ($p = 0.015$, $\omega^2 = 0.92\%$) were significant. Results indicated that as pH and wetness index decreased, E4:E6 increased – suggesting more fulvic compounds. Sulphate was positively correlated to E4:E6 ratio; as with other water chemistry measures, this contrasted with the correlation found with soil pore water, which had a negative correlation. Slope (Figure 2.33) was still significant ($p = 0.017$, $\omega^2 = 1.63\%$), though the lower mid-slope (4.88) was only significantly different from the upper mid-slope

(5.87). The ANCOVA model increased the coefficient of determination (R^2 = 24.30%) compared to the ANOVA model but the overall percentage variance explained by the model was nonetheless still low. As such, the error term included unexplained factors and interaction effects.

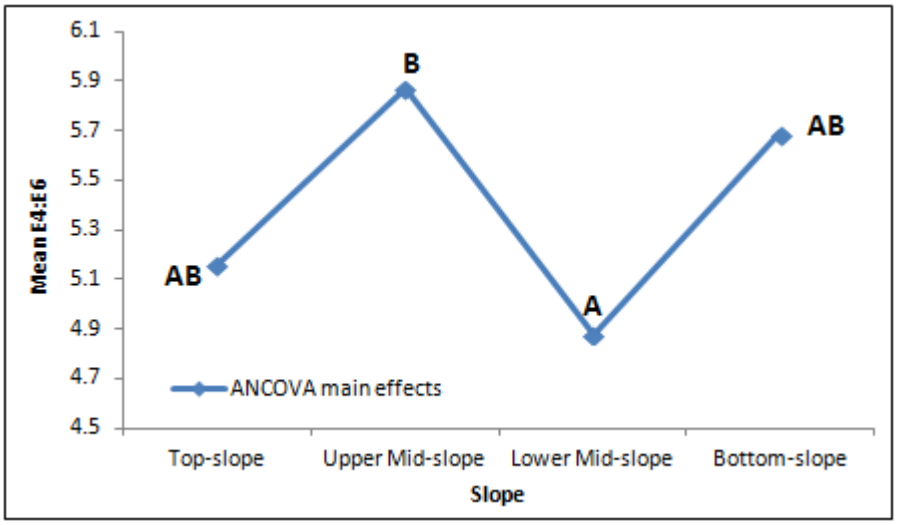

Figure 2.33 Runoff water E4:E6 ANCOVA main effects: significant differences denoted where letters are not shared between slope positions

2.5 Discussion

2.5.1 Limitations

There were a number of limitations to the study. The primary limitation was the inability to fully control the vegetation communities and incorporate vegetation as part of the factorial design. Vegetation on Alport Low was predominantly hummock based, with a mixture of *Vaccinium myrtillus* and *Eriophorum spp*. dominant, yet the upper mid-slope also had non-*Sphagnum* moss *spp*. where water tables were much deeper. Percentage *Eriophorum spp*. as the dominant vegetation community was used as a covariate and variation to some extent was

accounted for by incorporating sub-slope as a nested factor within the model given most vegetation change was across different sub-slopes. Given the extensive erosion on the Alport Low mid-slope, it was also not possible to place all plots on the same interfluve, meaning there was not a uniform slope profile on Alport Low. This did allow more variation across the mid-slope to be observed however, which was particularly useful for sub-slope hydrology.

It was not possible in this study to provide higher resolution monitoring of WTD and runoff beyond monthly sampling. More frequent monitoring has been used to provide more extensive insights into water table and runoff behaviour, particularly in response to rainfall events (Evans et al., 1999, Holden and Burt, 2003). The hydrological behaviour of intact and eroded peat has been studied in detail across the Peak District, including on Alport Low and Featherbed Moss (Allott et al., 2009) and would have provided further insights for this study as well.

2.5.2 Hydrology

Slope position was the most important variable in explaining variation in WTD and having accounted for factors including site and seasonal variation, the ANOVA model predicted high water tables on flat areas at the top and bottom-slope and drawdown on mid-slopes. The increase in WTD on mid-slopes was correlated with slope angle and therefore an increase in hydraulic gradient. Wilson et al. (2010) noted that post drain-blocking, slope angle was a significant control on WTD, whilst it has also been related to runoff response and mean residence time of water on the catchment scale, across multiple soil types (Capell et al., 2011, Soulsby and Tetzlaff, 2008).

Holden and Burt (2003) found at Moor House National Nature Reserve in the North Pennines that hillslope was important in the generation of runoff and subsurface flow. Steeper

mid-slopes generated surface overland flow less frequently than flatter areas at the top and bottom of the hillslope. This meant more sub-surface flow was generated on the mid-slope, which helped to maintain saturated conditions at the foot of the slope. The pattern observed by Holden and Burt (2003) would support the interpretation of the ANOVA model whilst the reduced frequency of runoff on the upper mid-slope also lends credence to such an explanation. Indeed, Holden (2009) found that although saturation-excess overland flow was common across all hillslope positions, flatter top-slope and bottom-slope positions remained saturated for a greater number of months, with the bottom-slope experiencing a greater number of overland flow events and a greater duration of both overland flow and saturation conditions. This supports the water table results and it is probable that higher water tables on the bottom-slope were the result of down-slope transfer of surface runoff (Holden and Burt, 2002c) and / or subsurface flow that maintains WTDs closer to the surface.

The mechanisms outlined above may explain some of the runoff processes and WTD patterns, but they are not wholly satisfactory. The lower mid-slope was observed to have the highest proportion of runoff, which was consistent across both study sites (Table 2.35). It is possible that the rapid transfer of water down-slope is the cause of higher runoff frequencies on Alport Low. As outlined above, Holden and Burt (2003) indicated subsurface flow from steeper mid-slopes generated return flow at the base of the slope and the proportion of runoff observed on the Alport Low bottom-slope (0.993) was higher than the top-slope (0.883) and upper mid-slope (0.671). Given the high proportion of runoff on the steep mid-slope, with deeper water tables, it may be that subsurface flow from higher up the mid-slope caused a rapid rise in water table further down the mid-slope, in spite of the steep slope angles. Furthermore, water tables at eroded sites across the Peak District have been observed to experience rapid wet-up towards the surface during rainfall events (Allott et al., 2009). Alternatively, although saturation-excess overland flow is considered the dominant overland process in peatlands, it is nonetheless possible that infiltration-excess overland flow occurs

(Evans et al., 1999) on mid-slopes, particularly on Alport Low. The considerably lower pH values observed in the lower mid-slope runoff traps compared to the overall trend of higher pH and conductivity values in runoff water could suggest that on Featherbed Moss, runoff water is due to ponding of soil pore water.

Table 2.35 Proportion of observed runoff between study sites

Site	All data runoff proportion	Alport Low runoff proportion	Featherbed Moss runoff proportion
Top-slope	0.841	0.883	0.742
Upper mid-slope	0.708	0.671	0.746
Lower mid-slope	0.921	0.945	0.896
Bottom-slope	0.864	0.933	0.708

The ANOVA main effects model predicted an overall WTD pattern, but it was not ubiquitous and conditions local to a given site were intrinsically linked to the overall hydrology of the hillslope. Intact peatlands should maintain high water tables close to the ground surface for most of the year, with saturation excess overland flow and near surface through-flow in the acrotelm the dominant forms of water movement across peatlands (Burt et al., 1997). Despite this, the concept of high hydraulic conductivity in the acrotelm with lower hydraulic conductivity in more decomposed catotelmic peat is not universal (Baird et al., 1997). Nonetheless, high antecedent water tables and reduced fluctuation of WTD should be a feature of intact peatlands compared to those that have experienced drainage, either through land management or natural erosion (Price, 1997, Daniels et al., 2008a, Wilson et al., 2010, Holden et al., 2011). The mean range of water table depths across the hillslope on Featherbed Moss was within those observed on intact blanket bogs (Allott et al., 2009), indicating that although Featherbed Moss is not a pristine bog, the slope was hydrologically intact.

Alport Low was markedly different, with large water table drawdown on the mid-slopes. Alport Low has linear, type II, gullies (Bower, 1961) on the mid-slope and dendritic, type I gullies on the top-slope. Erosion of peatlands is widespread in the South Pennines, with three quarters of the 300 km^2 blanket peat affected (Tallis, 1985). Water tables and drainage have been known to be affected within one to two metres of gullies and drainage ditches (Stewart and Lance, 1991, Allott et al., 2009, Wilson et al., 2010), though Wilson et al. (2010) observed this within 5 m of drainage ditches. Daniels et al. (2008a) also suggested that adjacent to gullies, water tables experienced rapid increases during rainfall events, followed by a rapid decline after the cessation of rainfall. This behaviour has also been observed on the eroded parts of Featherbed Moss (Tallis, 1973). Despite the extensive drawdown observed on Alport Low, water tables were placed beyond the zone expected to experience gully edge drawdown effects (Allott et al., 2009).

Covariates could not explain all the variation associated with slope position, site and sub-slope. Allott et al. (2009) suggested that eroded sites exhibited a water table drawdown effect beyond that explained by gully drawdown. It was suggested that erosion leads to a reduced contributing area, a feature also attributed to drainage ditches (Wilson et al., 2010, Holden et al., 2011). As such it may be that gullies divert flow away from the hillslope on Alport Low, lowering the water table to the extent observed. It is also possible that preferential flow routes such as macropores or soil pipes further enhanced drainage. A soil pipe outlet was observed near the bottom-slope on Alport Low (Figure 2.34) and though more common on flatter top-slopes and bottom-slopes (Holden and Burt, 2002c, Holden, 2005a), they also occur on mid-slopes as well.

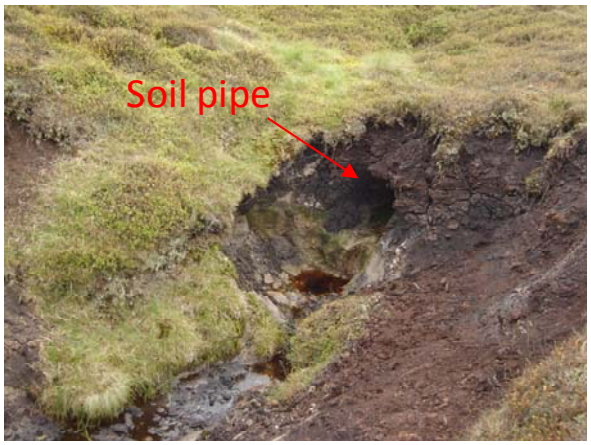

Figure 2.34 Soil pipe near Alport Low bottom-slope

It is possible that variation in soil properties also explains some of the effects caused by site and slope. Hydraulic conductivity has been shown to be both anisotropic and heterogeneous (Beckwith et al., 2003) and this may explain some of the variation associated with sub-slope. Low hydraulic conductivity at the bog margins of Cors Fochno, an estuarine raised bog in West Wales, has been suggested to help maintain higher water tables in the centre of the bog (Baird et al., 2008). Lewis et al. (2012) found that high bulk densities caused low hydraulic conductivity in riparian zones that helped to maintain higher water tables of a peat interior. Holden (2005a) suggested that hydraulic conductivity was less variable on mid-slopes and also slightly higher than top-slopes and bottom-slopes and speculated that an increase in drainage on mid-slopes may therefore be related. This may explain the lower runoff proportion observed on the upper mid-slope. It is also possible that peat depth (Wilson et al., 2010) has an effect upon water table, though this was not analysed here.

2.5.3 CO_2 flux

Hillslope position was a significant control upon CO_2 flux, with rates of R_{eco}, P_G and NEE all varying across the hillslope, though its importance was small compared to seasonal

variation. Ecosystem respiration was higher on the mid-slopes, but the exact nature of the relationship with hillslope position was not clear. ANOVA indicated that significant differences were found between the mid-slopes and bottom-slope, while the Kruskal-Wallis test and relative R_{eco} data suggested the top-slope had a lower rate of R_{eco} than the other hillslope positions. Nonetheless, each test indicated that the mid-slopes had the highest rate of R_{eco}.

Why do we get a slope effect? ANCOVA analysis indicated that P_G was the most important driver of R_{eco}, with seasonal variation and WTD also explaining a large amount of variation in R_{eco}. Consequently, though slope position was still significant in the ANCOVA model, nearly all the variation associated with slope was explained by differences with the covariates. More localised variation, reflected by sub-slope, was still significant and as in the ANOVA model, was more important than slope, possibly due to micro-topographic variation (Sommerkorn, 2008, Wu et al., 2011). It was surprising that temperature was not significant in the ANCOVA model, given its importance to respiration (Lloyd and Taylor, 1994, Burrows et al., 2005, Lafleur et al., 2005, Bortoluzzi et al., 2006, Dorrepaal et al., 2009, Bahn et al., 2010). This is likely due to it being collinear with P_G, an effect noted by Clay et al. (2012). The importance of P_G or gross primary productivity to respiration is well established, on a large scale across multiple biomes (Raich and Schlesinger, 1992) due to respiration of labile carbon sources (Crow and Wieder, 2005, Hardie et al., 2011) from photosynthates (Fenner et al., 2004, Ward et al., 2009). As such it is probable that much of the variation in R_{eco} across the hillslope was caused by variation in P_G. Water table conditions were also important and the negative relationship with R_{eco} suggested that water table drawdown increased efflux of CO_2. This is due to an increase in decomposition associated with aerobic respiration (Martikainen et al., 1995, Silvola et al., 1996a, Komulainen et al., 1999, Dalva et al., 2001).

Regression modelling was undertaken to explain how the response of R_{eco} to the covariates changes with slope position. It might be expected that WTD would be the cause of

higher rate of respiration on the mid-slopes, yet it was only important on the top-slope. This may reflect differences on the Alport Low top-slope, where *Eriophorum spp.* plots had higher water tables than hummocks with a mixture of vegetation (*Eriophorum* and *Vaccinium*). Relationships between WTD and R_{eco} are not uniform across peatlands and can be insensitive relative to other variables (Lafleur et al., 2005), or otherwise the response of R_{eco} to WTD can vary with vegetation and micro-topographic form (Pelletier et al., 2011) and can become limited due to moisture stress at very low water tables (Tuittila et al., 2004, Berglund and Berglund, 2011). The upper mid-slope had a negative correlation between R_{eco} and wetness index so it is possible that lower levels of saturation, on Alport Low at least, to some extent explain the higher rates of respiration. However, the correlation between wetness index and R_{eco} on the bottom-slope was the reverse of that on the upper mid-slope.

Respiration on the lower mid-slope was driven by seasonality and P_G, whereas a temperature dependent control was identified beyond these effects on the upper mid-slope and bottom-slope. However, the 1/T coefficients for the upper mid-slope and bottom-slope were within error of one another and while P_G was a significant driver across the hillslope, its contribution to R_{eco} appears to be larger on the top-slope and bottom-slope, which had lower rates of R_{eco}. As such it is not fully apparent what causes higher rates of R_{eco} on the mid-slopes. It may be that the response to seasonal variation is different, given the different responses to month variable (sin M and cos M) across the slope, though it is nonetheless expected that respiration rates will be low during winter months with lower temperatures and vegetation senescence.

Sub-slope in both the ANOVA and ANCOVA models explained more variation in R_{eco} than slope itself, highlighting the heterogeneous nature of peatland carbon fluxes. It could be that variation in soil properties, such as soil organic matter quality, explain differences between sub-slopes.

As with R_{eco}, month was the most important factor explaining variation in P_G, but slope position was significant nonetheless. Unlike R_{eco}, sub-slope and an interaction effect between slope and month were not important. Gross photosynthesis was significantly higher on the bottom-slope compared to the top-slope, while there were no significant differences on the mid-slopes. Inclusion of covariates accounted for the variance in P_G attributed to slope position. Temperature explained 32.12% of the variation in P_G, with PAR (ω^2 = 4.37%) and WTD (ω^2 = 3.59%) also important. Temperature was found to be an important driver of photosynthesis (Alm et al., 1999), though the effect reported here was considerably greater than that reported by Clay et al. (2012). Photosynthetically active radiation is also widely acknowledged as an important control upon P_G (Shurpali et al., 1995, Bubier et al., 2003). As with R_{eco}, the response of P_G to water table was an increase with higher WTD.

Regression analysis showed that the independent variables that explain variation in P_G differed with slope position. An increase in WTD had a positive effect upon rates of P_G on the top-slope and lower mid-slope, but was not important on the bottom-slope and had the opposite response on the upper mid-slope. This suggested that for the upper mid-slope, rates of P_G were lower with deeper water tables and increased when closer to the surface. Tuittila et al. (2004) found that for *Sphagnum*, maximum rates of P_G occurred at -120 mm WTD, decreasing with an increase in WTD beyond this level. It could be that such an effect was apparent in the relationship between P_G and WTD on the upper mid-slope, while the generally higher water tables on the top-slope did not exhibit such a response. Given that the top-slope was sensitive to both changes in WTD and temperature, this may explain why it had a lower rate of P_G than the bottom-slope, which was driven by seasonal variation and increased PAR. Though the response to PAR was different between the top-slope and bottom-slope, the coefficients were within standard error of one another.

Besides having a larger rate of P_G than the top-slope, NEE was a significantly greater carbon sink during daylight hours on the bottom-slope compared to all other slope positions.

ANCOVA analysis accounted for the effect of slope, though slope angle was significant. Gross photosynthesis was the most important covariate, with high rates of P_G increasing the NEE CO_2 sink. Unlike R_{eco} and P_G, WTD was not significant, though the percentage of *Eriophorum spp.* cover was. There was a negative relationship between *Eriophorum* cover and NEE, therefore showing that *Eriophorum spp*. increased the carbon sink potential of NEE. *Eriophorum* has been shown to accumulate carbon compared with *Carex* due to a high efficiency at carbon binding (Alm et al., 1997), with the physiology of the lacunar system present in *Eriophorum* proposed as an explanation for high rates of P_G and NEE (Komulainen et al., 1999), though this has also been noted to enhance CO_2 efflux as well. Given the importance of *Eriophorum spp.* to NEE on the top-slope and lower mid-slope, it could be that high levels of carbon sequestration were associated with high levels of *Eriophorum spp.* cover, which was low in some collars on the Alport Low mid-slope (Table 2.3) and on the hummock plots on the top-slope. The response of NEE on the bottom-slope may be universally high across all vegetation types, or otherwise the *Eriophorum spp.* cover on the hummocks on the Alport Low bottom-slope was higher than recorded at the top-slope and it may consequently be insensitive to *Eriophorum spp.* cover.

However, the difference in NEE between the top-slope and bottom-slope was most likely due to the lower rates of P_G at the top-slope. The coefficient for the top-slope was outside the standard error of bottom-slope, indicating that a larger proportion of P_G contributed to NEE on the bottom-slope, consequently increasing the overall net CO_2 sink during daylight hours. The response to P_G did not differ between the bottom-slope and the mid-slopes though and it is likely other explanations are important. The upper and lower mid-slope had a seasonal response not present on the bottom-slope, where the significant covariates were temperature, P_G and PAR. As stated above, the change in vegetation may be significant in explaining lower rates of NEE CO_2 sink on the lower mid-slope, while slope angle had a positive correlation on the upper mid-slope, suggesting NEE increased towards a CO_2

efflux with increasing slope angle. Furthermore, it is likely that the higher rates of R_{eco} on the mid-slopes were important to the reduced NEE sink relative to the bottom-slope, as has been observed at Mer Bleue in Canada (Moore et al., 2002).

Micro-topography has been shown to effect carbon cycling (Wu et al., 2011) and variation in CO_2 exchange associated with spatial heterogeneity can be important for carbon modelling (Laine et al., 2009). Landscape heterogeneity has been recognised as important, often across multiple scales (Dunn et al., 2009, Schrier-Uijl et al., 2010, Riveros-Iregui et al., 2011) and across peatlands, topographic features such as gullies have been shown to impact upon carbon cycling (Evans and Lindsay, 2010b), even if such effects are associated with vegetation (McNamara et al., 2008, Clay et al., 2012). As such, although slope position may only have a small impact upon CO_2 flux, it could yet have important implications for carbon budget models given the importance of recognising spatial heterogeneity.

2.5.4 DOC

DOC concentration was shown to significantly vary with slope position. Median DOC concentration on the top-slope was 96.2 mg C l^{-1}, with a decrease to 72.5 mg C l^{-1} at the bottom-slope, confirmed by ANOVA. A slope effect on DOC concentration and DOC flux has been observed for other catchments, with low concentrations on the hillslope and higher concentrations in riparian zones more important to DOC export in the stream (Morel et al., 2009, Laudon et al., 2011, Mei et al., 2012). However, these studies were from catchments where soils on the hillslope had low organic content, with organic wetland soils in the riparian zone contributing to higher DOC concentrations. As such the impact of hillslope on DOC across the peatland catchments studied here is quite different.

As with WTD, study site had a strong influence upon DOC concentration. Alport Low had higher DOC content than Featherbed Moss and the response of slope position was

dependent upon the interaction between slope and site. DOC concentration was higher on the mid-slopes of Alport Low than the top-slope, further reflected in the relative DOC data, yet decreased in concentration relative to the top-slope on Featherbed Moss. Some of the site differences may have been due to Alport Low having a south-facing aspect, but water table removed site effects from the model (see below). The seasonal trend identified in soil pore water DOC concentration was most likely due to a flushing mechanism, which has been noted in the stream water chemistry of Moor House in the North Pennines (Worrall et al., 2005, Worrall et al., 2006b) and soil pore water across varying gully morphologies on the Bleaklow Plateau in the South Pennines (Clay et al., 2012). This is because DOC that builds up during summer months is flushed out during autumn and as productivity is low, concentrations do not immediately return to their previous level (Worrall et al., 2005). This explained the large decrease in DOC between November and December, which was nearly 100 mg C l^{-1} on the upper mid-slope. However the decrease on the bottom-slope was to a much smaller extent and in December the bottom-slope had a larger DOC concentration than the top-slope. The flushing trend was repeated between January and May 2011, during a prolonged dry spell. The above results could suggest that the flushing mechanism did not dilute DOC concentrations on the bottom-slope compared to other slope positions.

Inclusion of covariates in the ANCOVA model helped to explain some of the variation in DOC. WTD, NO_3^-, pH, conductivity and E4:E6 ratio were significant. Multiple linear regression indicated a negative correlation between DOC and WTD. Increased oxidation of peat has been observed to enhance water DOC production on drained sites with lower water tables than where ditches have been blocked (Wallage et al., 2006, Höll et al., 2009) while increased colour content in water has been related to water table drawdown (Mitchell and McDonald, 1995). Clark et al. (2009) found in a laboratory based study that water table drawdown enhanced DOC production, but only after restoration of water tables close to the surface because reduction of sulphur to SO_4^{2-} increased acidity and lowered DOC solubility. Such an

effect was observed at Moor House in the North Pennines (Clark et al., 2005) and with the presence of erosion gullies (Daniels et al., 2008b). No relationship between SO_4^{2-} and DOC was observed here, although there was a positive correlation between DOC and pH. Given the negative relationship between DOC and WTD, it is likely that oxidation of soil organic matter and enhanced production of DOC elevated DOC concentrations. Regression modelling showed that such an effect was apparent across all hillslope positions and the correlation coefficients for WTD were within standard error of one another. It is likely therefore that WTD was most important in explaining site differences. Indeed, site, nor sub-slope, was significant in the ANCOVA model. As such, the elevated DOC concentrations on the Alport Low upper mid-slope were because of water table drawdown.

Nitrate was shown to have a strong correlation to DOC. The detection limit of NO_3^- was <<0.05 mg l^{-1} and of soil pore water samples where NO_3^- was detected, only two had concentrations <0.1 mg l^{-1}. A negative relationship was found by Jackson-Blake et al. (2012) when DOC was used to predict NO_3^- concentration and it was suggested that this represented changes in biological uptake, while Daniels et al. (2012) speculated that the negative relationship between DOC and NO_3^- could be because high concentrations of organic carbon suppress nitrification. Given the negative relationship between DOC and NO_3^- observed here, it is possible that such an explanation is also relevant and that the presence of NO_3^- is indicative of reduced DOC concentrations, rather than implying a direct influence of NO_3^- upon DOC.

pH and conductivity were positively correlated to DOC. As stated above, low pH can suppress the solubility of DOC and although SO_4^{2-} was not significant in explaining variation in DOC, it was for Abs_{400}, along with Cl^-. However, this was not consistent with the DOC results and it may be that changes in pH, conductivity and anion concentrations were related to flow pathway, water source and possible mixing effects (Worrall et al., 2003a, Worrall et al., 2006a, Worrall and Adamson, 2008). Consequently, it is possible that conductivity and pH were a

proxy for flowpath and possible dilution effects. Indeed, the lack of a slope effect on runoff water DOC may be indicative of overall dilution effects, given the lower DOC concentrations in surface runoff water compared to soil pore water. Furthermore, the differing water chemistry of soil pore water and runoff water could imply that changes in pH, conductivity and anion concentrations represent mixing of different water sources or changing flow paths. Site specific trends in runoff water pH could imply a mixing effect between soil pore water and surface runoff water on Featherbed Moss, where higher water tables are more likely to lead to ponding, which was observed in the field. Ponding also occurred on Alport Low top-slope and bottom-slope plots however where water tables were closer to the surface.

Even though much of the variation in DOC can be explained by water table and changes in water chemistry, possibly associated with hydrological changes, there was still a significant slope effect that remained unaccounted for. It could be that differences in soil organic matter composition can provide an explanation. Aitkenhead and McDowell (2000) used soil C:N ratio to predict DOC flux from 164 rivers across multiple biomes, while a strong relationship between catchment C:N and DOC has also been observed by Aitkenhead-Peterson et al. (2007). Positive correlations between C:N and DOC have been observed for non-peat soils (Kindler et al., 2011), and across multiple habitats and soil classes in the UK, including heathland and moorland (van den Berg et al., 2012). It may therefore be pertinent to investigate whether there are compositional differences in the soil substrate that could explain differences in DOC across the slope.

2.6 Conclusions

This study has found a significant slope effect upon the hydrology, CO_2 flux and DOC concentration of two contrasting sites in the Peak District. Slope position was the most

important factor explaining variation in WTD, yet the behaviour of the water table was not uniform and was intrinsically dependent upon site specific conditions. Across the entire hillslope scale, slope angle was the dominant determinant upon WTD, yet the link between slope angle and WTD for individual hillslope sites was sensitive to the amount of variation in slope angle. Geomorphic features such as drainage gullies caused by erosion can further affect WTD, lowering the upslope contributing area by diverting flow away from the slope on mid-slopes. The effect of slope position was not completely explained and variation in the structural properties and composition of peat across the slope may be important. The proportion of runoff generated across the slope was highest on the lower mid-slope and lower on the bottom-slope. Differences in flowpath and the response to rainfall events may explain the differences in generation of surface water, but further work is needed to validate this.

Ecosystem respiration was higher on the mid-slopes than the bottom-slope. Although P_G, WTD and for individual slope positions temperature, were shown to affect rates of R_{eco}, the exact response of individual slope positions to these variables was not fully apparent and more work is needed to clarify the response of distinct slope positions to the abiotic and biotic drivers of R_{eco}. There was as yet unaccounted for variation with sub-slope scale heterogeneity. Gross photosynthesis was higher on the bottom-slope than the top-slope and was linked to different responses to temperature, PAR and water table variation, with a possible altitudinal effect as well. Consequently, the NEE CO_2 sink was greatest on the bottom-slope. This was related to changes in the response of the slope to P_G, vegetation cover, air temperature, PAR and slope angle. The lower NEE CO_2 sink on the top-slope was related to the lower levels of P_G relative to the bottom-slope, while it was likely that the greater rates of R_{eco} were important in determining the size of the NEE sink on the mid-slopes. Given that slope position has been found to affect R_{eco}, P_G and NEE, it is important to establish what effect incorporating slope position into carbon budget models has.

Slope position was the second most important factor controlling DOC concentration after the observed seasonal pattern associated with flushing mechanisms. There was a large decrease in DOC down-slope, but as with WTD, there was also a site-specific slope effect. Water table drawdown increased DOC concentration, most likely due to enhanced DOC production and though this trend was observed at all slope positions, its influence was most keenly observed on the mid-slopes. This was because of the deeper water tables on the steeper, eroded slope of Alport Low. There was a general trend of decreasing DOC down-slope on Featherbed Moss where water tables were close to the surface across all slope positions and the much lower concentrations of DOC in runoff water may suggest there is a dilution of DOC as water moves down the slope. Further analysis of the relationship between DOC, water chemistry and water source could provide insights into the transport of DOC across the slope. Even when water table and hydrological effects were accounted for, the top-slope had a significantly higher DOC concentration that was unaccounted for. Table 2.36 summarises the significance of slope for WTD, R_{eco}, P_G, NEE and DOC.

Table 2.36 Summary table of significance of slope position, denoted by 'X'

Response variable	ANOVA slope effect	ANCOVA slope effect
WTD	X	X
R_{eco}	X	X
P_G	X	
NEE	X	
Soil pore water DOC	X	X
Runoff water DOC		

Chapter 3 The effect of organic matter composition on carbon flux

3.1 Introduction

Soil organic matter can have an impact upon the production and export of carbon from peatlands. Silvola et al. (1996b) suggested that root respiration contributed 35-45% of total soil respiration and was associated with root exudates, litter and detritus. Furthermore, Fenner et al. (2004) linked recently assimilated carbon in soil from plant photosynthates to CO_2 efflux. The link between CO_2 efflux and labile carbon sources is well established; Hardie et al. (2011) found respired CO_2 was enriched in ^{14}C, indicating microbial decomposition favoured young, labile sources of soil organic matter. Moreover, mineralisation of root exudates has been shown to decrease in the presence of an external source of labile organic matter (glucose amendment), providing further evidence linking CO_2 efflux to soil organic matter quality (Crow and Wieder, 2005).

Reiche et al. (2010) found that production of CO_2 was greater with thermally labile organic matter, while Leifeld et al. (2012) inferred a decrease in soil respiration down a soil profile due to increasing recalcitrance of organic matter. Modelling soil respiration, Rowson et al. (2013) used a two zone model associated with rooting depth. Carbon dioxide efflux was greatest in the upper zone than deeper peat, suggesting labile carbon sources enhanced CO_2 production towards the surface, though no empirical quantification of soil organic matter quality was used (Rowson et al., 2013). The origin of peat substrate, such as the type of vegetation soil organic matter is derived from, can be important to rates of CO_2 production (Moore and Dalva, 1997), while changes in peat substrate quality have been observed with drainage (Blodau and Siems, 2012).

Soil organic matter quality has also been linked to dissolved organic carbon (DOC) production and export. Clair et al. (1994) linked high aquatic C:N ratios to terrestrially derived humic substances, suggesting aquatic carbon was derived from terrestrial plants with a low nitrogen content due to microbial decomposition. Across 164 rivers, Aitkenhead and McDowell (2000) found a positive correlation between C:N ratio and soil solution DOC concentration and export. A positive relationship was found between soil organic matter concentration and C:N ratio in Scottish moorland podzols (White et al., 1996), while Aitkenhead-Peterson et al. (2007) also linked mean catchment C:N ratio to DOC export. Across multiple soil types and land uses, Kindler et al. (2011) similarly found a positive link between topsoil C:N ratio and DOC concentration.

Kindler et al. (2011) have suggested that DOC may build-up as more easily degradable soil organic matter associated with low C:N ratios is respired or re-assimilated, preserving less easily decomposed, recalcitrant organic matter (Kindler et al., 2011, van den Berg et al., 2012). However, incubation experiments have shown that enhanced nitrogen deposition can increase DOC production, possibly by stimulating microbial activity (Bragazza et al., 2006), and the relationship between C:N and DOC is not always evident (Moore et al., 2008). In a laboratory study, Fenner et al. (2004) linked DOC to young, recently assimilated carbon and Palmer et al. (2001) suggested that young DOC produced in surface soil layers was the primary source of DOC in streamwater for Brocky Burn, North East Scotland. If peat composition can alter both soil respiration and both the concentration and composition of DOC then can it explain the differences with slope position observed in the previous chapter?

Nitrogen content has been observed to decrease down-slope between an upland oak forest and peat filled cedar swamp (Reiners and Reiners, 1970), while changes in total organic carbon content have been related to anthropogenic influence and drainage (Heller and Zeitz, 2012). Hydrothermal treatment of peat has been shown to decrease oxygen content, while

increasing carbon content and the calorific value of peat, associated with increased aromaticity (Mursito et al., 2010). Thus the content of carbon, hydrogen, nitrogen and oxygen can vary across the landscape and with land use and can be used to infer substrate quality.

Atomic ratios derived from elemental analysis are useful indicators of the origin and quality of soil organic matter. Talbot and Livingstone (1989) found H:C ratios between 0.8 – 1.3 were indicative of terrestrial plant sources of organic matter, woody and ligno-cellulosic tissue, with values between 1.3 – 1.7 indicative of herbaceous organic matter. Klavins et al. (2008) stated H:C and O:C ratios decreased with increasing humification, while Zaccone et al. (2008) associated decreasing O:C ratios with depth to carbohydrate degradation and an increase in recalcitrant phenolic constituents. Kracht and Gleixner (2000) similarly noted differences in H:C and O:C ratios between cellulose and lignin-like compounds. Use of CHNO content can also be used to derive information regarding the carbon oxidation state (C_{OX}) and oxidative ratio (OR) of soil organic matter (Masiello et al., 2008, Hockaday et al., 2009).

Thermogravimetric analysis (TG) has been widely employed to assess the weight loss of soil organic matter (Barros et al., 2007), from which the thermal stability and composition of organic matter can be established (Plante et al., 2009). Weight loss between different temperature ranges can be indicative of labile, recalcitrant and refractory carbon (Lopez-Capel et al., 2008, de la Rosa Arranz et al., 2009), while Lopez-Capel et al. (2005) and Manning et al. (2005) related changes in the response of soil organic matter weight loss to the proportion of labile cellulose or more thermally stable lignin compounds. Chen et al. (2011) identified three stages to peat pyrolysis following moisture dehydration, related to hemicellulose, cellulose and lignin; and Reiche et al. (2010) used thermogravimetric analysis to develop a peat quality index. Thus thermogravimetry can be a useful technique to assess soil, vegetation and litter. However, it can be difficult to identify differences in weight loss using qualitative methods and consequently multivariate techniques have proved effective in separating different groups of

organic material (Bergner and Albano, 1993). Indeed, Persson et al. (1986) suggested univariate techniques were inadequate when analysing peat using thermogravimetric analysis, supporting multivariate analysis and methods such as principal components analysis can be used as a data reduction technique (Leinweber et al., 2001).

This chapter shall assess the composition and quality of organic matter derived from soil, vegetation and litter, employing a variety of analytical and statistical techniques to identify potential changes in organic matter composition across the hillslope and between substrate source and depth down a soil profile. The data shall be used in conjunction with CO_2 flux and DOC concentration data from Chapter 2 to establish whether differences in soil organic matter source, composition and quality can be related to carbon cycling.

3.2 Aims and objectives

The aim of this chapter is to identify potential changes in the physical and chemical composition of soil organic matter and relate these to slope position, sample depth and substrate origin. The objectives are:

- Establish the influence of slope position upon the physical and chemical composition of organic matter.
- Identify changes in soil organic matter quality down the soil profile.
- Understand how organic matter composition changes between vegetation types, litter and the topsoil.
- Incorporate measures of soil organic matter composition in CO_2 and DOC ANOVA models to establish whether they influence carbon production and export.

3.3 Materials and methods

3.3.1 Soil and vegetation

Between July and August 2011, 20, one metre deep soil cores were collected; one for each sub-slope position on Featherbed Moss and Alport Low (Figure 2.1, section 2.3.1). Samples were divided into multiple subsections. The top 5 cm was divided into 2.5 cm sections to allow more detailed measurement of surface samples, with a further subdivision of 5 cm sections comprising the remainder of the top 20 cm. From 20 cm to 100 cm depth, cores were separated into 10 cm increments. Samples were sealed in polyethylene bags prior to analysis. On return to the laboratory, samples were air dried to remove surface moisture. Alport Low cores were oven dried from ~0900 - 1700 at ~70°C, then at 105°C overnight for more than 12 hours. Featherbed Moss cores were dried at 105°C for 24 hours. Bulk density (Eq. 3.1) was determined as follows:

$$\rho_{bd} = \frac{m_d}{V} \quad 3.1$$

Where: ρ_{bd} = dry bulk density (g cm^{-3}); m_d = dry mass of sample (g); and V = volume of sample (cm^{-3}) determined from the length (cm) x height (cm) x width (cm) of sample. Woody and vegetative tissue was subsequently removed and soil samples homogenised using a pestle and mortar and sieved to pass through a 500 µm sieve.

Vegetation and litter samples were collected for each sub-slope in April 2012. *Eriophorum spp.* was collected on Featherbed Moss and the *Eriophorum spp.* plots on Alport Low. Hummock plots on Alport Low were composed of a mixture of *Eriophorum spp.* and *Vaccinium myrtillus*. Non-*Sphagnum* moss *spp.* was collected for one sub-slope on the Alport Low upper mid-slope and bottom-slope. On return to the laboratory, samples were air dried, oven dried at 105°C for 24 hours and homogenised using a SPEX SamplePrep 6770 Freezer/Mill (Stanmore, UK) for three minutes at 12 CPS.

3.3.2 Elemental analysis

CHNO analysis was performed on a COSTECH ECS 4010 Elemental Combustion System with pneumatic autosampler. The ECS 4010 was set up for separate CHN and O analysis. For CHN, two reactors were used: Reactor 1 consisted of chromium (III) oxide / Silvered cobaltous-cobaltic oxide catalysts at 1020 °C. Reactor 2 consisted of reduced high purity copper wires at 650 °C. Helium was used as the carrier gas at a flow rate of 120 – 140 cc min^{-1}. This was filtered for hydrocarbons upstream of the instrument. A packed (Porous Polymer, HayeSep Q) 2m GC column was used for separation of the gases. A thermal conductivity detector (TCD) was used to calculate the signal of each sample, set to a temperature of 60-70 °C. For O analysis, the reactor contained nickelised carbon, nickel wool, silica chips, silica wool and a water trap to remove moisture. Helium was used as the carrier gas at a flow rate of 130 – 140 cc min^{-1} and chloropentane added as a doping agent to aid combustion. The furnace was run at 1060 °C and oven temperature 60-65 °C

CHN calibration was conducted using a suite of acetanilide standards across a weight range of 0.5 – 2.5 mg. Extra standards at ~4.0 and 5.0 mg were used in oxygen analysis. Calibration curves were based on linear or quadratic regression, with an R^2 >0.999. Samples were weighed in triplicate in tin capsules, between 1.5 – 2.5 mg. Every 24 samples, acetanilide was measured in triplicate between 1.5 – 2.5 mg to check for drift. As a further check against analytical error or sample heterogeneity, if the relative standard error for a given sample was >5%, the sample was analysed again.

All soil samples were analysed for CHN content, but it was not possible to conduct a complete analysis of oxygen content. The top 20 cm samples and 90 – 100 cm were analysed for one sub-slope core across both study sites. All cores were analysed for oxygen content at 0 – 2.5 cm and 90 – 100 cm. If no sample could be obtained from the soil cores at 90 – 100 cm, the deepest sample was used. Vegetation and litter samples underwent complete analysis of

CHNO content. Cellulose (Whatman 90 mm filter papers, GE Healthcare UK Ltd, Buckinghamshire, UK), humic acid (humic acid crystalline powder, Alfa Aesar A Johnson Matthey Company, Massachusetts, USA) and lignin (lignin, alkali, SIGMA-ALDRICH, Steinheim, Germany) reference materials were also analysed for CHNO.

CHNO content was converted from weight percent into molar concentration, from which the atomic ratios of C:N, H:C and O:C were determined. C_{OX} was derived as below in Eq. 3.2:

$$C_{OX} = \frac{2O-H+3N}{C} \quad (3.2)$$

Where O, H, N, and C are the molar concentrations of each element. Using C_{OX}, OR was determined (Eq. 3.3):

$$OR = 1 - \frac{C_{OX}}{4} + \frac{3N}{4C} \quad (3.3)$$

Derivation of C_{OX} and OR was based upon equations 3 & 5 from Masiello et al. (2008)

3.3.3 Energy content (gross heat value)

Energy content, gross heat value, was determined using a 6200 Isoperibol Calorimeter (0.1% Precision Classification, Parr Instrument Company, Illinois, USA) with 1108(P) Oxygen Bomb. Calibration was performed as a rolling average of 10 benzoic acid standards (Parr Instrument Company, Illinois, USA). Samples were placed in crucibles and compressed to stabilise the peat surface and weighed between 0.5 - 1.1 g. Below 0.5 g benzoic acid spikes were added to aid combustion. Prior to combustion, de-ionised water was added, again to aid complete sample combustion. Following analysis, fuse corrections were performed by measuring the length of any remaining fuse wire, measured in calories and converting to MJ

Kg^{-1}. Each measurement was monitored for incomplete combustion (the presence of soot or sample in the bomb) with the results discarded and samples reanalysed.

All soil, vegetation and litter samples were analysed for energy content, but it was not possible to conduct repeat measurements due to the mass of sample required for analysis (unless required due to incomplete combustion, as stated above) and time constraints. As with CHNO content, cellulose, humic acid and lignin were measured as reference substances in triplicate. It was therefore possible to determine the standard error associated with instrument error for these substances, though not error due to sample heterogeneity.

3.3.4 Thermogravimetric analysis

Thermal stability of soil and vegetation was assessed using thermogravimetric analysis (TG) on a STA *i* 1200 (Instrument Specialists Inc., Wisconsin, USA). Samples were heated in a nitrogen atmosphere (analytical gas flow rate 25 - 30 cc min^{-1}, purge flow rate 25 – 40 cc min^{-1}) from ambient temperature to 700 °C at a heating rate of 10 °C min^{-1} to determine weight loss across the temperature range associated with organic material. The top 20 cm and deepest sample of all soil cores were analysed, with complete analysis of vegetation and litter. Between 200 – 335 mg of sample was used, but on four occasions <200 mg of sample was used due to limitations of available sample. It was not possible to conduct repeat measurements but cellulose, humic acid and lignin were measured in triplicate. The sample mass of reference substances was less than that of soil and vegetation samples due to the highly responsive nature of the samples. Cellulose varied between 30.2 – 38.7 mg, humic acid 100.7 – 109.1 mg and lignin 61.1 – 217.6 mg. This allowed an assessment of whether the response of weight loss characteristics varied with changing sample mass.

3.3.5 Statistical analysis

Prior to statistical analysis, ρ_{bd}, elemental composition, atomic ratios, C_{OX}, OR and energy content had outlying values removed by identifying values beyond three standard deviations. If log transformation was performed (section 3.3.5.1, below), log transformed datasets also had outlying values removed. Outlier removal was performed to remove extreme values and improve dataset distribution.

3.3.5.1 Analysis of variance and covariance

Analysis of variance (ANOVA) was performed on ρ_{bd}, elemental composition, atomic ratios, C_{OX}, OR, energy content and key principal components from multivariate analysis (see below). Prior to analysis, the Anderson-Darling test was used to assess the distribution of each dataset. If a given dataset failed the assumption of normality, it was natural-log transformed. If this failed to normalise the distribution, the dataset with the lowest Anderson-Darling statistic was used. This was not done for principal component scores (see below), which were both positive and negative. The Kruskal-Wallis non-parametric test was performed on non-normal datasets to determine whether significant variation with slope position held true. Levene's test was performed to assess whether each dataset passed the assumption of homogeneity of variance between factor levels.

Separate analyses were performed for soil and vegetation. Significant differences were performed on soil samples using three factor levels: site (Featherbed Moss and Alport Low); slope (top-slope, upper mid-slope, lower mid-slope and bottom-slope); and depth (0-2.5 cm, 2.5-5 cm, 5-10 cm, 10-15 cm, 15-20 cm, thereon 10 cm increments). Interactions were also assessed. For all datasets but ρ_{bd}, vegetation was assessed using factors of site, slope and vegetation (*Eriophorum spp., Eriophorum-Vaccinium* mix, non-*Sphagnum* moss *spp.* and litter).

The topsoil (0-2.5 cm) sample was included to assess compositional change during decomposition of vegetation to litter and soil. For multivariate principal component ANOVA, site, slope and substrate were used as factor levels. Substrate was classed as peat sample depth and vegetation type in this analysis.

3.3.5.2 Principal components analysis

Thermogravimetric weight loss was assessed using principal components analysis (PCA). Weight loss was determined every 10 °C between 180 – 600 °C (after the dehydration peak and after most weight loss associated with organic matter) to identify key weight loss intervals associated with labile, recalcitrant or refractory organic matter. Each weight loss interval had values outside three standard deviations removed. Cellulose, humic acid and lignin were included to determine whether sample weight loss reflected that of a reference substrate. Principal components (PCs) used were all PCs with an eigenvalue >1 and the first PC with an eigenvalue <1. Analysis of variance was performed on key principal components to identify significant trends.

Thermogravimetric principal components that showed an important trend were added to a multivariate dataset including atomic ratios, C_{OX}, OR and energy content. Each variable was z transformed (Eq. 3.4) to standardise the scales. The same selection procedure outlined above was used to determine the number of principal components used in the analysis. Analysis of variance was similarly performed on individual components, while regression analysis was performed on the TG principal components included in the multivariate PCA, to identify what compositional characteristics were associated with weight loss for a given component.

$$z = \frac{(x - \bar{x})}{\sigma} \qquad 3.4$$

Where: x = the measured value, $\bar{x}$ = the dataset mean and σ = the dataset standard deviation.

3.3.5.3 Impact upon hydrology and carbon flux

To test whether changes in organic matter composition affected CO_2 flux and DOC concentration, C:N, H:C and energy content were averaged across the top 20 cm for peat samples and included in the final Analysis of covariance (ANCOVA) models from Chapter 2 as covariates. Each core represented a sub-slope. Carbon oxidation state, OR and O:C were not included as they were not complete datasets. Backwards and forwards modelling was applied. A complete suite of atomic ratios, C_{OX}, OR and energy content was included from litter samples to test whether compositional changes in litter were significant; this was performed as a separate analysis to the soil covariates. Bulk density was used as a covariate in the WTD model; no composition variables were included.

Regression analysis was performed, incorporating any significant covariates from the ANCOVA model, to determine the nature of the correlation between a response variable and the covariate. Variance inflation factors were used to assess covariance, while residuals were tested for normal distributions.

3.4 Results

Table 3.1 shows the percentage of data removed as outliers for each variable analysed using ANOVA or PCA, by soil and substrate (vegetation, litter, 0 -2.5 cm) datasets. The largest percentage removed belonged to the TGA dataset at 7.14%. However, this was because PCA must be performed without data gaps and the number of data points removed was an accumulation of 42 columns of data (180 – 600 °C, at 10 °C weight loss steps) that had outliers

removed. Although 11 rows were removed, the maximum from an individual column was five (3.25%). The highest number of data points removed from a soil dataset was three (1.20%) while for substrate datasets, two data points from the energy content dataset meant 3.33% of data was removed.

Table 3.1 Percentage of data removed from each dataset

Variable	Dataset	N	N removed	% removed
ρ_{bd}	Soil	223	1	0.45
C	Soil	249	0	0.00
	Substrate	60	1	1.67
N	Soil	249	0	0.00
	Substrate	60	0	0.00
H	Soil	249	3	1.20
	Substrate	60	0	0.00
O	Soil	89	0	0.00
	Substrate	60	0	0.00
C:N	Soil	249	0	0.00
	Substrate	60	0	0.00
H:C	Soil	249	1	0.40
	Substrate	60	0	0.00
O:C	Soil	89	0	0.00
	Substrate	60	0	0.00
C_{OX}	Soil	89	0	0.00
	Substrate	60	1	1.67
OR	Soil	89	0	0.00
	Substrate	60	1	1.67
Energy content	Soil	249	2	0.80
	Substrate	60	2	3.33
TGA	TGA	154	11	7.14

Table 3.2 – Table 3.4 provide details of reference material CHNO content, atomic ratios, C_{OX}, OR and energy content. Descriptive statistics of all response variables are provided for slope (Table 3.5) and substrate (Table 3.6). To observe changes with depth, graphs of the raw data are used for each analytical section. For reasons of brevity, only significant

differences from ANOVA *post hoc* tests associated with slope position are shown, as this is the main focus of the research. Significant trends associated with sample depth are nonetheless discussed in the text. Kruskal-Wallis test results are only reported where distributions were non-normal and the non-parametric test disagreed with the ANOVA model for the relevant response variable.

Table 3.2 Reference material CHNO content ± standard error (SE)

	C (%)		N (%)		H (%)		O (%)	
Material	**Mean**	**SE Mean**	**Mean**	**SE Mean**	**Mean**	**SE Mean**	**Mean**	**SE Mean**
Cellulose	42.81	0.02	N/A	N/A	6.2	0.2	51.0	0.1
Humic acid	35.90	0.07	0.86	0.04	3.68	0.09	32.4	0.3
Lignin	61.63	0.09	0.82	0.01	6.0	0.1	29.0	0.2

Table 3.3 Reference material atomic ratios, C_{OX}, and OR

	C:N	H:C	O:C	C_{OX}	OR
Material	**Mean**	**Mean**	**Mean**	**Mean**	**Mean**
Cellulose	N/A	1.74	0.89	0.049	0.988
Humic acid	48.51	1.23	0.68	0.185	0.969
Lignin	87.33	1.17	0.35	-0.434	1.117

Table 3.4 Reference material energy content ± standard error (SE)

Energy content (MJ Kg^{-1})		
Material	**Mean**	**SE Mean**
Cellulose	16.6	0.2
Humic acid	12.57	0.03
Lignin	25.53	0.03

Table 3.5 Descriptive statistics for response variables by slope across entire one metre core: SE = standard error

Variable	Slope	N	Mean	SE Mean	Maximum	Minimum	Variable	Slope	N	Mean	SE Mean	Maximum	Minimum
ρ_{bd} (g cm^{-3})	Top-slope	63	0.219	0.009	0.543	0.094	H:C	Top-slope	74	1.289	0.008	1.48	1.15
	Upper Mid-slope	42	0.207	0.009	0.359	0.117		Upper Mid-slope	49	1.271	0.007	1.36	1.09
	Lower Mid-slope	47	0.20	0.01	0.370	0.094		Lower Mid-slope	50	1.296	0.008	1.41	1.19
	Bottom-slope	71	0.195	0.007	0.382	0.111		Bottom-slope	76	1.311	0.007	1.46	1.19
C (%)	Top-slope	74	51.4	0.3	56.52	46.04	O:C	Top-slope	30	0.51	0.01	0.63	0.38
	Upper Mid-slope	49	52.0	0.2	54.99	48.72		Upper Mid-slope	18	0.497	0.008	0.54	0.43
	Lower Mid-slope	50	51.6	0.3	54.45	47.06		Lower Mid-slope	16	0.49	0.01	0.57	0.41
	Bottom-slope	76	50.5	0.2	52.95	46.54		Bottom-slope	25	0.534	0.008	0.60	0.41
N (%)	Top-slope	74	1.30	0.04	2.43	0.81	C_{OX}	Top-slope	30	-0.22	0.02	-0.061	-0.425
	Upper Mid-slope	49	1.36	0.05	2.32	0.85		Upper Mid-slope	18	-0.19	0.01	-0.093	-0.324
	Lower Mid-slope	50	1.34	0.05	2.48	0.81		Lower Mid-slope	16	-0.23	0.02	-0.076	-0.321
	Bottom-slope	76	1.23	0.04	2.13	0.81		Bottom-slope	25	-0.17	0.02	-0.027	-0.308
H (%)	Top-slope	74	5.52	0.03	6.44	4.90	OR	Top-slope	30	1.074	0.005	1.128	1.027
	Upper Mid-slope	49	5.50	0.03	5.93	4.86		Upper Mid-slope	18	1.068	0.004	1.110	1.039
	Lower Mid-slope	50	5.57	0.03	6.06	5.06		Lower Mid-slope	16	1.077	0.005	1.114	1.033
	Bottom-slope	76	5.51	0.02	6.28	4.96		Bottom-slope	25	1.060	0.004	1.094	1.019
O (%)	Top-slope	30	33.8	0.7	39.97	26.37	Energy content (MJ Kg^{-1})	Top-slope	74	20.3	0.1	22.4204	17.6353
	Upper Mid-slope	18	34.0	0.7	38.41	28.89		Upper Mid-slope	49	20.5	0.1	22.1792	18.9742
	Lower Mid-slope	16	33.3	0.9	40.41	27.71		Lower Mid-slope	50	20.5	0.1	21.8645	18.6448
	Bottom-slope	25	35.5	0.6	40.45	27.54		Bottom-slope	76	19.74	0.07	21.0453	17.2890
C:N	Top-slope	74	49	1	75.40	22.22							
	Upper Mid-slope	49	47	2	75.31	25.52							
	Lower Mid-slope	50	48	2	78.30	22.14							
	Bottom-slope	76	51	1	74.97	25.49							

Table 3.6 Descriptive statistics for response variables by substrate: SE = standard error

Variable	Substrate	N	Mean	SE Mean	Maximum	Minimum	Variable	Substrate	N	Mean	SE Mean	Maximum	Minimum
	Eriophorum spp.	12	46.66	0.08	46.98	46.01		*Eriophorum spp*.	12	1.67	0.05	1.79	1.14
	Mixed	7	48.3	0.3	49.46	47.28		Mixed	7	1.70	0.02	1.79	1.62
C (%)	NSM	2	48.1	0.5	48.51	47.62	H:C	NSM	2	1.67	0.09	1.76	1.59
	Litter	19	47.3	0.2	49.52	46.01		Litter	19	1.72	0.01	1.82	1.63
	0 - 2.5	20	48.6	0.4	52.23	46.28		0 - 2.5 cm	20	1.31	0.02	1.46	1.15
	Eriophorum spp.	12	1.34	0.04	1.58	1.10		*Eriophorum spp*.	12	0.634	0.003	0.65	0.62
	Mixed	7	1.6	0.2	2.24	1.11		Mixed	7	0.584	0.006	0.60	0.56
N (%)	NSM	2	2.0	0.3	2.24	1.68	O:C	NSM	2	0.59	0.06	0.65	0.53
	Litter	19	1.33	0.05	1.79	0.88		Litter	19	0.623	0.008	0.72	0.57
	0 - 2.5 cm	20	1.98	0.06	2.48	1.22		0 - 2.5 cm	20	0.49	0.01	0.59	0.38
	Eriophorum spp.	12	6.5	0.2	6.96	4.43		*Eriophorum spp*.	12	-0.32	0.05	0.183	-0.438
	Mixed	7	6.85	0.06	7.12	6.64		Mixed	7	-0.45	0.02	-0.389	-0.517
H (%)	NSM	2	6.7	0.3	6.98	6.42	C_{OX}	NSM	2	-0.38	0.02	-0.368	-0.400
	Litter	19	6.77	0.05	7.25	6.45		Litter	19	-0.40	0.02	-0.270	-0.549
	0 - 2.5 cm	20	5.30	0.06	5.72	4.9		0 - 2.5 cm	20	-0.22	0.02	-0.089	-0.403
	Eriophorum spp.	12	39.5	0.2	40.83	38.64		*Eriophorum spp*.	12	1.10	0.01	1.130	0.974
	Mixed	7	37.6	0.2	38.29	36.64		Mixed	7	1.134	0.004	1.148	1.113
O (%)	NSM	2	38	4	41.28	34.58	OR	NSM	2	1.123	0.008	1.130	1.115
	Litter	19	39.2	0.4	44.77	37.33		Litter	19	1.118	0.005	1.156	1.086
	0 - 2.5 cm	20	31.9	0.6	37.37	26.37		0 - 2.5 cm	20	1.081	0.005	1.123	1.049
	Eriophorum spp.	12	41	1	49.38	34.51		*Eriophorum spp*.	12	18.03	0.07	18.4405	17.7448
	Mixed	7	38	4	51.98	24.63	Energy content ($MJ\ Kg^{-1}$)	Mixed	7	19.1	0.1	19.5933	18.7741
C:N	NSM	2	29	4	33.07	25.27		NSM	2	19.0	0.2	19.2729	18.8059
	Litter	19	43	2	62.01	31.06		Litter	19	18.4	0.1	19.2723	17.7273
	0 - 2.5 cm	20	29	1	49.95	22.14		0 - 2.5 cm	20	19.4	0.2	21.6008	17.2890

3.4.1 Bulk density

Mean ρ_{bd} (Table 3.5) decreased down-slope from 0.219 ± 0.009 g cm^{-3} on the top-slope to 0.195 ± 0.007 g cm^{-3} on the bottom-slope. The maximum ρ_{bd} was 0.543 g cm^{-3} on the top-slope, with a minimum of 0.094 g cm^{-3} on the top-slope and lower mid-slope. The ρ_{bd} values were higher than those reported by Lewis et al. (2012) but within the range of Holden and Burt (2002a) for peat surfaces covered by *Eriophorum spp*.

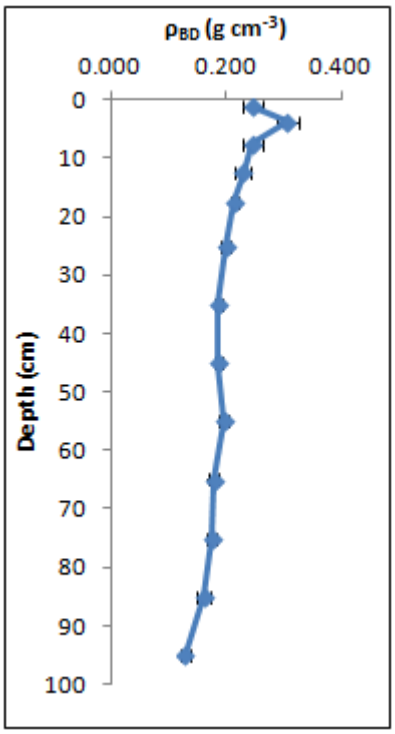

Figure 3.1 Mean bulk density with depth ± standard error

Bulk density decreased with depth, from a mean high of 0.31 ± 0.02 g cm^{-3} at 2.5 – 5 cm, to 0.128 ± 0.008 g cm^{-3} at 90 – 100 cm depth (Figure 3.1). Declining ρ_{bd} at depth goes against the acrotelm-catotelm model of ρ_{bd}, for which ρ_{bd} is expected to be higher in the catotelm than the acrotelm. Clymo (1992) reported ρ_{bd} values of 0.03 and 0.12 g cm^{-3} for the acrotelm and catotelm respectively, with an increase in ρ_{bd} through the acrotelm and

relatively stable ρ_{bd} in the catotelm. Although ρ_{bd} has been shown to increase with depth (Holden, 2005a), the relationship with depth can be variable, with Coggins et al. (2006) reporting both abrupt increases and decreases in ρ_{bd} at depth. Tallis (1985) found some cores on Featherbed Moss, including on the top-slope plateau and eroded areas, decreased in ρ_{bd} at depth.

Analysis of variance (Table 3.7) indicated that site ($p < 0.0001$, $\omega^2 = 4.51\%$), slope ($p = 0.001$, $\omega^2 = 1.74\%$) and depth ($p < 0.0001$, $\omega^2 = 41.58\%$) were significant factors explaining variation in ρ_{bd}, while there was also a significant interaction between site and slope ($p = 0.003$, $\omega^2 = 2.58\%$). *Post hoc* results confirmed a significant decrease in ρ_{bd} down-slope between the top-slope (0.202 g cm^{-3}) and upper mid-slope (0.208 g cm^{-3}) and bottom-slope (0.179 g cm^{-3}, Figure 3.2). The interaction effect suggested ρ_{bd} increased on the mid-slopes of Alport Low, while showing a general decrease down-slope on Featherbed Moss. The change in ρ_{bd} down the soil profile (Figure 3.1) was confirmed; ρ_{bd} in the top 15 cm was significantly higher than 60 – 100 cm and all depths but 80 – 90 cm were significantly higher than 90 - 100 cm. There was no significant interaction for depth with either site or slope, suggesting the depth profile was consistent across the study sites and between slope positions. The ANOVA error term is not reported, but includes unexplained factors and interactions alongside measurement error.

Table 3.7 Lnρ_{bd} ANOVA: ω^2 = % variance

ρ_{bd} ANOVA		
Factor	**P**	**ω^2**
Site	<0.0001	4.51%
Slope	0.001	1.74%
Depth	<0.0001	41.58%
Site*Slope	0.003	2.58%
N 222		**R^2 50.53%**

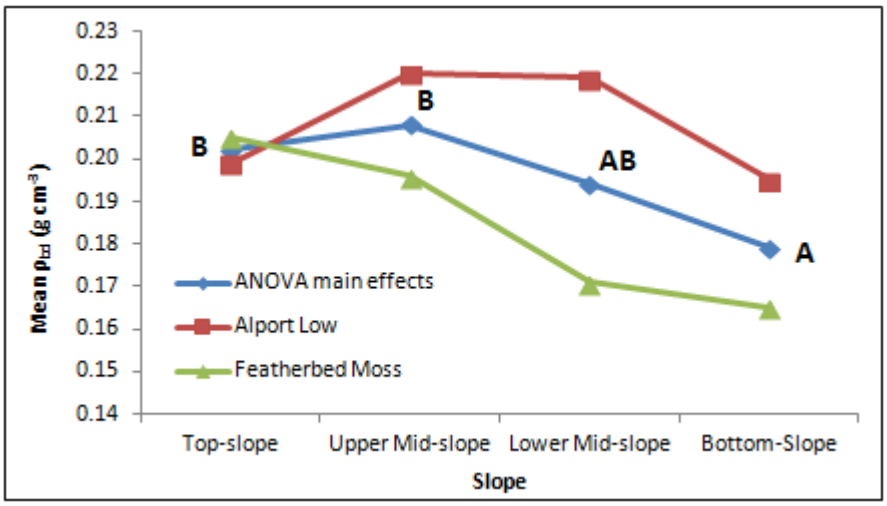

Figure 3.2 Lnρ_{bd} ANOVA main effects & interaction plot: significant differences denoted where letters are not shared between slope positions

3.4.2 Elemental composition

Soil carbon content (Table 3.5) was greatest on the upper mid-slope (52.0 ± 0.2%) and decreased to a low on the bottom-slope (50.5 ± 0.2%), with a maximum of 56.52% and minimum of 46.04% on the top-slope. Carbon in peat was therefore between cellulose (42.81 ± 0.02%, Table 3.2) and lignin (61.63 ± 0.09%). Andersson et al. (2012) found a mean total carbon content of 45.3% in bog peat. Carbon increased with depth (Figure 3.3), from 48.6 ± 0.4% at 0 – 2.5 cm to 52.9 ± 0.3% at 90 – 100 cm depth. There was a noticeable spike in carbon observed at 2.5 – 5 cm relative to the top 15 cm, with an increase to 50.5 ± 0.3%. Reiche et al. (2010) observed both increases and decreases in carbon content with depth from cores at an acidic fen in Germany.

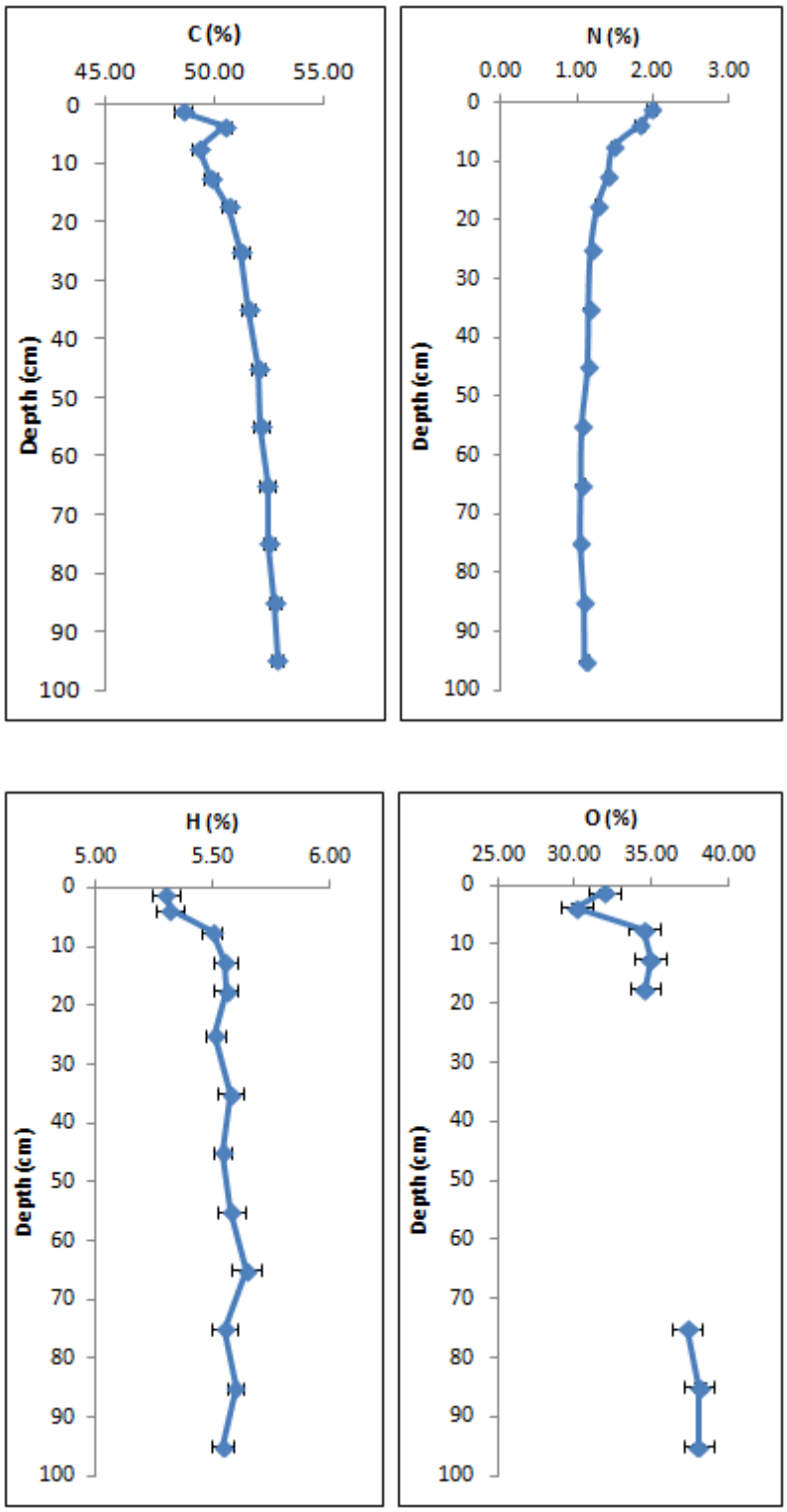

Figure 3.3 Mean CHNO content with depth ± standard error

Table 3.8 CHNO soil and substrate ANOVA: ω^2 = % variance

Soil Carbon ANOVA			**Substrate LnCarbon ANOVA**		
Factor	**P**	**ω^2**	**Factor**	**P**	**ω^2**
Site	<0.0001	1.09%	Substrate	<0.0001	25.17%
Slope	<0.0001	9.47%			
Depth	<0.0001	45.88%			
Site*Slope	<0.0001	3.61%			
N 249		**R^2 60.15%**	**N 59**		**R^2 25.50%**
Soil LnNitrogen ANOVA			**Substrate LnNitrogen ANOVA**		
Factor	**P**	**ω^2**	**Factor**	**P**	**ω^2**
Slope	<0.0001	2.52%	Slope	0.038	4.65%
Depth	<0.0001	67.93%	Substrate	<0.0001	51.28%
N 249		**R^2 70.54%**	**N 59**		**R^2 56.35%**
Soil Hydrogen ANOVA			**Substrate Hydrogen ANOVA**		
Factor	**P**	**ω^2**	**Factor**	**P**	**ω^2**
Depth	<0.0001	12.87%	Substrate	<0.0001	76.48%
N 246		**R^2 12.92%**	**N 60**		**R^2 76.78%**
Soil Oxygen ANOVA			**Substrate Oxygen ANOVA**		
Factor	**P**	**ω^2**	**Factor**	**P**	**ω^2**
Site	0.023	1.85%	Substrate	<0.0001	72.41%
Slope	0.014	4.31%			
Depth	<0.0001	56.84%			
N 89		**R^2 63.26%**	**N 60**		**R^2 72.74%**

ANOVA (Table 3.8) showed site ($p < 0.0001$, $\omega^2 = 1.09\%$), slope ($p < 0.0001$, $\omega^2 = 9.47\%$), depth ($p < 0.0001$, $\omega^2 = 45.88\%$) and an interaction between site and slope were significant ($p < 0.0001$, $\omega^2 = 3.61\%$). Slope was consequently the second most important factor to explain variation in carbon content after sample depth. *Post hoc* results revealed that the bottom-slope (50.33%, Figure 3.4) had significantly lower carbon content than all other slope positions. Carbon was higher on Alport Low than Featherbed Moss, showing a decrease down-slope on Featherbed Moss but with elevated carbon content on the Alport Low mid-slopes. There was a significant increase in carbon content with depth. 0 – 2.5 cm was significantly lower than 15 – 100 cm, while 5 – 15 cm depths were significantly lower than 20 – 100 cm. 20 – 30 cm carbon

content was lower than 80 – 100 cm, but higher than 0 – 2.5 cm and 5 – 15 cm. The increase in carbon content at 2.5 – 5 cm was significant compared to 0 – 2.5 cm.

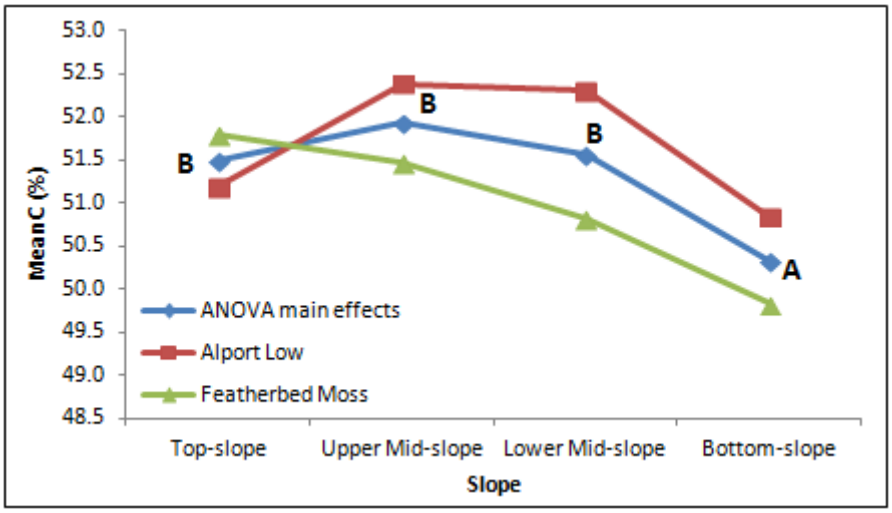

Figure 3.4 Carbon ANOVA main effects & interaction plot by slope: significant differences denoted where letters are not shared between slope positions

Comparing substrate, carbon content (Table 3.6) was greatest in the topsoil (48.6 ± 0.4%) and was also high in non-*Sphagnum* moss *spp*. (48.1 ± 0.5%) and mixed vegetation (48.3 ± 0.3%) of *Eriophorum spp.* and *Vaccinium myrtillus*. Carbon was lower in litter (47.3 ± 0.2%) and *Eriophorum spp.* (46.66 ± 0.08%). Clay and Worrall (2011) reported litter and vegetation carbon content of ~45 – 50%, while Thormann and Bayley (1997) reported 43.5 – 45.3% for *Eriophorum vaginatum*. As with the soil cores, carbon content was higher than in cellulose but lower than lignin (Table 3.2). ANOVA (Table 3.8) showed that substrate ($p < 0.0001$, $\omega^2 = 25.17\%$) was the only significant factor to explain variation in carbon content. There was a significant increase (Figure 3.5) in carbon content between *Eriophorum spp.* vegetation and

litter to topsoil, while there was also a significant difference between *Eriophorum spp.* and mixed vegetation.

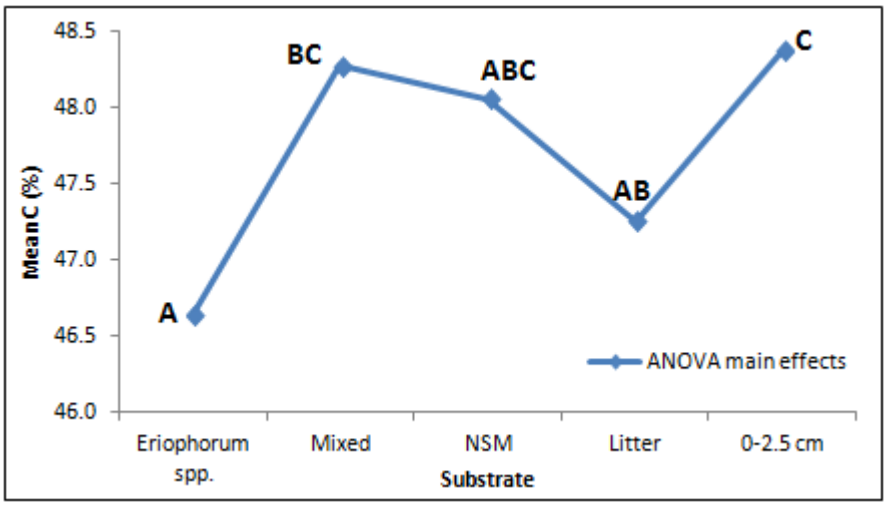

Figure 3.5 Carbon ANOVA main effects plot by substrate: significant differences denoted where letters are not shared between substrates; NSM = Non-Sphagnum moss spp.

Nitrogen content in peat (Table 3.5) was greatest on the upper mid-slope (1.36 ± 0.05%) and lowest on the bottom-slope (1.23 ± 0.04%), with a range of 0.81 – 2.48%. This was higher than humic acid (0.86 ± 0.04, Table 3.2) and lignin (0.82 ± 0.01). Reiche et al. (2010) reported a range of 0.5 – 2.1% nitrogen. In contrast to carbon content, there was a preferential depletion of nitrogen down the soil profile (Figure 3.3), declining from 1.98 ± 0.06% at 0 – 2.5 cm depth to 1.11 ± 0.04% at the bottom of the core, though the lowest mean was 1.05 ± 0.03% at 70 – 80 cm. Much of the decrease occurred within the top 20 cm of the core, with a mean of 1.28 ± 0.04% at 15 – 20 cm depth. ANOVA (Table 3.8, R^2 = 70.54%) indicated that slope ($p < 0.0001$, ω^2 = 2.52%) and depth ($p < 0.0001$, ω^2 = 67.93%) were significant factors.

Figure 3.6 shows nitrogen content on the bottom-slope (1.18%) was significantly lower than all other slope positions, as with carbon. The significant differences with depth occurred within the top 20 cm, with the top 5 cm having significantly higher nitrogen content than the rest of the soil profile. Nitrogen at 5 – 10 cm depth was greater than 15 – 100 cm and at 10 – 15 cm it was more than 20 – 100 cm. Nitrogen content at 15 – 20 cm depth was only significantly higher than 50 – 60 cm, indicating little variation in nitrogen content beyond 20 cm depth, as was seen in Figure 3.3.

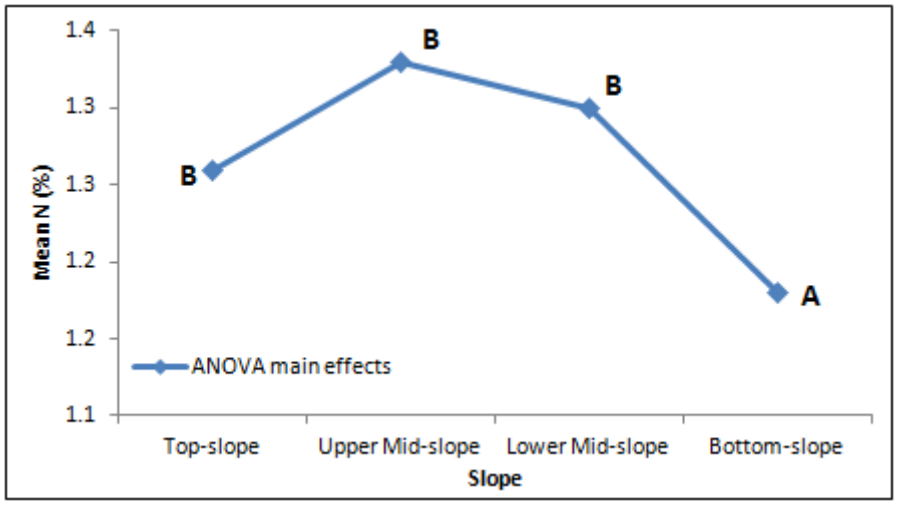

Figure 3.6 Soil nitrogen ANOVA main effects plot by slope: significant differences denoted where letters are not shared between slope positions

Nitrogen (Table 3.6) was lowest in *Eriophorum spp.* (1.34 ± 0.04%) and litter (1.33 ± 0.05%) and greatest in the topsoil (1.98 ± 0.06). This was higher than the nitrogen content of humic acid and lignin (Table 3.2). Thormann and Bayley (1997) reported *Eriophorum vaginatum* nitrogen content of 1.8%. ANOVA (R^2 = 56.35%, Table 3.8) indicated that slope (p 0.038, ω^2 = 4.65%) and substrate (p <0.0001, ω^2 = 51.28%) were significant. There was a

significant difference in nitrogen between the lower mid-slope (1.83%, Figure 3.7) and bottom-slope (1.54%). Nitrogen was higher in the topsoil (1.98%, Figure 3.8) than *Eriophorum spp.* (1.35%) and mixed (1.58%) vegetation, as well as litter (1.32%). Non-*Sphagnum* moss *spp*. (2.01%) had significantly greater nitrogen content than *Eriophorum spp.* and litter.

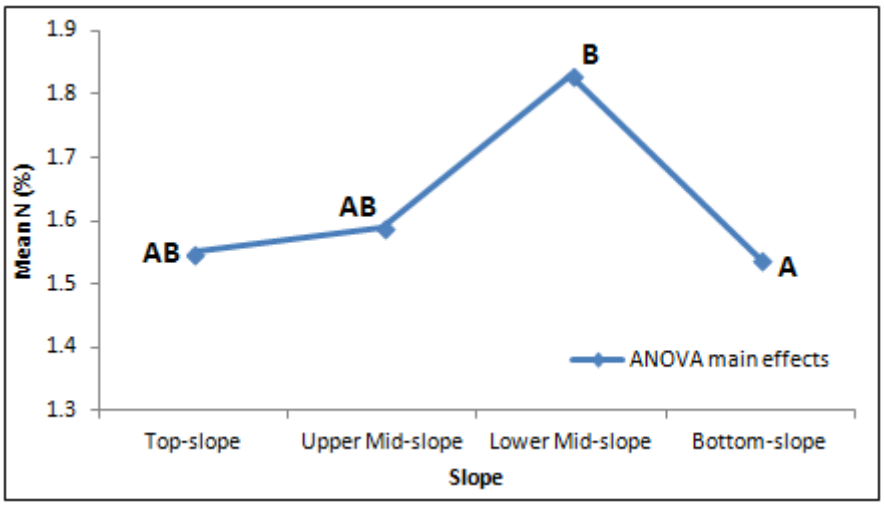

Figure 3.7 Substrate nitrogen ANOVA main effects by slope: significant differences denoted where letters are not shared between slope positions

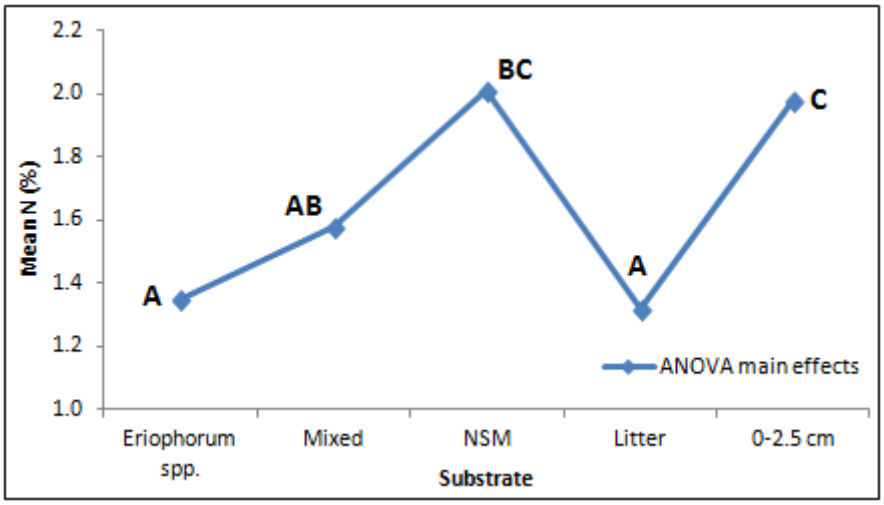

Figure 3.8 Substrate nitrogen ANOVA main effects plot by substrate: significant differences denoted where letters are not shared between substrates; NSM = Non-Sphagnum moss

Hydrogen was greatest on the lower mid-slope (5.57 ± 0.03%, Table 3.5) and lowest on the upper mid-slope (5.50 ± 0.03%), though there was little variation between the slope positions. Hydrogen ranged from 4.86 – 6.44%. Kracht and Gleixner (2000) reported a range of 5.3 – 6.65% hydrogen in the top 10 cm of peat, while Andersson et al. (2012) reported a range of 4.8 – 6.4% in bog peat. Across the slope, hydrogen was considerably higher than in humic acid (3.68 ± 0.09%) but lower than lignin (6.0 ± 0.1%) and cellulose (6.2 ± 0.2%). Hydrogen was lowest at 0 – 2.5 cm (5.30 ± 0.06%, Figure 3.3), with an observable increase from 5 – 10 cm (5.50 ± 0.04%), with hydrogen content peaking at 60 – 70 cm (5.65 ± 0.06%). Reiche et al. (2010) reported both increases and decrease in hydrogen content with depth. Sample depth ($p < 0.0001$, $\omega^2 = 12.87\%$) was the only significant factor in the ANOVA model ($R^2 = 12.92\%$, Table 3.8), with hydrogen at 0 – 2.5 cm significantly lower than 10 – 20 and from 30 – 100 cm, while 2.5 – 5 cm had significantly lower nitrogen than 10 – 20, 40 – 50 and 60 – 100 cm sample depths. There was more unexplained variance for hydrogen than carbon and nitrogen and the error term included factors and interactions not be accounted for in the research design.

Though 0 – 2.5 cm had the highest nitrogen and carbon content (Table 3.6) it had the lowest hydrogen content (5.30 ± 0.06%). Vegetation and litter varied between 6.85 ± 0.06% for mixed vegetation and 6.5 ± 0.2% for *Eriophorum spp.* This was higher than the hydrogen content of humic acid, cellulose and lignin (Table 3.2), though cellulose and lignin were also composed of more than 6% hydrogen. ANOVA (Table 3.8) indicated substrate ($p < 0.0001$, $\omega^2 = 76.78\%$) was the only significant factor. Hydrogen content was significantly lower in the topsoil (Figure 3.9) than all other substrate types, with no significant differences among vegetation. The surface of the soil profile was therefore depleted in hydrogen relative to vegetation and litter.

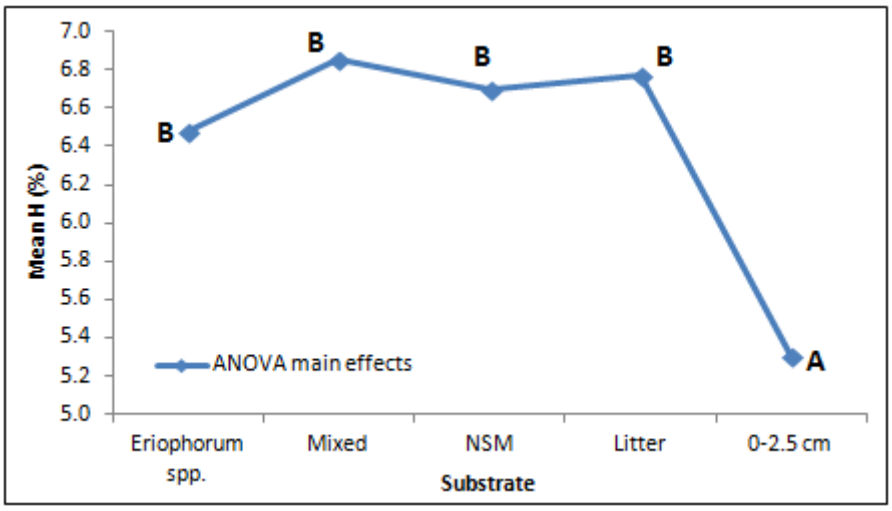

Figure 3.9 Hydrogen ANOVA main effects by substrate: significant differences denoted where letters are not shared between substrates: NSM = Non-sphagnum moss spp.

Oxygen content (Table 3.5) was highest on the bottom-slope (35.5 ± 0.6%) and lowest on the lower mid-slope (33.3 ± 0.9%). There was large variation in oxygen content compared to the mean values, 26.37 - 40.45%. Oxygen was closest to humic acid (32.4 ± 0.3%) but was much lower than cellulose (51.0 ± 0.1%). This variation was evident in the soil profile (Figure 3.3). Oxygen content was 31.9 ± 0.6% at 0 – 2.5 cm and increased to 34.5 ± 0.6% at 5 – 10 cm, outside the standard error of the top 5 cm. Mean oxygen content at 90 – 100 cm was 38.1 ± 0.4%, indicating a further increase in oxygen with depth. Kracht and Gleixner (2000) reported a range of 30.1 – 42.9% in the top 10 cm of peat samples. Site ($p = 0.023$, $\omega^2 = 1.85\%$), slope ($p = 0.014$, $\omega^2 = 4.31\%$) and depth ($p < 0.0001$, $\omega^2 = 56.84\%$) were all significant in the soil ANOVA model ($R^2 = 63.26\%$, Table 3.8). The bottom-slope (35.84%, Figure 3.10) had significantly higher oxygen content than the top-slope (34.28%) and lower mid-slope (33.77%), in contrast to the significantly lower carbon and nitrogen content. The observed change in oxygen with depth (Figure 3.3) was confirmed by *post hoc* results; oxygen at 0 – 2.5 cm was significantly lower than 5 – 20 and 80 – 100 cm, while at 2.5 – 5 cm it was lower than all other sample depths

aside from 0 – 2.5 cm. Between 5 – 20 cm, oxygen content was significantly lower than at 90 – 100 cm.

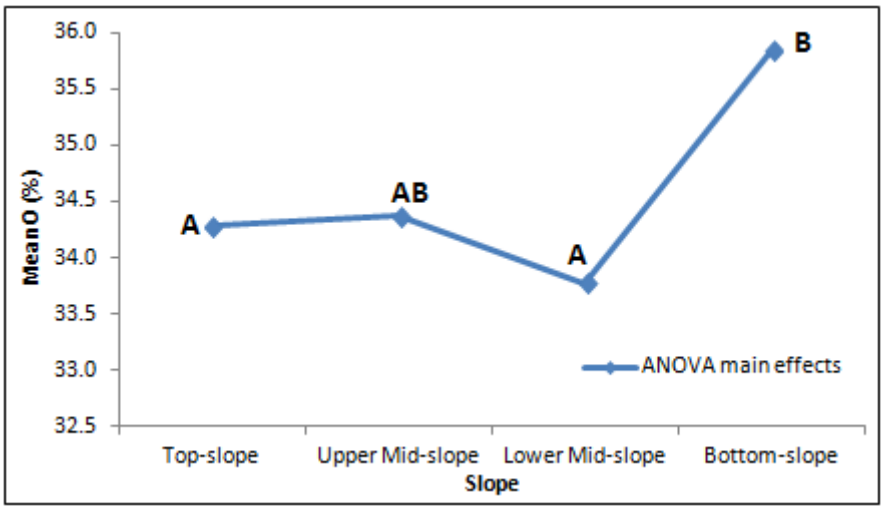

Figure 3.10 Oxygen ANOVA main effects plot by slope: significant differences denoted where letters are not shared between slope positions

As with hydrogen, oxygen content was lowest in the topsoil (31.9 ± 0.6%) compared to vegetation and litter (Table 3.6). *Eriophorum spp.* (39.5 ± 0.2%) and litter (39.2 ± 0.4%), had higher oxygen content than non-*Sphagnum* moss *spp*. (38 ± 4%) and mixed vegetation (37.6 ± 0.2%). This was higher than the oxygen content of lignin and humic acid (Table 3.2) but lower than cellulose. Topsoil was significantly different to all vegetation types and litter (Figure 3.11). This concurred with the hydrogen results (Figure 3.9), suggesting that while the topsoil is enriched in carbon and nitrogen relative to vegetation, it is depleted in oxygen and hydrogen. This would indicate soil formation is a reduction process. Slope and site were not significant (Table 3.8).

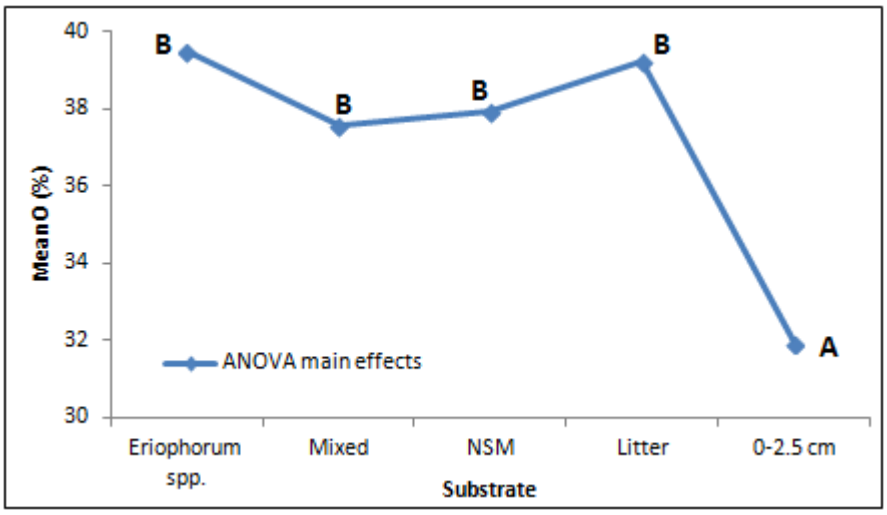

Figure 3.11 Oxygen ANOVA main effects by substrate: significant differences denoted where letters are not shared between substrates: NSM = Non-Sphagnum moss spp.

3.4.3 Atomic ratios

C:N ratio (Table 3.5) was highest on the bottom-slope (51 ± 1) and lowest on the upper mid-slope (47 ± 2). There was large variation between samples (22.14 – 78.30). The large variation was evident down the peat profile (Figure 3.12), with mean C:N changing from 29 ± 1 at 0 – 2.5 cm to a high of 59 ± 2 at 60 – 70 cm. Some studies have observed decreases in C:N at depth (Almendros et al., 1982, Zaccone et al., 2008) but Worrall et al. (2012a) found C:N ratio increased from 31 – 45 between the top of the peat profile and 50 cm depth in the Trout Beck catchment, North East England – similar to this study changing from 29 ± 1 to 53 ± 1. Mean C:N ratios across the slope were close to humic acid (48.51, Table 3.3), while the increased C:N with depth was still somewhat lower than that of lignin (87.33).

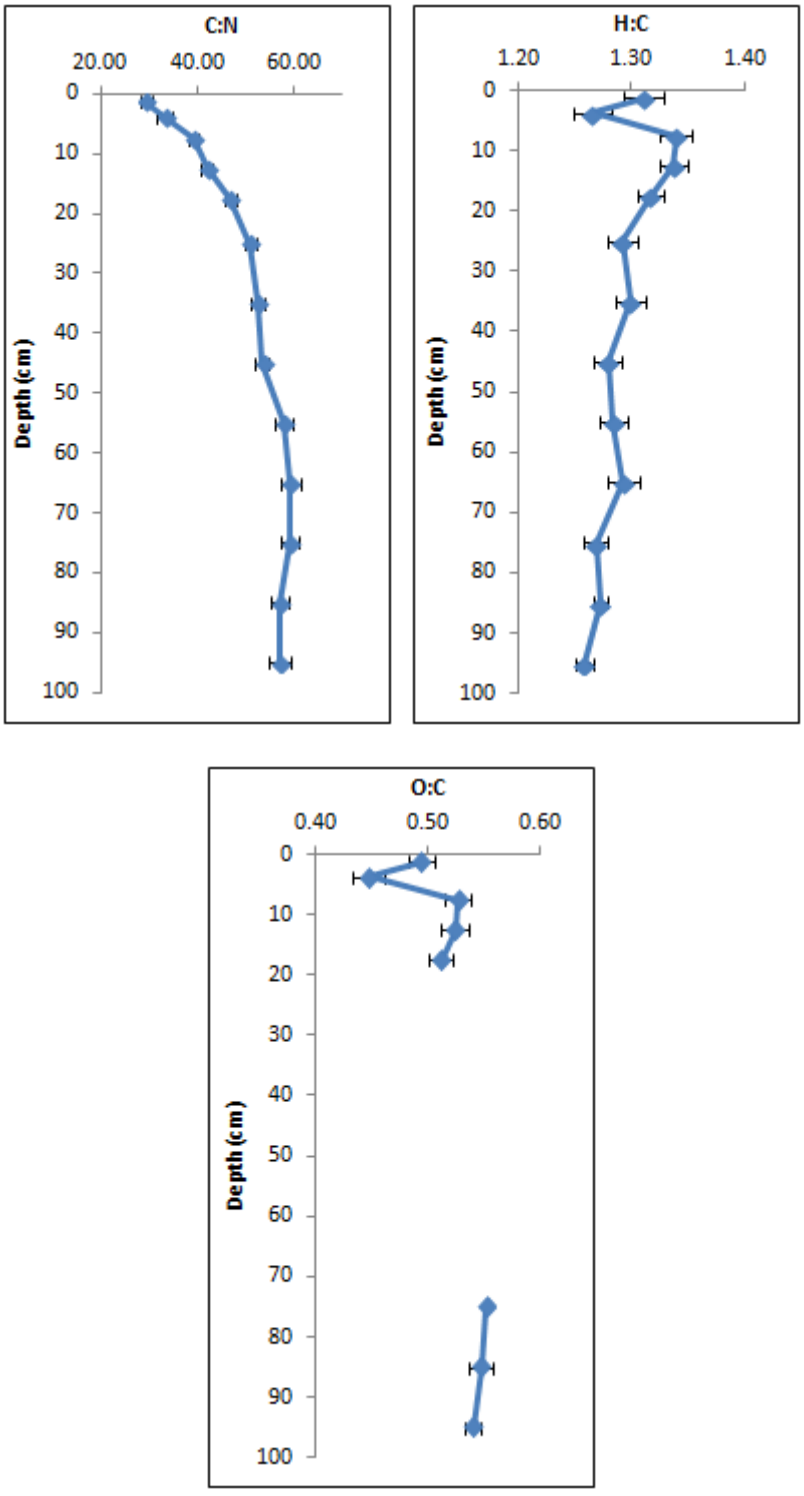

Figure 3.12 Mean atomic ratios with depth ± standard error

Slope ($p = 0.002$, $\omega^2 = 1.13\%$) and depth ($p < 0.0001$, $\omega^2 = 65.16\%$) were significant factors in the C:N ANOVA model ($R^2 = 66.38\%$, Table 3.9). Bottom-slope C:N ratio (51.39, Figure 3.13) was significantly higher than that of the upper mid-slope (46.82) and lower mid-slope (47.70), though slope was not significant according to the Kruskal-Wallis test ($p = 0.097$, Table 3.10). However, the distribution of the data was very close to normal (A/D statistic 0.807, $p = 0.036$). There was a significant increase in C:N down the soil profile. *Post hoc* tests indicated C:N at 0 – 2.5 cm was lower than 5 – 100 and 2.5 – 5 cm lower than 10 – 100 cm. Significant differences between depths progressively decreased and stopped beyond 20 – 30 cm, which had a C:N lower than 60 – 80 cm.

Table 3.9 Atomic ratio soil and substrate ANOVA: ω^2 = % variance

Soil C:N ANOVA			**Substrate C:N ANOVA**		
Factor	**P**	**ω^2**	**Factor**	**P**	**ω^2**
Slope	0.002	1.13%	Substrate	<0.0001	38.97%
Depth	<0.0001	65.16%			
N 249		**R^2 66.38%**	**N 60**		**R^2 39.37%**
Soil LnH:C ANOVA			**Substrate H:C ANOVA**		
Factor	**P**	**ω^2**	**Factor**	**P**	**ω^2**
Site	0.002	1.90%	Substrate	<0.0001	76.70%
Slope	0.002	4.26%			
Depth	<0.0001	12.06%			
N 248		**R^2 18.28%**	**N 60**		**R^2 77.00%**
Soil O:C ANOVA			**Substrate O:C ANOVA**		
Factor	**P**	**ω^2**	**Factor**	**P**	**ω^2**
Slope	0.004	8.21%	Substrate	<0.0001	71.05%
Depth	<0.0001	30.02%			
N 89		**R^2 38.50%**	**N 60**		**R^2 71.39%**

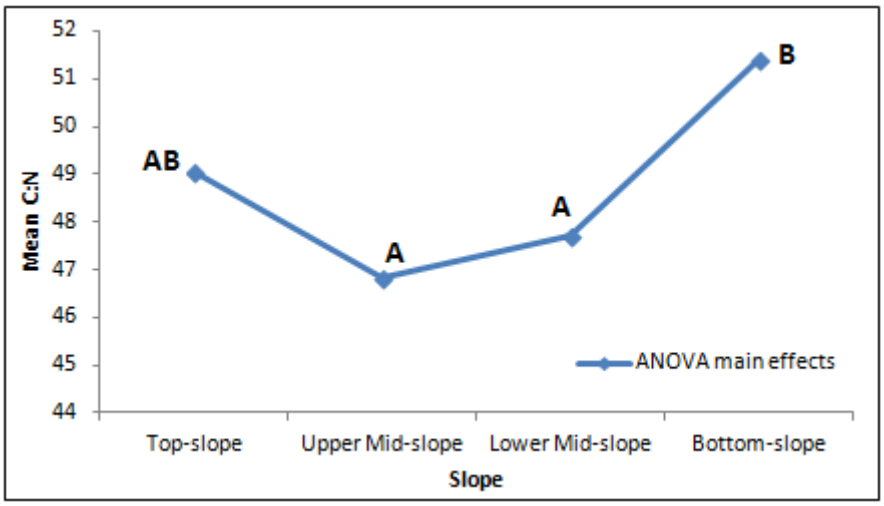

Figure 3.13 C:N ANOVA main effects by slope: significant differences denoted where letters are not shared between slope positions

Table 3.10 C:N Kruskal-Wallis results

Slope	N	Median	Ave Rank	Z
Top-slope	74	49.59	124.1	-0.13
Upper Mid-slope	49	47.90	111.4	-1.48
Lower Mid-slope	50	48.36	115.5	-1.04
Bottom-slope	76	52.67	140.9	2.30
Overall	249		125.0	
H = 6.32		**DF = 3**		**P = 0.097**

Substrate C:N (Table 3.6) varied to a large degree. Non-*Sphagnum* moss *spp*. (29 ± 4) and 0 – 2.5 cm (29 ± 1) C:N ratios were the lowest, increasing to 41 ± 1 for *Eriophorum spp.* and 43 ± 2 for litter. This reflected the higher nitrogen content of the topsoil, despite its higher carbon content as well. C:N ratio for topsoil and all vegetation and litter was below that of humic acid (48.51, Table 3.3). ANOVA (R^2 = 39.37%, Table 3.9) revealed that site and slope were insignificant, with substrate ($p < 0.0001$, ω^2 = 38.97%) the only significant factor. C:N was significantly lower in topsoil 0 – 2.5 cm peat than litter and *Eriophorum spp.* vegetation (Figure 3.14).

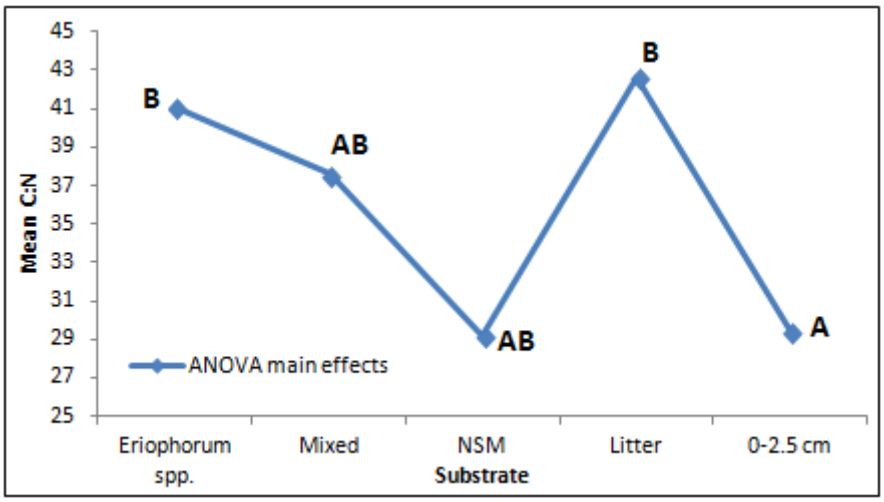

Figure 3.14 C:N ANOVA main effects plot by substrate: significant differences denoted where letters are not shared between substrates; NSM = Non-Sphagnum moss spp.

Talbot and Livingstone (1989) stated H:C ratios of 1.3 – 1.7 indicated herbaceous plant materials as the source of organic matter, with ratios of 0.8 – 1.3 implying more woody sources and H:C ratio decreasing in aerobic conditions due to degradation of labile compounds (Ortiz et al., 2004). The highest mean H:C ratio was on the bottom-slope (1.311 ± 0.007, Table 3.5) and the lowest was on the upper mid-slope (1.271 ± 0.007). The mean for all slope positions was much lower than cellulose (1.74, Table 3.3) but higher than lignin (1.17) and humic acid (1.23). The minimum H:C ratio of 1.09 was lower than that of lignin. H:C ratio fluctuated with depth (Figure 3.12), but was typically higher in the top 20 cm (1.34 ± 0.01 at 5 – 15 cm) and lowest at the bottom of the soil profile (1.258 ± 0.008). As observed with carbon content, there was a spike at 2.5 – 5 cm depth, with a lower H:C ratio of 1.27 ± 0.02 compared to the rest of the top 20 cm. ANOVA (R^2 = 18.28%, Table 3.9) suggested that site ($p = 0.002$, ω^2 = 1.90%), slope ($p = 0.002$, ω^2 = 4.26%) and depth ($p < 0.0001$, ω^2 = 12.06%) were significant, though of the atomic ratio ANOVA models, the amount of variation explained by the factors was the lowest, with unexplained variation in the error term caused by factors and interactions

that could not be measured. H:C ratio on the bottom-slope (1.31, Figure 3.15) was significantly higher than the upper mid-slope (1.27). Between 5 – 15 cm, H:C ratio was significantly higher than 70 – 100 cm, as well as the observed drop at 2.5 – 5 cm.

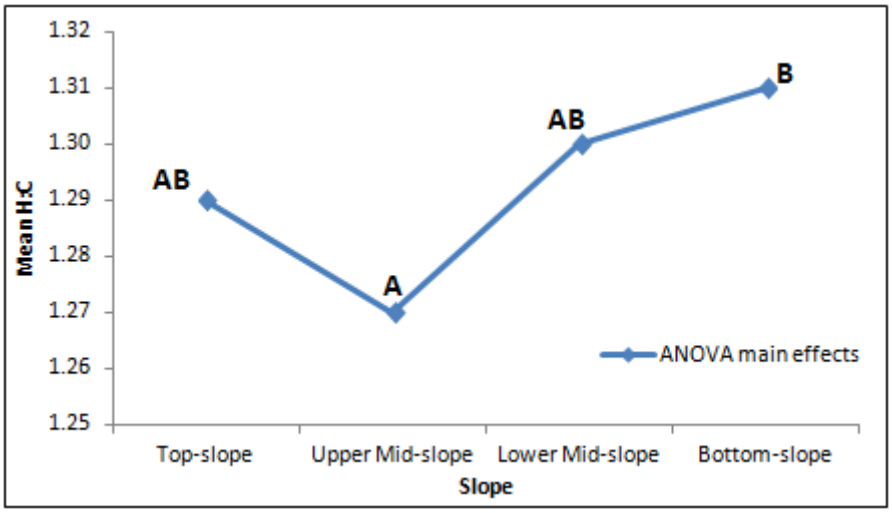

Figure 3.15 H:C ANOVA main effects plot by slope: significant differences denoted where letters are not shared between slope positions

Topsoil peat (1.31 ± 0.02) had a considerably lower H:C ratio than vegetation and litter (1.72 ± 0.01). A mean H:C of 1.67 was shared by *Eriophorum spp.* and moss. The H:C ratio of vegetation and litter was similar to cellulose (1.74, Table 3.3). Given the large change in H:C ratio between vegetation and litter and the topsoil, substrate ($p < 0.0001$ $\omega^2 = 76.70\%$), was the only significant factor in the ANOVA model ($R^2 = 77.00\%$, Table 3.9). Consequently, H:C at 0 – 2.5 cm depth in the peat profile was significantly lower than all vegetation types and litter (Figure 3.16).

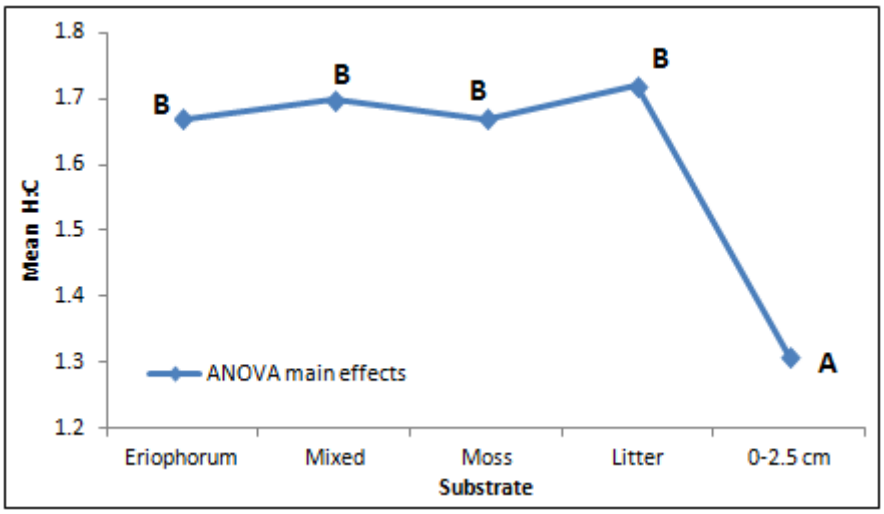

Figure 3.16 H:C ANOVA main effects plot by substrate: significant differences denoted where letters are not shared by substrates; NSM = Non-Sphagnum moss spp.

Mean O:C ratio was lowest on the lower mid-slope (0.49 ± 0.01, Table 3.5) and highest on the bottom-slope (0.534 ± 0.008), with a maximum of 0.63 and minimum of 0.38, both on the top-slope. Mean O:C ratios were between humic acid (0.68, Table 3.3) and lignin (0.35) and were much lower than cellulose (0.89). The O:C ratio fluctuated with depth, decreasing to 0.45 ± 0.01 at 2.5 – 5 cm but increasing to 0.53 ± 0.01 at 5 – 10 cm depth. At 90 – 100 cm, O:C ratio was 0.540 ± 0.007. ANOVA (R^2 = 38.50%, Table 3.9) indicated slope ($p = 0.004$, ω^2 = 8.21%) and depth ($p < 0.0001$, ω^2 = 30.02%) were significant. As with C:N ratio, O:C ratio was significantly higher on the bottom-slope (0.54, Figure 3.17) than the upper and lower mid-slopes (0.50), reflecting both the higher oxygen content and lower carbon content found on the bottom-slope. O:C ratio at 90 – 100 cm was significantly higher than the top 5 cm, though the drop in O:C ratio at 2.5 – 5 cm this depth was significantly lower than 5 – 20 cm.

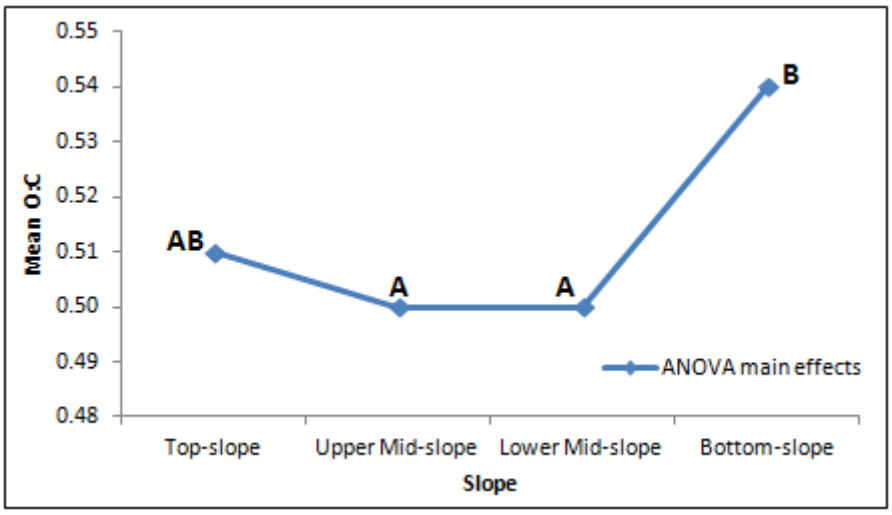

Figure 3.17 O:C ANOVA main effects plot by slope: significant differences denoted where letters are not shared between slope positions

The ratio of O:C was higher in vegetation and litter than soil, with *Eriophorum spp.* having the highest mean of 0.634 ± 0.003 but 0.49 ± 0.01 at 0 – 2.5 cm (Table 3.6). The ratio of O:C for vegetation was therefore closest to that of humic acid (0.68, Table 3.3). Substrate ($p < 0.0001$, $\omega^2 = 71.05\%$) was the only significant factor in the ANOVA model (R^2 71.39%, Table 3.9), with O:C ratio for topsoil significantly lower than all vegetation and litter (Figure 3.18).

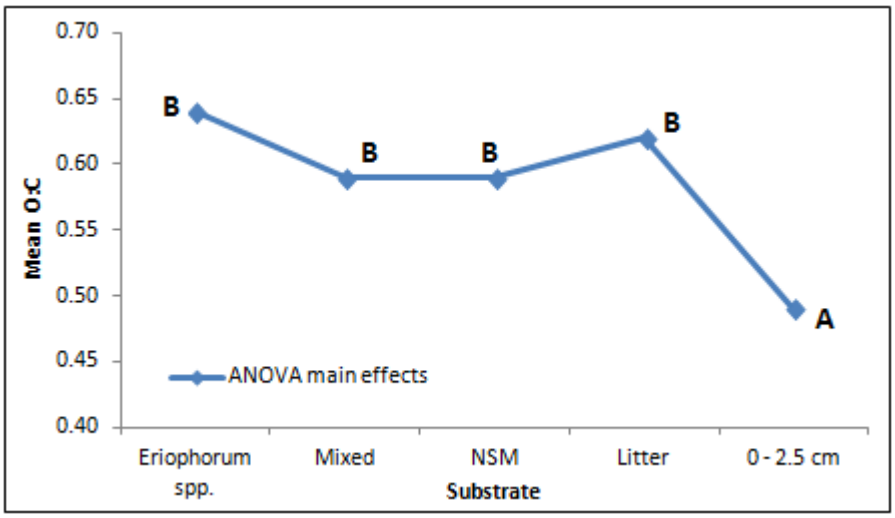

Figure 3.18 O:C ANOVA main effects by substrate: significant differences denoted where letters are not shared between substrates: NSM = Non-Sphagnum moss spp.

3.4.4 Carbon oxidation state & oxidative ratio

Mean carbon oxidation state (C_{OX}, Table 3.5) values were -0.22 ± 0.02, -0.19 ± 0.01, -0.23 ± 0.02 and -0.17 ± 0.02 for the top-slope, upper mid-slope, lower mid-slope and bottom-slope respectively. Carbon oxidation state ranged from -0.425 to -0.027. The minimum C_{OX} value was close to that of lignin (-0.434, Table 3.3) but mean values were typically between lignin and cellulose (0.049). Baldock et al. (2004) reported C_{OX} values of 0.000 and -0.381 for carbohydrates and lignin, respectively. Carbon oxidation state increased with depth (Figure 3.19), from -0.22 ± 0.02 at 0 – 2.5 cm to -0.12 ± 0.02 at 90 – 100 cm depth. The increase in C_{OX} with depth was the reverse of what would be expected. There was some degree of fluctuation; the decrease in C_{OX} at 2.5 – 5 cm depth (-0.27 ± 0.03) was in line with the reduced oxygen but higher carbon content observed at this depth.

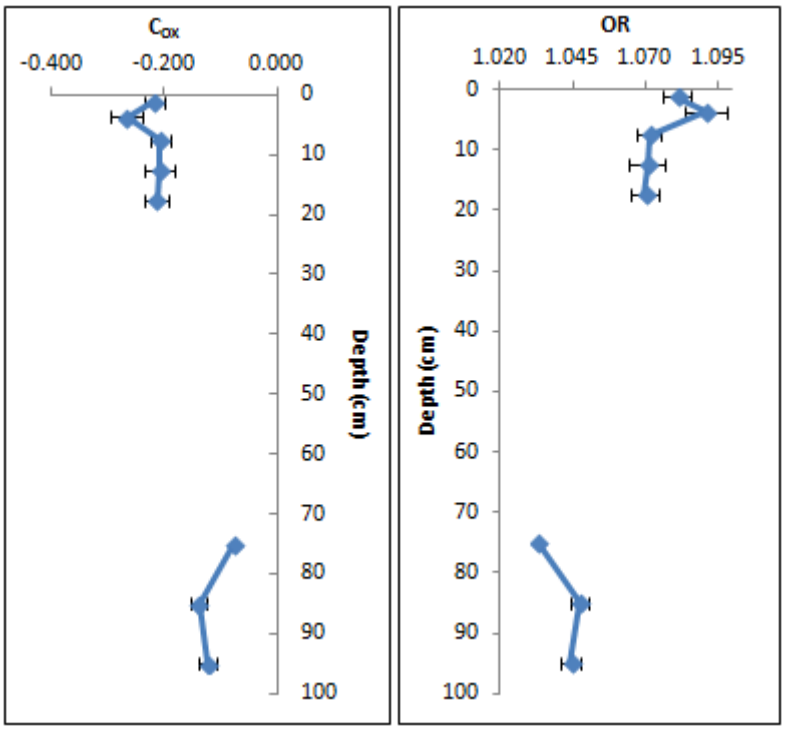

Figure 3.19 Mean carbon oxidation state (C_{OX}) and oxidative ratio (OR) with depth ± standard error

ANOVA (R^2 = 37.36%, Table 3.11) revealed that site (p = 0.023, ω^2 = 3.17%), slope (p = 0.004, ω^2 = 4.77%), depth (p <0.0001, ω^2 = 23.78%) and a site-slope interaction (p = 0.019, 5.38%) were all significant factors. Mean C_{OX} (Figure 3.20) was significantly lower on the top-slope (-0.224) and lower mid-slope (-0.216) than the bottom-slope (-0.151). The interaction effect showed that top-slope C_{OX} was lower on Featherbed Moss (-0.273) than Alport Low (-0.174) and steadily increased down-slope on Featherbed Moss, while the highest value on Alport Low was for the upper mid-slope (-0.147). The observed increase in C_{OX} with depth was confirmed, as all samples from the top 20 cm were significantly lower than 90 – 100 cm.

Table 3.11 C_{OX} and OR soil and substrate ANOVA: ω^2 = % variance

Soil C_{OX} ANOVA			Substrate C_{OX} ANOVA		
Factor	**P**	**ω^2**	**Factor**	**P**	**ω^2**
Site	0.023	3.17%	Site	0.017	5.21%
Slope	0.004	4.77%	Substrate	<0.0001	56.99%
Depth	<0.0001	23.78%			
Site*Slope	0.019	5.38%			
N 89		**R^2 37.36%**	**N 59**		**R^2 62.60%**
Soil OR ANOVA			**Substrate OR ANOVA**		
Factor	**P**	**ω^2**	**Factor**	**P**	**ω^2**
Site	0.018	2.97%	Site	0.038	6.06%
Slope	0.002	4.92%	Substrate	<0.0001	47.88%
Depth	<0.0001	38.82%			
Site*Slope	0.010	5.03%			
N 89		**R^2 52.01%**	**N 59**		**R^2 54.36%**

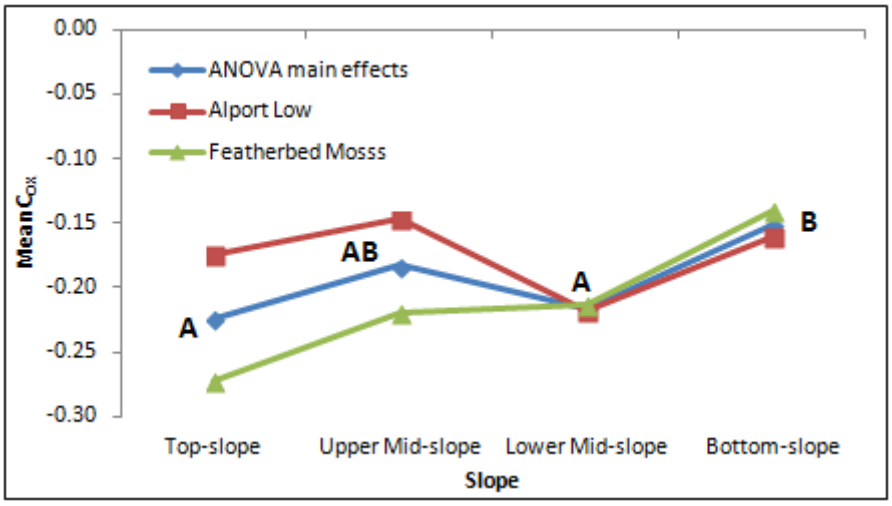

Figure 3.20 C_{OX} ANOVA main effects & interaction plot: significant differences denoted where letters are not shared between slope positions

Carbon oxidation state changed with substrate origin. Peat samples from 0 – 2.5 cm depth (– 0.22 ± 0.02) had a higher C_{OX} value than vegetation and litter samples (Table 3.6). *Eriophorum spp.* had the highest C_{OX} value of -0.32 ± 0.05, while mixed vegetation had the lowest value of -0.45 ± 0.02. The C_{OX} values were most like lignin (-0.434, Table 3.3), with

mixed vegetation having a lower oxidation state than lignin. Consequently, C_{OX} was significantly higher in 0 – 2.5 cm peat samples than *Eriophorum spp.*, mixed vegetation and litter (Figure 3.21). The ANOVA model (R^2 = 62.60%, Table 3.11) suggested that substrate ($p < 0.0001$, ω^2 = 56.99%) and site were significant ($p = 0.017$, ω^2 = 5.21%). Alport Low (-0.380) had a lower C_{OX} value than Featherbed Moss (-0.330).

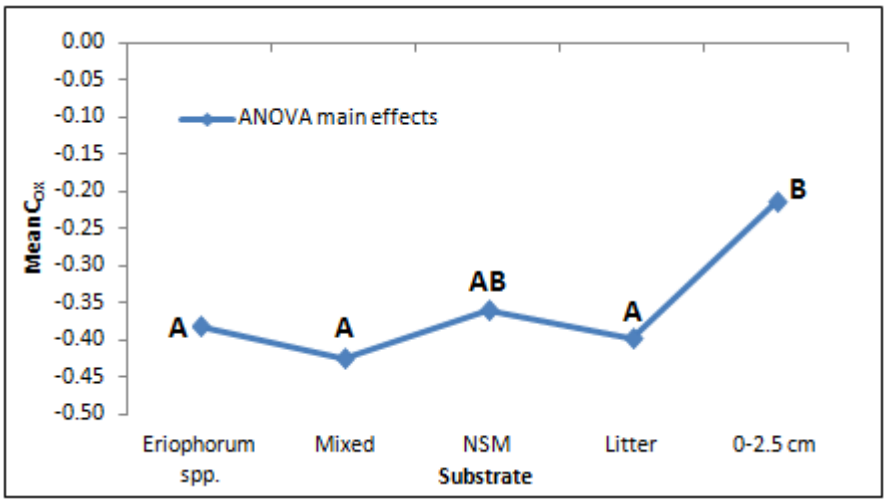

Figure 3.21 C_{OX} ANOVA main effects plot by substrate: significant differences denoted where letters are not shared between substrates; NSM = Non-Sphagnum moss spp.

Oxidative ratio (Table 3.5) was highest on the lower mid-slope (1.077 ± 0.005) and lowest on the bottom-slope (1.060 ± 0.004). Oxidative ratio varied between 1.019 – 1.128, with mean OR values between cellulose (0.988, Table 3.3) and lignin (1.117). Randerson et al. (2006) reported OR values of 1.00, 1.14 and 1.37 for carbohydrates, lignin and lipids respectively, while values reported by Masiello et al. (2008) of 1.00 and 1.13 for cellulose and lignin were also close to results from this study. Oxidative ratio decreased down the soil profile, from 1.081 ± 0.005 at 0 – 2.5 cm depth to 1.044 ± 0.004 at 90 – 100 cm (Figure 3.19). As with C_{OX}, site (p 0.018, ω^2 = 2.97%, Table 3.11), slope ($p = 0.002$, ω^2 = 4.92%), depth (p

<0.0001, ω^2 = 38.82%) and a site-slope interaction (p = 0.010, ω^2 = 5.03%) were significant. Similarly, *Post hoc* tests revealed that the significant differences reflected those of C_{OX}. Mean OR on the top-slope (1.074, Figure 3.22) and lower mid-slope (1.073) was significantly higher than the bottom-slope (1.055). The oxidative ratio of the top 20 cm was significantly different from the bottom of the soil core.

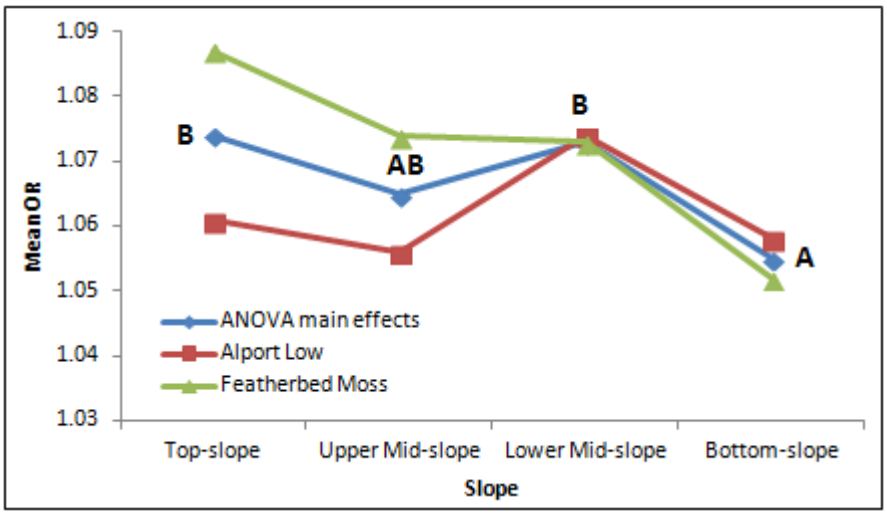

Figure 3.22 OR ANOVA main effects & Interaction plot by slope: significant differences denoted where letters are not shared between slope positions

Oxidative ratio (Table 3.6) varied from 1.081 ± 0.005 for peat at 0 – 2.5 cm depth to 1.134 ± 0.004 for mixed vegetation. The maximum observed OR was for litter (1.156) and minimum for *Eriophorum spp.* (0.974). Mean OR for vegetation and litter was higher than lignin (1.117, Table 3.3), aside from *Eriophorum spp.* (1.099 ± 0.012). Site (p = 0.038, ω^2 = 6.06%) and substrate (p <0.0001, ω^2 = 47.88%) were significant factors explaining variation in OR (R^2 = 54.36%, Table 3.11). Alport Low (1.117) had a higher mean OR than Featherbed Moss (1.106), while OR for *Eriophorum spp.*, mixed vegetation and litter was significantly higher than topsoil peat (Figure 3.23).

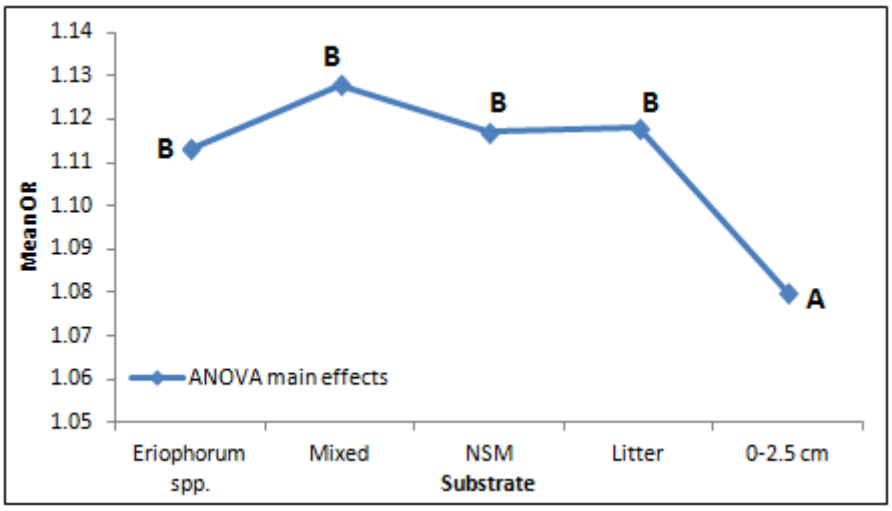

Figure 3.23 OR ANOVA main effects plot by substrate: significant differences denoted where letters are not shared between substrates; NSM = Non-Sphagnum moss spp.

3.4.5 Energy content

Mean energy content was highest on the upper mid-slope (20.5 ± 0.1 MJ Kg^{-1}, Table 3.5) and lowest on the bottom-slope (19.74 ± 0.07 MJ Kg^{-1}) and ranged between 17.2890 – 22.4204 MJ Kg^{-1}. Mean energy content across the hillslope was towards the low end of values for peat reported by Persson et al. (1986) but was in general agreement. Mean energy content was between cellulose (16.6 ± 0.2 MJ Kg^{-1}, Table 3.4) and lignin (25.53 ± 0.03 MJ Kg^{-1}). Trofimov and Emelyanenko (2000) reported values of 17.57 and 26.36 KJ g^{-1} for cellulose and lignin, higher than this study. The higher energy content of lignin would suggest a higher degree of recalcitrance. Although it was not possible to repeat energy content measurements for soil samples, the standard error of the reference materials was within the range of and often lower than CHNO content (Table 3.2). This would suggest a good degree of constraint on the analytical error, though sample heterogeneity was not accounted for. Energy content increased down the soil profile from 19.4 ± 0.2 MJ Kg^{-1} at 0 – 2.5 cm to 21.0 ± 0.2 MJ Kg^{-1} at 90 – 100 cm depth (Figure 3.24).

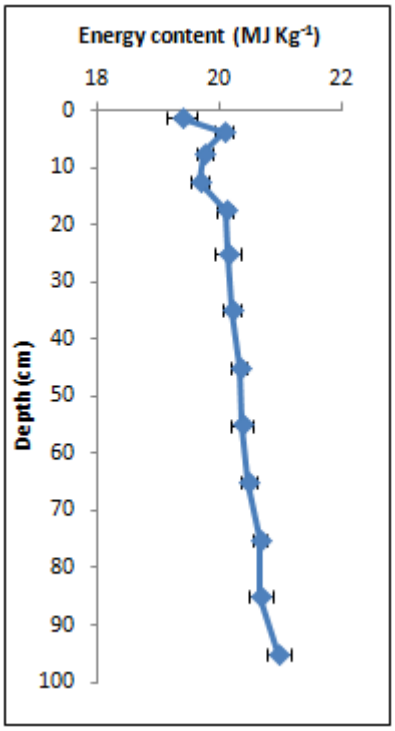

Figure 3.24 Mean energy content with depth ± standard error

Slope ($p < 0.0001$, $\omega^2 = 14.08\%$) and depth ($p < 0.0001$, $\omega^2 = 22.09\%$) were significant factors in the ANOVA model ($R^2 = 36.27\%$, Table 3.12). Energy content on the bottom-slope (19.7821 MJ Kg^{-1}) was significantly lower than all other hillslope positions (Figure 3.25). The progressive increase in energy content with depth was significant, with the top 0 – 2.5 cm sample significantly lower than 30 – 100 cm samples. From 5 – 15 cm, energy content was lower than from 50 – 100 cm, while 2.5 – 5 cm sample and 15 – 40 cm samples were significantly lower in energy content than at 90 – 100 cm.

Table 3.12 Energy content ANOVA: ω^2 = % variance

Soil energy content ANOVA			Substrate energy content ANOVA		
Factor	**P**	**ω^2**	**Factor**	**P**	**ω^2**
Slope	<0.0001	14.08%	Site	0.001	20.30%
Depth	<0.0001	22.09%	Substrate	<0.0001	25.59%
N 247		**R^2 36.27%**	**N 58**		**R2 46.33%**

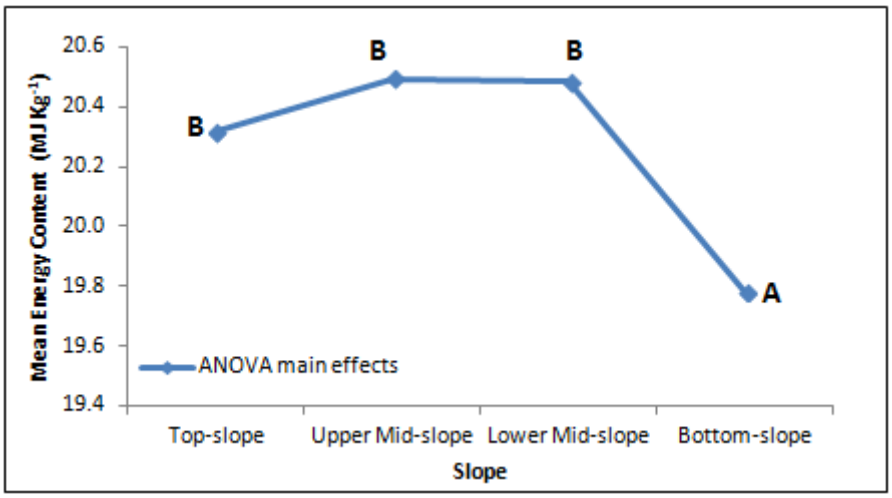

Figure 3.25 Energy content ANOVA main effects plot: significant differences denoted where letters are not shared between slope positions

Eriophorum spp. (18.03 ± 0.07 MJ Kg^{-1}, Table 3.6) had the lowest mean energy content of vegetation and litter, while mixed vegetation (19.1 ± 0.1 MJ Kg^{-1}) had the highest. This was still lower than the topsoil 0 – 2.5 cm peat samples (19.4 ± 0.2 MJ Kg^{-1}). Analysis of variance (R^2 = 46.33%, Table 3.12) showed that site (p = 0.001, ω^2 = 20.30%) and substrate were significant (p <0.0001, ω^2 = 25.59%) factors, with no apparent slope effect. Mean energy content for the substrate dataset from the ANOVA main effects was 18.8983 MJ Kg^{-1} on Alport Low, which was significantly higher than Featherbed Moss (18.3704 MJ Kg^{-1}). *Eriophorum spp.* (18.1161 MJ Kg^{-1}) and litter (18.3287 MJ Kg^{-1}) had significantly lower energy content than peat at 0 – 2.5 cm depth (19.1008 MJ Kg^{-1}, Figure 3.26).

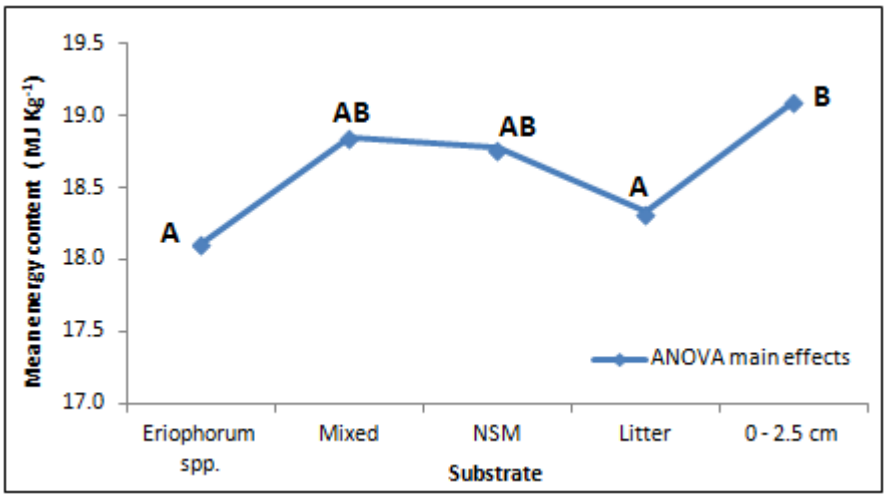

Figure 3.26 Energy content ANOVA main effects plot by substrate: significant differences denoted where letters are not shared between substrates: NSM = Non-Sphagnum moss

3.4.6 Thermogravimetric analysis

Thermogravimetric (TG) and derivative thermogravimetric curves (DTG) are shown in Figure 3.27. Cellulose TG curves indicated good repeatability, with total weight loss between 87.60 – 89.62%. There was a rapid onset of weight loss between ~310 – 400 °C, peaking at ~366 °C. Cellulose has been shown to undergo rapid weight loss to 350 °C, with a secondary weight loss step related to decomposition of char formed during pyrolysis (Lopez-Capel et al., 2005), but this was not evident here. Weight loss of lignin was more attenuated than cellulose, occurring from ~200 – 450 °C, peaking at ~385 °C and with total weight loss between 54.67 – 55.20%. Lignin weight loss was lower and with an earlier peak than Manning et al. (2005) had for sugarcane lignin. Humic acid had a large dehydration peak at 100 °C, fluctuated between ~300 – 380 °C and had a second peak associated with recalcitrant material at ~450 °C. Examples of peat at 0 – 2.5 cm and vegetation (Figure 3.27) peaked on DTG curves at ~280 °C, prior to cellulose and lignin. Weight loss for peat (57.73%) was lower than vegetation and litter (69.41 – 71.50 %), while both continued past 400 °C with the loss of more recalcitrant material.

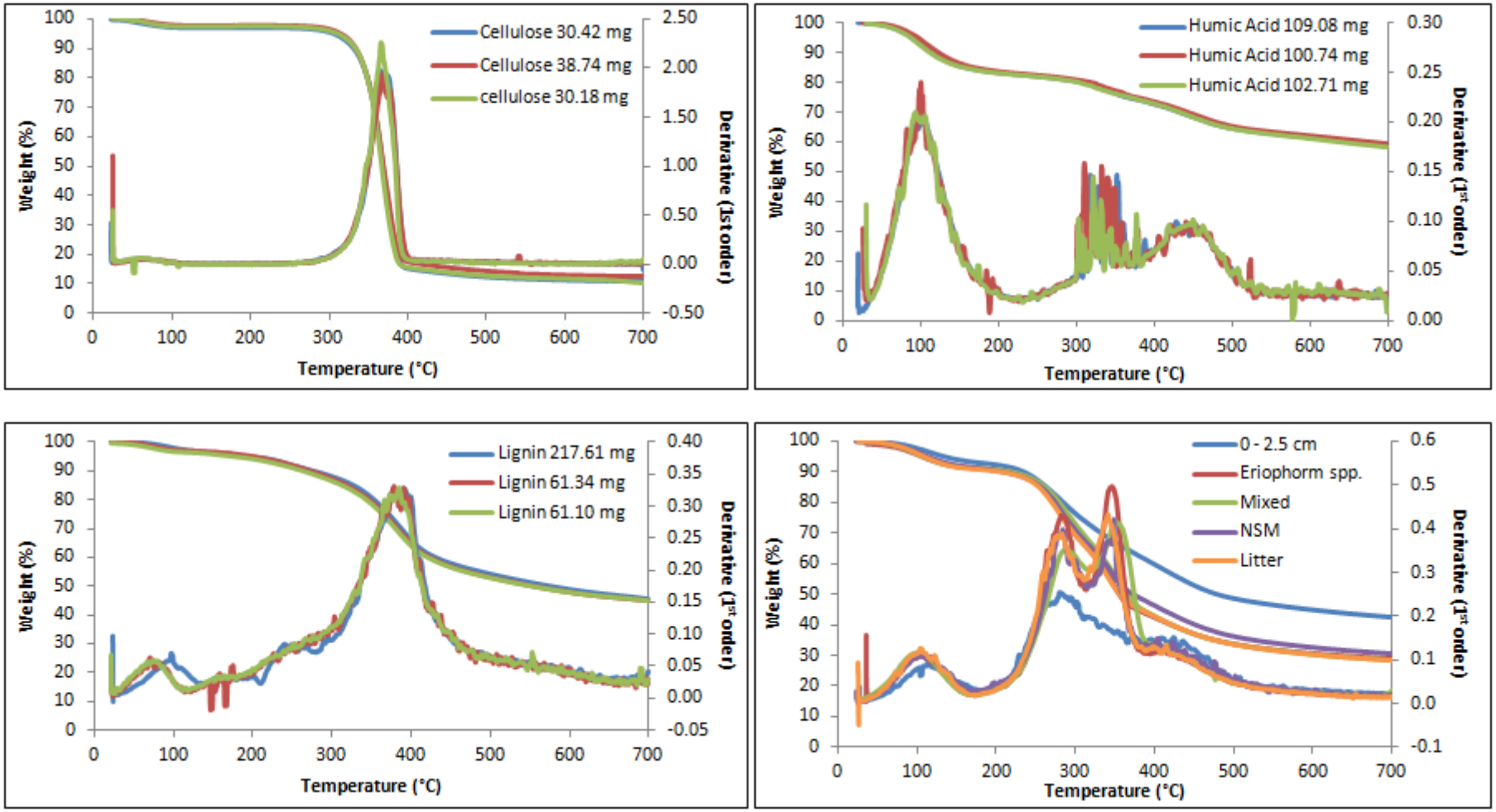

Figure 3.27 TG and DTG curves for cellulose, humic acid, lignin, soil and vegetation: NSM = Non-Sphagnum moss spp.

Weight loss was calculated every 10 °C between temperature ranges of 180 – 600 °C and assessed using PCA. Cellulose was excluded from the analysis after initial results indicated it was an outlying value. Seven principal components (PCs) were retained, based upon the rule of selecting all PCs with an eigenvalue >1 and the first PC with an eigenvalue <1 (Table 3.13). No one temperature range dominated weight loss on PC1, suggesting it represented a general unloading pattern. Principal component one (Figure 3.28) distinguished vascular vegetation from peat samples. Non-*Sphagnum* moss spp., though only based on two samples, plotted either between the two groups or within the topsoil peat samples. Principal component three (Figure 3.29) separated humic acid (negative loading) from lignin (positive loading), while PC2 represented the amount of humic acid or lignin. This suggested there were three compositional end-members (prefix EM); topsoil peat samples (0 – 2.5 cm, 2.5 – 5 cm) trended towards humic acid (EM-A), while deeper peat samples and vegetation trended towards lignin (EM-B). There appeared to be a transition between peat samples of 5 – 15 cm depth (EM-C), where low values on PC2 were associated with high weight loss up to around 300 °C.

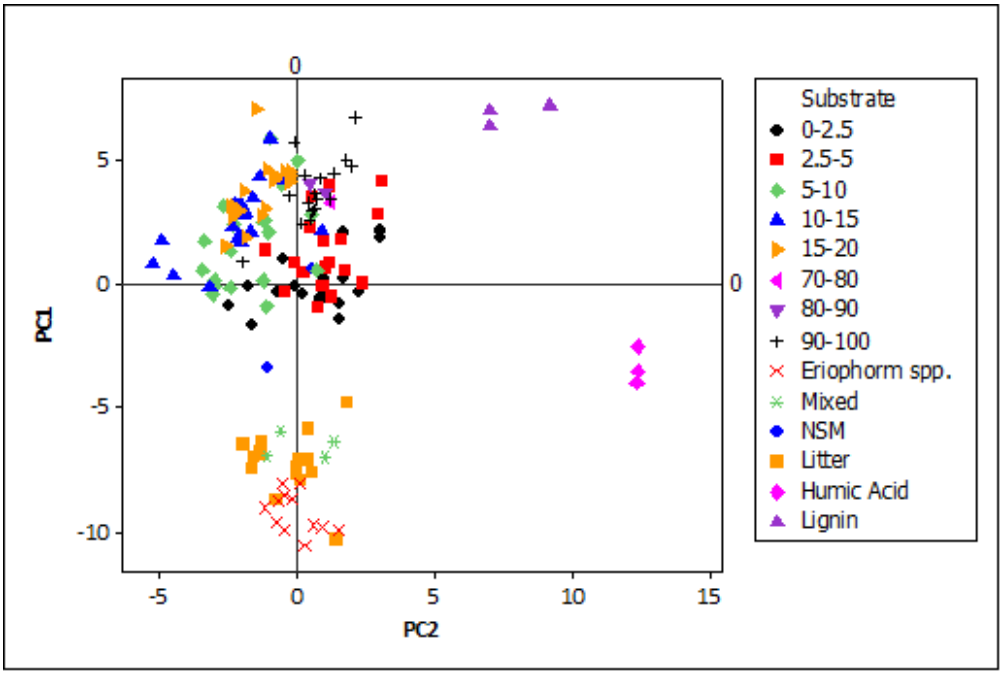

Figure 3.28 Scatterplot of TG weight loss PC1 & PC2; NSM = Non-Sphagnum moss spp.

Table 3.13 The first seven principal components of weight loss by temperature range

Temperature Range (°C)	PC1	PC2	PC3	PC4	PC5	PC6	PC7
180-190	0.149	-0.098	-0.085	-0.113	-0.200	-0.412	-0.319
190-200	0.111	-0.145	-0.064	-0.073	-0.314	-0.538	-0.070
200-210	0.094	-0.246	-0.035	0.022	-0.339	-0.267	0.218
210-220	0.105	-0.266	-0.048	0.058	-0.267	-0.009	0.291
220-230	0.090	-0.300	-0.048	0.074	-0.216	0.171	0.155
230-240	0.078	-0.313	-0.080	0.077	-0.120	0.260	-0.101
240-250	0.042	-0.335	-0.079	0.064	-0.069	0.260	-0.226
250-260	-0.024	-0.355	-0.025	0.016	0.012	0.217	-0.238
260-270	-0.105	-0.312	0.039	-0.007	0.077	0.078	-0.243
270-280	-0.133	-0.257	0.079	-0.013	0.166	-0.043	-0.258
280-290	-0.129	-0.240	0.108	-0.034	0.244	-0.094	-0.132
290-300	-0.109	-0.253	0.135	-0.067	0.234	-0.100	0.151
300-310	-0.129	-0.231	0.138	-0.070	0.150	-0.062	0.366
310-320	-0.160	-0.187	0.126	-0.004	0.065	-0.052	0.390
320-330	-0.188	-0.092	0.119	0.070	0.061	-0.096	0.206
330-340	-0.194	-0.044	0.115	0.091	0.076	-0.157	0.004
340-350	-0.193	-0.019	0.129	0.096	0.087	-0.191	-0.110
350-360	-0.183	-0.004	0.152	0.132	0.094	-0.210	-0.152
360-370	-0.126	0.011	0.256	0.260	0.035	-0.159	-0.115
370-380	0.038	0.049	0.316	0.336	-0.158	0.010	-0.079
380-390	0.109	0.052	0.270	0.289	-0.159	0.081	-0.028
390-400	0.126	0.057	0.236	0.297	-0.141	0.054	-0.060
400-410	0.153	0.024	0.160	0.320	-0.028	0.039	0.010
410-420	0.176	-0.023	0.026	0.289	0.108	-0.008	0.101
420-430	0.179	-0.038	-0.078	0.215	0.189	-0.037	0.123
430-440	0.177	-0.046	-0.120	0.191	0.205	-0.070	0.086
440-450	0.178	-0.050	-0.147	0.139	0.225	-0.047	0.052
450-460	0.180	-0.044	-0.165	0.116	0.200	-0.075	0.045
460-470	0.181	-0.032	-0.175	0.099	0.198	-0.076	0.022
470-480	0.185	-0.036	-0.163	0.080	0.176	-0.090	-0.012
480-490	0.191	-0.042	-0.123	0.063	0.196	-0.077	-0.062
490-500	0.200	-0.024	-0.023	0.004	0.137	-0.137	-0.110
500-510	0.194	-0.028	0.108	-0.044	0.108	-0.093	-0.038
510-520	0.178	-0.034	0.187	-0.108	0.086	-0.027	-0.036
520-530	0.177	-0.029	0.223	-0.118	0.034	0.005	0.000
530-540	0.170	-0.032	0.219	-0.149	0.055	-0.004	0.024
540-550	0.174	-0.028	0.213	-0.157	0.045	0.013	-0.049
550-560	0.173	-0.011	0.220	-0.161	0.020	0.044	0.011
560-570	0.173	-0.013	0.201	-0.188	0.026	0.010	-0.013
570-580	0.179	-0.016	0.190	-0.167	0.035	0.038	0.044
580-590	0.180	0.000	0.169	-0.194	0.038	0.077	0.000
590-600	0.180	0.006	0.154	-0.190	0.024	0.044	0.056
% Variance	**51.10%**	**67.90%**	**79.80%**	**87.40%**	**92.40%**	**94.90%**	**96.10%**

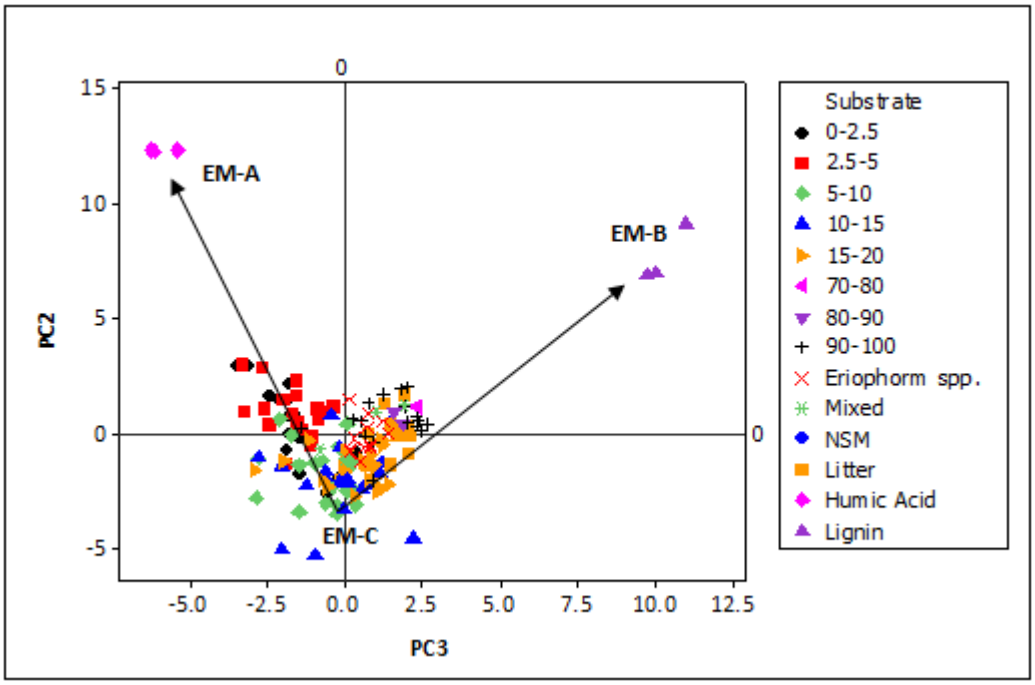

Figure 3.29 Scatterplot of TG weight loss PC2 & PC3: NSM = Non-Sphagnum moss spp.; prefix EM = end-member; A – C = labels

It was not possible to ascertain clear trends related to slope position due to the overriding importance of peat sample depth and substrate origin. ANOVA of PC2 and PC3 was used to determine whether slope position and study site were significant. Table 3.14 showed that slope was significant in explaining variation in scores on PC2 and PC3, along with site and substrate. For PC2 ANOVA, mean scores (Figure 3.30) decreased down-slope, from 0.089 on the top-slope to -0.740 on the bottom-slope, suggesting more organic matter weight loss between the 210 – 220 and 290 – 300 °C temperature ranges down-slope. For PC3, the mid-slopes had lower scores than the top-slope and bottom-slope. This could imply the top-slope and bottom-slope trended towards lignin-type compounds in weight loss characteristics, while the higher PC2 score for the top-slope suggested it plotted closer to lignin than the bottom-slope. Alport Low (0.102 PC2, 0.162 PC3, Figure 3.31) had a higher PC2 score than Featherbed

Moss (-0.663 PC2, 0.831 PC3) and while both had positive PC3 scores (towards lignin), Featherbed Moss had a significantly more positive loading.

Table 3.14 TG ANOVA: ω^2 = % variance

TG PC2 ANOVA			TG PC3 ANOVA		
Factor	**P**	**ω^2**	**Factor**	**P**	**ω^2**
Site	0.001	2.70%	Site	0.001	1.03%
Slope	0.022	2.87%	Slope	0.003	2.36%
Substrate	<0.0001	45.31%	Substrate	<0.0001	57.44%
N 143		**R^2 51.05%**	**N 143**		**R^2 61.00%**

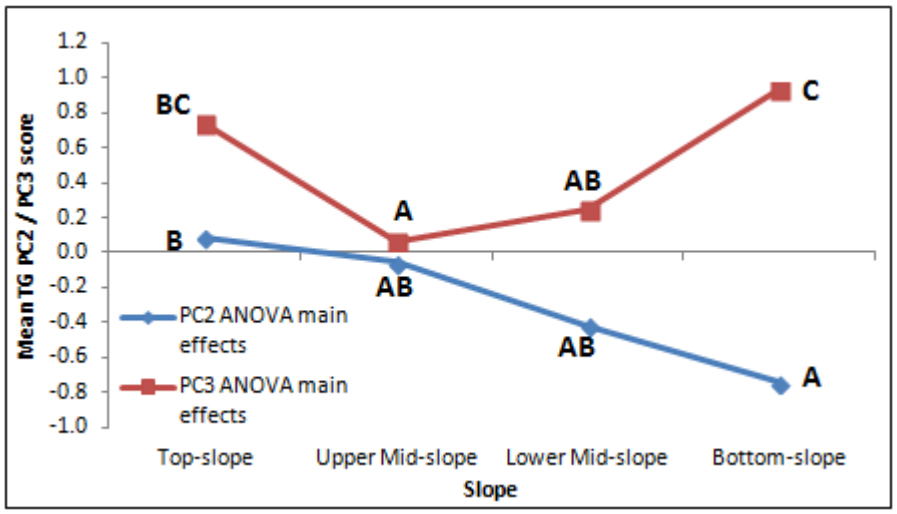

Figure 3.30 TG PC2 & PC3 ANOVA main effects plot by slope: significant differences denoted where letters are not shared between slope positions

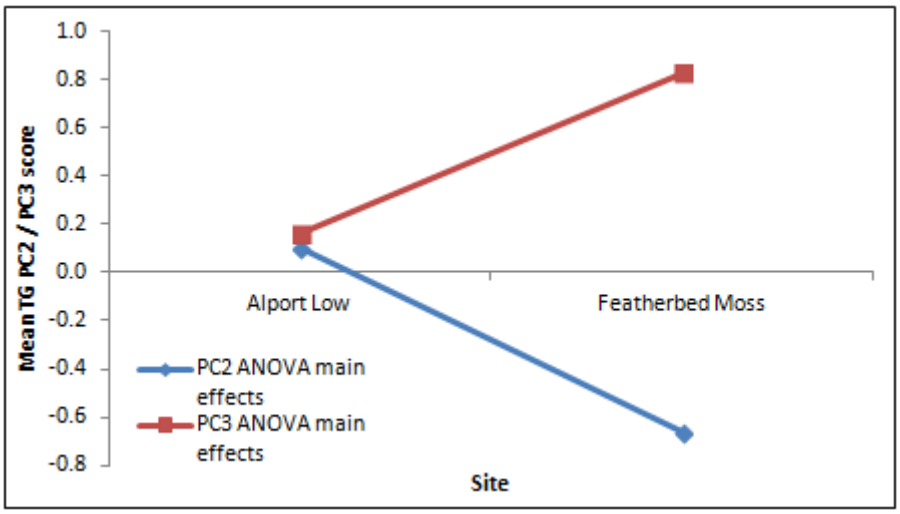

Figure 3.31 TG1 PC2 & PC3 ANOVA main effects plot by site

The trends indicated in Figure 3.29 related to substrate were confirmed by ANOVA. Between 5 – 20 cm depth samples, PC2 scores were significantly lower than 0 – 5 cm, 90 – 100 cm, *Eriophorum spp*. and litter samples (though specific to each substrate this was variable). This would support the possibility that 5 – 20 cm depths act as a transition point between surface and deeper peat samples, while PC3 separated 0 – 5 cm samples from deeper samples along with vegetation. The error in the ANOVA model likely included unexplained factors and interactions. For instance, it was not possible to test for interaction effects. Kruskal-Wallis of PC3 (Table 3.15) indicated slope was not significant (p 0.713), but the Anderson-Darling statistic of 0.914 (p = 0.019) implied a distribution close to normal.

Table 3.15 TG PC3 Kruskal-Wallis results

Slope	N	Median	Ave Rank	Z
Top-slope	41	0.083	75.6	0.66
Upper Mid-slope	28	0.212	66.7	-0.76
Lower Mid-slope	44	-0.042	69.0	-0.59
Bottom-slope	30	0.084	76.5	0.67
Overall	143		72.0	
HF = 1.37		**DF = 3**		**P = 0.713**

3.4.7 Multivariate analysis

PCA using multiple datasets (Table 3.16) was performed upon soil, vegetation and litter samples as well as lignin and humic acid. Four components explained 91.70% of variation in the dataset. Principal component one was dominated by negative loadings of H:C and OR, with positive loadings of C_{OX}, C:N and energy content. Scores from TG PC3 were important in explaining data for PC2, alongside C:N and O:C ratio. Plotting PC1 against PC2 (Figure 3.32) indicated a transition from vegetation and litter samples (EM-A) to topsoil peat samples (EM-B). Vegetation and litter had more negative C_{OX} and larger OR values. Though deeper peat samples and vegetation and litter had high TG PC3 (Figure 3.29), C_{OX}, OR, C:N ratio and energy content separated them. Peat samples changed from low C:N to high C:N ratio at depth (EM-C); consequently the change between vegetation and litter samples was defined the degree of oxidation, while peat samples were separated by C:N ratio.

Table 3.16 The first four principal components of multivariate analysis

Variable	PC1	PC2	PC3	PC4
Energy content	0.294	-0.039	-0.595	-0.395
C:N	0.283	-0.524	-0.172	0.148
H:C	-0.508	-0.096	0.004	0.346
O:C	0.039	-0.484	0.515	0.122
C_{OX}	0.509	0.217	0.131	0.336
OR	-0.527	-0.129	-0.099	-0.370
TG PC2	0.191	-0.186	0.483	-0.647
TG PC3	0.021	-0.618	-0.300	0.140
% Variance	**36.30%**	**61.00%**	**79.20%**	**91.70%**

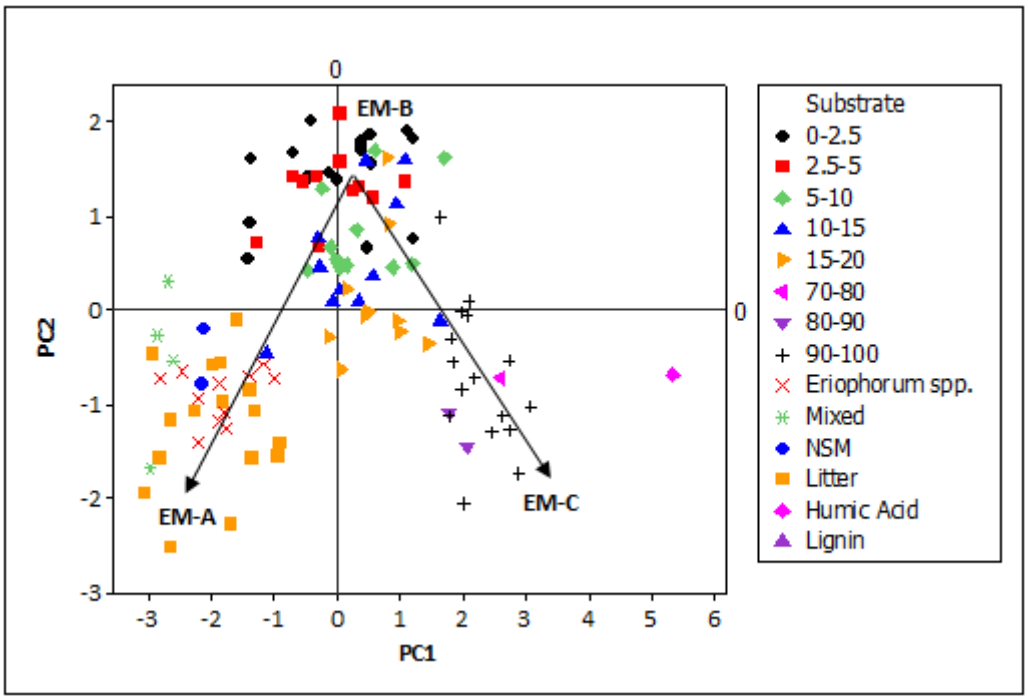

Figure 3.32 Scatterplot of Multivariate PC1 & PC2: NSM = Non-Sphagnum moss spp.; prefix EM = end-member; A-C = labels

Plots of PC1 against PC3 (Figure 3.33) further separated vegetation and litter from deeper peat samples. Vegetation and litter samples were defined by high H:C and O:C ratios and high OR. Though lignin, like vegetation and litter, had high OR and low C_{OX} values, it plotted adjacent to bottom-core peat samples due to high C:N ratios and energy content. High values of TG PC3 as well could therefore suggest that deeper peat samples and lignin were more recalcitrant. Despite this, 90 – 100 cm samples had lower OR values and higher C_{OX} values than vegetation, implying a higher level of oxidation, while vegetation also had high TG PC3 scores. Nonetheless, high H:C and O:C ratios and lower energy content in vegetation and litter may be indicative of less decomposed organic matter and consequently a lower degree of recalcitrance.

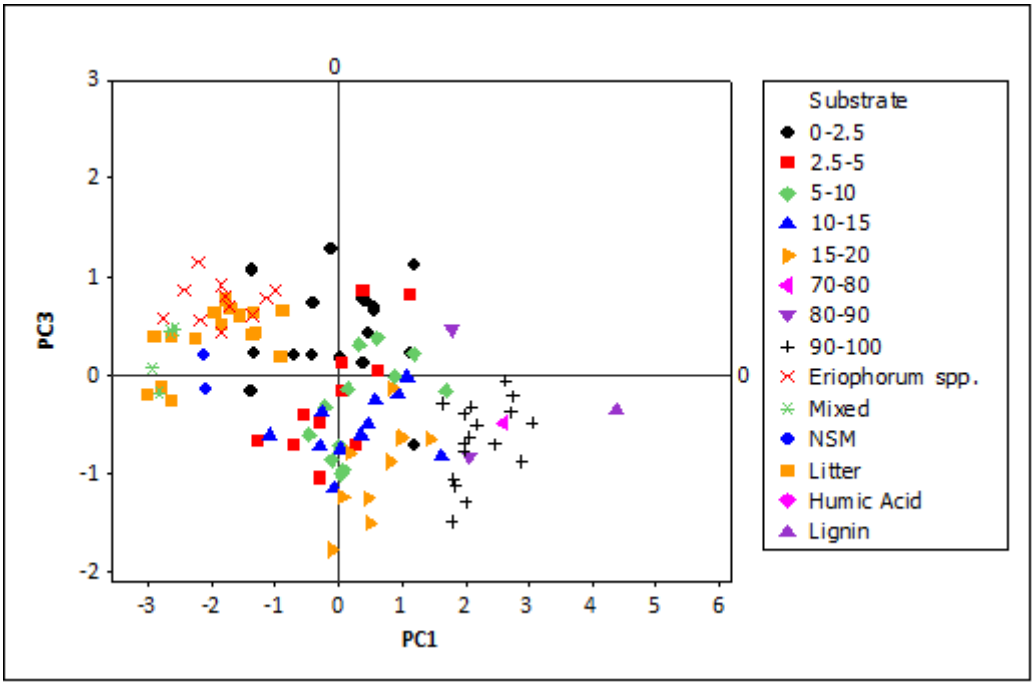

Figure 3.33 Scatterplot of Multivariate PC1 & PC3: NSM = Non-Sphagnum moss spp.

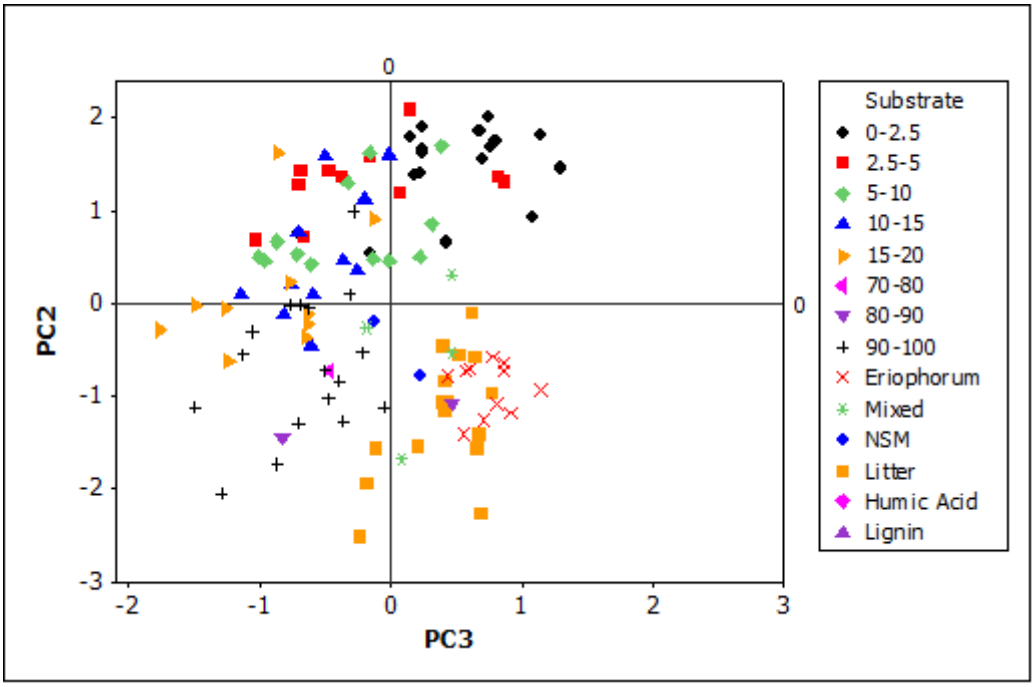

Figure 3.34 Scatterplot of Multivariate PC2 & PC3: NSM = Non-Sphagnum moss spp.

Figure 3.34 showed that 90 – 100 cm peat samples typically grouped with negative loadings of PC2 and PC3, indicating high C:N ratios, energy content and a positive TG PC3 score. The change to the top of the core was defined by low C:N ratios and negative TG PC3 scores. Vegetation was characterised by low energy content and high O:C ratios, while the most positive vegetation and litter samples on PC3 had high TG PC2 scores.

ANOVA of the multivariate principal components (Table 3.17) indicated that although substrate origin was the dominant factor dictating variation for PC1 – PC4, slope was significant for PC2 ($p = 0.002$, $\omega^2 = 1.64\%$) and PC4 ($p = 0.008$, $\omega^2 = 5.89\%$). Significant differences for PC2 (Figure 3.35) indicated the mid-slopes had higher scores on PC2, indicative of lower C:N and H:C ratios and TG PC3 scores. This was consistent with analysis of the individual variables that dominated the PC2 trend. The bottom-slope (0.407) had a significantly higher mean on PC4 than the top-slope (-0.163), reflecting lower energy content, TG PC2 score and OR value. Kruskal-Wallis (Table 3.18) suggested that slope was not significant in explaining variation for PC2.

Table 3.17 Multivariate ANOVA: ω^2 = % variance

Multivariate PC1 ANOVA			**Multivariate PC2 ANOVA**		
Factor	**P**	**ω^2**	**Factor**	**P**	**ω^2**
Substrate	<0.0001	83.47%	Slope	0.002	1.64%
			Substrate	<0.0001	74.92%
N 114		**R^2 83.59%**	**N 114**		**R^2 76.72%**
Multivariate PC3 ANOVA			**Multivariate PC4 ANOVA**		
Factor	**P**	**ω^2**	**Factor**	**P**	**ω^2**
Substrate	<0.0001	58.65%	Slope	0.008	5.89%
			Substrate	<0.0001	32.55%
N 114		**R^2 58.87%**	**N 114**		**R^2 38.66%**

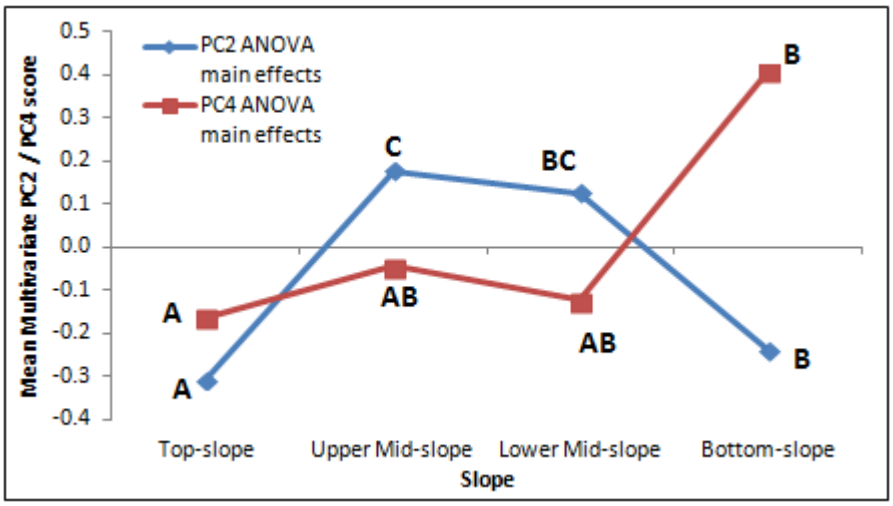

Figure 3.35 Multivariate PC2 & PC4 ANOVA main effects plots by slope: significant differences denoted where letters are not shared between slope positions

Table 3.18 Multivariate PC2 Kruskal-Wallis results

Slope	N	Median	Ave Rank	Z
Top-slope	35	0.002	54.9	-0.56
Upper Mid-slope	23	0.102	63.0	0.89
Lower Mid-slope	23	0.113	63.8	1.02
Bottom-slope	33	-0.352	52.1	-1.12
Overall	114		57.5	
H = 2.58		**DF = 3**		**P = 0.461**

Regression analysis (Table 3.19) of TG PC2 suggested it was positively correlated to O:C ratio and OR and negatively correlated to energy content and H:C ratio. This would imply the amount of humic or lignin-type compounds was higher with less oxidised material, despite the positive correlation with O:C ratio. More interestingly, TG PC3 was positively correlated to energy content, C:N, O:C and H:C ratios and OR. This suggested that as energy content increased and nitrogen was depleted, more recalcitrant substances that reflect lignin-type compounds lose weight during pyrolysis. However, the higher O:C and H:C are indicative of less decomposed organic matter, perhaps reflecting that vegetation and litter had positive TG PC3

values as well. The O:C ratio also increased with sample depth due to the increase in oxygen alongside higher carbon content.

Table 3.19 TG PC2 & PC3 MLR: SE = standard error

Variable	Predictor	Coef	SE Coef	P
TG PC2	Constant	-13	6	0.040
	Energy content	-0.3	0.1	0.037
	O:C	7	1	<0.0001
	H:C	-7	1	<0.0001
R^2 39.80%	OR	22	6	<0.0001
TG PC3	Constant	-31	4	<0.0001
	Energy content	0.6	0.1	<0.0001
	C:N	0.08	0.01	<0.0001
	O:C	6	1	<0.0001
	H:C	3.0	0.7	<0.0001
R^2 65.50%	OR	9	4	0.044

3.4.8 Impact of organic matter on hydrology & carbon

Bulk density was incorporated as a covariate in the ANCOVA WTD model from Chapter 2 to determine whether it explained any variation in WTD. Bulk density ($p < 0.0001$, $\omega^2 = 5.00\%$) was significant (Table 3.20) and removed the effect of slope angle from the ANCOVA model. This resulted in a small improvement in the model's coefficient of determination ($R^2 = 89.82\%$). The model suggested that WTD was significantly higher on the bottom-slope (32 mm, Figure 3.36) relative to all other hillslope positions, while the upper mid-slope was significantly deeper (-311 mm). Although the model appeared to give reasonable results on the site-slope interaction for Alport Low, it suggested WTD was 156 mm above the surface on the Featherbed Moss bottom-slope. The regression model (Table 3.21) indicated a negative correlation between WTD and ρ_{BD}. In the regression model, slope angle was still significant, while wetness index was not.

Table 3.20 Organic matter ANOVA: ρ_{BD} = bulk density; WI = wetness index; ω^2 = % variance

WTD ρ_{BD} ANOVA			LnR_{eco} Litter ANOVA			LnP_G Top 20 cm ANOVA		
Factor	**P**	**ω^2**	**Factor**	**P**	**ω^2**	**Factor**	**P**	**ω^2**
WI	<0.0001	1.64%	WTD	<0.0001	6.12%	1/T	<0.0001	35.14%
ρ_{BD}	<0.0001	5.00%	LnP_G	<0.0001	43.24%	LnPAR	<0.0001	5.46%
Site	<0.0001	22.69%	WI	0.035	0.28%	Energy content	0.004	0.71%
Slope	<0.0001	25.73%	C:N	0.017	0.59%	Month	<0.0001	11.35%
Sub-slope	<0.0001	8.88%	H:C	0.001	0.68%			
Month	<0.0001	5.18%	Month	<0.0001	12.97%			
Site*Slope	<0.0001	20.47%						
Site*Month	0.005	0.23%						
N 707		**R^2 89.82%**	**N 564**		**R^2 59.0%**	**N 562**		**R^2 52.71%**

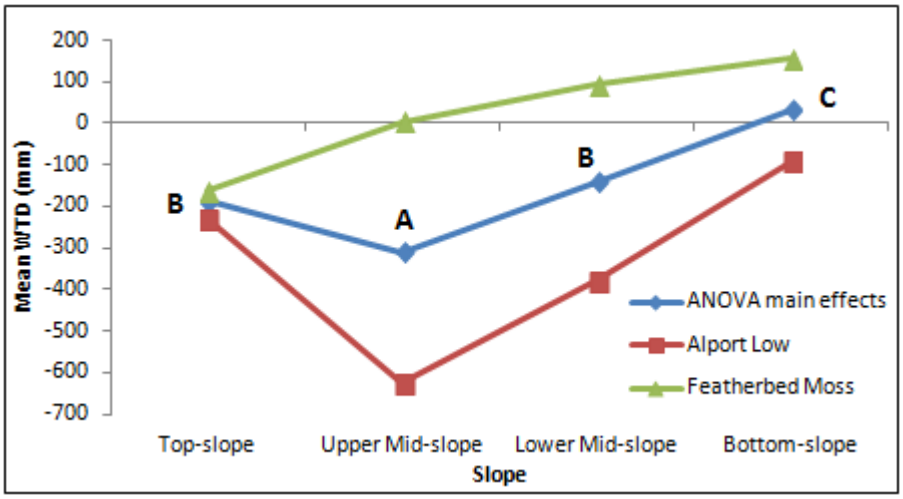

Figure 3.36 WTD ANOVA main effects & interactions plot: significant differences denoted where letters are not shared between slope positions

Litter C:N ($p = 0.017$, $\omega^2 = 0.59\%$, Table 3.20) and H:C ($p = 0.001$, $\omega^2 = 0.68\%$) ratio were significant in explaining variation in R_{eco}, though only to a small degree. However, the ANCOVA model ($R^2 = 59.0\%$) was not as successful in explaining variation in R_{eco} as the original ANCOVA model ($R^2 = 65.83\%$, Table 2.13). This was because slope position was insignificant and resulted in the removal of sub-slope from the model. Regression analysis (Table 3.21) indicated a negative correlation between R_{eco} and C:N and H:C ratios. Despite the lower R^2 in the ANCOVA

model, the R^2 of the regression model was improved (R^2 = 58.80%; original model R^2 = 57.80%, Table 2.17) despite the removal of wetness index as insignificant.

Table 3.21 Organic matter MLR: Sin M & Cos M = sin and cos by month; SE = standard error

Variable	Predictor	Coef	SE Coeff	P value
WTD	Constant	180	30	<0.0001
	Sin M	-18	7	0.012
	Cos M	39	7	<0.0001
	Slope angle	-50	2	<0.0001
R^2 55.3%	ρ_{BD}	-400	100	0.003
LnR_{eco} Litter	Constant	1.1	0.8	0.151
	Sin M	-0.14	0.04	<0.0001
	Cos M	-0.47	0.05	<0.0001
	WTD	-0.0005	0.0001	<0.0001
	LnPG	0.35	0.02	<0.0001
	C:N	-0.010	0.004	0.005
R^2 58.8%	H:C	-1.3	0.5	0.007
Soil LnP_G	Constant	5	4	0.241
	Sin M	-0.47	0.06	<0.0001
	Cos M	-0.40	0.10	<0.0001
	1/T	-3800	900	<0.0001
	LnPAR	0.42	0.05	<0.0001
	Altitude	-0.007	0.002	0.007
R^2 50.0%	Energy content	0.4	0.1	<0.0001

For P_G, energy content averaged across the top 20 cm of peat was significant (p = 0.004, ω^2 = 0.71%) and slightly improved model performance (R^2 = 52.71%; original ANCOVA model R^2 = 52.06%, Table 2.13), with WTD and altitude no longer significant. Regression analysis (Table 3.21) indicated that altitude was still significant, while energy content was positively correlated to P_G. The regression model R^2 increased by 0.90%. Litter H:C was significant when litter organic matter quality parameters were tested, but the model did not perform as well as the soil ANCOVA. No organic matter quality parameters were significant in explaining variation in NEE and DOC.

3.5 Discussion

3.5.1 Limitations

There were a number of limitations to this study that must be outlined before putting the results into context. It was only possible to analyse one core per sub-slope, meaning there were only two cores per study site slope position and no replicates on a sub-slope level. Given the number of samples collected in the study and the time constraints involved in many of the analyses, it was not possible to gather a complete dataset for all measures used in this study. Thermogravimetric analysis required two hours per analysis and consequently it was not possible to analyse the full length of the soil profile, with a focus upon the top 20 cm and deepest samples to assess the change down the soil profile. No intermediate depths were analysed. This proved sufficient to separate different sample depths using PCA (Figure 3.28 and Figure 3.29). It was also not possible to perform repeated measurements on TG, though weight loss was broadly consistent for repeated reference substances (Figure 3.27), suggesting variation was likely associated with sample heterogeneity than analytical precision. Though it was intended to gather a complete dataset, time constraints limited oxygen analysis, with vegetation and litter analysed completely and topsoil and bottom samples prioritised for peat samples. Consequently, O:C ratio, C_{OX} and OR measurements were limited in dataset size as well.

Atomic ratios and weight loss characteristics can be useful in providing information about decomposition and how labile a substrate is, particularly if referred back to known reference materials as in this study. However, the specific composition of organic matter was not determined. Many studies have related TG weight loss and elemental composition to specific compounds and structural properties, using techniques such as NMR and GC-MS. Almendros et al. (2003) used NMR to show that during thermal treatment of peat, there was

an enrichment in heterocyclic and aromatic N and a decrease in amide N. In a study of black carbon, de la Rosa Arranz et al. (2009) related peaks from TG-DSC to pyrolysis GC-MS and NMR results, classing pyrolysis products as alkanes and alkenes, carbohydrates, proteins and aromatics, something also done by Pereira et al. (2011). As such, techniques like GC-MS and NMR can complement the study and aid interpretation of elemental composition and TG by identifying specific compounds. Consequently, although organic matter was inferred to be similar in composition to cellulose, humic acids or lignin, the presence of such compounds in samples could not be confirmed in this study.

A further limitation was in the interpretation of vegetation results. Samples were collected on the basis of being analysed as an end-member at the top of the soil surface, distinct from soil samples. This meant that for hummock plots with both *Eriophorum spp.* and *Vaccinium myrtillus*, vegetation was not separated into distinct functional groups of sedge or shrub and were prone to error due the mass of one vegetation type over the other. *Calluna vulgaris* has been shown to have a different C:N ratio than *Eriophorum spp*. (Worrall et al., 2012a) for instance and thus the approach used in this study was limited in its interpretation of vegetation results. Nonetheless, PCA results showed distinct groupings of vegetation and litter separate from peat samples (Figure 3.32), lending support to the original intention of using vegetation as a probable end-member in organic matter composition.

3.5.2 Bulk density

Bulk density significantly decreased down-slope, with values lower on the bottom-slope compared to the top-slope and upper mid-slope. Landscape scale variation in ρ_{bd} was noted by Lewis et al. (2012), who found that ρ_{bd} was higher at peat margins near the riparian zone than the centre of a blanket bog. Variation in ρ_{bd} was also identified between peatland types including peat plateaus, fens and ombrotrophic bogs by Robinson and Moore (1999),

with significant microtopographic variation as well between hummocks and hollows. Holden (2005a) reported increased variability in ρ_{bd} on top-slopes and bottom-slopes compared with mid-slopes. Bulk density varied between 0.15 – 0.17 g cm^{-3} and was lowest on the mid-slope and highest on the bottom-slope (Holden, 2005a). Results in this study disagreed, given ρ_{bd} at the bottom of the hillslope was significantly lower than the top-slope and upper mid-slope.

Some studies have found ρ_{bd} increased with depth (Robinson and Moore, 1999, Holden and Burt, 2002a, Holden, 2005a) yet this relationship is not consistent. Clymo (2004) found no clear change in ρ_{bd} between 1 – 5 m depth, while it varied within the top metre. Tomlinson (2005) reported no consistent relationship with depth and Lewis et al. (2012) found no significant change with depth. At two lowland fen peats in England, higher ρ_{bd} at the surface of the soil profile was associated with increased decomposition and degradation of soil organic matter (Kechavarzi et al., 2010), while Heller and Zeitz (2012) suggested lower ρ_{bd} at depth was due to less disturbance from human impact. It could be that erosion near the surface on Featherbed Moss and Alport Low increased ρ_{bd}, with lower densities at depth due to a lower level of disturbance. Indeed, Lindsay (2010) argues the traditional acrotelm-catotelm model (Clymo, 1992) does not apply to British blanket bogs, suggesting that decreasing ρ_{bd} with depth could be due to disturbance or destruction of the acrotelm, with upper layers in fact catotelmic peat exposed to aerobic conditions, therefore being haplotelmic peat.

Increased ρ_{bd} has been shown to decrease hydraulic conductivity (Schlotzhauer and Price, 1999) and consequently it could be expected to cause an increase in the water table. This was not the case. The negative correlation indicated that as ρ_{bd} increased, the water table got lower. Tuittila (2000) noted lower ρ_{bd} on a rewetted peatland relative to a drained peatland. Other studies have noted an increase in ρ_{bd} as a result of drainage (Laiho et al., 2004, Minkkinen and Laine, 1998, Laiho et al., 1999). It was hypothesised that alongside effects associated with afforestation, physical collapse of pore structures and enhanced oxidation

could be a cause of increased ρ_{bd}. It may therefore be that for this study, the relationship between ρ_{bd} and water table is related more to site variation than slope. Indeed, correlation is not causation as the toes of slopes have low density and high water tables because they are the bottom of the slope, not because one explains the other. Mean ρ_{bd} on Alport Low from ANOVA main effects was 0.208 g cm^{-3}, as opposed to 0.183 g cm^{-3} on Featherbed Moss. Thus, given the much higher water tables on Featherbed Moss than Alport Low, it is not surprising that the correlation between ρ_{bd} and water table is negative. The site-slope interaction for ρ_{bd} lends this argument further credence, given the enhanced ρ_{bd} on the Alport Low mid-slopes. This may therefore reflect enhanced oxidation with water table drawdown and collapse of poor structures on Alport Low. Furthermore, slope angle was removed in the ANCOVA model, though not in the regression model, by the relationship between WTD and ρ_{bd}, which was also negatively correlated to WTD due to the high slope angles on the Alport Low mid-slope.

3.5.3 Organic matter composition and energy content

Carbon and nitrogen content was significantly lower on the bottom-slope relative to the other three hillslope positions, with C:N ratio significantly higher on the bottom-slope compared to the mid-slopes. This suggested a preferential depletion of nitrogen down-slope, possibly due to transportation. Kracht and Gleixner (2000) argued that changes in nitrogen content in the soil profile between 1 – 10 cm was caused by different microbial communities and possible effects related to fluctuations in the water table, from oxygenated to reduced conditions. Andersson et al. (2012) stated that loss of nitrogen under anaerobic conditions occurred through microbial denitrification with NO_3 reduced to N_20 and N_2 or otherwise by anaerobic ammonium oxidising bacteria. It is possible that differences in nitrogen content were therefore related to microbial community, or changes in moisture status; the bottom-slope had significantly higher water tables than other hillslope positions, though this did vary

with site. An alternative explanation could be that lower pH levels on the top-slope and mid-slopes caused a reduction in the mineralisation of carbon and nitrogen. Such an effect was noted by White et al. (1996) and although no covariates were included in compositional analysis to confirm such an effect, the pH of soil pore water was significantly higher on the bottom-slope than the top-slope and upper mid-slope (Figure 2.21).

Carbon content increased with depth, while nitrogen was depleted with depth, causing an increase in C:N with depth. Some studies have observed a decrease in C:N with depth, with Kuhry and Vitt (1996) suggesting a preferential loss of carbon in the catotelm was due to anaerobic decomposition. However, Reiche et al. (2010) and Anderson (2002) observed an increase in C:N ratio with depth. The increase in C:N observed in this study would imply a preferential loss of nitrogen and consequently more labile compounds, leading to an accumulation of more recalcitrant compounds at depth.

The C:N ratio significantly decreased between *Eriophorum spp*. compared to that of the topsoil at 0 – 2.5 cm. Although the decrease in C:N ratio between *Eriophorum spp.* and surface peat was noted by Worrall et al. (2012a), the C:N ratio of *Eriophorum spp.* from that study was considerably greater than the one found here. Furthermore, litter C:N ratio was not different from that of the topsoil, whereas here it was more reflective of vegetation C:N, perhaps indicating a lower state of decomposition as Worrall et al. (2012a) postulated that vegetation absorbs nitrogen during the transition to litter. Indeed, White et al. (1996) found C:N of fresh *Calluna* litter was 45, close to the mean value of litter in this study, while an increase in nitrogen content and decrease in C:N during litter decomposition has been observed elsewhere (Domisch et al., 2006, Rubino et al., 2007). The decrease in C:N ratio as vegetation is decomposed and transformed to peat (Worrall et al., 2012a) is consistent with results found here.

The increased level of decomposition and humification down the soil profile was further supported by the change in H:C ratio between vegetation and litter and with depth of

the peat profile. Kracht and Gleixner (2000) reported H:C ratios of surface peat samples and moss close to that of cellulose (1.67), with a decrease to 10 cm depth suggesting a dehydration process, or inhibition of oxidative degradation and preservation of phenolic compounds. Cellulose H:C ratio in this study was 1.74 and the values of litter (1.72) and *Eriophorum spp*. (1.67) would suggest a low state of decomposition, comparable with more labile carbohydrate compounds found in cellulose (LaRowe and Van Cappellen, 2011). Andersson et al. (2012) stated that a change from high H:C ratios to lower values towards those of lignin (1.27) was the result of decomposition of more readily degradable aliphatic compounds and the accumulation of aromatics. Indeed, Leifeld et al. (2012) noted a decrease in H:C with depth, with more recalcitrant compounds present, while Klavins et al. (2008) noted a decrease in H:C with humification due to dehydrogenation, leading to the accumulation of more thermally stable aromatic and polyaromatic compounds.

Decomposition of vegetation and litter during the transition in the peat profile could therefore be caused by selective degradation of more labile carbohydrate and aliphatic compounds, reflected in the decreased H content and H:C ratios in 0 – 2.5 cm peat relative to vegetation and litter, which was more akin to that of humic acid and lignin. The further decrease in H:C ratio with depth, though minimal compared to the transition between litter and soil, would imply a continuation of the decomposition process, despite an increase in hydrogen content with depth relative to surface layers. H:C ratio was higher on the bottom-slope and lower on the upper mid-slope, implying a higher level of degradation on the upper mid-slope. This would seem contrary to the observation inferred with the C:N ratio, but both mean values of 1.27 and 1.31 for the upper mid-slope and bottom-slope respectively are considerably lower than vegetation and litter. As such it seems likely that both slope positions have undergone considerable degradation, but the extent of this was more severe on the upper mid-slope. Furthermore, mean C:N ratios of 47.31 and 51.17 were nonetheless high for both the upper mid-slope and bottom-slope respectively.

Energy content was significantly lower on the bottom-slope than all other hillslope positions. Trofimov and Emelyanenko (2000) noted that energy content increased during decomposition, owing to preservation of lignin-type compounds that had a high energy content, with mineralisation of cellulose occurring over a much shorter times-scale. Gary et al. (1995) noted an increase in energy of woody tissue with increased lignin content, with energy content related to humification by Lahdesmaki and Piispanen (1988). The lower energy content on the bottom-slope may suggest a lower level of decomposition, as with H:C ratio but in contrast to C:N ratio. In likelihood, the lower energy content reflected the lower carbon content on the bottom-slope. Energy content increased with depth and was significantly higher in surface peat than *Eriophorum spp*. and litter, reflecting the transition that took place during decomposition of vegetation and litter and subsequent humification at depth with the preservation of more recalcitrant, energy rich, compounds. Such an interpretation was supported by multivariate analysis, with Figure 3.33 indicating a transition towards energy-rich, lignin-type compounds with depth as phenolic compounds were less easily degraded.

The top-slope and lower mid-slope had significantly lower oxygen content than the bottom-slope, while O:C ratio was significantly lower on the mid-slopes compared to the bottom-slope. O:C ratio is an indicator of carbohydrate and carboxylic content (Zaccone et al., 2008) and decreases with increasing humification due to decarboxylation (Klavins et al., 2008). As such, the bottom-slope may have higher quantities of oxygen-containing functional groups. This was reflected in the overall stoichiometry, with the less negative C_{OX} and lower OR values on the bottom-slope compared to the top-slope and lower mid-slope implying a more oxidised substrate. However, the C_{OX} and OR values would suggest a more reduced substrate than organic acids and carbohydrates, with the OR values closest to those of soluble phenolics reported by Masiello et al. (2008).

Randerson et al. (2006) used OR to show that lignin, lipids, humic acids and humins were more reduced and recalcitrant than compounds such as cellulose. Baldock et al. (2004)

reported decomposition lead to a decrease in carbohydrate content and an increase in lignin and lipids. As such, the change in OR and C_{OX} with depth and during the transition between vegetation and litter to soil is surprising. Given the observed changes in energy content and H:C and C:N ratios between vegetation and soil, it was expected that soil would be more reduced, with a further decline in C_{OX} with depth due to increased decomposition and selective preservation of more recalcitrant organic matter. Yet *Eriophorum spp*., mixed vegetation and litter had significantly lower C_{OX} and higher OR values than 0 – 2.5 cm peat, while peat at 90 – 100 cm was more oxidised than the top 20 cm. The values of OR for cellulose and lignin suggested that although 0 – 2.5 cm peat was more reduced than cellulose, it was not to the same degree as vegetation and litter, which seemed to trend towards lignin in C_{OX} and OR. The significantly higher oxygen content of vegetation and litter and concomitant higher O:C ratios would imply they were more oxidised than topsoil peat; it may be that C_{OX} and OR reflected the greater hydrogen content of vegetation and litter and thus although the high H:C ratios were indicative of cellulose or similar carbohydrates, C_{OX} and OR were indicative of lignin-type compounds within the vegetation and litter – something which would be expected given their physical structure. The cause of the increase in carbon oxidation state with depth was unclear, but may reflect different compositional processes, dehydrogenation rather than decarboxylation.

3.5.4 Thermogravimetric analysis

Thermogravimetric analysis was most useful in determining changes with depth in the peat profile and substrate. Chen et al. (2011) suggested weight loss in peat was related to hemicellulose, cellulose and lignin, observing a peak in the DTG curve at 300 °C and another at 340 °C. This may suggest the peaks in vegetation and soil between 280 – 300 °C were related to hemicellulose. Sutcu (2007) related peat weight loss between 200 – 340 °C as

decomposition of phenolic compounds and carbonyl and carboxyl structural groups; later weight loss was associated with aromatic compounds. Reiche et al. (2010) similarly suggested labile compounds caused weight loss between 205 – 360 °C, with gradual weight loss of stable organic matter following. Thus it may be that the second DTG peak observed for vegetation and litter was related to mass loss of lignin-type compounds. The gradual mass loss of peat, with a second peak at ~410 °C, could be indicative of thermally stable, possibly aromatic, compounds.

Principal components analysis indicated two trends: the separation of soil from vegetation and litter; and a distinction between humic acid and lignin-type compounds. The separation of soil from vegetation was likely caused by the secondary peaks in mass loss for vegetation and litter, perhaps indicative of lignin type compounds. It may also have suggested the presence of cellulose, yet this was not important in PCA. The trend towards lignin-type compounds in vegetation was indicated by plotting PC2 against PC3 and could lend support to the results inferred by C_{OX} and OR. However, deeper soil samples also trended towards lignin, supporting the observed increase in energy content and C:N ratio with depth and concomitant decrease in H:C ratio. This may reflect the variety of degradation processes that occur between the transition of vegetation and litter to soil and further decomposition with depth. Weight loss in surface peat samples was more towards humic acid, perhaps indicating the presence of aromatic compounds in surface soil layers. It was possible to separate PC3 across the slope and suggested that the top-slope and bottom-slope trended more towards lignin-type compounds.

3.5.5 Multivariate analysis

As with PCA of the TG dataset, the multivariate dataset was most useful in distinguishing substrate and sample depths. PC1 was dominated by C_{OX} and OR and when plotted against PC2 (Figure 3.32) distinguished between soil and vegetation and litter. However, the second trend between peat depth was dominated by C:N ratio and TG PC3 weight loss, reflecting the increased carbon and energy content at depth. Furthermore, PC1 did not appear to plot based upon C_{OX} and OR in Figure 3.33. Despite the strong trend of vegetation and litter being more reduced in composition towards lignin, lignin plotted close to deep peat samples, a reflection of the low H:C ratios and high C:N ratio and energy content at depth. This would lend support to the interpretation of increased humification with depth and preservation of recalcitrant, energy rich compounds. Furthermore, it shows the advantage of using multivariate datasets given the complexity of degradation trends. Indeed, it was possible to separate hillslope characteristics, with PC2 reflecting the reduced C:N and H:C scores on the mid-slopes, and lower energy content and higher oxidation state of the bottom-slope.

3.5.6 Organic matter and carbon cycling

Ecosystem respiration was negatively correlated to litter C:N and H:C ratio. Though the effects were small (<1%) it demonstrated the sensitivity of the experiment in establishing effects on carbon flux associated with organic matter composition. The relationship between litter composition and R_{eco} implied the utilisation of litter by microbial communities, which would be expected during the transformation to soil. The presence of litter has been shown to increase CO_2 efflux (Ward et al., 2010, Rubino et al., 2007), though the latter study was comparable only to bare soil controls. The negative correlation between R_{eco} and C:N would suggest that more labile substrates increased CO_2 efflux. This was consistent with previous research; selective mineralisation of younger labile carbon sources has been observed (Crow

and Wieder, 2005, Hardie et al., 2011) or otherwise the addition of labile carbon sources has been shown to stimulate decomposition of recalcitrant organic matter (Fontaine et al., 2007). Furthermore, increased nitrogen content has been related to increased CO_2 efflux (Bragazza et al., 2006), while Reiche et al. (2010) found anaerobic CO_2 production was negatively related to C:N ratio. Such findings lend support to the notion of both litter as a source of heterotrophic respiration and preferential assimilation of more labile compounds.

The negative correlation between H:C ratio and R_{eco} contradicted the pattern suggested by C:N and R_{eco}. It must be noted however that H:C ratio was high for all litter samples, with a minimum of 1.63 (Table 3.6) still indicative of a less degraded substrate, whereas C:N ratio of litter varied between 31.06 and 62.01. Nonetheless, it is possible for stable organic matter to contribute to R_{eco}; Reiche et al. (2010) demonstrated thermally recalcitrant compounds can be used by microorganisms alongside labile compounds, while Hardie et al. (2011) also suggested old carbon sources affected CO_2 efflux under certain conditions. This may lend support to the positive correlation between energy content and P_G, suggesting a relationship between more energy rich, thermally stable compounds. It may otherwise imply a relationship between lignin-type compounds and consequently vascular species contributing to organic matter in the soil profile.

Organic matter compositional data were not found to affect DOC concentration, either with topsoil peat or litter. Many studies have found positive correlations between soil C:N ratio and DOC export or production (Aitkenhead and McDowell, 2000, Aitkenhead-Peterson et al., 2007, Kindler et al., 2011). Other studies have emphasised the importance of labile soil organic matter in the top of the peat profile as the primary source of DOC (Palmer et al., 2001) or otherwise acknowledged the importance of litter to DOC production (Ward et al., 2010, Tang et al., 2013). However, neither Michel and Matzner (1999) or Moore et al. (2008) found a

relationship between C:N ratio and DOC. Such findings agree with the results from this study, with no effect found either from surface peat or litter as the source of DOC.

3.6 Conclusions

The purpose of this chapter was to investigate whether the physical properties of peat and its organic matter composition varied across the hillslope, while also identifying changes in composition down the soil profile and during the decomposition of vegetation and litter into the soil profile. The final objective was to determine if organic matter composition affected carbon cycling and ρ_{bd} affected WTD. Bulk density was significantly higher on the top-slope and upper mid-slope compared to the bottom-slope, while it decreased with depth in the soil profile, possibly caused by disturbance at the surface as result of erosion. Bulk density was negatively correlated to WTD, indicating that water tables were lower with higher bulk density. This could be related to site-specific slope effects and the collapse of pore structures under oxidised conditions where water tables are lower.

Organic matter composition varied with hillslope. Carbon and nitrogen content was lower on the bottom-slope, with C:N ratios significantly higher than mid-slopes. This indicated more labile substrates on the mid-slope, but H:C ratio suggested the upper mid-slope was more degraded than the bottom-slope and may therefore reflect selective decomposition processes such as dehydrogenation. The higher O:C ratio on the bottom-slope relative to the mid-slopes suggested the bottom-slope was less decomposed, while the higher C_{OX} and lower OR values indicated that peat was more oxidised on the bottom-slope than the top-slope and lower mid-slope.

There was a clear transition between vegetation and surface peat samples but litter was similar to vegetation in its composition, suggesting it was in a low state of decomposition.

C:N ratios decreased during degradation of vegetation and litter and its transition into the soil profile, while higher H:C ratios in vegetation and litter indicated possible labile carbohydrate and aliphatic compounds that were preferentially degraded. Consequently, C:N ratio and energy content increased with depth, while H:C ratios decreased, indicating preservation of more recalcitrant compounds. O:C ratio increased with depth in the soil profile however, while C_{OX} and OR values indicated vegetation and litter was more reduced than peat. TG analysis suggested a change between humic and lignin-type compounds with increasing depth of the soil profile and multivariate analysis supported the notion that thermally stable, energy rich compounds accumulated preferentially with depth during humification.

Litter C:N ratio was negatively correlated to rates of R_{eco}, indicating that CO_2 efflux was enhanced in the presence of more labile substrates for heterotrophic respiration. H:C ratio was negatively correlated to R_{eco} as well, though litter H:C ratios were still indicative of low levels of decomposition. Energy content was positively correlated to P_G, possibly indicative that recalcitrant organic matter can be important to carbon cycling, or otherwise reflective of the importance of vascular species to rates of P_G. C:N ratio has been shown to affect DOC production and export, but no effect was found here.

Chapter 4 Carbon flux of a hillslope transect

4.1 Introduction

Chapter 2 identified significant changes in water table depth (WTD), CO_2 flux and dissolved organic carbon (DOC) across the hillslope. Water table depth was highest at the bottom-slope due to lateral down-slope flow maintaining high water tables and slope angle was suggested to be an important control upon WTD. Ecosystem respiration (R_{eco}) was higher on mid-slopes, possibly due to water table drawdown effects, but spatial heterogeneity was not fully accounted for and gross photosynthesis (P_G) was higher on the bottom-slope. Furthermore, DOC concentration decreased down-slope and was significantly related to WTD and possibly changes in hydrological flowpath across the slope. However, it is important to establish whether the patterns found with WTD, CO_2 flux and DOC flux are consistent across the slope with more detailed monitoring.

This chapter will explore the hillslope in more detail by increasing the frequency of monitoring points across the slope and extending the study towards the stream in the riparian zone. A transect of 12 slope positions was used to explore in further detail the role of hillslope in carbon cycling.

4.2 Aims and objectives

The aim of this chapter was to establish whether variation in water table and carbon cycling is consistent along the hillslope by assessing WTD, CO_2 flux and DOC down a single slope transect. The objectives are:

- Assess the change in WTD and surface runoff at multiple points along a slope transect to establish whether there is a consistent hydrological response at different hillslope units.
- Determine whether CO_2 flux varies uniformly along the slope units or whether spatial heterogeneity is more important.
- Establish whether DOC concentration continues to decrease down-slope along a transect towards the riparian zone and look at differences in DOC between soil pore water, runoff water and stream sources.
- Relate findings back to results from Chapter 2 to determine whether consistent slope affects are evident.

4.3 Materials and methods

4.3.1 Experimental design

The study was conducted on Alport Low, with the four hillslope positions used in Chapter 2 realigned into a transect from the top-slope to the riparian zone (Figure 4.1). The hillslope on Featherbed Moss did not have a riparian zone and was not used. Twelve hillslope positions were used as part of the slope transect (Table 4.1), numbered 1 – 11 from the top-slope to riparian zone. The topmost slope position was divided into 1-E and 1-H, comprised of former top-slope *Eriophorum spp.* plots 1 – 3 (1-E) and top-slope hummock plots 4 – 6 (1-H). Slope position 4 was formerly upper mid-slope plots 1 – 3. Ostensibly, the top-slope, mid-slope

and bottom-slope were represented by four slope positions each: 1-E & 1-H – 3 = top-slope; 4 – 7 = mid-slope; and 8 – 11 = bottom-slope. Such a derivation was supported by altitudinal and slope angle variation (Table 4.1), whereby change in elevation was more rapid between slope positions 4 – 7 which also had slope angles more than five degrees. Slope position 9 had a slope angle of 6.4°, but was located in a small depression to capture more variation across the bottom-slope. Peat depth decreased on mid-slopes to less than 1.5 metres with a low of less than 1 metre, while it was typically above 2 metres on flat locations other than slope position 3. Two stream points were used to collect samples for water quality analysis; one from a stream draining the catchment and another directly draining the bank of peat adjacent to slope position 11, denoted bank-stream, though this was not a soil pipe.

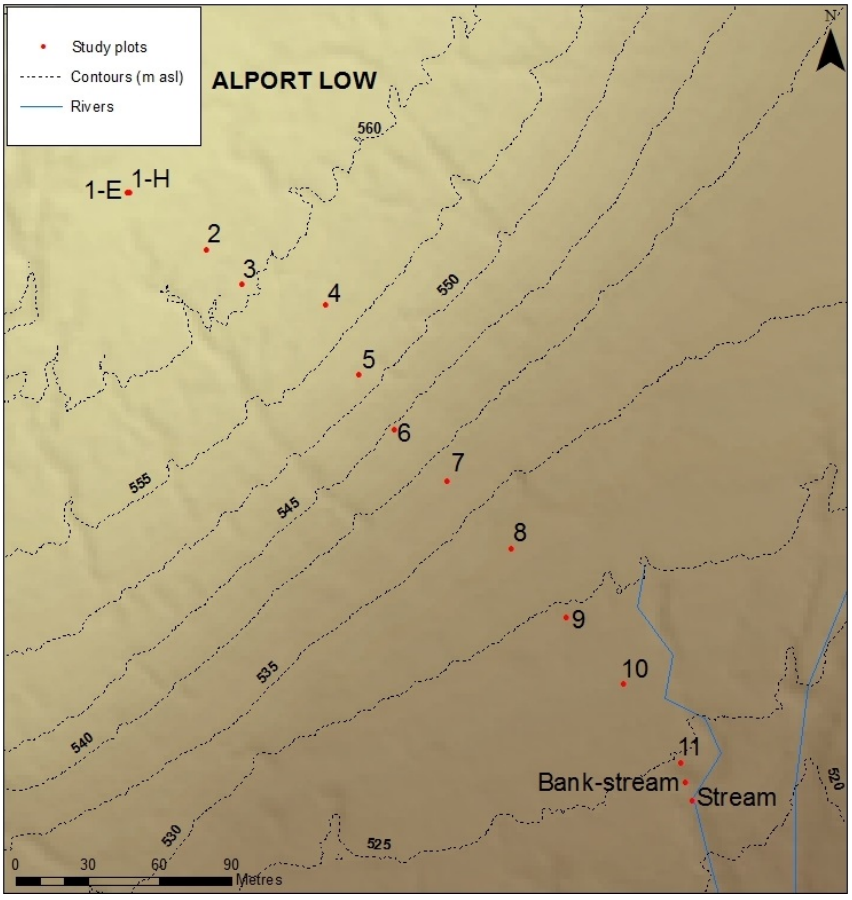

Figure 4.1 Map of Alport Low slope transect

Table 4.1 Alport Low transect site details

Slope position	Plot	*Eriophorum* dominance (%)	Peat depth (m)	Altitude (m)	Aspect (°)	Slope angle (°)	Wetness index
1-E	1	100					
1-E	2	100		563.7	166.9	4.4	4.8
1-E	3	100					
1-H	4	24					
1-H	5	32		563.9	188.6	4.3	5.1
1-H	6	20					
2	1	20	-2.55				
2	2	56	-2.58	561.8	136.1	4.0	4.4
2	3	80	-2.42				
3	1	88	-1.69				
3	2	68	-1.83	560.4	108.0	3.8	5.9
3	3	80	-1.92				
4	1	24	-1.25				
4	2	40	-1.44	557.4	131.3	7.4	7.1
4	3	48	-1.29				
5	1	12	-0.82				
5	2	60	-0.87	552.3	144.2	11.3	5.9
5	3	52	-0.92				
6	1	68	-1.00				
6	2	20	-1.16	544.5	142.3	11.2	6.2
6	3	24	-1.09				
7	1	20	-1.48				
7	2	44	-1.49	537.1	135.1	10.2	6.7
7	3	100	-1.44				
8	1	100	-2.00				
8	2	68	-2.03	532.5	135.0	4.1	6.0
8	3	56	-2.04				
9	1	24	-2.30				
9	2	60	-2.31	529.5	176.8	6.4	7.9
9	3	92	-2.36				
10	1	96	-2.52				
10	2	100	-2.52	527.4	146.3	4.8	7.3
10	3	96	-2.61				
11	1	76	-2.68				
11	2	88	-2.73	525.0	145.9	4.5	6.9
11	3	100	-2.42				

Each slope position was comprised of three plots, each with uPVC gas collar, 1 metre uPVC dipwell and surface runoff trap, as detailed in section 2.3.2. Study plots were installed during August 2011, with sampling of CO_2 flux measurements, soil pore water and surface runoff water and WTD taking place from September 2011 – August 2012. Sampling commenced after a one month gas collar and WTD stabilisation period, following the protocols of Rowson (2008), wherein no anomalies were observed using this time frame. It was not possible to conduct sampling for most slope positions during December 2011 due to extensive snow cover. Although data collected for December was included in raw datasets, it was not included in statistical analysis. A factorial design was employed, comprising slope position (1-E – 11), sample month and slope-month interaction. Vegetation surveys were conducted for each plot in November 2012 to determine the percentage cover of *Eriophorum spp*. classed as dominant vegetation to be used as a covariate in statistical analysis.

4.3.2 Field monitoring

4.3.2.1 Gaseous CO_2 flux

Ecosystem respiration and net ecosystem exchange (NEE) were measured using an infra-red gas analyser (IRGA) connected to an acrylic CPY-2 closed canopy chamber using the method outlined in section 2.3.3.1. Gross photosynthesis was derived as the residual of NEE – R_{eco}. A negative sign convention indicates sequestration of CO_2 from the atmosphere.

4.3.2.2 Water table depth & water collection

Water table depth was measured concurrently with CO_2 flux using a conductivity probe inserted into the dipwell until the water surface was reached. Values were corrected for

the height of the dipwell above the surface, which was measured for each plot every month in case dipwell height changed. Soil pore water samples were collected from dipwells after CO_2 flux measurements were completed. Surface runoff water was collected from runoff traps, which were emptied each month.

4.3.2.3 Basic water chemistry measurements

Prior to analysis, samples were filtered at 0.45 µm to remove particulate matter using cellulose acetate syringe filters. Process blanks of deionised water underwent the same analytical procedures as soil pore water and surface runoff water samples. These process blanks were not used to correct for measurement error but rather to highlight and acknowledge potential sources of error. pH, electrical conductivity and UV-visible absorbance measurements at 400, 465 and 665 nm were made as outlined in section 2.3.4.1. Measurements at 465 and 665 nm were used to determine the E4:E6 ratio, a basic compositional measurement.

4.3.2.4 Dissolved organic carbon

Dissolved organic carbon concentration was determined using a colourimetric method (Bartlett and Ross, 1988), as outlined in section 2.3.4.2. Regression of standards against absorbance measurements allowed determination of detection limits. Measurements below the lower confidence limit were deleted.

4.3.2.5 Anion concentrations

A Metrohm 761 compact IC connected to an 813 Compact Auto-sampler was used to determine concentrations of F^-, Br^-, NO_3^-, PO_4^{3-} and SO_4^{2-}. Further details of the analytical procedure are outlined in section 2.3.4.3. Blanks were run between each slope position, approximately every six samples, which was more frequent than outlined in section 2.3.4.3 due to fewer samples collected at each slope position in this study.

4.3.3 Statistical analysis

Values that contradicted the micro-meteorological sign convention used for R_{eco} and P_G were removed, as were measurements below the lower confidence limit of DOC measurements. Descriptive statistics used in section 4.4 were based upon raw datasets that had not undergone any data treatment beyond that described above. Prior to statistical analysis, each dataset had values outside three standard deviations of the mean removed as outlying values. Outlier removal amounted to a small percentage of each dataset (discussed in section 4.4) and improved dataset distributions.

4.3.3.1 Analysis of variance and covariance

Prior to conducting analysis of variance (ANOVA) and covariance (ANCOVA) dataset distribution was established using the Anderson-Darling test. If a dataset failed the assumption of normality, natural-log transformation was performed. Analysis of variance was conducted on the untransformed or transformed dataset that had the lowest Anderson-Darling statistic if neither passed the assumption of normality. For non-normal datasets, the non-parametric Kruskal-Wallis test was performed to confirm ANOVA results. Levene's test was conducted to test the assumption of homogeneity of variances.

Analysis of variance was performed on WTD, R_{eco}, P_G, NEE and DOC using a General Linear Modelling approach. Backwards modelling was performed, incorporating slope, month and slope-month interactions as factors in the ANOVA model, removing insignificant factors until only significant factors remained. Analysis of covariance applied backwards and forwards modelling. Covariates included in ANCOVA of WTD, CO_2 fluxes and DOC are shown in Table 2.6, though terrain parameters could not be used as they were co-linear with slope position. Soil pore water and runoff water were analysed separately, and water type (soil pore water, runoff water, stream) was analysed separately. To test for differences in CO_2 flux between Chapter 2 and this chapter, study year (Chapter 2 = one, this chapter = two) was included as a factor in additional analyses for slope positions 1-E, 1-H and 4.

4.3.3.2 Multiple linear regression

Slope angle, wetness index and altitude were co-linear with slope and could not be included in ANCOVA models. The significance of the terrain parameters was assessed using multiple linear regression (MLR), adopting backwards and forwards modelling techniques. Regression was not performed for individual slope positions or where slope was not significant in ANCOVA models.

4.3.3.3 Runoff occurrence

The frequency that runoff was observed for each slope position was assessed using the χ^2 method outlined in equation 2.6, followed by *post hoc* tests. Observations were not included in the analysis if bungs were missing on a given month, due to removal by grazing sheep.

4.4 Results

Kruskal-Wallis non-parametric results did not reveal significant differences to ANOVA models and are therefore not discussed further in the results. Table 4.2 shows the percentage of outliers removed from datasets used for ANOVA, ANCOVA and MLR. Individual results tables for ANOVA and ANCOVA show whether datasets were untransformed or log-transformed. Only one dataset, runoff water conductivity, had >2% of data removed.

Table 4.2 Percentage data removed from each variable dataset: SPW = soil pore water; RO = runoff water; and water type = combined SPW, RO and stream water

Variable	Dataset	N	N removed	% removed
WTD	WTD	403	0	0.00
R_{eco}	CO_2 flux	249	0	0.00
P_G	CO_2 flux	293	1	0.34
NEE	CO_2 flux	329	6	1.82
Air temperature	Environmental	335	0	0.00
1/T	Environmental	335	0	0.00
PAR	Environmental	334	2	0.60
DOC	SPW	389	0	0.00
	RO	292	0	0.00
	Water type	703	0	0.00
pH	SPW	394	6	1.52
	RO	335	3	0.90
	Water type	751	0	0.00
Conductivity	SPW	392	5	1.28
	RO	328	8	2.44
	Water type	742	3	0.40
E4:E6	SPW	383	6	1.57
	RO	266	1	0.38
	Water type	671	2	0.30
Cl^-	SPW	391	1	0.26
	RO	335	1	0.30
	Water type	748	12	1.60
SO_4^{2-}	SPW	391	1	0.26
	RO	335	4	1.19
	Water type	748	7	0.94
NO_3^-	SPW	391	7	1.79
	RO	335	1	0.30
	Water type	748	14	1.87

4.4.1 Hydrology

4.4.1.1 Water table depth

Water table depth ranged from -826 mm to 22 mm above the surface (Table 4.3). The deepest mean WTD was at slope 4 (-660 ± 10 mm). This was previously denoted as upper mid-slope and was consistent with results from Chapter 2. There was a progressive increase in water table towards the surface further down-slope; slope positions 5 (-521 ± 9 mm), 6 (-280 ± 30 mm) and 7 (-220 ± 20 mm) had mean WTDs more than 200 mm. However, although WTD increased towards the surface on the flatter bottom-slope, it was deep at slope position 9 (-390 ± 20 mm), located in the depression. Mean WTD was different between 1-E (-30 ± 10 mm) and 1-H (-250 ± 10 mm). Water table was deepest in May 2012 (-340 ± 30 mm), September 2011 (-300 ± 30 mm) and July 2012 (-280 ± 30 mm).

Table 4.3 WTD (mm) descriptive statistics according to slope position and month: SE = standard error

Slope	N	Mean	SE Mean	Maximum	Minimum	Month	N	Mean	SE Mean	Maximum	Minimum
1-E	33	-30	10	-230	22	9	35	-300	30	-826	-16
1-H	33	-250	10	-414	-75	10	36	-200	30	-680	14
2	33	-105	10	-223	-20	11	36	-250	40	-782	22
3	32	-220	20	-386	-12	12	4	-20	4	-30	-11
4	33	-660	10	-826	-535	1	36	-230	40	-817	20
5	33	-521	9	-600	-371	2	36	-190	30	-604	18
6	33	-280	30	-403	-43	3	36	-280	40	-805	2
7	33	-220	20	-371	-20	4	36	-200	30	-640	10
8	33	-130	10	-384	-22	5	36	-340	30	-812	-65
9	33	-390	20	-595	-180	6	35	-250	30	-730	11
10	35	-90	20	-346	20	7	36	-280	30	-713	-30
11	34	-120	20	-357	-11	8	36	-260	30	-723	-10

Slope ($p < 0.0001$, $\omega^2 = 80.14\%$, Table 4.4) and month ($p < 0.0001$, $\omega^2 = 4.24\%$) were significant factors in the WTD ANOVA model ($R^2 = 84.41\%$). As the ANOVA model explained a large amount of variation in WTD, the error term was more likely composed of measurement error than unexplained factors and interactions. The main effects (Figure 4.2) were in good agreement with mean WTD from Table 4.3, reflecting the increase in WTD on the mid-slope, hummock plots and in the bottom-slope depression. Slope positions 1-H, 3, 6 and 7 were significantly deeper than 1-E, 2, 8, 10 and 11 while 4, 5 and 9 were deeper than most slope positions; slope position 4 was deeper than all others (Table 4.5). For month, October, February and April had the highest WTD while September, May and July were deepest.

Table 4.4 WTD ANOVA / ANCOVA; ω^2 = % variance

ANOVA			ANCOVA		
Factor	**P**	**ω^2**	**Factor / covariate**	**P**	**ω^2**
Slope	<0.0001	80.14%	% *Eriophorum spp.*	0.005	25.52%
Month	<0.0001	4.24%	Slope	<0.0001	54.89%
			Month	<0.0001	4.25%
N 394		**R^2 84.41%**	**N 394**		**R^2 84.69%**

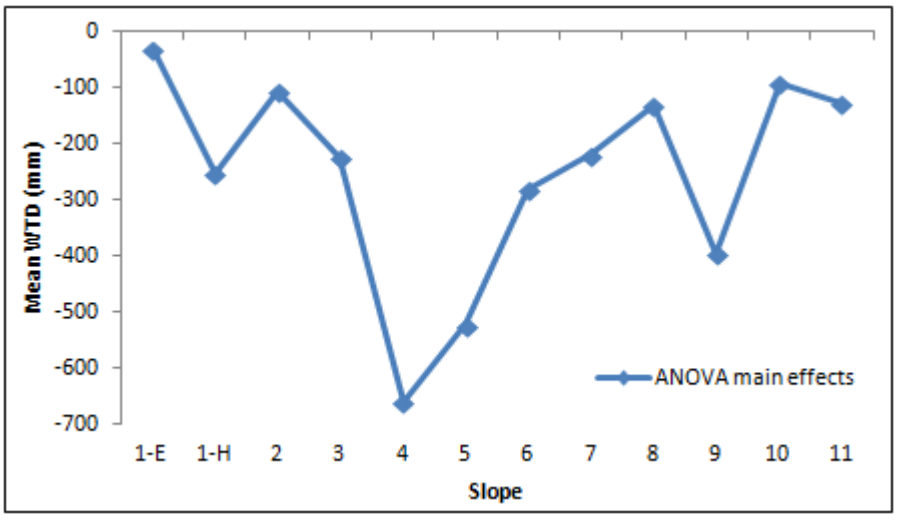

Figure 4.2 WTD ANOVA main effects plot

Table 4.5 Significant differences for WTD

Slope	ANOVA	ANCOVA
1-E	<1-H - 9, 11	<All but 2, 10
1-H	>1-E, 2, 8, 10, 11; <4,5,9	>1-E, 2, 8, 10, 11; <4,5,9
2	>1-E; <1-H, 3-7, 9	<1-H, 3-7, 9
3	>1-E, 2, 8, 10, 11;<4,5,9	>1-E, 2, 8, 10, 11; <4,5,9
4	>All	>All
5	>All but 4; <4	>All but 4; <4
6	>1-E, 2, 8, 10, 11; <4,5,9	>1-E, 2, 8, 10, 11; <4,5,9
7	>1-E, 2, 8, 10, 11; <4,5,9	>1-E, 2, 8, 10, 11; <4,5,9
8	> 1-E; <1-H, 3-7, 9	>1-E; <1-H, 3-7, 9
9	>All but 4, 5; <4, 5	>All but 4, 5; <4, 5
10	<1-H, 3-7, 9	<1-H, 3-7, 9
11	>1-E; <1-H, 3-7, 9	>1-E; <1-H, 3-7, 9

Percentage *Eriophorum spp*. ($p = 0.005$, $\omega^2 = 25.52\%$) was significant in the ANCOVA model ($R^2 = 84.69\%$, Table 4.4), along with slope ($p < 0.0001$, $\omega^2 = 54.89\%$) and month ($p < 0.0001$, $\omega^2 = 4.25\%$). The only change to the ANOVA model was that slope position 2 was no longer significantly different to 1-E, perhaps because the lower percentage of *Eriophorum spp*. at slope position 2 was accounted for. Indeed, there was a positive correlation between percentage *Eriophorum spp*. and WTD, indicating higher water tables with increased *Eriophorum spp*. dominance. Multiple linear regression (Table 4.6) showed that slope angle had a negative correlation to WTD, consistent with results from Chapter 2 (Table 2.11), though negative correlations for wetness index and altitude were not significant for the complete dataset regression from chapter 2. A temperature effect was found that was not significant in the ANCOVA model, suggesting a negative correlation between WTD and air temperature.

Table 4.6 WTD MLR: R^2 = 67.50%; SE = standard error

Predictor	Coef	SE Coef	P
Constant	6000	400	<0.0001
% *Eriophorum spp*.	1.8	0.2	<0.0001
Air Temperature	-3.0	0.7	<0.0001
Slope angle	-17	3	<0.0001
Wetness index	-160	10	<0.0001
Altitude	-9.5	0.7	<0.0001

4.4.1.2 Runoff occurrence

Measurement of runoff occurrence from slope positions 7 – 11 was affected by grazing sheep removing bungs from the top of runoff traps, resulting in lower expected runoff totals than further upslope. Nearly all slope positions had a runoff proportion of 1.00 (Table 4.7). Slope position 6, towards the lower part of the mid-slope, had a significantly lower runoff proportion of 0.844. These results contradict those of Chapter 2, for which each slope position had instances when no runoff was observed and the lower mid-slope had the highest proportion of observed runoff (Table 2.12). Table 4.8 shows monthly rainfall patterns for the Chapter 2 dataset (2010 – 2011) and current chapter (2011 – 2012). Despite a lower *N* (due to data gaps) the 2011 – 2012 dataset had a higher total rainfall, suggesting rainfall differences were the cause of the change in runoff pattern. For instance, April 2011 had 21.30 mm of rain, compared to 238.44 mm in April 2012. Similarly, June 2011 had 77.17 mm of rain compared to 283.74 mm in June 2012.

Table 4.7 Chi-squared results for runoff (RO) occurrence by slope

Slope	Expected RO	Observed RO	RO Proportion
1-E	33	33	1.000
1-H	33	32	0.970
2	33	33	1.000
3	33	33	1.000
4	32	32	1.000
5	33	33	1.000
6	32	27	0.844
7	26	26	1.000
8	27	27	1.000
9	21	21	1.000
10	27	27	1.000
11	24	24	1.000
χ2 = 42.60			**P <0.0001**

Table 4.8 Monthly rainfall for study years 2010 – 2011 & 2011 – 2012: Starting month = first month of sampling; NB data gaps present (see N for comparisons); Two data points removed as outliers: 23.23 mm from 14/7/2010 & 22.23 mm from 12/8/2012

Study year 2010 - 2011				Study year 2011 - 2012			
Year	**Month**	**N**	**Total Rain (mm)**	**Year**	**Month**	**N**	**Total Rain (mm)**
2010	6	720	73.21				
2010	7	742	122.21	2011	9	718	84.01
2010	8	743	116.55	2011	10	721	226.90
2010	9	720	146.05	2011	11	720	59.13
2010	10	573	97.52	2011	12	516	142.92
2010	11	720	128.93	2012	1	467	73.78
2010	12	743	37.36	2012	2	695	59.65
2011	1	443	75.00	2012	3	816	37.94
2011	2	468	85.19	2012	4	648	238.44
2011	3	743	21.85	2012	5	743	95.79
2011	4	720	21.30	2012	6	720	283.74
2011	5	743	135.55	2012	7	744	190.96
2011	6	719	77.17	2012	8	742	146.19
Total		**8797**	**1137.89**	**Total**		**8250**	**1639.45**

4.4.2 Gaseous fluxes

Descriptive statistics for slope positions are provided in Table 4.9 and for month in Table 4.10. Due to the number of missing data points it was not possible to test for any inter-factor interaction effects with respect to the CO_2 flux datasets.

Table 4.9 Descriptive statistics for response variables by slope; SE = standard error

Variable	Slope	N	Mean	SE Mean	Maximum	Minimum
R_{eco} (g CO_2 m^2 h^{-1})	1-E	26	0.16	0.04	0.843	0.008
	1-H	25	0.47	0.08	1.590	0.040
	2	26	0.25	0.04	0.815	0.020
	3	24	0.20	0.05	1.027	0.023
	4	27	0.30	0.06	1.209	0.020
	5	27	0.16	0.03	0.758	0.038
	6	27	0.26	0.04	0.833	0.022
	7	26	0.24	0.04	0.686	0.029
	8	30	0.39	0.09	2.228	0.020
	9	26	0.27	0.05	0.949	0.010
	10	32	0.45	0.08	1.931	0.019
	11	30	0.19	0.03	0.746	0.032
P_G (g CO_2 m^2 h^{-1})	1-E	23	-0.34	0.07	-1.269	-0.018
	1-H	24	-0.8	0.1	-1.901	-0.001
	2	24	-0.25	0.04	-0.843	-0.011
	3	22	-0.29	0.06	-1.164	-0.013
	4	26	-0.44	0.06	-1.158	-0.037
	5	27	-0.17	0.02	-0.427	-0.021
	6	22	-0.29	0.04	-1.051	-0.019
	7	21	-0.29	0.06	-0.885	-0.026
	8	26	-0.5	0.1	-2.457	-0.005
	9	24	-0.26	0.05	-0.773	-0.006
	10	26	-0.7	0.1	-2.243	-0.013
	11	29	-0.30	0.06	-1.075	-0.004
NEE (g CO_2 m^2 h^{-1})	1-E	26	-0.15	0.03	0.051	-0.768
	1-H	26	-0.24	0.08	0.475	-1.222
	2	26	0.04	0.04	0.528	-0.338
	3	27	-0.07	0.04	0.487	-0.600
	4	28	-0.12	0.08	0.917	-0.920
	5	27	-0.01	0.03	0.332	-0.267
	6	28	0.02	0.03	0.312	-0.231
	7	26	0.02	0.05	0.650	-0.466
	8	27	-0.09	0.05	0.524	-1.053
	9	28	0.02	0.03	0.367	-0.325
	10	33	-0.07	0.04	0.269	-0.752
	11	30	-0.10	0.04	0.171	-0.573

Table 4.10 Descriptive statistics for response variables by month; SE = standard error

Variable	Month	N	Mean	SE Mean	Maximum	Minimum
R_{eco} (g CO_2 m^{-2} h^{-1})	9	18	0.30	0.04	0.828	0.122
	10	34	0.20	0.03	1.111	0.041
	11	35	0.23	0.04	1.337	0.046
	12	2	0.06	0.03	0.091	0.037
	1	22	0.052	0.007	0.145	0.010
	2	32	0.043	0.004	0.116	0.008
	3	36	0.062	0.006	0.182	0.020
	4	27	0.20	0.03	0.839	0.030
	5	18	0.44	0.05	0.989	0.126
	6	30	0.35	0.05	1.404	0.051
	7	36	0.82	0.07	2.228	0.254
	8	36	0.37	0.04	1.243	0.135
P_G (g CO_2 m^{-2} h^{-1})	9	18	-0.32	0.06	-1.045	-0.070
	10	34	-0.33	0.06	-1.529	-0.028
	11	35	-0.37	0.05	-1.474	-0.036
	12	1	-0.024	*	-0.024	-0.024
	1	12	-0.028	0.005	-0.059	-0.004
	2	26	-0.06	0.01	-0.266	-0.001
	3	28	-0.058	0.009	-0.236	-0.005
	4	22	-0.34	0.08	-1.316	-0.007
	5	18	-0.7	0.1	-1.708	-0.129
	6	30	-0.59	0.09	-2.457	-0.030
	7	35	-0.70	0.09	-2.243	-0.056
	8	35	-0.50	0.06	-1.469	-0.091
NEE (g CO_2 m^{-2} h^{-1})	9	18	-0.02	0.04	0.207	-0.361
	10	36	-0.12	0.04	0.135	-0.901
	11	36	-0.14	0.03	0.133	-0.682
	12	3	0.06	0.01	0.085	0.040
	1	21	0.044	0.008	0.127	-0.022
	2	36	0.003	0.010	0.115	-0.221
	3	34	0.03	0.02	0.468	-0.083
	4	27	-0.09	0.06	0.650	-0.920
	5	18	-0.23	0.07	0.059	-1.222
	6	31	-0.23	0.05	0.179	-1.053
	7	36	0.14	0.06	0.917	-0.520
	8	36	-0.12	0.05	0.366	-0.800

4.4.2.1 Ecosystem respiration

Mean R_{eco} (Table 4.9) was greatest at slope position 1-H (0.47 ± 0.08 g CO_2 m^{-2} h^{-1}) and ≥0.30 g CO_2 m^{-2} h^{-1} on slope positions 4, 8 and 10. Ecosystem respiration was lowest at 1-E (0.16 ± 0.04 g CO_2 m^{-2} h^{-1}) and 5 (0.16 ± 0.03 g CO_2 m^2 h^{-1}) and ranged from 0.008 – 2.228 g CO_2 m^{-2} h^{-1}. Ecosystem respiration was greatest in July (0.82 ± 0.07 g CO_2 m^{-2} h^{-1}, Table 4.10) and lowest in February (0.043 ± 0.004 g CO_2 m^{-2} h^{-1}), with R_{eco} typically decreasing during autumn months to a low during winter before increasing in spring.

Slope ($p < 0.0001$, $\omega^2 = 8.32\%$) and month ($p < 0.0001$, $\omega^2 = 70.02\%$) were significant factors in the ANOVA model ($R^2 = 78.39\%$, Table 4.11). Mean R_{eco} from the ANOVA main effects (Figure 4.3) was lower than reported in Table 4.9 having accounted for the effect of seasonal variation. Slope positions 1-H and 10 had significantly higher R_{eco} than all others excluding slope positions 4 and 8 (Table 4.12), while R_{eco} on slope position 1-E was significantly lower than all others bar slope positions 3 and 5. Ecosystem respiration between January – March was significantly lower than all other months, while May – August had significantly higher R_{eco} than October – April and R_{eco} in July was greater than all other months.

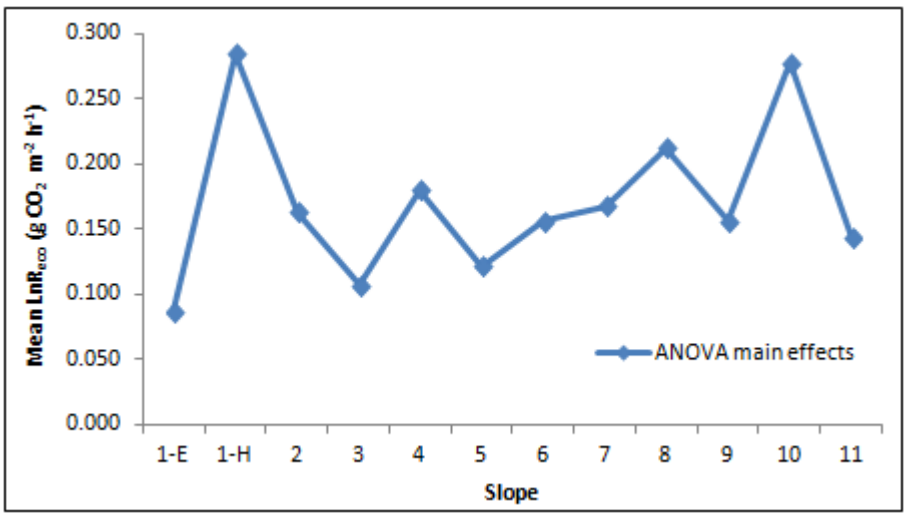

Figure 4.3 LnR_{eco} ANOVA main effects plot (values unlogged)

Table 4.11 CO_2 flux ANOVA / ANCOVA; ω^2 = % variance

LnR_{eco} ANOVA			**LnR_{eco} ANCOVA**		
Factor	**P**	**ω^2**	**Factor**	**P**	**ω^2**
Slope	<0.0001	8.32%	LnP_G	<0.0001	61.49%
Month	<0.0001	70.02%	Slope	<0.0001	4.89%
			Month	<0.0001	16.92%
N 324		**R^2 78.39%**	**N 292**		**R^2 83.35%**
LnP_G ANOVA			**LnP_G ANCOVA**		
Factor	**P**	**ω^2**	**Factor**	**P**	**ω^2**
Slope	<0.0001	8.93%	% *Eriophorum spp.*	0.002	0.03%
Month	<0.0001	53.80%	Air Temperature	0.006	25.79%
			LnPAR	<0.0001	13.72%
			Slope	<0.0001	7.18%
			Month	<0.0001	25.45%
N 292		**R^2 62.81%**	**N 291**		**R^2 72.23%**
NEE ANOVA			**NEE ANCOVA**		
Factor	**P**	**ω^2**	**Factor**	**P**	**ω^2**
Slope	<0.0001	7.96%	LnP_G	<0.0001	25.08%
Month	<0.0001	13.93%	Slope	<0.0001	7.50%
			Month	<0.0001	21.03%
N 323		**R^2 21.94%**	**N 286**		**R^2 53.70%**

Table 4.12 Significant differences for LnR_{eco}

Slope	ANOVA	ANCOVA
1-E	<All but 3 & 5	<All but 3
1-H	>1-E-3, 5-7, 9, 11	>1-E, 3, 5
2	<1-H, 10; >1-E	<10; >1-E
3	<1-H, 4, 8, 10	<1-H; 7-10
4	>1-E, 3	<10; >1-E
5	<1-H, 8, 10	<1-H, 10; >1-E
6	<1-H, 10; >1-E	<10; >1-E
7	<1-H, 10; >1-E	>1-E, 3
8	>1-E, 3, 5	>1-E, 3, 5
9	<1-H, 10; >1-E	>1-E, 3
10	>1-E, 2-3, 5-7, 9, 11	>1-E, 2-6, 11
11	<1-H, 10; >1-E	<10; >1-E

The only significant covariate in the ANCOVA model (R^2 = 83.35%, Table 4.11) was P_G (p <0.0001, ω^2 = 61.49%) and was the most important predictive variable. Slope (Figure 4.4)

reflected the broad pattern of the ANOVA model (Figure 4.3) but many of the significant differences were removed by accounting for P_G (Table 4.12). Though 1-E was significantly different in R_{eco} to all but slope position 3, 1-H was no longer different to most slope positions – only 1-E, 3 and 5. Slope position 3 was no longer significantly different to slope position 4, but was to 7 and 9. Water table depth explained 6.13% of variation in R_{eco} in Chapter 2 (Table 2.13), but was not significant in this study.

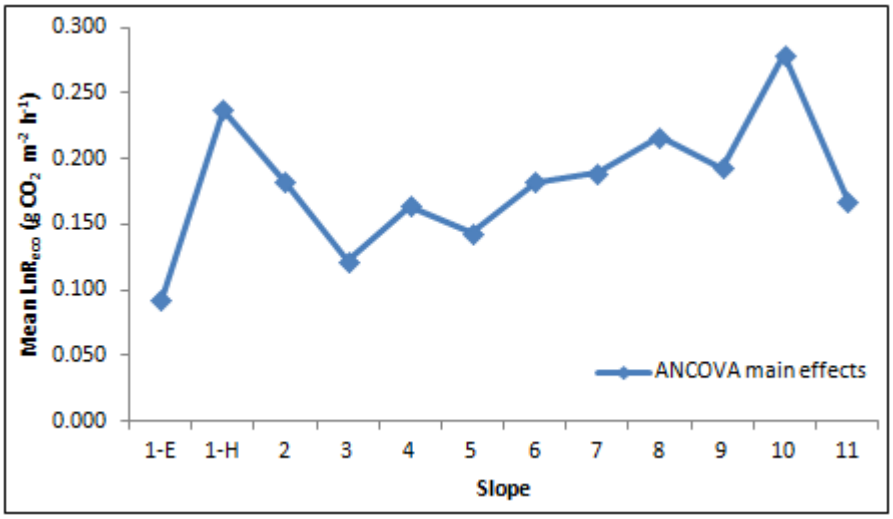

Figure 4.4 LnR_{eco} ANCOVA main effects plot (values unlogged)

Regression analysis (Table 4.13) indicated that of the terrain parameters, only altitude was significant, suggesting R_{eco} decreased with increasing elevation. A temperature effect was evident beyond that which was co-linear with P_G in the ANCOVA model. The correlation between R_{eco} and sin M, cos M and LnP_G was the same direction as Chapter 2 (2010 – 2011).

Table 4.13 LnR_{eco} MLR; Sin M & Cos M = sin and cos by month; 1/T = temperature coefficient; SE = standard error

Year	Predictor	Coef	SE Coef	P
2011 - 2012	Constant	8	2	<0.0001
	sin M	-0.35	0.05	<0.0001
	cos M	-0.39	0.07	<0.0001
	1/T	-1100	500	0.014
	LnP_G	0.41	0.03	<0.0001
R^2 = 74.50%	Altitude	-0.011	0.002	<0.0001
2010 - 2011	Constant	-1.9	0.2	<0.0001
	Sin M	-0.14	0.04	<0.0001
	Cos M	-0.48	0.05	<0.0001
	WTD	-0.0006	0.0001	<0.0001
	LnP_G	0.35	0.02	<0.0001
R^2 = 57.80%	WI	0.06	0.02	0.016

4.4.2.2 Gross photosynthesis

Mean P_G (Table 4.9) was considerably greater at 1-H (-0.8 ± 0.1 g CO_2 m^{-2} h^{-1}) than other slope positions, though as with R_{eco}, slope position 10 (-0. 7 ± 0.1 g CO_2 m^{-2} h^{-1}) had the second highest mean rate of P_G. The lowest mean P_G was on slope position 5 (-0.17 ± 0.02 g CO_2 m^{-2} h^{-1}). Gross photosynthesis was greatest between May – August (Table 4.10) peaking in July (-0.70 ± 0.0.090 g CO_2 m^{-2} h^{-1} and was much lower in winter months than spring – autumn.

Slope ($p < 0.0001$, ω^2 = 8.93%) and month ($p < 0.0001$, ω^2 = 53.80%) were both significant (R^2 = 62.81%, Table 4.11). Mean P_G was highest on 1-H (Figure 4.5), as with the raw data, yet accounting for seasonal variation indicated that slope position 4 had the second highest rate of P_G (-0.299 g CO_2 m^{-2} h^{-1}). Gross photosynthesis on 1-H was significantly greater than all sites bar 4, 8 and 10 (Table 4.14), while slope position 4 was significantly greater than 2, 3, 5, 9 and 11. Slope position 10 (-0.245 g CO_2 m^{-2} h^{-1}) had significantly greater P_G than slope position 11 (-0.114 g CO_2 m^{-2} h^{-1}) despite the plots being adjacent. Gross photosynthesis in

January – March was significantly lower than all other months, as with R_{eco}, while May – August also had significantly greater P_G than April.

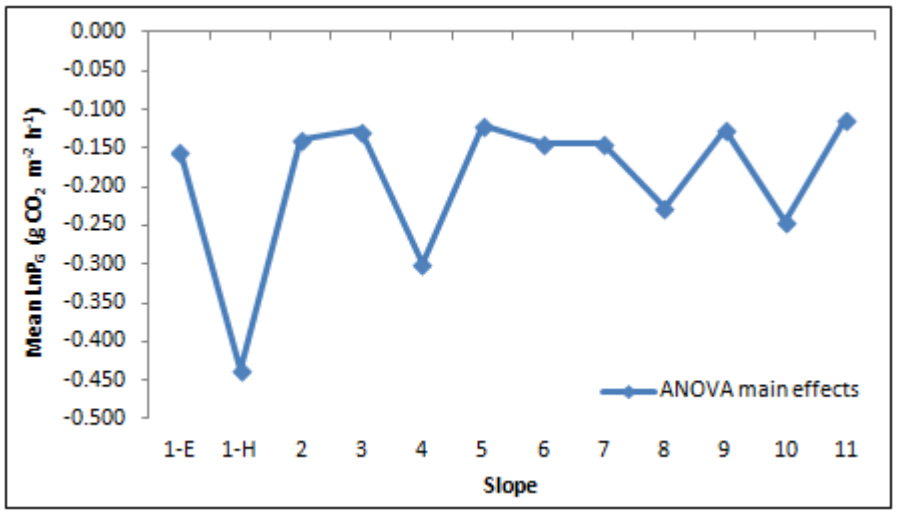

Figure 4.5 LnP_G ANOVA main effects plot (values unlogged)

Table 4.14 Significant differences for LnP_G

Slope	ANOVA	ANCOVA
1-E	<1-H	<1-H, 4
1-H	>All but 4, 8, 9	>All but 4
2	<1-H, 4	<1-H, 4
3	<1-H, 4	<1-H, 4
4	>2-3, 5, 9, 11	>1-E, 2-3, 5-6, 9, 11
5	<1-H, 4	<1-H, 4
6	<1-H	<1-H, 4
7	<1-H	<1-H
8		<1-H
9	<1-H, 4	<1-H, 4
10	>11	<1-H
11	<1-H, 4, 10	<1-H, 4

The ANCOVA model (R^2 = 72.23%, Table 4.11) indicated that air temperature (p = 0.006, ω^2 = 25.79%) and PAR (p <0.0001, ω^2 = 13.72%) were significant and explained a lot of variation in P_G. Although percentage *Eriophorum spp*. was significant (p = 0.002, ω^2 = 0.03%) it explained only a minimal amount of variation in P_G. Slope (p <0.0001, 7.18%, Figure 4.6) was still significant and accounting for air temperature and PAR meant slope position 1-H was significantly different to all but slope position 4 (Table 4.14), which also had significantly greater P_G than most, but not all, other slope positions. Many of the significant differences between months were removed, but March had significantly lower P_G than all months other than January, whilst October and November were larger than January – March and September. No relationship with WTD was observed, unlike in Chapter 2 (Table 2.13).

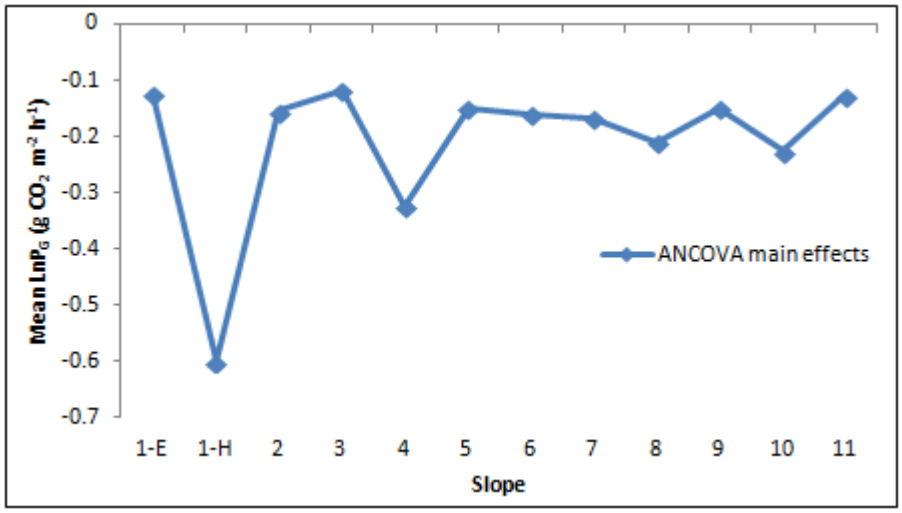

Figure 4.6 LnP_G ANCOVA main effects plot (values unlogged)

Regression analysis (Table 4.15) indicated that slope angle, wetness index and altitude did not explain any variation in P_G, while percentage *Eriophorum spp*. dominance was not significant, which concurred with the very low percentage variance from the ANCOVA model.

Regression analysis suggested a positive correlation to 1/T, the equivalent of a negative correlation to untransformed air temperature, meaning P_G decreased at higher temperatures (as log-transformed P_G was used). Furthermore, using untransformed air temperature in the model in place of 1/T indicated a negative correlation, perhaps suggesting moisture stress limited P_G at higher temperatures. This was the opposite of the relationship suggested by the ANCOVA model, which indicated a positive correlation between air temperature and P_G.

Table 4.15 LnP_G MLR: R^2 = 55.90%; Sin M & Cos M = sin & cos by month; 1/T = temperature coefficient; SE = standard error

Predictor	Coef	SE Coef	P value
Constant	-14	3	<0.0001
Sin M	-0.79	0.08	<0.0001
Cos M	-0.7	0.1	<0.0001
1/T	2500	900	0.006
LnPAR	0.66	0.07	<0.0001

4.4.2.3 Net ecosystem exchange

Mean NEE (Table 4.9) was lowest at 1-H (-0.24 ± 0.08 g CO_2 m^{-2} h^{-1}), reflecting the high rates of P_G. 1-E (-0.15 ± 0.03 g CO_2 m^{-2} h^{-1}) was the second largest daytime CO_2 sink, reflecting the low level of R_{eco} as well as high P_G. Net ecosystem exchange ranged from -1.222 to 0.917 g CO_2 m^{-2} h^{-1} and the large variation was reflected in slope positions 2, 6, 7 and 9 having positive mean NEE values, indicating efflux of CO_2 to the atmosphere. Net ecosystem exchange (Table 4.10) was negative during the daytime in September, October, November, April, May, June and August, peaking in May (-0.23 ± 0.07 g CO_2 m^{-2} h^{-1}). However, NEE was positive in July (0.14 ± 0.06 g CO_2 m^{-2} h^{-1}), despite high temperatures and PAR and the highest mean P_G.

Slope ($p < 0.0001$, $\omega^2 = 7.96\%$) and month ($p < 0.0001$, $\omega^2 = 13.93\%$) were significant factors in the ANOVA model ($R^2 = 21.94\%$, Table 4.11). Less variation was explained than in the R_{eco} and P_G models. Lower coefficients of determination and larger error terms can occur for NEE over R_{eco} and P_G because it includes the concomitant processes of respiration and photosynthesis. As with the raw data, slope position 1-H (-0.188 g CO_2 m^{-2} h^{-1}, Figure 4.7) was the largest NEE sink, significantly different from the four slope positions that were sources of CO_2. Slope position 1-E was significantly different from slope positions 2 and 6 (Table 4.16), but despite slope position 4 (-0.144 g CO_2 m^{-2} h^{-1}) being similar to 1-E (-0.150 g CO_2 m^{-2} h^{-1}) in mean NEE from the main effects, only the two topmost slope positions had significantly lower NEE. The significantly higher NEE values on the top-slope contrasted to Chapter 2 results that suggested the bottom-slope had significantly higher daytime NEE than all other slope positions. January and March, which had positive NEE values, were significantly different to May, June and August – months with the highest NEE. February was significantly different in NEE to June, while July, which had the lowest level of NEE, was significantly different in NEE to October, November, May, June and August.

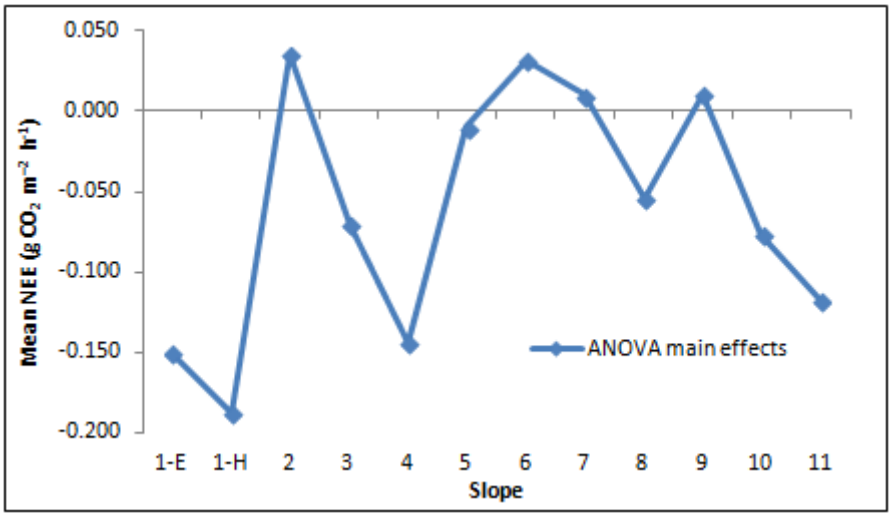

Figure 4.7 NEE ANOVA main effects plot

The ANCOVA model (R^2 = 53.70%, Table 4.11) indicated that P_G ($p < 0.0001$, ω^2 = 25.08%) was the only significant covariate, with slope ($p < 0.0001$, ω^2 = 7.50%) and month ($p < 0.0001$, ω^2 = 21.03%) still significant factors. The importance of P_G was less than Chapter 2 (ω^2 = 45.02%, Table 2.13), which also found a significant influence of percentage *Eriophorum spp*., PAR and slope angle but no slope effect in the ANCOVA model. Accounting for P_G, all slope positions (Figure 4.8) were net CO_2 daytime sinks but only 1-E and 11 were significantly lower than 2, 6, 8 and 9 (Table 4.16). Slope position 1-H, which had the largest CO_2 daytime sink in the ANOVA model was not significantly different to any other slope positions in the ANCOVA model. Significant differences associated with month changed in the ANCOVA model, with winter months the largest CO_2 sinks. This was because the influence of P_G had been accounted for by its inclusion as a covariate and therefore the model did not reflect the actual data, in which winter months had lower rates of NEE and may have been sources to the atmosphere, rather it reflected the effect P_G had upon the model. This effect was also observed in Chapter 2.

Table 4.16 Significant differences for NEE

Slope	ANOVA	ANCOVA
1-E	<2, 6	<2, 6, 8-9
1-H	<2, 6-7, 9	
2	>1-E, 1-H	>1-E, 11
3		
4		
5		
6	>1-E, 1-H	>1-E, 11
7	>1-H	
8		>1-E, 11
9	>1-H	>1-E, 11
10		
11		<2, 6, 8-9

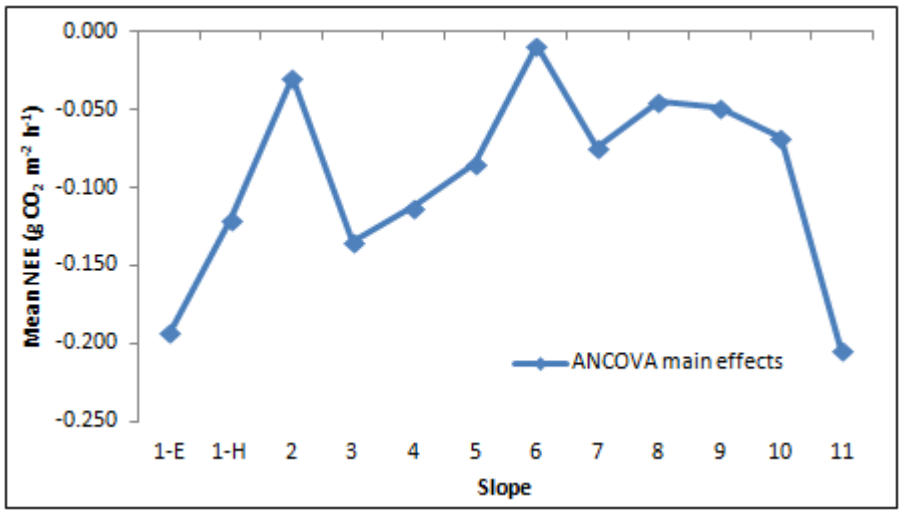

Figure 4.8 NEE ANCOVA main effects plot

Regression analysis (Table 4.17) indicated a positive correlation to air temperature that was not found in the ANCOVA model, while the negative correlation between NEE and logged P_G suggested that as would be expected, higher rates of P_G increased values of NEE. Slope angle, wetness index and altitude did not have a significant effect upon rates of NEE.

Table 4.17 NEE MLR: R^2 = 38.30%; Sin M & Cos M = sin & cos by month; SE = standard error

Predictor	Coef	SE Coef	P value
Constant	-0.42	0.04	<0.0001
Sin M	-0.10	0.02	<0.0001
Cos M	-0.06	0.02	0.013
Air Temperature	0.005	0.002	0.007
LnP_G	-0.14	0.01	<0.0001

4.4.2.4 CO_2 flux and study year

Because of the different results in CO_2 flux between Chapter 2 and the current chapter, CO_2 fluxes were analysed for slope positions 1-E, 1-H and 4 with slope, study year,

month and interactions included in the analysis to determine whether changes between study year 1 (Chapter 2) and 2 (current chapter) affected CO_2 flux. Only ANOVA analysis was conducted. Results for R_{eco} (Table 4.18) suggested slope ($p < 0.0001$, $\omega^2 = 15.37\%$) and month ($p < 0.0001$, $\omega^2 = 45.09\%$) were significant but not study year. ANOVA main effects (Figure 4.9) showed 1-E (0.081 g CO_2 m^{-2} h^{-1}) had a lower mean rate of R_{eco} than slope position 4 (0.153 g CO_2 m^{-2} h^{-1}) and 1-H (0.227 g CO_2 m^{-2} h^{-1}), which were also significantly different. Results from this chapter suggested 1-E had lower rates of R_{eco} than slope position 4 but not 1-H, while the first year found no significant differences between the top-slope and mid-slope. For P_G, study year was significant ($p = 0.001$, $\omega^2 = 3.25\%$), indicating that P_G in year 1 (-0.168 g CO_2 m^{-2} h^{-1}, Figure 4.10) was lower than year 2 (-0.261 g CO_2 m^{-2} h^{-1}). Gross photosynthesis on slope position 1-E was lower than slope positions 1-H and 4 (Figure 4.9). Results from Chapter 4 suggested a difference between slope positions 1-E and 1-H but not with slope position 4. No slope effect was significant for NEE, but study year ($p = 0.020$, $\omega^2 = 2.51\%$) was significant, with a greater daytime CO_2 sink found in year 2 (Figure 4.10). No significant difference in NEE between slope positions 1-E, 1-H and 4 was consistent with results from both chapters.

Table 4.18 CO_2 flux ANOVA for study year; ω^2 = % variance

LnR_{eco} ANOVA			**LnP_G ANOVA**			**NEE ANOVA**		
Factor	**P**	**ω^2**	**Factor**	**P**	**ω^2**	**Factor**	**P**	**ω^2**
Slope	<0.0001	15.37%	Slope	<0.0001	5.17%	Study year	0.020	2.51%
Month	<0.0001	45.09%	Study year	0.001	3.25%	Month	<0.0001	17.76%
			Month	<0.0001	45.59%			
			Slope*month	0.007	5.63%			
N 177		**R^2 60.60%**	**N 166**		**R^2 59.78%**	**N 179**		**R^2 20.36%**

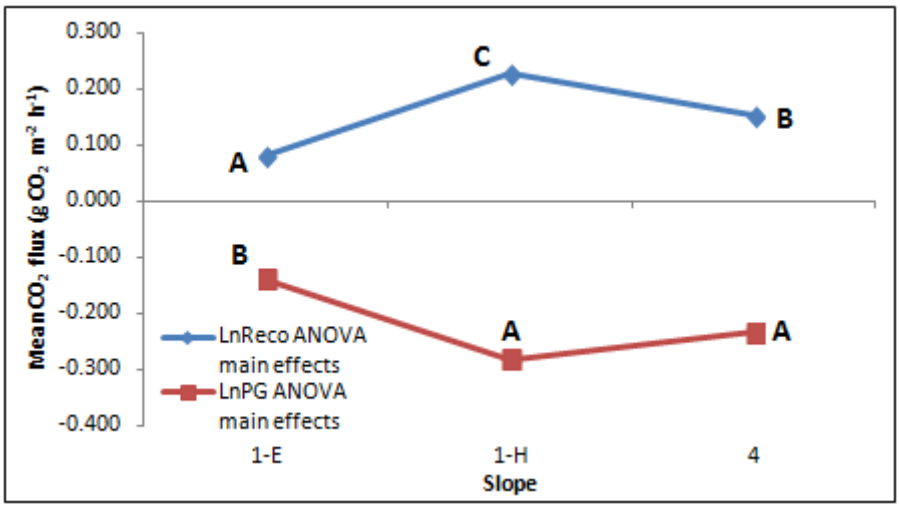

Figure 4.9 Study year LnR_{eco} and LnP_G ANOVA main effects plot (values unlogged): significant differences denoted where letters are not shared between slope positions

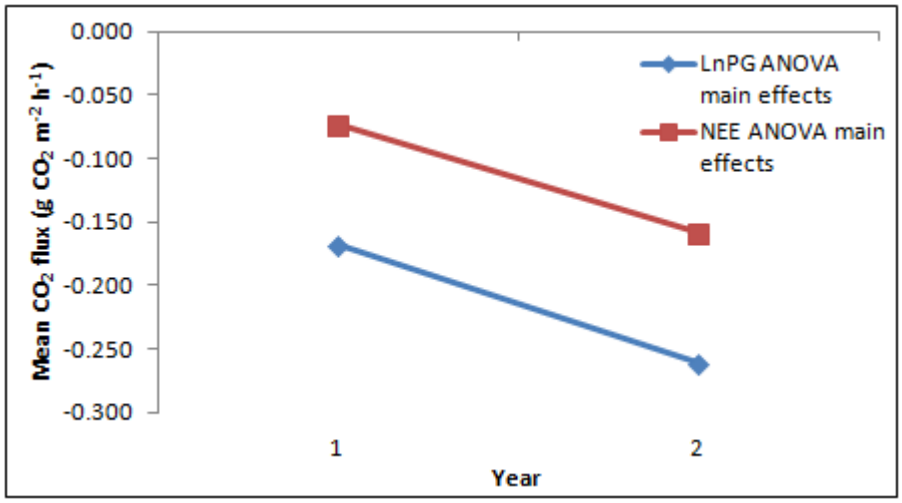

Figure 4.10 Study year LnP_G and NEE ANOVA main effects plots (P_G values unlogged)

4.4.3 Dissolved organic carbon

Descriptive statistics for slope are provide in Table 4.19 and month in Table 4.20.

Table 4.19 DOC descriptive statistics for response variables by slope: SE = standard error

Variable	Slope	N	Mean	SE Mean	Maximum	Minimum
Soil pore water DOC (mg C l^{-1})	1-H	33	89	6	197.3	22.2
	1-E	30	94	7	205.1	16.9
	2	33	90	9	213.5	9.5
	3	33	107	9	204.1	6.7
	4	33	140	10	234.3	19.4
	5	32	170	10	236.1	13.0
	6	33	110	10	226.4	13.9
	7	32	98	8	172.8	18.0
	8	33	92	8	186.7	16.9
	9	33	150	10	237.0	9.5
	10	34	81	7	196.2	9.3
	11	35	90	10	213.0	5.8
Runoff DOC (mg C l^{-1})	1-H	30	43	5	110.3	6.5
	1-E	29	50	5	149.1	20.0
	2	28	35	4	92.1	6.5
	3	29	56	9	186.9	5.6
	4	28	50	7	181.7	8.4
	5	27	48	7	163.1	5.6
	6	23	70	10	231.7	11.4
	7	21	42	5	83.0	8.1
	8	22	44	6	116.0	9.3
	9	19	48	5	86.7	15.3
	10	25	46	6	116.3	8.4
	11	16	44	5	80.3	10.2
Stream DOC (mg C l^{-1})	Bank-stream	12	80	10	159.4	12.0
	Stream	12	88	8	117.4	34.1

Table 4.20 DOC descriptive statistics for response variables by month: SE = standard error

Variable	Month	N	Mean	SE Mean	Maximum	Minimum
Soil pore water DOC (mg C l^{-1})	9	36	143	7	213.0	70.8
	10	36	127	8	226.4	34.8
	11	36	150	8	234.8	46.0
	12	5	90	20	160.7	64.4
	1	33	90	10	234.5	16.9
	2	34	67	8	196.1	11.1
	3	36	110	10	237.0	9.3
	4	35	52	5	102.6	5.8
	5	36	140	10	230.8	26.5
	6	36	103	7	205.1	31.0
	7	35	105	8	216.1	23.8
	8	36	103	8	225.6	23.6
Runoff DOC (mg C l^{-1})	9	17	50	10	170.6	9.6
	10	27	37	6	148.5	7.5
	11	34	53	5	183.9	18.3
	12	5	48	8	68.1	32.6
	1	21	42	6	110.3	8.1
	2	24	40	9	186.9	8.4
	3	34	41	4	90.5	8.4
	4	32	66	9	181.7	6.7
	5	30	64	7	231.7	31.0
	6	22	34	7	98.7	5.6
	7	22	33	4	74.2	13.5
	8	29	55	4	99.2	28.0

4.4.3.1 Soil pore water

Mean DOC concentration (Table 4.19) was largest on slope position 5 (170 ± 10 mg C l^{-1}) and was very high on slope position 9 (150 ± 10 mg C l^{-1}) and slope position 4 (140 ± 10 mg C l^{-1}). Dissolved organic carbon was lower on the topmost slope positions (89 ± 6 mg C l^{-1}, 1-H) and decreased down-slope from slope position 5, to a low at slope position 10 (81 ± 7 mg C l^{-1}). Mean DOC was greatest in autumn months (Table 4.20), peaking at 150 ± 8 mg C l^{-1} in November but was also high in May (140 ± 10 mg C l^{-1}) following a low in April (52 ± 5 mg C l^{-1}).

Slope ($p < 0.0001$, $\omega^2 = 19.61\%$), month ($p < 0.0001$, $\omega^2 = 24.56\%$) and a slope-month interaction ($p = 0.001$, $\omega^2 = 9.55\%$) were significant in the ANOVA model ($R^2 = 53.78\%$, Table 4.21). Slope positions 4, 5 and 9 all had significantly higher DOC concentrations than most other slope positions. There was no significant difference in DOC concentration between top-slope collars and those on the bottom-slope beyond slope position 9 (Table 4.22). Such results would appear to contradict Chapter 2 yet the main effects (Figure 4.11) were broadly similar to the Alport Low site-slope interaction from Chapter 2 (Figure 2.17). Slope position 4 (Alport Low upper mid-slope collars 1 - 3) had a mean of 140.6 mg C l^{-1} from the ANOVA main effects, similar to the mean of 138.2 mg C l^{-1} in Chapter 2. The Alport Low top-slope mean was 98.2 mg C l^{-1}, while 1-E was 93.4 and 1-H 89.3 mg C l^{-1}. The decrease in DOC concentration further down the mid-slope was also consistent with results from Chapter 2, though DOC concentrations on the bottom-slope collars were higher than in Chapter 2. Slope position 9 (148.3 mg C l^{-1}) had significantly higher DOC than adjacent slope positions, reflecting the importance of microtopographic variation given its location in a depression.

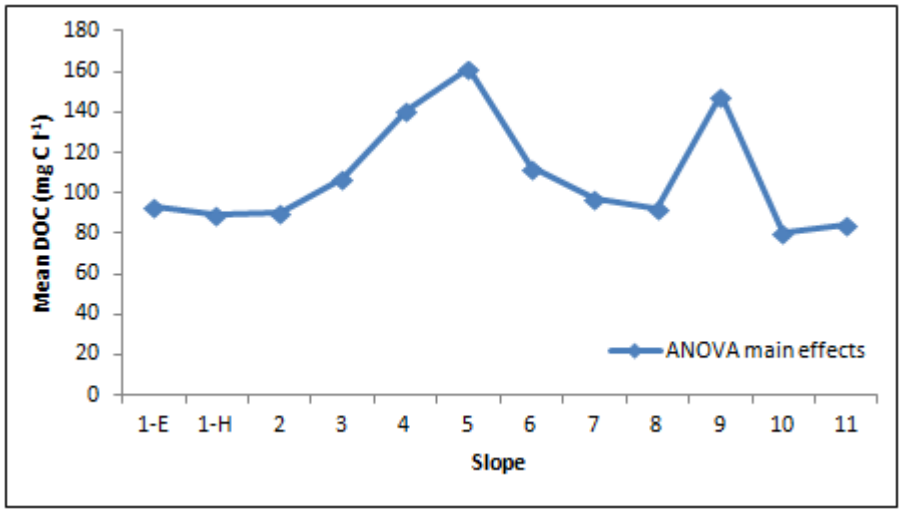

Figure 4.11 Soil pore water DOC ANOVA main effects plot

Table 4.21 Soil pore water (SPW) and runoff (RO) water DOC ANOVA / ANCOVA: ω^2 = % variance

SPW DOC ANOVA			SPW DOC ANCOVA		
Factor	**P**	**ω^2**	**Factor**	**P**	**ω^2**
Slope	<0.0001	19.61%	WTD	<0.0001	27.27%
Month	<0.0001	24.56%	LnConductivity	<0.0001	8.78%
Slope-month	0.001	9.55%	NO_3^-	<0.0001	7.21%
			$LnSO_4^{2-}$	0.014	0.52%
			Slope	<0.0001	4.78%
			Month	<0.0001	7.44%
			Slope-month	<0.0001	10.26%
N 411		**R^2 53.78%**	**N 371**		**R^2 66.32%**
LnRO DOC ANOVA			**LnRO DOC ANCOVA**		
Factor	**P**	**ω^2**	**Factor**	**P**	**ω^2**
Month	<0.0001	13.13%	pH	<0.0001	0.22%
			LnE4:E6	<0.0001	14.75%
			$LnSO_4^{2-}$	<0.0001	19.02%
			Month	0.019	3.49%
N 292		**R^2 13.17%**	**N 215**		**R^2 37.59%**

Table 4.22 Significant differences for soil pore water DOC

Slope	ANOVA	ANCOVA
1-E	<4-5, 9	>1-H
1-H	<4-5, 9	<All but 4, 7, 10
2	<4-5, 9	>1-H
3	<4-5, 9	>1-H
4	>All but 5-6, 9	<5
5	>All but 4, 9	>1-H, 4
6	<5, 9; >10	>1-H
7	<4-5, 9	
8	<4-5, 9	>1-H
9	>All but 4, 5	>1-H
10	<4-6, 9	
11	<4-5, 9	>1-H

DOC concentrations in the autumn were significantly higher than most months excluding May, showing a significant decrease in DOC in January. Although DOC concentrations

in Chapter 2 were not higher in the autumn than the summer, the decrease in DOC between November and January in Chapter 2 was consistent with Chapter 4. DOC concentration between June – August was significantly higher than February and April.

ANCOVA analysis (R^2 = 66.32%, Table 4.21) indicated that WTD ($p < 0.0001$, ω^2 = 27.27%), conductivity ($p < 0.0001$, ω^2 = 8.78%), NO_3^- ($p < 0.0001$, ω^2 = 7.21%) and SO_4^{2-} ($p = 0.014$, ω^2 = 0.52%) were significant covariates, reducing the importance of slope ($p < 0.0001$, ω^2 = 4.78%). The high DOC concentrations on the mid-slope positions were reduced (Figure 4.12) compared to the ANOVA model, while slope position 1-H decreased to a mean of 74.3 mg C l^{-1}, significantly lower than all slope positions other than 4, 7 and 10 (Table 4.22). Indeed, slope position 4 was significantly lower than slope position 5 having accounted for the effect of WTD and the other hydrological covariates. The high DOC concentrations observed at slope position 9, a bottom-slope position, were no longer significantly different to adjacent plots.

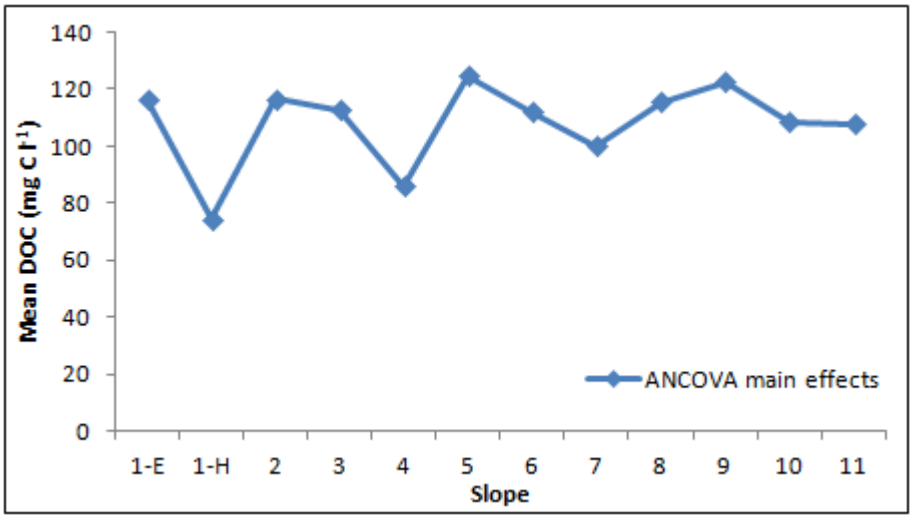

Figure 4.12 Soil pore water DOC ANCOVA main effects plot

The main significant differences suggested that 1-H, a top-slope position, was lower in DOC than most others in ANCOVA. The ANCOVA model from Chapter 2 removed interaction effects and showed the top-slope was higher in DOC than all other slope positions, suggesting a different pattern to here. However, slope position 1-E had a mean of 116.4 mg C l^{-1}, which was significantly higher than slope position 1-H and closer to the top-slope mean of 103.9 mg C l^{-1} in the ANCOVA model of Chapter 2 (Figure 2.18). Furthermore, slope position 4 was remarkably similar in its ANCOVA mean (85.8 mg C l^{-1}) as Chapter 2 (upper midslope 82.5 mg C l^{-1}), albeit without collars 4-6 on Alport Low or Featherbed Moss plots. As such this corroborated the results from Chapter 2, emphasising the importance of WTD in controlling DOC concentration and removing most of the slope effects observed in the ANOVA model. Moreover, the increased importance of conductivity compared to Chapter 2 may suggest the slope transect better captured variation in DOC associated with hydrological changes.

Backwards MLR (Table 4.23) indicated that wetness index (p = 0.046) and altitude (p = 0.024) were negatively correlated to DOC concentration. However, they were not significant in the forwards model and only improved the R^2 by 0.40%. Results for other covariates agreed well with Chapter 2, showing a negative correlation between DOC and WTD and NO_3^- and a positive correlation with conductivity.

Table 4.23 Soil pore water DOC MLR: R^2 = 47.50%; Sin M = sin by month; SE = standard error

Predictor	Coef	SE Coef	P Value
Constant	300	200	0.167
Sin M	-15	3	<0.0001
WTD	-0.14	0.02	<0.0001
LnConductivity	80	10	<0.0001
NO_3^-	-10	2	<0.0001
$LnSO_4^{2-}$	-14	7	0.037
Wetness index	-9	5	0.046
Altitude	-0.7	0.3	0.024

4.4.3.2 Runoff water

Runoff water DOC concentration (Table 4.19) was lower than that of soil pore water. The highest mean DOC concentration was at slope position 6 (70 ± 10 mg C l^{-1}) and lowest at slope position 2 (35 ± 4 mg C l^{-1}). DOC ranged from 5.6 – 231.7 mg C l^{-1}, and was highest in April (66 ± 9 mg C l^{-1}, Table 4.20), with a low in July (33 ± 4 mg C l^{-1}). Only month was significant ($p < 0.0001$, $\omega^2 = 13.13\%$) in the ANOVA model ($R^2 = 13.17\%$, Table 4.21), in agreement with results from Chapter 2, meaning a large amount of unexplained variance was in the error term. Dissolved organic carbon concentration was highest in May and lowest in February and varied between months with no clear distinction between winter and summer, as in Chapter 2. pH ($p < 0.0001$, $\omega^2 = 0.22\%$), E4:E6 ($p < 0.0001$, $\omega^2 = 14.75\%$), $LnSO_4^{2-}$ ($p < 0.0001$, $\omega^2 = 19.02\%$) and month ($p = 0.019$, $\omega^2 = 3.49\%$) were significant in the ANCOVA model ($R^2 = 37.59\%$, Table 4.21). DOC concentration in January was significantly lower than June and October significantly lower than May, with no other significant differences. pH had a negative correlation to DOC, with a positive correlation for E4:E6 and SO_4^{2-} which agreed with results from Chapter 2.

4.4.3.3 Water type

Water type ($p < 0.0001$, $\omega^2 = 26.82\%$), month ($p < 0.0001$, $\omega^2 = 9.13\%$) and a water type-month interaction ($p < 0.0001$, $\omega^2 = 5.81\%$) were significant in the ANOVA model ($R^2 = 41.80\%$, Table 4.24). ANOVA main effects (Figure 4.13) indicated that soil pore water (89.6 mg C l^{-1}) had a higher DOC concentration than stream water (73.0 mg C l^{-1}) and runoff water (36.3 mg C l^{-1}). Runoff water DOC concentration was significantly lower than soil pore water and stream water, though there was no difference between the latter two. DOC concentration in February was lower than September – November, May and August. The interaction between water type and month suggested a large decrease in DOC content in stream water between January and February, from 60.1 to 20.2 mg C l^{-1}, meaning stream water DOC concentration was lower than

runoff water (26.3 mg C l^{-1}) in February. During April, soil pore water DOC concentration (40.6 mg C l^{-1}) was lower than runoff (50.1 mg C l^{-1}) and stream (83.9 mg C l^{-1}) water. ANCOVA analysis indicated that pH ($p = 0.002$, $\omega^2 = 26.33\%$), conductivity ($p < 0.0001$, $\omega^2 = 6.64\%$), E4:E6 ($p < 0.0001$, $\omega^2 = 2.54\%$) and NO_3^- ($p < 0.002$, $\omega^2 = 1.85\%$) were significant covariates. ANCOVA changed the significant differences, with soil pore water significantly higher in DOC than runoff water and stream water, which were no longer significantly different from one another. pH and NO_3^- were negatively correlated to DOC, with conductivity and E4:E6 positively correlated.

Table 4.24 Water type DOC ANOVA / ANCOVA; ω^2 = % variance

LnDOC ANOVA			**LnDOC ANCOVA**		
Factor	**P**	**ω^2**	**Factor**	**P**	**ω^2**
Water type	<0.0001	26.82%	pH	0.002	26.33%
Month	<0.0001	9.13%	LnConductivity	<0.0001	6.64%
Water type-month	<0.0001	5.81%	LnE4:E6	<0.0001	2.54%
			NO_3^-	0.002	1.85%
			Water type	<0.0001	4.90%
			Month	0.001	5.50%
			Water type-month	<0.0001	2.63%
N 703		**R^2 41.80%**	**N 597**		**R^2 50.44%**

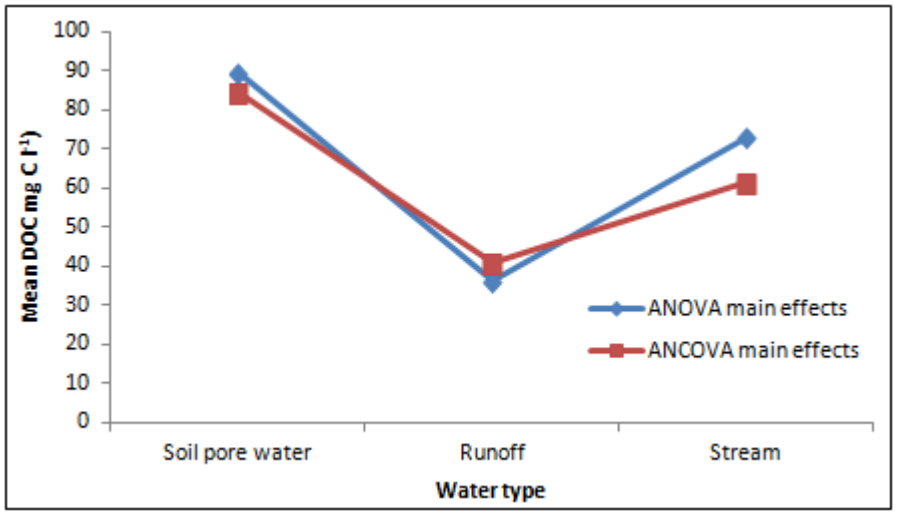

Figure 4.13 Water type DOC ANOVA / ANCOVA main effects plot

4.4.3.4 Process blanks

Process blanks were run to demonstrate potential sources of error in water chemistry analysis. pH (Table 4.25) had a mean of 5.8 ± 0.3 while conductivity was low (4.9 ± 0.5 µs cm^{-1}). Absorbance at 400 nm (Abs_{400}) was very low (0.003 ± 0.002 Abs_{400}) and though the mean E4:E6 was 1.3 ± 0.3, it was missing most values because of negative absorbance readings at 465 and 665 nm wavelengths. The main source of error was from DOC, with a mean concentration of 16 ± 4 mg C l^{-1} and range of 1.8 – 55.0 mg C l^{-1}. This implied possible contamination during DOC analysis, but this was not consistent given the sometimes higher concentration of DOC in process blanks than runoff samples, perhaps suggesting cleaning was not of a uniformly high standard.

Table 4.25 Process blank descriptive statistics for response variables; Abs_{400} = absorbance at 400 nm; SE = standard error

Variable	N	Mean	SE Mean	Maximum	Minimum
pH	11	5.8	0.3	6.76	4.20
Conductivity (µs cm^{-1})	11	4.9	0.5	8.1	2.7
Abs_{400}	11	0.003	0.002	0.018	-0.002
E4:E6	4	1.3	0.3	2.00	1.00
DOC (mg C l^{-1})	11	16	4	55.0	1.8

4.5 Discussion

4.5.1 Limitations

This study addressed whether carbon cycling varied in consistent patterns along a hillslope transect but was limited by its use of only one transect. It was not possible to conduct the study on Featherbed Moss as the study slope was not connected to a stream. However, Alport Low had much greater variation in slope angle along the hillslope than the more uniform Featherbed Moss and was an ideal site to assess the effects of rapid change in hillslope properties down to the riparian zone. The study was conducted using three replicate collars per slope position to increase the frequency of sampling locations along the hillslope. Where data gaps existed, such as with CO_2 flux from instrumentation failure or error, it meant it was not always possible to assess interaction affects between factor levels. Furthermore, terrain parameters of slope angle, wetness index and altitude were co-linear with slope position and it was not possible to include them as covariates in ANCOVA. However, the importance of terrain parameters was assessed with MLR.

It was not possible to control vegetation on Alport Low due to changes along the hillslope. This was most likely related to variation in slope angle and consequently WTD that affected vegetation communities along the slope. However, it did reflect the spatial heterogeneity of peat bogs and provided an insight into microtopographical variation across the hillslope. Although the research design focused upon variation along the hillslope and therefore limited the ability to fully account for specific mictropographical groups, it did allow the possibility to make inferences, such as between 1-E and 1-H *Eriophorum spp*. and hummock plots.

4.5.2 Hydrology

The highest water tables were found on the top-slope and bottom-slope with extensive drawdown apparent on the mid-slope, though water tables gradually increased further down the mid-slope. These results were in good agreement with those for Alport Low in Chapter 2 that showed deeper water tables on the mid-slope but which were closer to the surface on the lower mid-slope compared to the upper mid-slope. Furthermore, extending analysis of the hillslope along a more detailed transect increased the overall significance of slope position to over 80% of the original variance being explained and highlighted the importance of topographic variation such as occurred with the deeper water tables on slope position 9, located in a depression, as well as differences between 1-E and 1-H. The difference in WTD between slope positions 1-E and 1-H was reflected in the significance of *Eriophorum spp*. dominance as a covariate. Alm et al. (1997) observed large hydrological differences between *Eriophorum* lawns and hummocks, while Laine et al. (2006) distinguished wet and dry sites including shrub dominated hummocks and hollows that included *Eriophorum angustifolium* alongside *Sphagnum spp.* Furthermore, *Eriophorum vaginatum* was shown to increase in abundance following rewetting (Komulainen et al., 1999) and therefore the presence of *Eriophorum spp*. was indicative of higher water tables.

The importance of slope was reflected in the negative correlation between WTD and slope angle, suggesting that steeper slopes had deeper water tables, which was also observed by Wilson et al. (2010) following blocking of drainage ditches at a peatland in Wales. Altitude was similarly negatively correlated to WTD and may reflect the deeper water tables on the mid-slope compared to the bottom-slope, where return flow can maintain higher water tables (Holden and Burt, 2003). However, the negative correlation between WTD and wetness index was unusual, given that high water tables would be expected in areas with a high wetness index (Allott et al., 2009). Top-slope locations (Table 4.1) had a lower wetness index than those

on the bottom-slope yet the mid-slopes also had high wetness index values and may be the cause of the negative correlation.

Runoff frequency was at or close to 100% for all slope positions other than slope position 6, a mid-slope location, which only had 84.38% runoff occurrence. Slope position 6 had a higher water table than mid-slope locations further upslope so it could have been expected that it would experience more runoff events. Results from Chapter 2 indicated that the lower mid-slope had the highest runoff frequency, though slope position 7 (altitude 537.1 m) did have a high runoff frequency, like the lower mid-slope in Chapter 2 (altitude 537.8 – 538.8 m). The difference in runoff frequencies in this study were likely caused by different rainfall patterns compared to the Chapter 2 study. Holden and Burt (2003) observed higher frequencies of surface runoff on gently sloping top-slopes and foot-slopes compared to mid-slopes. The lower runoff frequency at mid-slope position 6 may suggest this pattern can be observed, yet it had a higher mean WTD than other mid-slope positions with more runoff. The high proportion of runoff observed across the slope showed the value of a second year of monitoring and the differences between this study and Holden and Burt (2003) could be due to different years of study as well as taking place at different locations. Holden and Burt (2003) also had a higher frequency of sampling.

4.5.3 CO_2 flux

Carbon dioxide flux varied with slope position, though not in a distinct manner that supported results from Chapter 2. The upper mid-slope was shown to have higher rates of R_{eco} than the bottom-slope in Chapter 2, yet this study indicated top-slope position 1-H and bottom-slope position 10 had significantly higher R_{eco} than other slope positions, notably top-slope 1-E which had lower rates of R_{eco} than most other locations. Evidence of topographic

affects can vary across the literature. For a non-peat forest soil in Ohio, McCarthy and Brown (2006) found no evidence of a change in soil respiration between uplands and lowlands, while Pacific et al. (2011) suggested accumulative growing season soil CO_2 efflux was higher in riparian zones than uplands, relating it to increased soil moisture and C:N content. Webster et al. (2008) suggested soil respiration was higher on transitional foot-slope areas compared to mid-slopes and wetland areas (the only location with significant peat deposits) due to soil moisture and substrate, a product of DOC accumulation hotspots (Creed et al., 2013). These studies did not consider autotrotrophic respiration and were not across uniformly peat dominated soils, but do show that respiration can vary with topographic position, albeit not in a uniform manner.

It could be that R_{eco} results reflected spatial heterogeneity and microtopographical variation that is prevalent across particularly bog peatlands, and can complicate modelling of CO_2 fluxes (Sulman et al., 2012). Across both study years, R_{eco} on slope position 1-E was lower than that of 1-H, as well as slope position 4. Variance in R_{eco} has often been observed to be related to microtopographic change (Alm et al., 1997, Wu et al., 2011) and consequently variation in WTD (Sommerkorn, 2008). Such a relationship is not always consistent across microforms (Pelletier et al., 2011) but the relationship in Chapter 2 between R_{eco} and WTD on the top-slope could suggest WTD and microtopographic variation was important. However, no relationship between R_{eco} and WTD was found in this study, while the high rates of R_{eco} at 1-H were reduced having accounted for the influence of P_G. Gross photosynthesis did not explain high rates of R_{eco} at slope position 10 but the importance of sub-slope variation in Chapter 2 indicated that spatial heterogeneity was an important cause of change in rates of R_{eco}, something which was supported by results here. Indeed, slope position 10 had significantly higher rates of R_{eco} than the adjacent position 11 despite both having high *Eriophorum spp*. dominance, demonstrating spatial variation in R_{eco}.

Gross photosynthesis was greatest at slope positions 1-H and 4, the former upper mid-slope of Chapter 2. Chapter 2 indicated that P_G was greater on the bottom-slope than the top-slope, but this was not corroborated, rather the reverse was found between slope positions 1-H, 9 and 11. Air temperature and PAR were significant in explaining variation in P_G, as would be expected (Alm et al., 1999, Bubier et al., 2003, Clay et al., 2012), and accounted for many but not all of the significant differences between months due to seasonal variation. However, air temperature and PAR did not account for the high rates of P_G at slope positions 1-H and 4. It is possible that the lower dominance of *Eriophorum spp*. was important. At slope position 1-H there was more than 32% *Eriophorum spp*. dominance and plots were characterised by higher percentages of *Vaccinium myrtillus*. Though *Eriophorum spp*. have been shown to be efficient at sequestering CO_2, this has also been observed for ericaceous shrub dominated hummocks (Komulainen et al., 1999). It must be noted though that many slope positions had a high presence of *Vaccinium myrtillus* as a subdominant species.

Net ecosystem exchange was higher on the top-slope 1-E and 1-H plots than top-slope position 2, mid-slopes 6 and 7 and bottom-slope 9, which were net sources of CO_2 to the atmosphere in the ANOVA main effects model, though not the raw data. Results from Chapter 2 indicated the bottom-slope was a significantly greater net CO_2 sink than other slope positions during daylight hours, which was not supported by results here. As with P_G, there was significant annual variation, with NEE sinks much greater across the year of study in this chapter than Chapter 2, and this may partly explain the discrepancy between results. Significant differences were related to R_{eco} and P_G. Slope position 1-E had low rates of R_{eco} but relatively high, though not significant, rates of P_G and it was unsurprising that it was a net carbon sink during daylight hours. The high rates of P_G on slope position 1-H explained the net CO_2 sink. Inclusion of P_G in the ANCOVA model removed significant differences between slope position 1-H and those slope positions that were net sources of CO_2 became minor CO_2 sinks, suggesting the cause of the daytime CO_2 efflux was low rates of P_G. Slope position 1-E had a

significantly greater CO_2 sink during daylight hours having accounted for the effect of P_G, indicative of low rates of R_{eco}.

4.5.4 DOC

Dissolved organic carbon results were in good agreement with those of Chapter 2. Although top-slope locations did not have significantly higher DOC concentrations than bottom-slope locations, there was a significant increase in DOC on the mid-slope, at slope positions 4 and 5. The increase in DOC on the mid-slope reflected the site-specific slope affect observed on Alport Low using the four-component slope model. Dissolved organic carbon concentration was significantly lower further down the mid-slope and showed that DOC decreased to the bottom-slope locations, though slope position 9, in a depression on the bottom-slope, also had a significantly higher DOC concentration than most other slope positions.

Slope specific DOC affects have been observed across many environments. Boyer et al. (1997) reported higher DOC concentrations on hillslopes than in the riparian zone due to increased throughflow of subsurface water flushing DOC into the stream from the riparian zone, thus lowering DOC concentrations in the riparian zone. The results of Boyer et al. (1997) would support observations found in this study, but the study was not in peatlands and the scale was limited, classing hillslope as an area 10 metres from the stream where a break in slope was observed, with the riparian zone on steeper ground. Other studies have also commented upon the importance of the riparian zone or wetland areas across different soil types in contributing to stream water DOC (Mei et al., 2012, Hinton et al., 1998, Strohmeier et al., 2013), with little affect from the hillslope. Hinton et al. (1998) and Cory et al. (2007) found mineral soil hillslopes had lower DOC concentrations than lower wetland areas that had

organic rich soils, though Creed et al. (2013) suggested mid-slope areas and lower wetland zones had lower DOC concentrations than at the base of the hillslope in accumulation areas.

Thus the response of the hillslope and the hydrological connection between the hillslope, riparian zone and stream can depend upon soil type. For this study, it was evident that DOC concentrations in peatlands decreased down-slope and emphasises both the importance of monitoring DOC concentrations at the hillslope scale and the dominant affect that hydrology can have in controlling DOC concentration. Indeed, Chapter 2 suggested that elevated DOC concentrations on Alport Low compared to Feathered Moss were the consequence of water table drawdown and this was confirmed using the slope transect. The significance of WTD to DOC concentration would imply the importance of oxidative production of DOC (Wallage et al., 2006, Scott et al., 1998). Furthermore, high DOC concentrations could be found on the bottom-slope where water table drawdown was observed, such as with slope position 9, located in a depression. This further emphasised the importance of WTD while also highlighting the value of locating collars within the depression to capture spatial heterogeneity.

As with Chapter 2, soil pore water DOC concentration was negatively correlated to NO_3^-, but was also correlated to SO_4^{2-} and conductivity. Sulphur oxidation has been observed to lower acidity and suppress DOC solubility (Clark et al., 2005, Daniels et al., 2008b). No such affect was apparent in Chapter 2 and is therefore equivocal. Indeed, lower water tables would be expected to demonstrate suppression of DOC production if this was the case, while pH was not significant, but has been found to be of overall importance in lowering DOC concentration by affecting organic matter solubility (Evans et al., 2012). The concentration of SO_4^{2-} only explained a small amount of variation in DOC and may reflect dilution of DOC, given higher SO_4^{2-} content in surface runoff samples. However, although surface runoff water had higher conductivity than soil pore water, it may be that the positive correlation between DOC in soil

pore water and conductivity was indicative of deeper ground water sources (Worrall et al., 2008).

Slope position was not significant in explaining variation in DOC for surface runoff water, as was observed in Chapter 2. Soil pore water DOC concentration was significantly higher than that of runoff water. Robroek et al. (2010) similarly observed lower DOC concentrations in surface runoff water compared to soil pore water at Moor House in the North Pennines, reporting much lower DOC concentrations across both water types than observed here. Stream water DOC was greater than runoff water, and represented an intermediate concentration between soil pore water and surface runoff water. Stutter et al. (2012) noted that for peat soils stream water DOC decreased as it was diluted by precipitation inputs, while Billett et al. (2006) similarly observed lower DOC concentrations in the stream while acknowledging inputs from shallow depth peat soils. This was also observed by Palmer et al. (2001). While stream water and soil pore water were not significantly different in the ANOVA model, they were having accounted for water chemistry covariates. Thus uniform surface runoff water across the slope was caused by dilution, while stream water represented a mixture of DOC from soil pore water and dilution effects. The relationship between DOC, water chemistry and water type will be explored in detail in Chapter 5.

4.6 Conclusions

This chapter has explored the importance and relevance of the hillslope in detail by assessing variation in WTD, CO_2 flux and DOC along a slope transect. Analysis of WTD corroborated results from Chapter 2 and slope position explained over 80% of variation in WTD, confirming the importance of hillslope in controlling WTD across the landscape, while also highlighting the importance of microtopographic variation.

CO_2 fluxes did not agree with results from Chapter 2 and no distinct trend could be associated with slope position. Variation in R_{eco} was most closely associated with microtopographic variation and highlighted the importance of spatial heterogeneity, while high rates of P_G on top-slope hummocks may have been due to ericaceous shrub dominance. Net ecosystem exchange was greatest on the two top-most locations on the slope and was the result of high rates of P_G or low rates of R_{eco}.

Dissolved organic carbon concentration was greatest on the mid-slopes, where water table drawdown enhanced production of DOC. DOC concentration decreased further down-slope due to rising water tables towards the surface and possible flushing by lateral throughflow of water. Studying DOC concentration along a detailed slope transect confirmed the trends observed in the site-slope interaction on Alport Low from Chapter 2 and emphasised the need to account for the effect of hillslope and water table in controlling DOC concentrations when modelling carbon budgets across large spatial scales. Water chemistry was another important control upon DOC concentration for multiple water sources, be it soil pore water, surface runoff or stream water. Chapter 5 will examine the importance of these relationships and of different flowpaths across the hillslope.

Chapter 5 Hillslope hydrology and water chemistry

5.1 Introduction

Chapters 2 and 4 identified important changes in hydrology across the hillslope and towards the riparian zone, while also observing changes in dissolved organic carbon (DOC) concentration. Soil pore water DOC concentration along the hillslope was negatively correlated to changes in water table depth (WTD), with DOC concentration increasing as the water table got deeper. However, for soil pore water, surface runoff water and stream water, DOC concentration was affected by other hydrochemistry variables, as summarised below:

- Soil pore water: In Chapter 2, DOC was positively correlated to pH and conductivity but negatively correlated to NO_3^- concentration and E4:E6 ratio, though the latter was a very small effect. In Chapter 4, pH and E4:E6 ratio were not significant, but conductivity and NO_3^- were. There was a small negative correlation to SO_4^{2-}.
- Runoff water: Chapter 2 indicated conductivity, E4:E6 ratio and SO_4^{2-} concentration were positively correlated to DOC concentration; no significant relationship to conductivity was found in Chapter 4, but pH had a small negative correlation to DOC.
- Water type: Chapter 4 assessed soil pore water, runoff water and stream water together, suggesting conductivity and E4:E6 ratio were positively correlated to DOC concentration, while pH and NO_3^- concentration had a negative correlation.

The exact nature of the relationship between water chemistry variables and DOC was unclear and it was suggested that dilution effects or changes in flowpaths with mixing of different water sources may be important controls on DOC dynamics.

Variation in water chemistry in peatlands has been related to different flowpaths, water sources or both. At an uneroded blanket peatland in the North Pennines, Adamson et al. (2001) observed an increase in pH and Cl^- concentration with depth in soil pore water while SO_4^{2-} and DOC concentration decreased; ionic concentrations were related to WTD, and indicated that while water table drawdown stimulated ammonification, there was limited evidence of nitrification. Prévost et al. (1999) found at a forested peatland in Canada an increase in nutrients and SO_4^{2-} with increased proximity to drainage ditches. As well as relating variation in hydrochemistry to WTD and oxidation or reduction processes, it is possible to observe changes in water source, flowpaths and mixing processes. Kværner and Kløve (2006) used variation in anions and cations to distinguish water sources; Si and Al^{3+}, as well as DOC, were particularly useful in distinguishing between precipitation, stream water, groundwater and peat soil pore water, while Ca^{2+} was characteristic of groundwater sources. Major ions in peat water also included SO_4^{2-} and Cl^- (Kværner and Kløve, 2006).

Multivariate techniques have been used when analysing water chemistry and inferring flowpaths (such as near surface throughflow or runoff water) or distinct end-members. On blanket bog in the North Pennines, Worrall and Adamson (2008) assessed changes in soil pore water under different burning and grazing management regimes and used principal components analysis (PCA) to identify compositional trends in soil pore water and rainwater. Two dominant trends were identified, associated with rainwater and shallow soil water, while groundwater components were characterised as base-rich with high ionic strength but were found to be excluded as a water source following burning (Worrall and Adamson, 2008). Clay et al. (2010a) were able to detect compositional changes in soil water following burning,

identifying a decrease in deep water components and an increased influence of shallow soil pore water components from sites where the water table was closer to the surface, typically on 20 year burn plots. However, following burning surface runoff water was shown to almost exclusively reflect the composition of rainwater, whereas pre-burn it plotted on the shallow water trend as well (Clay et al., 2010a).

Proctor (2008) used PCA analysis to distinguish between the water chemistry of ombrotrophic bogs and minerotrophic fens with ombrotrophic bog chemistry reflecting distance from the sea by virtue of Na^+ and Cl^- content, as they are marine derived. Furthermore, PCA has been used to characterise the transition of stream water chemistry in a headwater system with distance downstream (Daniels et al., 2012). Consequently, PCA is an extremely useful statistical method to explore patterns in flowpaths and water sources. Moreover, Worrall et al. (2003a) outlined why PCA is preferable to using end-member mixing analysis (EMMA) as a method for determining compositional trends. While EMMA requires identification of end-members prior to analysis, PCA makes no assumptions regarding a given dataset. Furthermore, EMMA does not reflect temporal variation in compositional trends as it assumes steady-state water sources and can only use conservative tracers as it is not a multivariate technique (Worrall et al., 2003a).

Although multivariate techniques are extremely useful when assessing hydrochemistry, tracer experiments provide explicit evidence of water movement across the landscape. Shabaga and Hill (2010) used NaBr as a conservative tracer and suggested it provided evidence of storage zones in the riparian zone due to a delay in Br^- flushing. Hedin et al. (1998) established water velocity, hydraulic conductivity and subsurface flowpaths by applying KBr^- as a tracer. Bromide has also been used to identify preferential flowpaths (Parsons et al., 2004). Thus Br^- has numerous applications as a tracer and has several advantages over other tracers. Though Cl^- is conservative it is naturally abundant in UK

ombrotrophic bogs owing to the oceanic climate and can dominate anion trends (Proctor, 2008, Worrall and Adamson, 2008). Consequently, while Adamson et al. (2001) used naturally occurring concentrations of Cl^- as a standard by which to compare other ion concentrations, tracer studies are better served using a solute such as Br^- which has naturally low background concentrations (Gilley et al., 1990) that can be below the detection limit of ion chromatographs (Hedin et al., 1998). Furthermore, although plant uptake of Br^- has been observed (Parsons et al., 2004) it is considered to be a generally conservative tracer (Shabaga and Hill, 2010) and its detection would be indicative of water movement at a given location or depth in the peat profile.

This chapter will use a multi-tracer approach to explore patterns in water chemistry and flowpaths across the hillslope. Sodium bromide will also be used in a tracer experiment to detect both water movement and how flowpaths change along the hillslope. As part of this, soil pore water, 10 cm depth water, surface runoff water and stream water samples will be analysed.

5.2 Aims and objectives

The overall aim of this chapter is to determine how hydrochemistry varies along the hillslope and to use this to evaluate different water sources, how these mix on the hillslope and the relationships with flowpaths. The objectives are:

- Identify compositional trends in water chemistry using multivariate techniques and establish unique end-members.
- Determine how water chemistry varies along the hillslope and relate this to changes in flowpath and compositional mixing.

- Use a conservative tracer to identify water movement along the hillslope to the riparian zone and determine the origin of different water sources.

5.3 Materials and methods

5.3.1 Experimental design

5.3.1.1 Annual datasets

This chapter uses the water chemistry datasets from Chapters 2 and 4. Consequently, data was gathered from June 2010 – June 2011 for Featherbed Moss and Alport Low across four slope positions (top-slope, upper mid-slope, lower mid-slope and bottom-slope); and between September 2011 – August 2012 along the Alport Low slope transect to the stream. As an additional data source, the 2011 – 2012 dataset contained data from 10 cm depth water traps which were installed in March 2012. These traps were designed to assess mixing between water sources and changes in flowpath given the observed differences between soil pore water and surface runoff water (Chapters 2 and 4) and the change in water chemistry and DOC concentration that can occur with depth (Adamson et al., 2001, Clark et al., 2008). Two 10 cm depth traps were installed at each slope position, in between collars 1 – 2 and collars 2 – 3. The 10 cm depth traps were composed of uPVC runoff traps with holes drilled to 10 cm below the peat surface when installed. Bungs were inserted at both ends to prevent mixing with soil pore water from other depths or precipitation. Samples were gathered for five months between April – August 2012, using a hand pump to extract water from the trap so as to prevent disturbance of the peat substrate. Samples from 10 cm depth traps shall herein be referred to as 10 cm water.

Field monitoring during 2010 – 2011 and 2011 – 2012 was undertaken to assess changes in DOC concentration along the hillslope and sampling focused upon gathering soil pore water and runoff water data. As such, precipitation data was not gathered. To compare soil pore water and runoff water to precipitation water chemistry, data gathered from the River Etherow (DEFRA, 2013) between 07/06/2010 – 04/01/2012 was used, covering the study period of Chapters 2 and 4 until no more data was available. The River Etherow drains the northern part of Bleaklow Plateau and the monitoring station (SK 12410 98884) was located approximately 5.2 and 7.2 km NNE of Alport Low and Featherbed Moss respectively.

5.3.1.2 Tracer study

A tracer study was conducted on the Alport Low slope transect during September 2012, incorporating soil pore water, surface runoff water, 10 cm water and stream water samples. On 14/09/2012 (day 0), water samples were collected for water chemistry analysis to determine background Br^- concentrations and all runoff / 10 cm traps emptied prior to application of the tracer. After water samples had been collected from all slope positions along the transect, 4 kg NaBr was applied as a solid to the peat surface at four locations (1 kg each, Figure 5.1) and doused with water (~2.5 litres at each location, stored in five, 2 litre polyethelene bottles) to stabilise the sample on the peat surface and initiate infiltration of the tracer. The tracer was not applied at the very top of the slope so as to avoid the tracer being diverted away from the hillslope by its loss in the extensive gully network. The four application points were at the same altitude, between slope positions 3 and 4 so as to remove possible drainage effects of linear gullies either side of the interfluve that the slope transect was located upon. As such, application of the tracer was done away from gullies so as to explicitly observe water flow down the hillslope. The tracer was applied across the interfluve,

approximately four metres between each application point and at least two metres away from gullies.

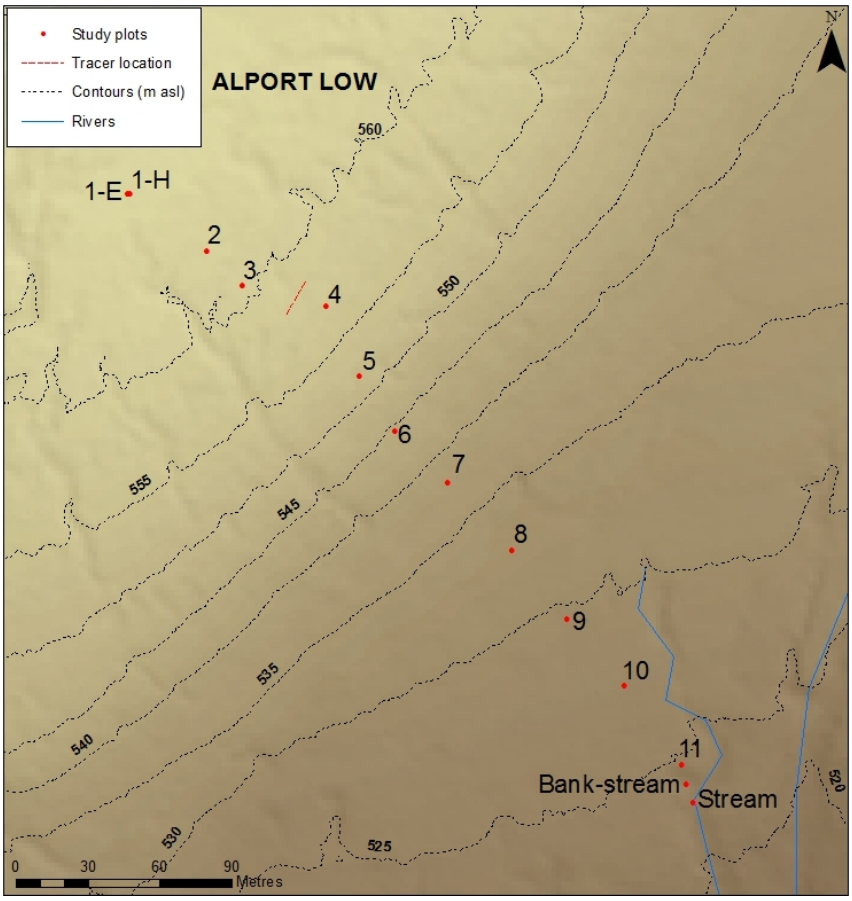

Figure 5.1 Map of Alport Low slope transect and bromide tracer application location

In the seven days prior to tracer application, 27 mm of rain fell, while mean temperature was 11 °C. Nearly all slope positions had water tables closer to the surface than the mean values in Table 4.3. Only slope position 5 had a deeper WTD, which was only 2 mm deeper than in Table 4.3. Slope position 1-E had two plots with saturated water tables. Following tracer application, samples were gathered on three subsequent occasions: 17/09/2012 (day 3); 20/09/2012 (day 6); and 27/09/2012 (day 13). The sampling design was

established to gather two lots of samples within the first week of tracer application and another a week later to observe progression of the tracer along the slope and its subsequent dilution. Heavy rainfall events between day 6 and day 13 (90.89 mm of rain 21 – 26 September) and after day 13 (30.87 mm in the seven days following the last sample date) meant that it was anticipated the NaBr would have been flushed out of the system and that further sample collection would be unnecessary. After each sample collection, surface runoff and 10 cm depth traps were emptied.

5.3.2 Laboratory analysis

All water samples were filtered at ≤0.45 µm using cellulose acetate-syringe filters to remove particulate material. Samples were analysed for pH; electrical conductivity; UV-Visible absorbance at 400, 465 and 665 nm; DOC; and anion concentrations (SO_4^{2-}, Cl^-, NO_3^-, Br^-, PO_4^{3-}, F^-). Details of methods are given in Chapter 2.

5.3.3 Statistical analysis

Prior to statistical analysis, datasets had values outside three standard deviations of the mean removed as outlying values. Outlier removal was conducted separately for each water type (soil pore water; surface runoff water; 10 cm water; and stream water). Outlier removal was conducted to remove any bias induced from extreme values and improve dataset distribution. The use of three standard deviations was a conservative approach that allowed an objective and consistent approach to be adopted, as done throughout the thesis. Details of outliers removed from the 2010 – 2011 and 2011 – 2012 datasets are provided in sections 5.4.1 and 5.4.2 respectively. The datasets used in this chapter were from untransformed

datasets only, meaning the number of outliers removed may differ to those reported in Chapter 2 and Chapter 4.

5.3.3.1 Principal components analysis

Principal components analysis was performed separately for the 2010 – 2011 and 2011 – 2012 datasets. Water chemistry variables included in the multivariate datasets were: pH; electrical conductivity; absorbance at 400 nm (Abs_{400}); E4:E6 ratio (absorbance 465 / 665 nm); specific absorbance (Abs_{400} / DOC concentration); DOC concentration; and SO_4^{2-}, Cl^-, and NO_3^- concentration. Nitrate concentration was included owing to its significance in explaining variation in DOC concentration (Table 2.22 & Table 4.21) but Br^-, PO_4^{3-} and F^- were excluded from analysis owing to their low concentrations often being below detection. Prior to analysis, all water chemistry variables were z transformed (equation 5.1) to standardise each variable to allow comparison between variables with different measurement units. Principal components (PCs) with an eigenvalue >1 explain more variance than any of the original variables in the standardised dataset and therefore selection of PCs used in analysis was based upon the convention of using all PCs with an eigenvalue >1 and the first PC that has an eigenvalue <1. Analysis of variance (ANOVA) was performed on PC1 to identify significant differences.

$$z = \frac{(x - \bar{x})}{\sigma} \qquad 5.1$$

Where: x = the measured value, $\bar{x}$ = the dataset mean and σ = the dataset standard deviation.

5.3.3.2 Analysis of variance / covariance

ANOVA was conducted on PC1 (given the observed results, for which PC1 distinguished water type) to identify factors that had a significant relationship to PC1 scores. For the 2010 –

2011 dataset, factors included: site (Alport Low, Featherbed Moss); slope (top-slope, upper mid-slope, lower mid-slope, bottom-slope); sub-slope; water type (soil pore water, runoff water); month; and interactions. Percentage *Eriophorum spp*., WTD and terrain indices (slope angle, wetness index and altitude) were included as covariates. For the 2011 – 2012 dataset, it was not possible to analyse slope and water type together. Water type had four factor levels: soil pore water; runoff water; 10 cm water; and stream water. Month was included as a second factor. Water type was assessed using solely ANOVA, with no covariates (given no percentage *Eriophorum spp*. and WTD for stream samples). The influence of slope position (12 factor levels, 1-E and 1-H – 11) was assessed separately for soil pore water, runoff water and 10 cm water, with month included as a factor as well. Covariates were included for ANCOVA of soil pore water and runoff water, but this was not done for 10 cm water samples as they were placed between plots 1 – 2 and 2 – 3 and had no individual WTD or percentage *Eriophorum spp*. to include as covariates. The non-parametric Kruskal-Wallis test was performed on any ANOVA dataset that did not have a normal distribution.

5.3.3.3 Runoff and 10 cm water occurrence

The frequency that runoff was observed for each slope position during the tracer study was assessed using the χ^2 method outlined in equation 2.6, followed by *post hoc* tests. The χ^2 test was also applied to observations of water collection in the 10 cm depth traps and performed on samples gathered between April – August 2012 and the tracer study dataset. The two 10 cm water datasets were analysed separately.

5.4 Results

5.4.1 2010 – 2011 dataset

Details of pH, conductivity, Abs_{400}, specific absorbance and E4:E6 were discussed in Chapter 2. Table 5.1 summarises variation in anion concentrations for soil pore water and runoff water. For soil pore water, mean SO_4^{2-} was highest on the top-slope (6.8 ± 0.3 mg l^{-1}) but was considerably lower than concentrations observed in the runoff water, which was much higher on the upper mid-slope (22 ± 3 mg l^{-1}), compared to the next highest concentration on the bottom-slope (16 ± 1 mg l^{-1}). Chloride content was relatively similar between water types compared to SO_4^{2-}, with the upper mid-slope runoff water mean of 5.7 ± 0.5 mg l^{-1} the highest and lower mid-slope soil pore water mean of 4.2 ± 0.1 mg l^{-1} the smallest. As with SO_4^{2-}, Cl^- was highest on the top-slope in soil pore water (4.9 ± 0.2 mg l^{-1}). Nitrate was greatest on the upper mid-slope (2.4 ± 0.3 mg l^{-1}). Nitrate concentration was highest on the upper mid-slope on both study sites, but was particularly high on the Alport Low upper mid-slope, possibly due to enhanced oxidation due to water table drawdown. Concentrations of other anions were low, though PO_4^{3-} had a top-slope mean of 0.7 ± 0.2 mg l^{-1} in runoff water.

Table 5.2 shows the water chemistry of precipitation for the River Etherow (DEFRA, 2013). Precipitation mean pH (5.6 ± 0.1) was higher than soil pore water but close to that of runoff water, which had a mean of 5.6 ± 0.1 – 6.02 ± 0.07 (Table 2.29) across the four slope positions. Precipitation conductivity (25 ± 4 µs cm^{-1}) was lower than both soil pore water and runoff water. Anion concentrations were much lower than soil pore water and runoff water, with Cl^- (3.5 ± 0.5 mg l^{-1}) concentrations higher than SO_4^{2-} and NO_3^- which were both <1 mg l^{-1}. The dominance of Cl^- over SO_4^{2-} contrasted soil pore water and in particular runoff water, which had mean SO_4^{2-} concentrations >12 mg l^{-1} on all slope positions.

Table 5.1 Descriptive statistics for 2010 – 2011 anion concentrations (detection limit <<0.05 mg l^{-1}): SPW = soil pore water; RO = runoff water; SE = standard error

Variable	Slope	SPW N	SPW Mean	SPW SE Mean	SPW Maximum	SPW Minimum	RO N	RO Mean	RO SE Mean	RO Maximum	RO Minimum
SO_4^{2-} (mg l^{-1})	Top-slope	224	6.8	0.3	33.4	0.0	162	12.2	0.9	89.3	0.0
	Upper Mid-slope	139	5.6	0.3	14.4	0.0	98	22	3	198.4	0.0
	Lower Mid-slope	134	5.1	0.3	15.4	0.0	108	14	2	170.0	0.0
	Bottom-slope	200	5.6	0.3	20.1	0.1	165	16	1	122.1	1.2
Cl^- (mg l^{-1})	Top-slope	225	4.9	0.2	26.1	0.2	162	5.0	0.7	107.7	1.5
	Upper Mid-slope	139	4.5	0.1	10.9	1.1	98	5.7	0.5	27.2	1.7
	Lower Mid-slope	140	4.2	0.1	9.2	1.0	114	4.9	0.5	34.2	1.3
	Bottom-slope	200	4.4	0.1	10.5	1.1	165	4.9	0.4	29.0	1.2
NO_3^- (mg l^{-1})	Top-slope	225	1.3	0.1	11.0	0.0	162	1.16	0.08	5.8	0.0
	Upper Mid-slope	139	2.4	0.3	24.5	0.0	98	1.0	0.2	12.5	0.0
	Lower Mid-slope	140	0.92	0.09	6.4	0.0	114	1.0	0.1	4.9	0.0
	Bottom-slope	200	0.99	0.08	5.3	0.0	165	0.80	0.06	3.4	0.0
PO_4^{3-} (mg l^{-1})	Top-slope	225	0.16	0.04	6.3	0.0	162	0.7	0.2	23.2	0.0
	Upper Mid-slope	139	0.37	0.09	5.8	0.0	98	0.4	0.2	16.1	0.0
	Lower Mid-slope	140	0.2	0.1	13.0	0.0	114	0.17	0.06	4.3	0.0
	Bottom-slope	200	0.13	0.06	10.2	0.0	165	0.5	0.3	51.6	0.0
Br^- (mg l^{-1})	Top-slope	225	0.26	0.02	1.5	0.0	162	0.22	0.08	12.7	0.0
	Upper Mid-slope	139	0.32	0.03	1.2	0.0	98	0.19	0.03	1.2	0.0
	Lower Mid-slope	140	0.27	0.03	1.1	0.0	114	0.18	0.03	1.6	0.0
	Bottom-slope	200	0.21	0.02	1.1	0.0	165	0.12	0.02	1.0	0.0
F^- (mg l^{-1})	Top-slope	225	0.23	0.01	1.1	0.0	162	0.14	0.02	3.1	0.0
	Upper Mid-slope	139	0.20	0.02	1.8	0.0	98	0.15	0.02	1.0	0.0
	Lower Mid-slope	140	0.18	0.02	1.0	0.0	114	0.13	0.02	1.3	0.0
	Bottom-slope	200	0.13	0.01	0.5	0.0	165	0.11	0.01	1.0	0.0

Table 5.2 River Etherow precipitation data 07/06/2010 – 04/01/2012: SE = standard error

Variable	N	Mean	SE Mean	Maximum	Minimum
SO_4^{2-} (mg l^{-1})	31	0.52	0.04	1.1	0.2
Cl^- (mg l^{-1})	31	3.5	0.5	13	0.6
NO_3^- (mg l^{-1})	31	0.33	0.04	1.1	0.1
pH	31	5.6	0.1	7.4	4.6
Conductivity (µs cm^{-1})	31	25	4	110.9	7.3

Table 5.3 shows the percentage of data removed as statistical outliers for the variables used in PCA, separated by water type. The maximum percentage data removed from a single dataset was 2.47% (soil pore water specific absorbance) and of the 18 individual datasets, only four had >2% of data removed as outlying values.

Table 5.3 Percentage data removed from 2010 – 2011 water chemistry variables: SPW = soil pore water; RO = runoff water; Abs_{400} = absorbance at 400 nm

Variable	Dataset	N	N removed	% removed
pH	SPW	716	15	2.09
	RO	552	0	0.00
Conductivity	SPW	715	6	0.84
	RO	532	13	2.44
Abs_{400}	SPW	716	9	1.26
	RO	578	5	0.87
E4:E6	SPW	709	14	1.97
	RO	529	10	1.89
DOC	SPW	688	5	0.73
	RO	518	9	1.74
Specific absorbance	SPW	688	17	2.47
	RO	516	10	1.94
SO_4^{2-}	SPW	697	12	1.72
	RO	533	12	2.25
Cl^-	SPW	704	7	0.99
	RO	539	9	1.67
NO_3^-	SPW	704	12	1.70
	RO	539	8	1.48

Principal components analysis combined variables from multiple datasets but could only be conducted on a dataset without data gaps, thus meaning any row that had a variable missing was excluded from the analysis, reducing the number of data retained. Table 5.4 shows the cell occupancy of the 2010 – 2011 dataset by site and slope each month. On 11 occasions, cell occupancy was zero. However, for only one dataset was this caused by statistical outlier removal. On the Featherbed Moss top-slope in March, three runoff traps either had no sample or not enough sample for a complete suite of water chemistry analyses, two samples had DOC concentrations below the detection limit and one sample had an outlier removed from NO_3^- concentration. Thus, out of the six possible samples that month, one sample was excluded due to removal of a statistical outlier, causing zero cell occupancy.

Other factors to cause zero cell occupancy included DOC concentrations and E4:E6 ratios (where absorbance at 465 or 665 nm was zero or negative) below the detection limit, meaning the sample could not be incorporated into PCA. Values below the detection limit were most common in runoff samples, meaning runoff water was subject to larger errors than soil pore water and had more rows of data excluded from analysis. Nonetheless, it was important to include E4:E6 ratio as a compositional measure given the amount of variation it explained in runoff water DOC analysis for both years of study. Additional factors that caused zero cell occupancy related to laboratory and field constraints. For instance, it was not possible to include anion concentration data on Featherbed Moss bottom-slope samples in November. Heavy snowfall prevented collection of soil pore water and runoff water samples on Featherbed Moss bottom-slope in December. Finally, not all runoff traps had collected water on a given month, reducing the number of samples available for analysis.

Table 5.4 2010 – 2011 PCA cell occupancy: all slope positions had six sample plots except Alport Low top-slope and bottom-slope that had 12; June was sampled in 2010 and 2011 on Alport Low; SPW = soil pore water; RO = runoff water

Site-Water type	Slope	Month												
		7	8	9	10	11	12	1	2	3	4	5	6	TOTAL
Alport Low SPW	Top-slope	11	12	10	11	11	8	11	10	9	12	8	13	126
	Upper Mid-slope	4	4	4	4	5	3	4	5	2	4	4	5	48
	Lower Mid-slope	2	6	5	4	5	5	5	6	4	6	6	6	60
	Bottom-slope	10	12	12	12	10	9	6	9	5	7	12	12	116
	TOTAL	27	34	31	31	31	25	26	30	20	29	30	36	
Alport Low RO	Top-slope	8	9	3	7	8	5	3	8	8	9	11	16	95
	Upper Mid-slope	2	2	1	1	1	3	3	1	2	3	5	1	25
	Lower Mid-slope	2	3	0	4	3	2	0	4	1	5	5	5	34
	Bottom-slope	6	8	7	8	8	7	2	7	6	6	8	18	91
	TOTAL	18	22	11	20	20	17	8	20	17	23	29	40	
Featherbed Moss SPW	Top-slope	5	5	6	5	6	4	6	6	4	6	5	2	60
	Upper Mid-slope	4	6	6	5	6	2	6	3	6	6	6	6	62
	Lower Mid-slope	6	6	0	6	6	6	4	6	5	3	4	6	58
	Bottom-slope	5	6	6	6	0	0	1	4	2	6	3	6	45
	TOTAL	20	23	18	22	18	12	17	19	17	21	18	20	
Featherbed Moss RO	Top-slope	2	1	4	5	4	3	0	5	0	1	0	3	28
	Upper Mid-slope	4	2	3	3	6	3	2	4	2	2	2	2	35
	Lower Mid-slope	4	3	0	4	6	3	2	3	4	1	3	3	36
	Bottom-slope	4	2	3	6	0	0	1	3	1	2	1	2	25
	TOTAL	14	8	10	18	16	9	5	15	7	6	6	10	

Of the total number of rows for which a complete suite of water chemistry variables was available, 86.86% of soil pore water and 89.56% of runoff water samples were retained following outlier removal. As such, a large sample size was retained nonetheless, with 944 data points incorporated into the analysis. Furthermore, the spread of data was sufficient for each slope position and month to be adequately represented (total N, Table 5.4), meaning cell occupancy was large enough to test interactions between factor levels in ANOVA of PC1 (Table 5.6). The dataset was therefore large and robust enough to cope with the data gaps that occurred.

Four components were retained for PCA based upon the rule of selecting all PCs with an eigenvalue >1 (PCs 1 – 3) and the first PC with an eigenvalue <1 (PC4). The four PCs explained 77.70% of variation in the data (Table 5.5). Principal component 1 was characterised by strong positive loadings for pH, SO_4^{2-} and conductivity and negative loadings for Abs_{400}, specific absorbance and E4:E6 (also shown in Figure 5.2). Principal component 2 was dominated by DOC concentration, which had a negative loading. Abs_{400} was correlated to DOC, sharing a negative loading, while specific absorbance had a strong positive loading.

Table 5.5 First four principal components of 2010 – 2011 dataset

Variable	PC1	PC2	PC3	PC4
pH	0.487	-0.019	-0.204	0.055
Conductivity	0.430	-0.213	0.333	-0.099
Abs_{400}	-0.415	-0.394	0.156	-0.081
E4:E6	-0.266	-0.143	0.463	0.130
DOC	-0.103	-0.726	0.025	0.018
Specific Absorbance	-0.328	0.381	0.237	-0.088
SO_4^{2-}	0.443	-0.187	0.302	0.115
Cl^-	0.134	0.148	0.461	-0.730
NO_3^-	0.058	0.222	0.498	0.640
% Variance	**33.70%**	**52.10%**	**67.80%**	**77.70%**

Principal component 1 (Figure 5.3) distinguished between soil pore water and runoff water while PC2 represented a concentration and compositional gradient of DOC, with two trend lines showing the separation of soil pore water from runoff water. Runoff water had much higher pH values and higher SO_4^{2-} concentrations; with SO_4^{2-} plotting with conductivity in Figure 5.2. However, it must be noted that cation concentrations could not be accounted for and the higher conductivity of runoff water was most likely caused by associated cations rather than SO_4^{2-}. Soil pore water had much higher Abs_{400} values than runoff water.

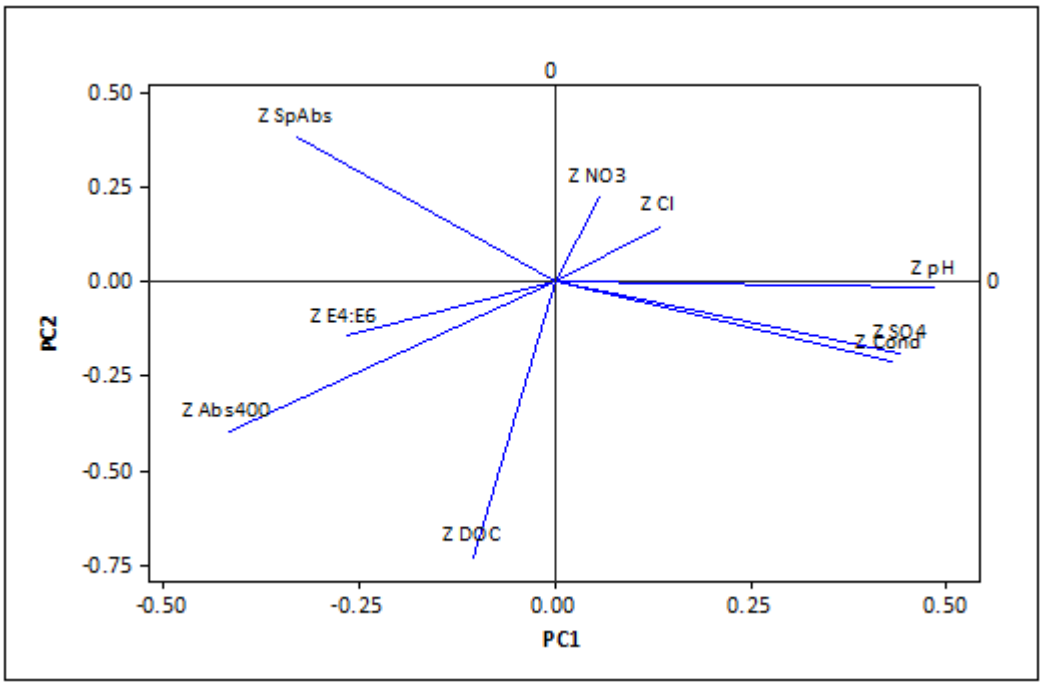

Figure 5.2 Loading plot of 2010 – 2011 PC1 & PC2

End-members on Figure 5.3 have been labelled with the prefix 'EM', while regions of interest discussed in the text have the prefix 'R'. End-members represented distinct compositions that were physically interpretable and from which compositional mixtures evolved. Two distinct end-members, of soil pore water (EM-A) and runoff water (EM-B), were identified, along with a mixing zone (R-C) where runoff water plotted along the soil pore water trend and was characterised by low pH and conductivity but high DOC, thus exhibiting the composition of soil pore water. Runoff water in the mixing zone often had higher Abs_{400} values compared to runoff water that was distinct from soil pore water, along the runoff water trend line. Runoff water samples in the mixing zone were typically from *Eriophorum spp*. plots or otherwise bottom-slope hummock plots on Alport Low, where water tables were high or even saturated.

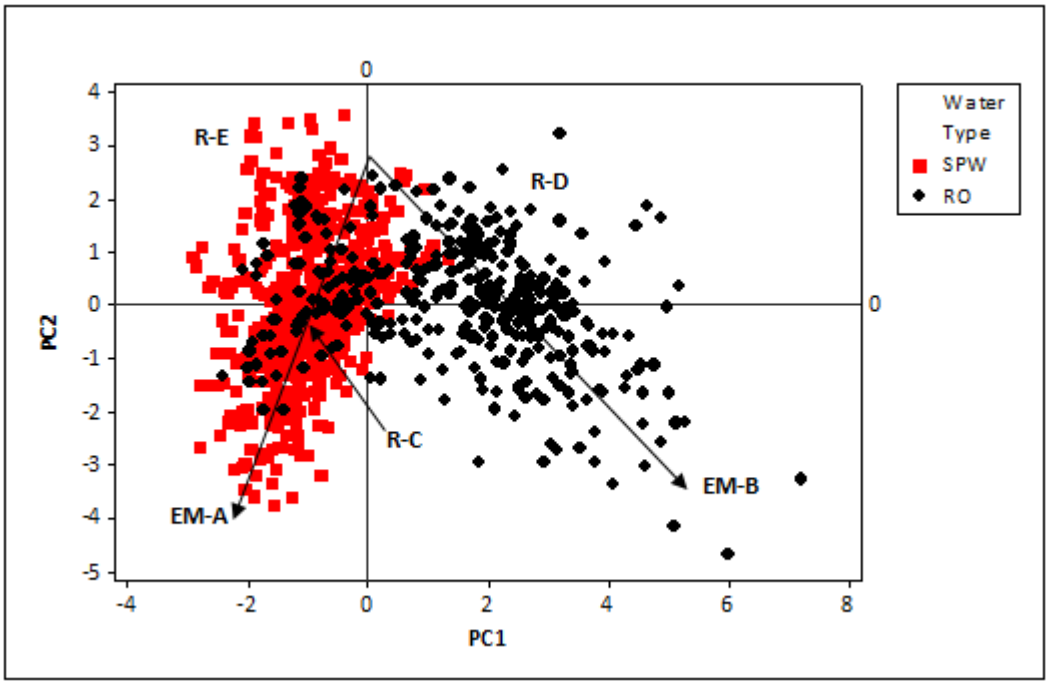

Figure 5.3 Scatterplot of 2010 -2011 PC1 & PC2: SPW = soil pore water; RO = runoff water; prefix EM = end-member; prefix R =region; A – E = labels

EM-A in Figure 5.3 was characterised by very high DOC and Abs_{400}, with low pH levels. EM-A was a deep soil pore water end-member composed of samples from the Alport Low mid-slopes and top-slope hummock plots where water tables were deeper. EM-B retained the dominant features of runoff water: high pH, conductivity and SO_4^{2-} but was also characterised by high DOC concentrations, thus making it a distinct end-member from runoff water compositions with lower DOC content. Despite samples from EM-B consisting of high DOC concentrations, they were distinct from soil pore water samples by virtue of low levels of Abs_{400} and specific absorbance, as well as the higher pH, conductivity and SO_4^{2-} characteristic of runoff water samples. Runoff water around R-D had low DOC concentrations but high SO_4^{2-} concentrations, while soil pore water samples at R-E had high specific absorbance but low DOC and conductivity.

To summarise, PC1 distinguished between compositions of soil pore water and runoff water while PC2 was a DOC concentration gradient, with Abs_{400} and specific absorbance DOC compositional measures further characterising water samples. The only other scatterplot of PCs where a coherent visual pattern was evident was PC1 against PC3 (Figure 5.4). Whereas DOC dominated PC2, it was not important to PC3, rather E4:E6 ratio, Cl^- and NO_3^- separated water samples. EM-A was dominated by high NO_3^- concentrations and high E4:E6 ratios in soil pore water. Although EM-A was dominated by Alport Low mid-slope and top-slope hummock plots with deeper water tables (as with Figure 5.3), it was not exclusively a deep soil pore water end-member as some samples were from *Eriophorum spp*. plots on Alport Low and Featherbed Moss samples. EM-B was a runoff water end-member of both high Cl^- and NO_3^- concentrations. Runoff water at R-C had low E4:E6 ratios and either low Cl^- or NO_3^- concentrations.

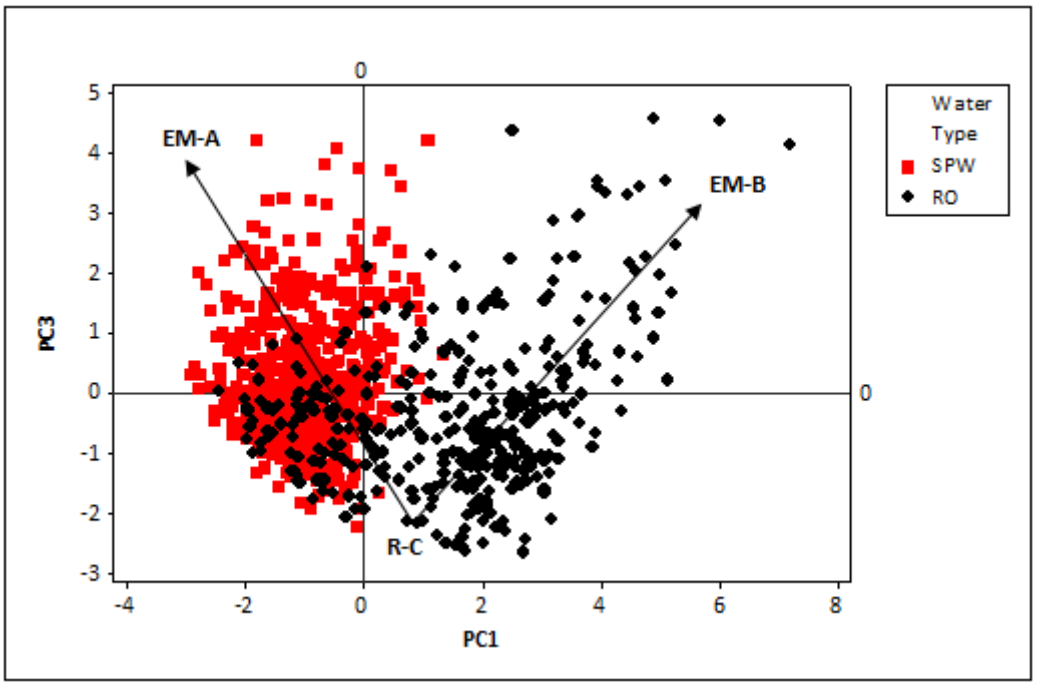

Figure 5.4 Scatterplot of 2010 – 2011 PC1 & PC3; SPW = soil pore water; RO = runoff water; prefix EM = end-member; prefix R =region; A – C = labels

Analysis of variance (R^2 = 70.07%, Table 5.6) was performed on PC1 due to its importance in separating water types. The error term in ANOVA accounted for the variation in the data that could not be explained by the ANOVA model and although it included measurement error, it also represented unexplained factors and interactions. Though slope was significant (p <0.0001, ω^2 = 0.43%) it explained only a small amount of variation in PC1. There were multiple interactions incorporating slope, including slope-water type (p <0.0001, ω^2 = 1.08%). Water type, as expected based upon PCA results, was the most important factor (p <0.0001, ω^2 = 48.00%) followed by month (p <0.0001, ω^2 = 8.51%), site-water type (p <0.0001, ω^2 = 3.29%) and site (p <0.0001, ω^2 = 2.46%).

Table 5.6 2010 – 2011 PC1 ANOVA: ω^2 = percentage variance

ANOVA			ANCOVA		
Factor	**P**	**ω^2**	**Factor**	**P**	**ω^2**
Site	<0.0001	2.46%	WTD	<0.0001	1.69%
Slope	<0.0001	0.43%	Wetness Index	0.008	0.15%
Sub-slope	0.014	0.64%	Altitude	0.013	0.61%
Water Type	<0.0001	48.00%	Site	0.007	0.68%
Month	<0.0001	8.51%	Slope	<0.0001	0.79%
Site*Slope	<0.0001	0.77%	Water Type	<0.0001	48.82%
Site*Water Type	<0.0001	3.29%	Month	<0.0001	7.86%
Site*Month	<0.0001	0.93%	Site*Slope	<0.0001	0.92%
Slope*Water Type	<0.0001	1.08%	Site*Water Type	<0.0001	3.20%
Slope*Month	0.002	1.07%	Site*Month	<0.0001	1.12%
Water Type*Month	<0.0001	2.09%	Slope*Water Type	<0.0001	1.17%
Site*Slope*Water Type	<0.0001	0.80%	Slope*Month	0.002	1.12%
			Water Type*Month	<0.0001	2.06%
			Site*Slope*Water Type	<0.0001	0.87%
N 941		**R^2 70.07%**	**N 904**		**R^2 71.09%**

Figure 5.5 shows the three-way interaction between site, slope and water type, though not based on the ANOVA model as three-way interaction plots could not be depicted. On Alport Low, soil pore water PC1 scores increased from 1.13 ± 0.06 on the top-slope to 1.2 ± 0.1

on the upper mid-slope. From the upper mid-slope, Alport Low soil pore water PC1 values became less negative down-slope, whereas PC1 values became more negative down-slope of the upper mid-slope on Featherbed Moss. Though runoff water on Alport Low had uniformly high PC1 means, they were lower on the top-slope (1.6 ± 0.2) and bottom-slope (1.8 ± 0.2). The upper mid-slope (1.6 ± 0.3) had a high PC1 score on Featherbed Moss, characteristic of high pH, conductivity and SO_4^{2-} concentrations, but PC1 scores were lower at the other slope positions, particularly the lower mid-slope (-0.1 ± 0.2) and top-slope (0.4 ± 0.3). Indeed, the PC1 score on the Featherbed Moss lower mid-slope would suggest a composition of runoff water more akin to that of soil pore water, lending credence to the possibility that runoff water was sourced from the ponding of soil pore water.

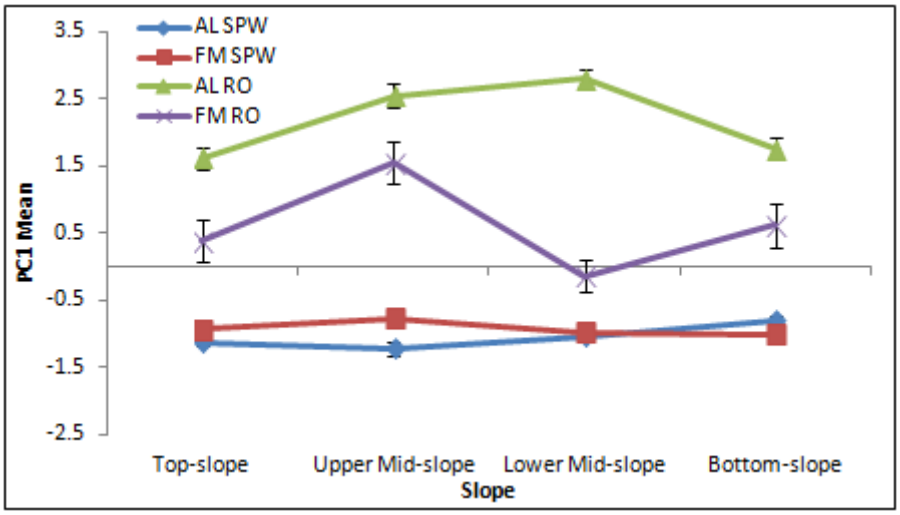

Figure 5.5 2010 – 2011 site-slope-water type interaction mean PC1 score ± standard error: AL = Alport Low; FM = Featherbed Moss; SPW = soil pore water; RO = runoff water

Figure 5.6 shows the ANOVA main effects for slope position as well as interactions between site-slope and slope-water type. The top-slope had a significantly lower PC1 mean

(0.044) than the bottom-slope (0.313) and upper mid-slope (0.586), which had a mean PC1 score significantly higher than all other slope positions. The significantly higher PC1 score on the upper mid-slope could be indicative of a greater separation of runoff water from soil pore water, given the slope-water type interaction means showed soil pore water had a negative mean and runoff water samples a positive mean. Furthermore, upper mid-slope runoff water had a much higher PC1 mean (2.092) compared to the other slope positions. Although PC1 means on Alport Low had entirely positive values for the site-slope interaction, PC1 means were lower on the top and bottom-slope while the top-slope and lower mid-slope had a negative PC1 mean for the ANOVA interaction on Featherbed Moss. This would support the interpretation suggested by Figure 5.5, indicating a greater influence of soil pore water composition over runoff water on Featherbed Moss and as such the occurrence of soil pore water ponding where water tables were above the surface.

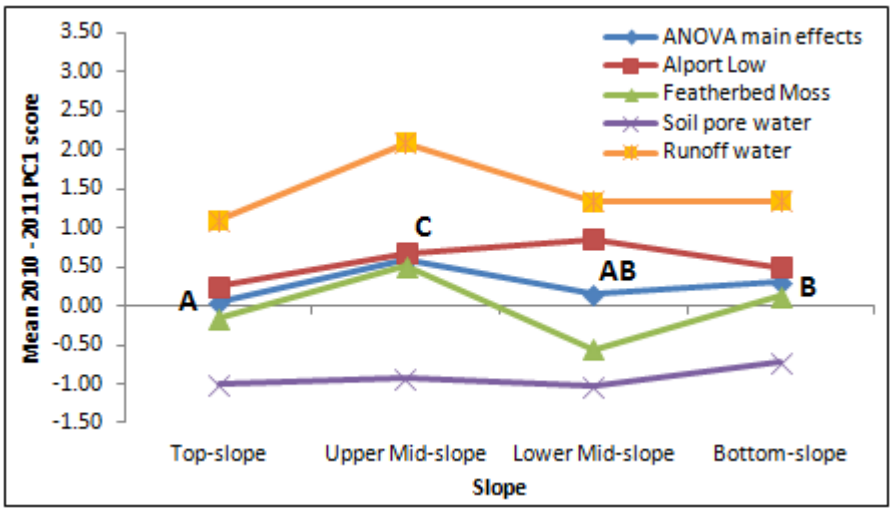

Figure 5.6 2010 – 2011 PC1 ANOVA main effects & interactions plot: significant differences denoted where letters are not shared between slope positions

The ANOVA model main effects predicted a mean PC1 score of 0.567 for Alport Low (Figure 5.7) compared to -0.022 on Featherbed Moss, suggesting that variation in runoff water compositions was more important on Featherbed Moss than on Alport Low. The interaction between site and water type showed PC1 scores of soil pore water and runoff water on Featherbed Moss were closer together than on Alport Low, perhaps supporting the interpretation that mixing of soil pore water and runoff water occurred predominantly on *Eriophorum spp*. plots, of which Featherbed Moss has more. Figure 5.8 displays ponding in more detail, showing runoff water samples on the PC1 and PC2 scatterplot. Slope positions with deeper water tables – Alport Low top-slope hummock plots and Alport Low mid-slope plots – did not have negative PC1 loadings, suggesting runoff water on these plots was compositionally distinct from soil pore water. Negative PC1 loadings were dominated by samples from Featherbed Moss, which was uniformly dominated by *Eriophorum spp*. vegetation, as well as *Eriophorum spp*. plots on Alport Low. Bottom-slope hummock plots on Alport Low also had some samples with negative PC1 scores as higher water tables and, compared to top-slope hummock plots, facilitated ponding.

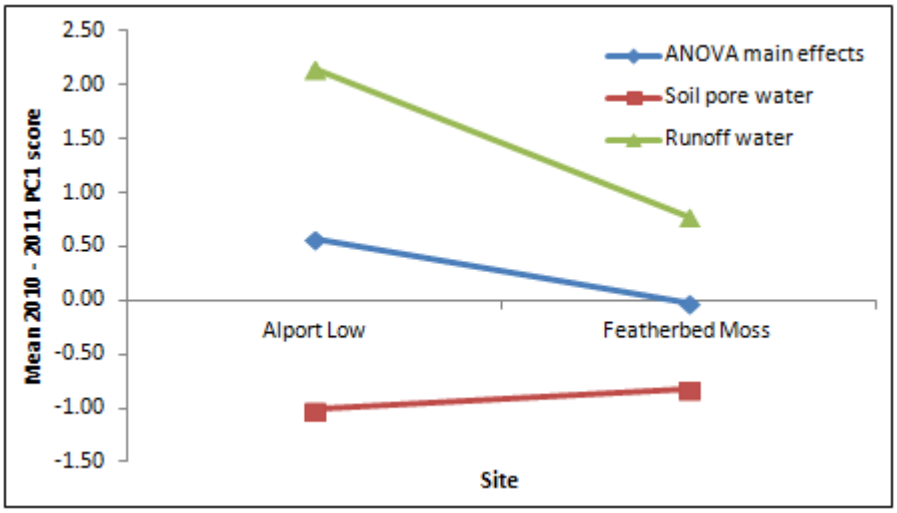

Figure 5.7 2010 – 2011 PC1 ANOVA main effects & interactions plot

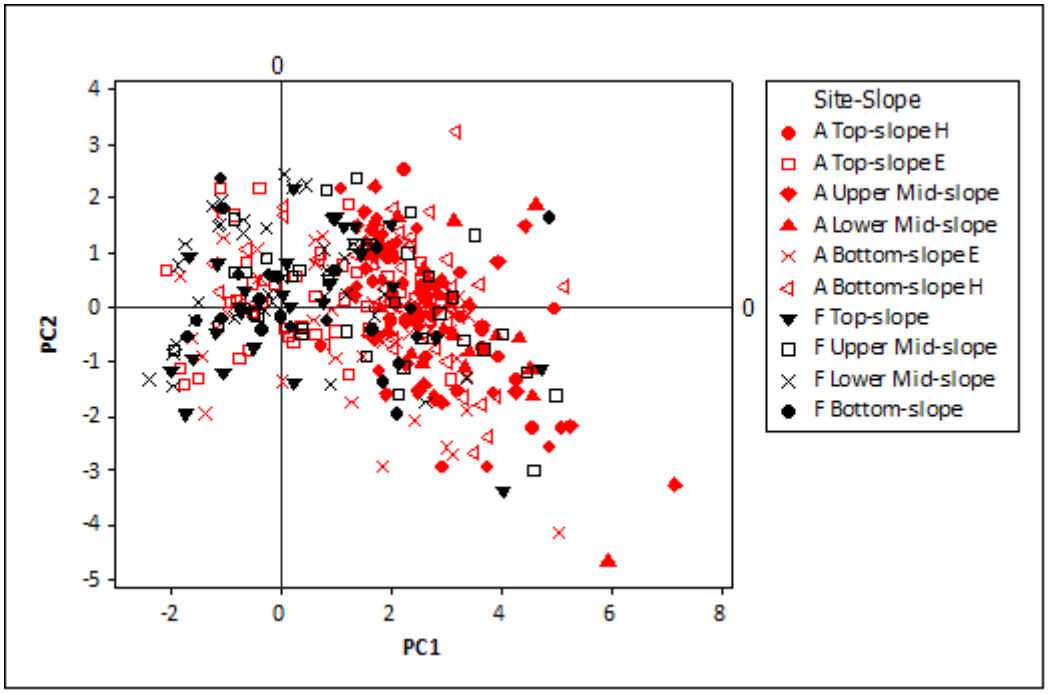

Figure 5.8 Scatter plot of 2010 – 2011 PC1 & PC2 runoff water samples: A = Alport Low; F = Featherbed Moss; E = Eriophorum spp. plots; H = Hummock plots

The ANCOVA model (R^2 = 71.09%, Table 5.6) showed that WTD ($p < 0.0001$, ω^2 = 1.69%) was significant and negatively correlated to PC1 scores, therefore suggesting that water tables towards the surface resulted in more negative PC1 scores, possibly indicative of greater mixing between water sources. Indeed, deeper water tables would cause higher PC1 scores, implying a greater influence of positive values from runoff water that was compositionally distinct from soil pore water – perhaps suggestive of dilution. Wetness index ($p = 0.008$, ω^2 = 0.15%) was significant but had little influence upon the ANCOVA model. Altitude ($p = 0.013$, ω^2 = 0.61%) was negatively correlated to PC1. It must be noted that distribution of the dataset was non-normal and failed Levene's test. Furthermore, slope was not significant ($p = 0.079$, Table 5.7) in the Kruskal-Wallis model.

Table 5.7 Kruskal-Wallis results of 2010 – 2011 PC1 dataset

Slope	N	Median	Ave Rank	Z
Top-slope	309	-0.6186	455.8	-1.2
Upper Mid-slope	168	-0.516	479.9	0.47
Lower Mid-slope	187	-0.763	442.4	-1.61
Bottom-slope	277	-0.413	501.9	2.25
Overall	941		471.0	
H = 6.80		**DF = 3**		**P = 0.079**

5.4.2 2011 – 2012 dataset

5.4.2.1 10 cm water occurrence

Five months of data were gathered April 2012 – August 2012 using 10 cm depth traps in addition to the complete soil pore water and runoff water 2011 – 2012 dataset (September 2011 – August 2012). With two traps per slope position, this meant a total of 10 expected water events were possible. However, this was not the case on the bottom-slope; slope position 11, for instance, only had four possible water observations owing to the removal of bungs by grazing sheep, therefore limiting the quality of the dataset. Only slope positions 1-H (0.80, Table 5.8) and 5 (0.90) had water proportions less than 1.00. This indicated that water collection was less frequent on raised hummocks and on the mid-slope; however the lower frequency of water collection was not significant (χ^2 = 13.92).

Table 5.8 April – August 2012 Chi-squared results for 10 cm water occurrence by slope;

Slope	Expected 10 cm	Observed 10 cm	10 cm Proportion
1-E	10	10	1.000
1-H	10	8	0.800
2	10	10	1.000
3	10	10	1.000
4	10	10	1.000
5	10	9	0.900
6	10	10	1.000
7	5	5	1.000
8	9	9	1.000
9	5	5	1.000
10	6	6	1.000
11	4	4	1.000
χ^2 = 13.92			**P ***

5.4.2.2 2011 – 2012 multivariate analysis

Table 5.9 shows the variation in water chemistry across the four different water types collected. Mean pH was 4.35 ± 0.03 for soil pore water, significantly lower than the pH of runoff water (6.41 ± 0.02). Despite this, soil pore water pH could be high with a maximum of 6.58. 10 cm water had a higher pH than soil pore water (mean = 5.98 ± 0.04), albeit lower than that of runoff. Stream water was the most acidic (mean = 4.19 ± 0.09). Conductivity was greatest in runoff water (mean = 86 ± 2 µs cm^{-1}) and lowest in soil pore water (mean = 47.4 ± 0.9 µs cm^{-1}), with high conductivity in 10 cm water (mean = 76 ± 8 µs cm^{-1}) as well. Mean DOC was highest in 10 cm water (114 ± 5 mg C l^{-1}), though sample collection was only during spring and summer. Soil pore water DOC was high (mean = 109 ± 3 mg C l^{-1}) compared to stream water (mean = 82 ± 7 mg C l^{-1}) and particularly runoff water (mean = 48 ± 2 mg C l^{-1}). Despite sharing high concentrations of DOC, Abs_{400} (mean Abs_{400} = 0.192 ± 0.007) and specific absorbance (mean = 0.00195 ± 0.00008) was much greater in soil pore water than 10 cm water (mean Abs_{400} = 0.098 ± 0.008; mean specific absorbance = 0.00097 ± 0.00009). Higher Abs_{400} and specific absorbance would indicate greater concentrations of humic compounds in DOC-

rich soil pore water, yet E4:E6 was greatest (mean = 8.5 ± 0.2) in soil pore water and lowest in runoff water (mean = 4.4 ± 0.2) suggesting a greater humic component in runoff water despite low absorbance.

Sulphate content was considerably higher in 10 cm water (mean = 14 ± 1 mg l^{-1}) and runoff water (mean = 11.7 ± 0.5 mg l^{-1}) than soil pore water (mean = 4.4 ± 0.1 mg l^{-1}) and stream water (mean = 4.6 ± 0.3 mg l^{-1}). Chloride content did not vary as much between different water types, but was greatest in steam water (mean = 5.9 ± 0.7 mg l^{-1}) and lowest in 10 cm throughflow water (mean = 3.3 ± 0.2 mg l^{-1}). Nitrate concentrations were >1 mg l^{-1} in soil pore water, 10 cm and stream water but were much lower than SO_4^{2-} and Cl^- concentrations. Phosphate was highest in soil pore water (mean = 0.5 ± 0.3 mg l^{-1}) and 10 cm water (mean = 0.4 ± 0.2 mg l^{-1}), with no PO_4^{3-} present in stream water and only very low concentrations in runoff (mean = 0.10 ± 0.06 mg l^{-1}). The highest Br^- (mean = 0.12 ± 0.03 mg l^{-1}) and F^- (mean = 0.16 ± 0.05 mg l^{-1}) concentrations indicated very low concentrations for all water types, which were below the detection limit for a large number of samples. Indeed, for runoff water, detectable concentrations of Br^- and F^- were both found in only 10.00% of samples for both anions. The percentage occurrence of Br^- and F^- was higher in soil pore water, 16.41% and 37.37% respectively.

Table 5.9 Descriptive statistics for 2011 – 2012 water chemistry: SPW = soil pore water; RO = runoff water; 10 cm = 10 cm water; SE = standard error

Variable	Water type	N	Mean	SE Mean	Maximum	Minimum	Variable	Water type	N	Mean	SE Mean	Maximum	Minimum
pH	SPW	399	4.35	0.03	6.58	3.22	SO_4^{2-} ($mg\ l^{-1}$)	SPW	396	4.4	0.1	14.0	0.1
	RO	340	6.41	0.02	7.17	4.74		RO	340	11.7	0.5	82.6	1.0
	10 cm	95	5.98	0.04	7.28	5.18		10 cm	95	14	1	98.5	3.6
	Stream	24	4.19	0.09	5.58	3.75		Stream	24	4.6	0.3	7.0	1.7
Conductivity ($\mu s\ cm^{-1}$)	SPW	397	47.4	0.9	196.8	15.8	Cl^- ($mg\ l^{-1}$)	SPW	396	4.14	0.08	10.4	0.0
	RO	333	86	2	290.0	15.3		RO	340	4.6	0.2	29.4	0.3
	10 cm	93	76	8	685.0	23.9		10 cm	95	3.3	0.2	10.4	1.1
	Stream	24	56	2	85.4	36.5		Stream	24	5.9	0.7	16.9	2.9
Abs_{400}	SPW	398	0.192	0.007	0.893	0.005	NO_3^- ($mg\ l^{-1}$)	SPW	396	1.06	0.08	14.9	0.0
	RO	343	0.023	0.001	0.222	-0.001		RO	340	0.84	0.05	8.3	0.0
	10 cm	95	0.098	0.008	0.477	0.015		10 cm	95	1.0	0.2	11.4	0.0
	Stream	24	0.23	0.02	0.490	0.055		Stream	24	1.1	0.2	3.3	0.0
E4:E6	SPW	388	8.5	0.2	40.00	1.29	PO_4^{3-} ($mg\ l^{-1}$)	SPW	396	0.5	0.3	129.3	0.0
	RO	270	4.4	0.2	21.00	0.50		RO	340	0.10	0.06	20.2	0.0
	10 cm	95	6.5	0.2	12.50	2.00		10 cm	95	0.4	0.2	21.5	0.0
	Stream	24	7.4	0.5	16.00	4.53		Stream	24	0.0	0.0	0.0	0.0
DOC ($mg\ C\ l^{-1}$)	SPW	394	109	3	237.0	5.8	Br^- ($mg\ l^{-1}$)	SPW	396	0.12	0.03	8.0	0.0
	RO	297	48	2	231.7	5.6		RO	340	0.09	0.03	7.7	0.0
	10 cm	95	114	5	226.5	28.4		10 cm	95	0.04	0.03	2.7	0.0
	Stream	24	82	7	159.4	12.0		Stream	24	0.0	0.0	0.0	0.0
Specific Absorbance	SPW	393	0.00195	0.00008	0.0183	0.0002	F^- ($mg\ l^{-1}$)	SPW	396	0.14	0.01	3.1	0.0
	RO	293	0.00067	0.00006	0.0142	0.0000		RO	340	0.04	0.01	4.0	0.0
	10 cm	95	0.00097	0.00009	0.0059	0.0002		10 cm	95	0.09	0.04	3.0	0.0
	Stream	24	0.0032	0.0004	0.0071	0.0010		Stream	24	0.16	0.05	0.8	0.0

Table 5.10 Percentage data removed from 2011 – 2012 water chemistry variables: SPW = soil pore water; RO = runoff water; Abs_{400} = absorbance at 400 nm

Variable	Dataset	N	N removed	% removed
pH	SPW	399	6	1.50
	RO	340	3	0.88
	10 cm	95	1	1.05
	Stream	24	1	4.17
Conductivity	SPW	397	5	1.26
	RO	333	7	2.10
	10 cm	93	2	2.15
	Stream	24	0	0.00
Abs_{400}	SPW	398	7	1.76
	RO	342	8	2.34
	10 cm	95	3	3.16
	Stream	24	0	0.00
E4:E6	SPW	388	7	1.80
	RO	270	3	1.11
	10 cm	95	1	1.05
	Stream	24	1	4.17
DOC	SPW	394	0	0.00
	RO	297	7	2.36
	10 cm	95	0	0.00
	Stream	24	0	0.00
Specific absorbance	SPW	393	2	0.51
	RO	293	0	0.00
	10 cm	95	1	1.05
	Stream	24	0	0.00
SO_4^{2-}	SPW	396	6	1.52
	RO	340	7	2.06
	10 cm	95	2	2.11
	Stream	24	0	0.00
Cl^-	SPW	396	2	0.51
	RO	340	3	0.88
	10 cm	95	1	1.05
	Stream	24	1	4.17
NO_3^-	SPW	396	7	1.77
	RO	340	1	0.29
	10 cm	95	2	2.11
	Stream	24	0	0.00

Table 5.10 shows the percentage data removed as outlying values from each water type dataset used in PCA. The maximum was 4.17% from stream water, though this amounted

to only one actual data point. The absolute maximum number of data points removed was eight, from runoff water Abs_{400}, amounting to 2.34% of the data. Based on the total number of rows with a full set of complete water chemistry variables prior to outlier removal, 91.56%, 90.13%, 86.17% and 87.5% of soil pore water, runoff water, 10 cm water and stream water respectively, was retained. PCA cell occupancy (Table 5.11) was lower than in the 2010 – 2011 dataset, predominantly because each slope position only had three replicate sample plots as opposed to six and DOC and E4:E6 ratio values were below detection limits, particularly in runoff water. Zero cell occupancy occurred 48 times but on only seven occasions did it include samples deleted due to outlier removal. However, zero cell occupancy was never caused by outlier removal alone as some samples were not included for additional reasons. Most samples were missing in December because heavy snow cover prevented sampling.

From a total of 650 data points, the first five principal components were used in PCA, explaining a total of 87.60% variation in the dataset (Table 5.12). The trends of PC1 were nearly identical to those of the 2010 – 2011 dataset (Table 5.5), with high positive loadings for pH, conductivity and SO_4^{2-}, while negative loadings were dominated by Abs_{400}, specific absorbance and E4:E6. Unlike the 2010 – 2011 dataset, DOC also had a strong negative loading; this was unsurprising given DOC compositional variables trended in this direction as well. As with the 2010 – 2011 dataset, DOC had the strongest loading on PC2 and Abs_{400} was correlated with it as well. However, conductivity, Cl^- and SO_4^{2-} also had positive loadings. The loadings plot of PC1 against PC2 is shown in Figure 5.9. PC3 was dominated by negative loadings of NO_3^- and E4:E6 ratio and PC4 had positive loadings of Cl^- and specific absorbance and a negative loading for DOC. Cl^- and specific absorbance dominated PC5, but unlike PC4, trended in opposite directions.

Table 5.11 2011 – 2012 PCA cell occupancy: three sample plots for SPW & RO water & two for 10 cm water per slope position; SPW = soil pore water; RO = runoff water; 10 cm = 10 cm water

Water type	Slope	Month												
		9	10	11	12	1	2	3	4	5	6	7	8	TOTAL
SPW	1-E	3	3	2		2	2	3	3	3	3	2	3	29
	1-H	3	3	3		3	3	3	2	3	3	3	3	32
	2	3	3	3		2	2	3	3	3	3	3	3	31
	3	3	3	2		3	3	3	2	3	3	3	3	31
	4	1	3	3		3	1	3	1	3	2	3	3	26
	5	2	2	2		2	3	2	2	2	3	3	3	26
	6	3	3	2		3	3	2	2	3	3	3	3	30
	7	3	3	2		3	2	3	0	3	3	3	2	27
	8	3	3	3		2	3	3	3	2	3	2	2	29
	9	1	2	2		3	3	2	3	2	3	3	3	27
	10	3	3	2	1	2	2	2	3	3	3	3	3	30
	11	2	3	1	1	2	3	3	2	3	3	3	3	29
	TOTAL	30	34	27	2	30	30	32	26	33	35	34	34	
RO	1-E	1	2	2		2	2	1	1	2	2	2	3	20
	1-H	2	1	0		1	2	0	1	3	0	1	3	14
	2	2	3	0		0	2	3	2	3	2	2	3	22
	3	2	2	1		2	1	2	3	3	1	2	3	22
	4	0	3	3		1	1	3	1	2	3	3	3	23
	5	0	3	3		3	0	1	0	3	3	2	3	21
	6	1	2	0		2	2	0	0	2	0	2	2	13
	7	1	3	3		2	0	2	0	0	0	2	3	16
	8	2	0	3		0	1	2	0	2	1	0	3	14
	9	0	0	0		1	0	0	0	3	0	0	0	4
	10	0	3	3	1	1	1	2	3	2	2	0	3	21
	11	0	0	2	3	0	1	1	1	3	0	0	0	11
	TOTAL	11	22	20	4	15	13	17	12	28	14	16	29	
10 cm	1-E								1	2	1	1	1	6
	1-H								2	0	2	2	1	7
	2								1	2	2	2	2	9
	3								1	2	2	2	2	9
	4								2	2	1	2	2	9
	5								2	2	2	2	1	9
	6								2	2	2	1	2	9
	7								1	2	0	0	0	3
	8								1	2	2	1	1	7
	9								2	1	1	1	0	5
	10								1	0	2	0	1	4
	11								2	0	2	0	0	4
	TOTAL								18	17	19	14	13	

Table 5.12 The first five principal components of 2011 – 2012 dataset

Variable	PC1	PC2	PC3	PC4	PC5
pH	0.476	-0.013	0.128	-0.080	-0.183
Cond	0.381	0.469	-0.176	0.079	-0.242
Abs_{400}	-0.415	0.397	0.037	-0.052	-0.246
E4:E6	-0.313	0.078	-0.435	-0.097	-0.094
DOC	-0.264	0.487	0.023	-0.557	0.250
Specific Absorbance	-0.346	0.056	-0.034	0.512	-0.558
SO_4^{2-}	0.404	0.364	-0.202	-0.125	-0.301
Cl^-	0.059	0.452	0.000	0.622	0.591
NO_3^-	0.045	-0.198	-0.848	0.014	0.160
% Variance	**39.10%**	**54.90%**	**67.10%**	**78.20%**	**87.60%**

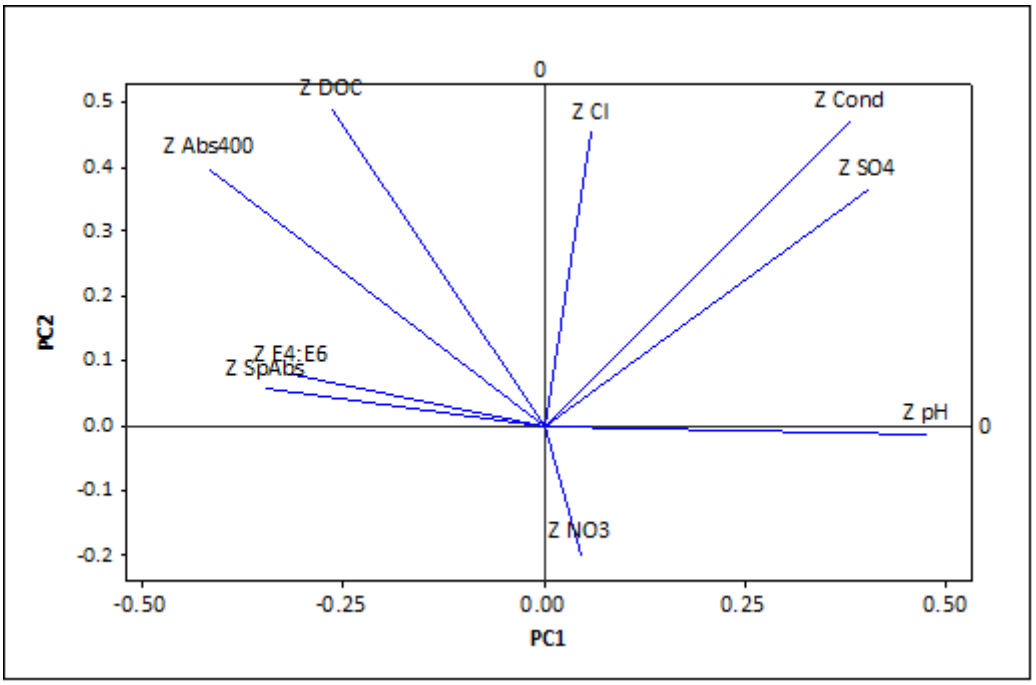

Figure 5.9 Loading plot of 2011 – 2012 PC1 & PC2

Figure 5.10 indicated that as with Figure 5.3, PC1 distinguished between water types but showed minimal overlap between soil pore water and runoff water. Instead, 10 cm water plotted predominantly between soil pore water and runoff water, reflecting the transition between the two water types and suggesting the mixing of soil pore water and runoff water

predominated in the upper layers. Three end-members were evident from Figure 5.10. EM-A was a compositional end-member from which soil pore water and runoff water evolved. EM-A was represented by two soil pore water samples, from slope position 2 in June 2012 and slope position 3 in February 2012. The characteristic features of EM-A were low: conductivity, SO_4^{2-} and Cl^- concentrations, DOC concentrations, E4:E6 ratios, Abs_{400} and specific absorbance. pH values distinguished between runoff and soil pore water as the two water types evolved distinct compositions from EM-A. Runoff water samples that plotted adjacent to EM-A were from April and June 2012.

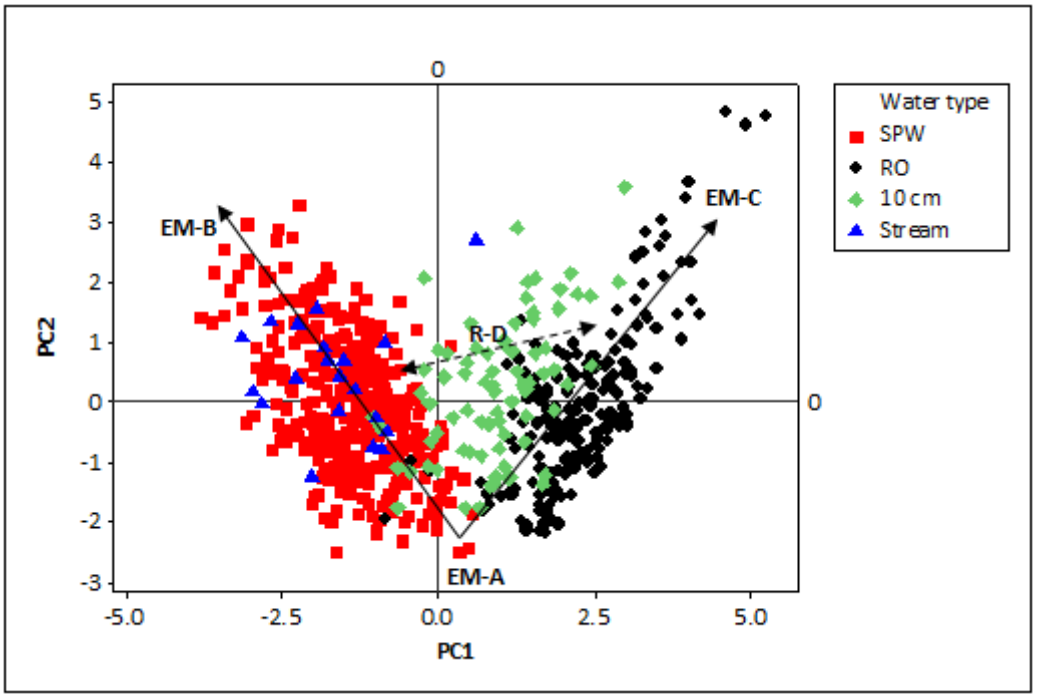

Figure 5.10 Scatterplot of 2011 – 2012 PC1 & PC2; SPW = soil pore water; RO = runoff water; 10 cm = 10 cm water; prefix EM = end-member; prefix R =region; A – D = labels

Soil pore water composition evolved from EM-A towards EM-B, which was characterised by very high DOC concentrations and specific absorbance but was particularly

distinguished by very high Abs_{400}. EM-B was typically a deep soil pore water end-member similar to EM-A in Figure 5.3 from the 2010 – 2011 dataset. Slope positions 9, 4 and 5, which had deep water tables, dominated EM-B. Top-slope positions 1-H and 3 also had some samples located in EM-B. Though Chapter 4 revealed that stream water DOC concentrations were between those of soil pore water and runoff water, multivariate analysis suggested its water chemistry plotted along the soil pore water trend, indicative of low conductivity, pH and SO_4^{2-} but high Abs_{400} and specific absorbance.

Runoff water evolved from EM-A towards EM-C, where samples had high conductivity, SO_4^{2-} and pH but very low specific absorbance and Abs_{400}. The composition of 10 cm water helped to demonstrate the change in water chemistry between soil pore water and runoff water, as shown along the area R-D. Where 10 cm water plotted with runoff water, pH was high, as was either SO_4^{2-} or Cl^-. Specific absorbance and Abs_{400} were low where 10 cm water and runoff water overlapped, but 10 cm water DOC concentration was high; as 10 cm water samples evolved along PC1 towards a soil pore water composition, specific absorbance and Abs_{400} increased (relative for 10 cm water). pH also decreased but was not as low as soil pore water or stream water.

Figure 5.11 of PC1 against PC5 again reflected the separation of water types but four different end-members suggested seasonal changes in water composition. Soil pore water EM-A had very high Abs_{400} and specific absorbance from samples in July and August while EM-B was from late autumn and winter, with low Abs_{400} and specific absorbance. However, Cl^- and DOC concentrations at EM-B were high. As such, EM-B may be indicative of the autumn flush. Runoff water EM-C was typically composed of spring and summer samples with high pH, conductivity and SO_4^{2-}; while EM-D was from autumn and winter samples up to March, with high Cl^- and pH but low DOC. It is possible a fifth end-member, representing dilute samples, exists where the arrows converge, though this was not sampled. The transition of 10 cm water

from adjacent to soil pore water towards runoff, denoted by R-E, was characterised by a change from high specific absorbance to low specific absorbance in the runoff zone; Cl^- concentrations were low for both.

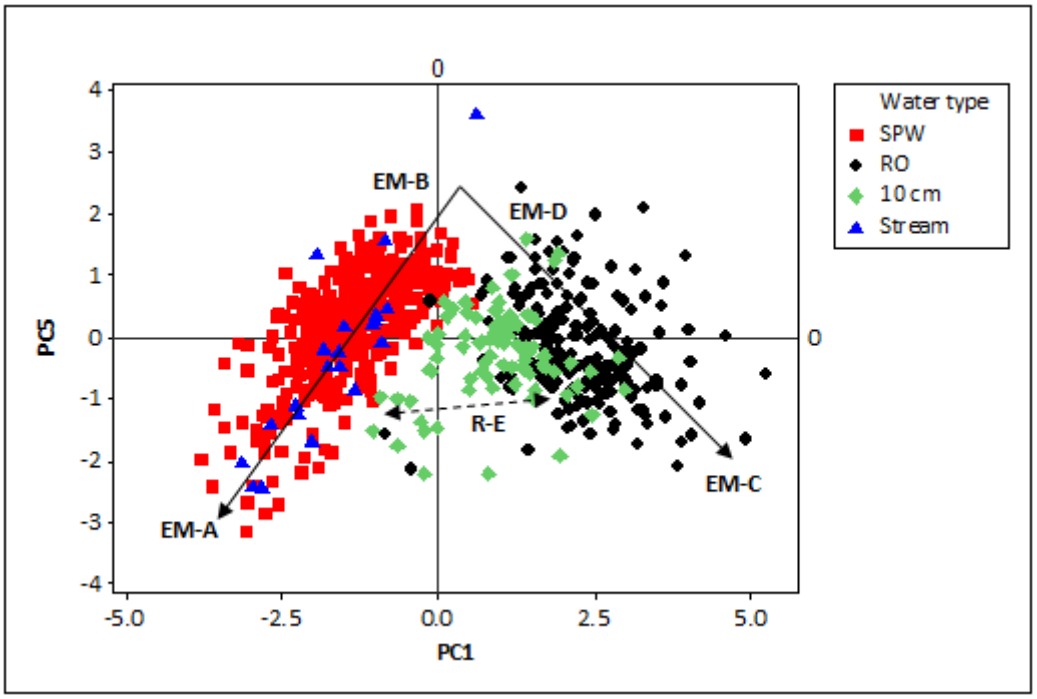

Figure 5.11 Scatterplot of 2011 – 2012 PC1 & PC5; SPW = soil pore water; RO = runoff water; 10 cm = 10 cm water; prefix EM = end-member; prefix R =region; A – E = labels

It was not possible to perform ANOVA using slope and water type together; runoff or 10 cm water trap bung removal by grazing sheep meant cell occupancy was too low to in some months for combined analysis. ANOVA was consequently performed separately for each water type by slope, while differences between water types were assessed without regarding slope position. Water type ($p < 0.0001$, $\omega^2 = 80.14\%$) was the most important factor in individual ANOVA models. Month ($p < 0.0001$, $\omega^2 = 2.83\%$) was also significant in the water type ANOVA model ($R^2 = 83.00\%$). The ANOVA main effects model (Figure 5.12) showed that negative PC1

loadings (soil pore water and stream water) were significantly different from positive loadings (runoff water and 10 cm water). The 10 cm water loading was significantly lower than that of runoff water as well. Loadings were positive in January – May and most negative in July.

Table 5.13 2011 – 2012 PC1 ANOVA; ω^2 = percentage variance; % Erio spp. = percentage Eriophorum spp.

Water type ANOVA			**Slope soil pore water ANOVA**			**Slope soil pore water ANCOVA**		
Factor	**P**	**ω^2**	**Factor**	**P**	**ω^2**	**Factor**	**P**	**ω^2**
Water type	<0.0001	80.14%	Slope	<0.0001	14.09%	*% Erio spp.*	0.013	0.83%
Month	<0.0001	2.83%	Month	<0.0001	29.31%	WTD	0.008	10.97%
						Slope	<0.0001	7.83%
						Month	<0.0001	25.60%
N 632		**R^2 83.00%**	**N 345**		**R^2 43.47%**	**N 342**		**R^2 45.30%**
Slope runoff ANOVA			**Slope runoff ANCOVA**			**Slope 10 cm throughflow ANOVA**		
Factor	**P**	**ω^2**	**Factor**	**P**	**ω^2**	**Factor**	**P**	**ω^2**
Month	<0.0001	13.93%	*% Erio spp.*	0.009	2.07	Slope	0.003	24.28%
			Month	<0.0001	14.52%	Month	0.001	13.99%
N 197		**R^2 14.00%**	**N 197**		**R^2 16.66%**	**N 80**		**R^2 38.56%**

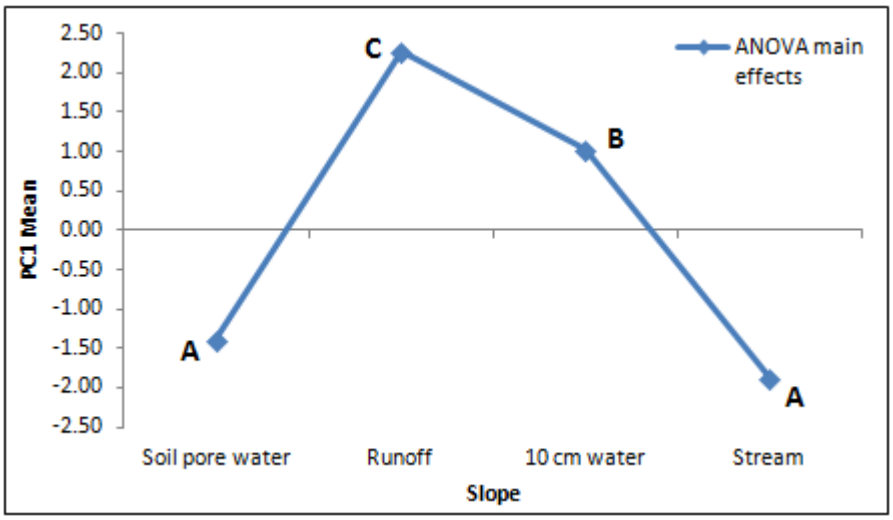

Figure 5.12 2011 – 2012 water type PC1 ANOVA main effects; significant differences denoted where letters are not shared between water types

Slope was significant in the soil pore water ANOVA ($p < 0.0001$, $\omega^2 = 14.09\%$, Table 5.13), with loadings at slope positions 1-H, 4, 5 and 9 significantly more negative than those of slope positions 2, 6, 7, 8 and 11 (Table 5.14, Figure 5.13). The ANCOVA model removed most of the significant differences; only 1-H remained significantly more negative for PC1. WTD ($p = 0.008$ $\omega^2 = 10.97\%$) was positively correlated to PC1 score while percentage *Eriophorum spp*. ($p = 0.013$, $\omega^2 = 0.83\%$) was negatively correlated.

Table 5.14 Significant differences 2011 – 2012 PC1 ANOVA / ANCOVA models

Slope	SPW ANOVA	SPW ANCOVA	10 cm ANOVA
1-E			
1-H	<2, 6-8, 10-11	<2, 6-8, 10-11	
2	>1-H, 3-5, 9	>1-H	<7
3	<2		<7
4	<2, 6-8, 11		<7
5	<2, 6-8, 11		<7
6	>1-H, 4-5, 9	>1-H	
7	>1-H, 4-5, 9	>1-H	>2-5
8	>1-H, 4-5, 9	>1-H	
9	<2, 6-8, 11		
10	>1-H	>1-H	
11	>1-H, 4-5, 9	>1-H	

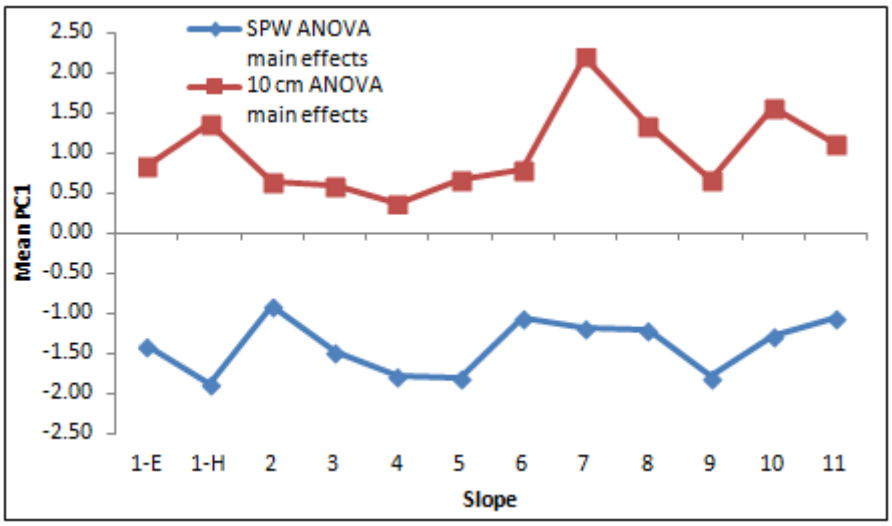

Figure 5.13 2011 – 2012 PC1 ANOVA main effects plot by slope; SPW = soil pore water; 10 cm = 10 cm water

Slope position 7 (Table 5.14, Figure 5.13) had a significantly higher PC1 mean than slope positions 2 – 5 in the ANOVA model for 10 cm water, suggesting a water composition more akin to runoff water. Slope position ($p = 0.003$, $\omega^2 = 24.28\%$) explained the most variance in PC1 score, ahead of month (p 0.001, $\omega^2 = 13.99\%$), for which April had a higher PC1 mean than June – August. Slope was not significant in the runoff water ANOVA model, with only month ($p < 0.0001$, $\omega^2 = 13.93\%$) significant. Mean PC1 loadings were greater in May than February, June, July and October. Percentage *Eriophorum spp*. ($p = 0.009$, $\omega^2 = 2.07\%$) was a significant covariate, indicating that as the dominance of *Eriophorum spp*. increased, PC1 loadings decreased – perhaps suggesting an increased mixing with soil pore water.

The error terms in ANOVA and ANCOVA models were large, particularly in the runoff water ANOVA model that explained only 14.00% of variance in PC1 score. The error term included measurement error, but also represented unexplained variance from factors and interactions that could not be included in the experimental design. For instance, it was not possible to test interaction effects in either the water type ANOVA or for individual ANOVA

models of soil pore water, runoff and 10 cm water. Furthermore, covariates such as slope angle, altitude and wetness index could not be included as they were co-linear with slope position.

5.4.3 Tracer experiment

5.4.3.1 Bromide concentrations

Bromide concentrations across the four sample days are shown in Figure 5.14. Day 0 concentrations of Br^- were typically 0.0 mg l^{-1}, though 0.9 mg l^{-1} was observed in one soil pore water sample from slope position 8 and 0.5, 3.4 and 1.9 mg l^{-1} detected in runoff water from slope positions 1-H, 5 and 8 respectively. In 10 cm water, 0.6 mg l^{-1} was found in a sample from slope position 2 and 1.0 mg l^{-1} from slope position 8; from the bank-stream, 0.7 mg l^{-1} was found. Thus Br^- was detected in seven samples from a possible 95, with one of these from soil pore water. The Br^- detected in the seven samples was above concentrations typically found in background levels, of 0.2-0.3 mg l^{-1}.

Mean Br^- concentration in soil pore water for all slope positions on day 3 was >1 mg l^{-1}. The tracer was applied between slope positions 3 and 4 and was therefore detected upslope of the application point. No Br^- was detected in any of the three process blanks run during the study or in any unknown blanks run between standards and samples from different slope positions. As such it seems unlikely there was an issue with contamination of the tracer through analytical processes. The source of Br^- upslope must be explained by other processes or sources of contamination. It is possible Br^- was transported on the author's boots upslope after application of the tracer but detection of the tracer at 1-H, a hummock plot, would imply an alternative explanation such as aeolian transport and deposition despite the tracer being

damped down at the time of application. In dry conditions, diffusion upslope may have occurred.

Mean Br^- concentration at slope position 4 on day 3 was 2.0 ± 0.6 mg l^{-1}. Concentrations of Br^- decreased at slope positions 5 and 6 but increased to 2.7 ± 0.8 mg l^{-1} at slope position 7, the last mid-slope plot. Bromide concentrations were greatest at bottom-slope plots, increasing to a mean of 4 ± 2 mg l^{-1} at slope position 8, with the increased standard error reflecting the larger variation in Br^- concentrations found between dipwells. The largest concentrations were observed at the last two slope positions; slope position 10 had a mean of 10 ± 4 mg l^{-1}, while concentrations showed a vast increase at slope position 11 (60 ± 20 mg l^{-1}). The maximum concentration observed at slope position 11 was 93.0 mg l^{-1}, indicating large delivery of the tracer down-slope to an accumulation area at the riparian zone. The accumulation of Br^- at the bottom-slope was in contrast to the observed decrease in DOC concentrations down-slope as seen in Chapters 2 and 4. No tracer was detected in runoff samples and only in slope positions 8 – 11 for 10 cm water. Mean concentrations were <1 mg l^{-1} at slope positions 8 and 9 in 10 cm water, but 20 ± 10 mg l^{-1} and 20 ± 20 mg l^{-1} at slope positions 10 and 11 respectively.

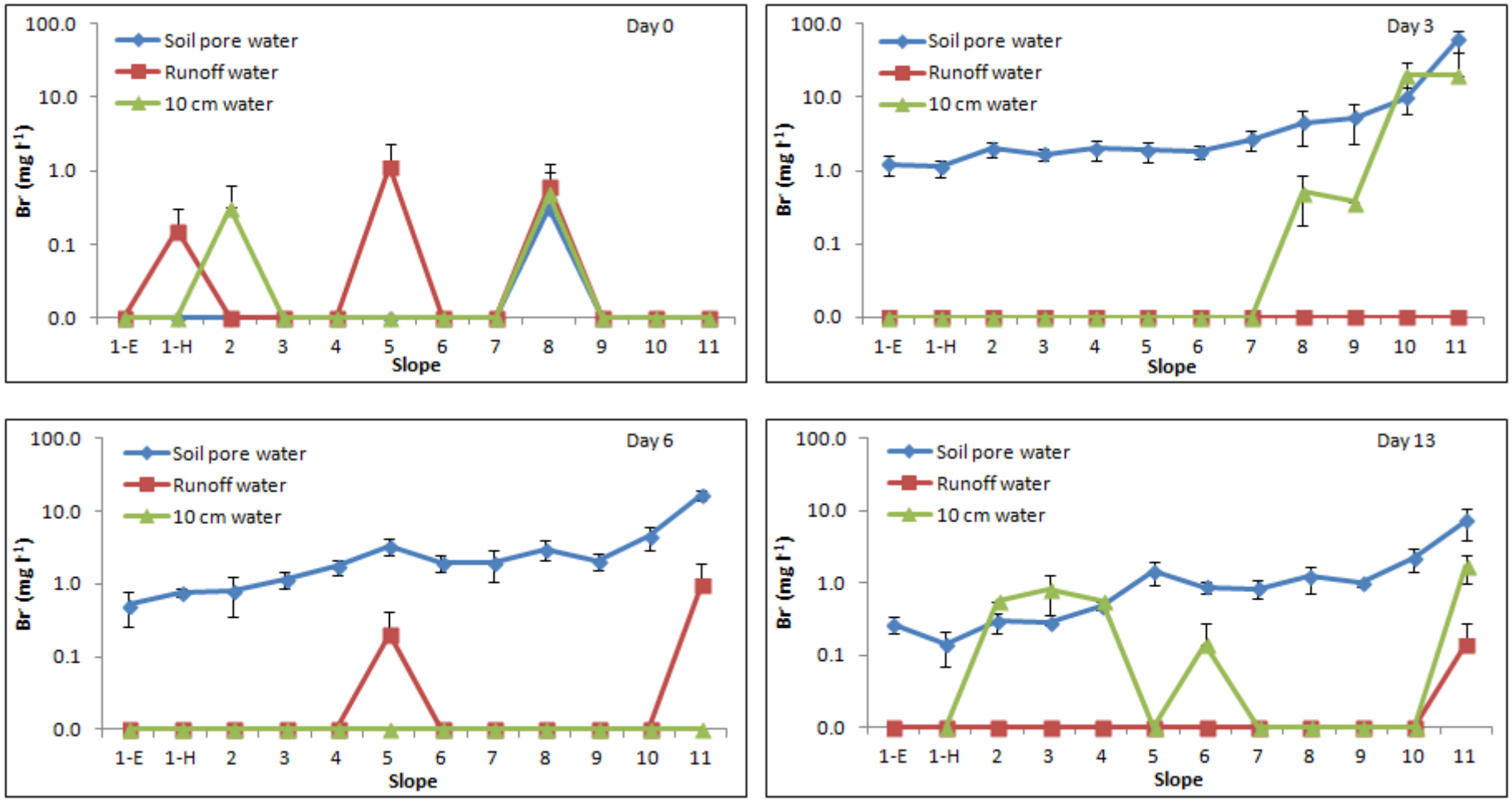

Figure 5.14 Mean Br^- concentrations ± standard error; tracer applied between slope positions 3 & 4

Mean Br^- concentration in soil pore water on day 6 was relatively similar on the mid-slope, though had decreased to 1.7 ± 0.4 mg l^{-1} at slope position 4 and increased to 3.3 ± 0.8 mg l^{-1} at slope position 5. Bromide concentration was marginally higher at slope position 6 as well. Concentrations of the tracer decreased more markedly on the bottom-slope, with a mean of 4 ± 2 mg l^{-1} at slope position 10 and 17 ± 3 mg l^{-1} at slope position 11. Despite the large decrease, concentration of Br^- at slope position 11 was much higher than all other slope positions. No tracer was detected in 10 cm water but was found in one runoff sample at slope position 5 (0.6 mg l^{-1}) and one sample at slope position 11 (2.9 mg l^{-1}). Down-slope of the application point, mean Br^- concentration in soil pore water was <1 mg l^{-1} at slope positions 4, 6, 7 and 9 on day 13. The highest concentrations were at slope position 10 (2.2 ± 0.8 mg l^{-1}) and 11 (7 ± 3 mg l^{-1}). Consequently, concentrations of the tracer gradually declined throughout the system but despite being diluted, remained high at slope positions 10 and 11 two weeks after the tracer was introduced to the system. Interestingly, mean Br^- concentration was >0.5 mg l^{-1}, in 10 cm water at slope positions 2, 3, 4 and 11 – which had a mean of 1.7 ± 0.7 mg l^{-1}. 0.3 mg l^{-1} Br^- was detected in one 10 cm water sample at slope position 6. Tracer was detected in only one runoff water sample, 0.3 mg l^{-1} at slope position 11.

In stream water samples, no tracer was found in the stream sample, but it was detected in the bank-stream samples: 0.6 mg l^{-1} (day 0); 0.9 mg l^{-1} (day 3); 0.3 mg l^{-1} (day 6); and 0.5 mg l^{-1} (day 13). The detection of Br^- on days 3, 6 and 13 could be indicative of transfer of the tracer towards the stream, despite a possible source of error implied by detection of the tracer on day 0. The presence of Br^- in the bank-stream indicated the direct link between the hillslope and the riparian zone and stream and finding no tracer in the zero-order stream could be explained by dilution.

5.4.3.2 Runoff and 10 cm water occurrence

Across the four sample days during the tracer experiment, slope position 9 on the bottom-slope (Table 5.15) had significantly lower runoff occurrence than all other slope positions, with only 50% occurrence. Despite slope position 1-E missing two 10 cm water samples, this was not significantly different to the other slope positions.

Table 5.15 Chi-squared results for runoff (RO) water and 10 cm water (10 cm) occurrence by slope

Slope	Expected RO	Observed RO	RO Proportion	Expected 10 cm	Observed 10 cm	10 cm Proportion
1-E	12	12	1.000	8	6	0.750
1-H	12	12	1.000	8	8	1.000
2	12	12	1.000	8	8	1.000
3	12	12	1.000	8	8	1.000
4	12	12	1.000	8	8	1.000
5	12	12	1.000	8	7	0.875
6	12	11	0.917	8	8	1.000
7	12	11	0.917	8	8	1.000
8	10	10	1.000	8	8	1.000
9	8	4	0.500	8	8	1.000
10	12	12	1.000	8	8	1.000
11	10	9	0.900	8	7	0.875
	χ^2 = 39.05		**P = <0.0001**	**χ^2 = 14.61**		**P***

5.5 Discussion

5.5.1 Limitations

This study assessed changes in water composition across the hillslope and with different sources of water. Multivariate analysis of water chemistry was extremely useful and provided valuable insights, yet would have been aided further were it possible to include

cation concentrations. Laboratory issues meant it was not possible to conduct ICP-OES to determine concentrations of cations as was intended. Such data can be useful, with high concentrations of Na^+ correlated to Cl^- as indicative of marine derived precipitation (Adamson et al., 2001, Proctor, 2008). High Ca^{2+}, K^+, Mg^{2+}, Na^+ for instance, could indicate interaction with base-rich groundwater or deep peat sources (Worrall and Adamson, 2008). High Al^{3+} and Fe^{2+} has been attributed to shallow near-surface waters (Clay et al., 2010a) but has also been shown to correlate with DOC (Worrall et al., 2006a, Knorr, 2013) and therefore can be used to distinguish flowpaths and identify mobilisation of DOC.

Although 10 cm water was included in the analysis, it was only gathered between April – August 2012; an annual dataset would have been useful in identifying seasonal variation. Nonetheless, 10 cm water was valuable in separating soil pore water and runoff water. Furthermore, specific absorbance and Abs_{400} were different in 10 cm water to soil pore water, implying compositional differences in DOC.

It was beyond the scope of this study to analyse high-resolution changes in water chemistry during the tracer experiment. Hourly monitoring would have provided information regarding the velocity of water movement down-slope, as has been achieved with other tracer experiments (Hedin et al., 1998, Anderson and Burt, 1978, Anderson et al., 2009). It would have been useful to see how water movement changed across various rainfall events, particularly with a change in response of the sampled stream which most likely resembled soil pore water as it was gathered during periods of low flow. However, the purpose of the tracer experiment was to observe water movement along the hillslope and identify whether the presence of the tracer was detected across all slope positions and across multiple water types. To this end, the experiment was successful.

5.5.2 Water chemistry and flowpaths

Use of a large, multivariate dataset analysed with PCA allowed changes in soil pore water composition and runoff water origin along the hillslope to be identified. It was possible to separate different water sources by virtue of changes in pH, conductivity, SO_4^{2-} concentration, DOC concentration and DOC composition. It was evident that runoff water and soil pore water had quite distinct water chemistries, with pH >6 and higher levels of conductivity in runoff water. The high conductivity appeared to be caused by high levels of SO_4^{2-}, though cation concentrations were not accounted for. Worrall et al. (2002) suggested conductivity was higher under low flow conditions due to the increased importance of old water, which reduced with the input of new water during rain events. Wilson et al. (2011) also suggested conductivity decreased post drain blocking as precipitation received less contact with water from deep peat layers. However, this study would appear to contradict Worrall et al. (2002) and Wilson et al. (2011) as higher conductivity was associated with runoff water and therefore SO_4^{2-} from new water. This study also took place in the South Pennines rather than the North Pennines and Wales and geographical differences could be expected to explain some of the differences between the studies.

Some studies have noted the dominance of Cl^- (Adamson et al., 2001, Proctor, 2008) for anion concentrations due to high inputs from marine derived precipitation, also represented by high levels of Na^+ in cation data. However, across both study years there was comparatively little difference in Cl^- concentration between water types. It is possible that SO_4^{2-} was more important in the South Pennines owing to higher levels of atmospheric deposition, whether sourced in precipitation or otherwise from historic pollution (Daniels et al., 2008b). It is likely however that the source of SO_4^{2-} was from near surface peat layers given the low concentrations found in precipitation (mean = 0.52 ± 0.04 mg l^{-1}, Table 5.2) as well as high levels of SO_4^{2-} found in peat deposits in the South Pennines, including on Featherbed

Moss (Coulson et al., 2005). Given the particularly high concentrations of SO_4^{2-} in 10 cm and runoff water, it is probable that SO_4^{2-} was sourced from the upper layers of peat where sulphur was oxidised and mobilised into 10 cm water and surface runoff. Indeed, Adamson et al. (2001) observed higher concentrations of SO_4^{2-} at 10 cm depth than 50 cm in soil pore water, which derived SO_4^{2-} through down profile diffusion. Sulphate concentrations at 10 cm depth correlated to WTD with a three week lag, suggesting that drying allowed SO_4^{2-} to be mobilised under aerobic conditions (Adamson et al., 2001).

Though pH and SO_4^{2-} had the same loadings on PCA, the relationship between pH and SO_4^{2-} was unclear. In soil pore water, SO_4^{2-} could be expected to lower pH (Clark et al., 2012) while it has been observed that as SO_4^{2-} decreases in reducing conditions, there is a concomitant increase in pH (Knorr, 2013). Runoff water contained higher SO_4^{2-} concentrations but also had higher pH than soil pore water. It may be that higher pH levels in runoff water were caused by the higher pH of precipitation compared to soil pore water and was not related to SO_4^{2-} content. As precipitation mixed with soil pore water, it may have mobilised SO_4^{2-} whilst also increasing the pH of runoff water.

The pH of precipitation (mean = 5.6 ± 0.1) was higher than soil pore water and the same as the lower mid-slope runoff water from the 2010 – 2011 dataset. This would suggest rainfall increased the pH of runoff water compared to soil pore water, though rainfall pH was lower than 10 cm water and runoff water (>pH6) from 2011 – 2012. Could an additional factor have increased pH levels in runoff water further beyond that caused by precipitation? High pH and high conductivity has been linked to buffering of acids by carbonate rich groundwater in streams (Worrall et al., 2007a, Worrall et al., 2008) and Vogt and Muniz (1997) noted a shift in water chemistry between baseflow with high pH due to bicarbonate buffering of pH through mineral soils and highflow with lower pH values from organic histosols. Soulsby et al. (2003) also observed a shift from baseflow dominated by cations and silica from weathering in

groundwater to high flow dominated by acidic, carbon rich waters from peatland plateau areas. Such an explanation of the high pH levels in runoff water seems unlikely in ombrotrophic bogs where there is no interaction between soil pore water and groundwater. Clay et al. (2010a) reported higher levels of Ca^{2+} in runoff water than soil pore water from a peatland in the north Pennines and it is possible Ca^{2+} further increased pH levels here. Moors for the Future undertook restoration projects across Bleaklow plateau during the study period and it is possible part of the study site was limed, further increasing the pH of runoff water.

Despite the different water chemistries of runoff water and soil pore water, a mixing zone was evident where runoff water chemistry reflected that of soil pore water. This suggested that mixing and evolution of water types could change across the slope. Indeed, samples where soil pore water and runoff water overlapped were dominated by high water tables that were sometimes saturated at the surface. As such, runoff samples mixed with soil pore water predominantly from *Eriophorum spp*. plots or otherwise hummock plots on the bottom-slope of Alport Low. Thus, the composition of runoff water was controlled by slope position, slope angle (with respect to increased ponding on Featherbed Moss) and vegetation. Daniels et al. (Daniels et al., 2008a) also attributed ponding to micro-topographical variation. Ponding took place at locations where the water table was close to the surface and frequent saturation was possible, causing runoff traps to be filled with soil pore water that underwent minimal dilution from precipitation and thus retained the chemical composition of soil pore water. Multivariate PCA has therefore confirmed the observation of ponding of soil pore water suggested in Chapter 2 by recognising a shared chemical signature in two different water types.

Soil pore water had characteristically higher DOC concentrations, Abs_{400} and specific absorbance than runoff water that was not in the mixed zone where runoff water overlapped with soil pore water. This was in agreement with Clay et al. (2009b) who also reported lower

DOC, Abs_{400} and specific absorbance in runoff water. Wilson et al. (2011) found Abs_{400} and specific absorbance in blocked drainage ditches decreased with an increase in precipitation, in part due to higher water tables and higher rates of saturation-excess overland flow. The decrease in absorbance in runoff was due to the same process of dilution by rainfall, as were lower DOC concentrations. Water colour has been used as an indicator of humic DOC and microbial mobilisation of older carbon stores (Yallop et al., 2010). Thus soil pore water appeared to be more humic in character than runoff water. However, E4:E6 ratio was lower in runoff water than soil pore water which would imply a higher component of humic acids in runoff water. Fulvic acids have a higher E4:E6 ratio due to their lower molecular weight, with a higher proportion of aliphatic compounds and fewer aromatic compounds (Gondar et al., 2005). Despite this, high water colour and specific absorbance is associated with humic substances (Wallage et al., 2006). As such there was an apparent disposition between the DOC Abs_{400} and compositional measures. It may be that absorbance in runoff water at 465 and 665 nm that comprised E4:E6 was so low it meant the ratio was subject to larger errors than soil pore water, as exemplified by the exclusion of runoff water samples below the limit of detection at these wavelengths.

The soil pore water trend had an end-member associated with very high DOC and Abs_{400}, which was characteristic of plots with deep water tables on the Alport Low mid-slope and top-slope hummock plots. The deep soil pore water end-member was also evident in the slope transect dataset, with slope positions 1-H (top-slope hummock), 4 & 5 (mid-slope) and 9 (bottom-slope depression) all having deep water tables with means of ≥250 mm depth (Table 4.3) and high DOC and / or Abs_{400}. The slope transect confirmed the water chemistry associations inferred from the 2010 – 2011 dataset, distinguishing water types based upon pH, conductivity, SO_4^{2-}, DOC, Abs_{400} and specific absorbance. However, there were far fewer runoff water samples that plotted on the soil pore water trend, rather 10 cm water composition represented an intermediary between runoff and soil pore water.

Adamson et al. (2001) noted changes in water chemistry between 10 cm and 50 cm depth at Moor House in the north Pennines. Using PCA on the Moor House dataset, Worrall et al. (2003a) observed evolution of soil pore water from 10 cm depth which plotted close to rainfall and 50 cm which had higher K^+ concentrations alongside greater water colour. The evolution of water between 10 and 50 cm depth was attributed to a change in residence time (Worrall et al., 2003a). As such it seems likely that runoff water is composed predominantly of a mixture of rainfall and near surface soil water, with mixing occurring between 10 cm water and precipitation. However, despite similarities in pH, conductivity and SO_4^{2-} content between 10 cm water and surface runoff, 10 cm water had much higher DOC concentrations – higher even than soil pore water. Robroek et al. (2010) noted an increase in DOC with depth between surface runoff and 10 cm water, but also a further increase to 50 cm depth, though the concentrations reported and variation in DOC with depth was much smaller than found here. Adamson et al. (2001) observed a decrease in DOC between 10 and 50 cm depth, with sensitivity to seasonal variation near the surface not observed at depth. Clark et al. (2008) noted high concentrations of DOC in upper surface layers up to 10 cm depth, with a decrease from 20 – 50 cm. In this study, there was relatively little difference between DOC concentrations in soil pore water and 10 cm water compared to the concentrations in runoff water and stream water. However, there was a difference in the characteristics of DOC.

Soil pore water had high Abs_{400} and specific absorbance, which showed a seasonal pattern by declining in late autumn and winter but peaking in July and August. Worrall et al. (2006b) noted seasonal change in specific absorbance of shallow soil pore water related to water table variation. Where 10 cm water plotted adjacent to soil pore water, it had a higher specific absorbance than when it plotted with surface runoff, indicating a greater influence of water colour and humic compounds in soil pore water. Wallage and Holden (2010) also noted a change in the relationship between DOC and colour with depth. The overall differences in Abs_{400} and specific absorbance between soil pore water and 10 cm water suggested that closer

to the surface, DOC was composed of labile material with low absorbance whereas at depth in soil pore water it was comprised of more coloured, humic substances – despite the trend suggested by E4:E6 ratio. As such the lower DOC concentrations found in surface runoff were likely due to dilution from precipitation but elevated concentrations in soil pore water may reflect increased residence time and old water rich in colour from humic substances.

Stream water plotted on the soil pore water trend, suggesting low signal strength of surface runoff when delivered to the stream, which had a composition more characteristic of soil pore water. In peatlands, DOC concentration could be expected to decrease with increased discharge due to dilution by precipitation and mixing with surface runoff water (Clark et al., 2008, Stutter et al., 2012). The lower DOC concentrations observed in the stream may be consistent with this, yet stream water retained the high Abs_{400} and low pH of soil pore water. Indeed, given that mean Abs_{400} was higher than soil pore water but DOC lower, stream water had a higher specific absorbance. This was because sampling took place under low flow conditions (the author's observation). Abs_{400} may have been diluted with increased inputs from surface runoff water and near surface throughflow and therefore a higher resolution sampling strategy when assessing stream water chemistry would have provided important insights into the change in water chemistry at high flow during rainfall events, as shown by Gazovic et al. (2013).

5.5.3 Tracer study

Results from the tracer experiment helped to illuminate some of the findings of the water chemistry data. By day 3 post-tracer application, a mass flux of Br^- to the bottom-slope was observed. Hoag and Price (1995) found tracer movement was fast at 2.3 m day^{-1}, equating to 70 m over 30 days, on a gently sloping (3.2°) blanket bog in Newfoundland. At a drained fen

in Somerset, Baird and Gaffney (2000) noted that tracer concentration decreased with distance from the injection well. Thus results here show the effect on tracer movement on a steeply sloping blanket bog hillslope; much quicker transport over longer distances than found by Hoag and Price (1995) but also the accumulation of tracer at the furthest distance from the application point.

Although the tracer was detected in the deeper soil pore water of the mid-slope, it accumulated at the bottom-slope, with much higher concentrations towards the riparian zone, while the tracer was only detected in 10 cm water at bottom-slope plots. This supported the findings of Holden and Burt (2003) who suggested mid-slopes produced more subsurface runoff that accumulated at the bottom-slope as return flow. As such, it seems probable that the increased presence of the tracer in 10 cm water at the bottom-slope reflected the return of deeper subsurface flow on the mid-slope returning towards the surface on the gently sloping bottom-slope which maintained higher water tables.

The lack of detection of the tracer in mid-slope surface runoff and 10 cm water traps could reflect the bypassing of the tracer from these flowpaths, or dilution as near surface water and runoff water was mixed with precipitation. Indeed, both arguments would lend support to the multivariate analysis that indicated, aside from where ponding took place, soil pore water and runoff water had distinct chemical compositions, suggesting a lack of mixing between deeper soil pore waters and runoff water. The bypassing of the tracer from layers by day 3, when concentrations of the tracer would have been greatest, reflected this. Likewise, 10 cm water was a boundary in the evolution of water composition between surface runoff water influenced by precipitation and soil pore water. In peatlands, surface runoff is dominated by saturation-excess overland flow (Evans et al., 1999). In a laboratory rainfall simulation experiment, Holden and Burt (2002b) indicated most surface runoff originated from near surface layers of peat, though the deepest layer in the study that was less related to surface

runoff was 10 cm. Consequently, the tracer may have percolated to deeper layers, perhaps through soil pipes or macropores, which did not mix with surface runoff. Otherwise, dilution in surface runoff prevented detection of the tracer.

The concentration of the tracer decreased between days 3 – 6 and further still by day 13. The decrease in concentration of the tracer was more apparent on the bottomslope and although concentrations remained much higher at slope position 11, it also experienced a much greater decrease in concentration compared to other slope positions. Indeed, slope positions 5 – 7 showed an increase in Br^- concentration and perhaps reflected the longer residence time of water found at deeper depths on the mid-slope, corroborating the assertion that DOC on the mid-slope had high Abs_{400} due to longer residence times and being old water. It was possible to detect tracer in runoff samples on day 6 while it was present in 10 cm water on mid-slope plots on day 13. Thus although there was less mixing of water it was nonetheless detectable across multiple water types and sample depths. However, concentrations were much lower than in soil pore water, supporting the assertion that water was diluted in surface runoff.

5.6 Conclusions

This chapter aimed to identify how water chemistry varied across the hillslope in relation to changes in flowpath and mixing of water sources. Soil pore water and surface runoff water had distinct water chemistries, separated by high conductivity, SO_4^{2-} content and much higher pH levels in runoff water. Dissolved organic carbon concentrations were much lower in surface runoff, caused by dilution by mixing with precipitation. The water chemistry signature in soil pore water was similar across the hillslope, except where deeper water tables were distinguished by higher concentrations of DOC and higher Abs_{400} as well, suggesting a

longer residence time of water on steeper mid-slopes due to a build up of humic substances. Despite the differences between soil pore water and surface runoff water, ponding could occur, particularly on Featherbed Moss where slope angles were low and *Eriophorum spp*. was the dominant form of vegetation. In this instance, runoff water took on the compositional characteristics of soil pore water.

10 cm water resembled an intermediate layer between soil pore water and surface runoff water, characterised by higher SO_4^{2-} concentrations, conductivity and pH than soil pore water but also much higher DOC concentrations than found in surface runoff water. As such, surface runoff water originated from near surface layers but DOC was diluted relative to 10 cm water. The high DOC concentrations found at 10 cm depth did not have the same compositional characteristics of soil pore water, with lower Abs_{400} and specific absorbance suggesting a younger more labile form of DOC in the upper surface was mobilised in the upper surface layers.

The bromide tracer experiment confirmed rapid transport of the tracer down-slope, while the presence of the tracer in bottom-slope 10 cm water traps was indicative of return flow of deeper sub-surface flow from the mid-slope towards the surface. The increase in tracer concentration over time on the mid-slope could suggest continued percolation of the tracer at depth but also increased residence time of water at greater depth. The accumulation of the tracer at the bottom-slope, particularly towards the riparian zone, was maintained throughout the 13 day experiment, though concentrations of the tracer on the bottom-slope also experienced more dilution than on the mid-slope.

Previous chapters have shown that DOC concentrations were high on the top-slope and on mid-slopes that experienced extensive water table drawdown. The importance of the relationship between DOC and WTD suggested that increased DOC concentrations at depth were caused by increased oxidation of peat and production of DOC. While this process is likely

to be important, the high DOC concentrations found at 10 cm depth have also shown that deep soil pore water DOC was characterised by humic substances that build up with longer residence times. The decrease in DOC down-slope demonstrated in previous chapters was contradicted by accumulation of tracer on the bottom-slope. Greater dilution of the tracer was observed on the bottom-slope than other slope positions, suggesting that the greater throughflow of water on the bottom-slope was the cause of lower DOC concentrations.

Chapter 6 Modelling the effects of hillslope position

6.1 Introduction

One of the most important assessments of peatland function is to derive complete carbon budgets and determine whether a peatland is likely to be a carbon sink or source. Moore et al. (2002) estimated a carbon budget for Mer Bleue bog in Canada of -60 g m^{-2} yr^{-1}, which was largely comprised of the difference between gross photosynthesis (P_G) and ecosystem respiration (R_{eco}). A six year study at Mer Bleue (Roulet et al., 2007) identified large inter-annual variation in net ecosystem exchange (NEE), ranging between -2 to -112 g m^{-2} yr^{-1}. The export of dissolved organic carbon (DOC) comprised an average 37% of mean NEE while CH_4 was 9%. Roulet et al. (2007) also compared the contemporary carbon balance (six year mean = -21.5 ± 39.0 g m^{-2} yr^{-1}) to the alternative method of estimating carbon balance by obtaining net carbon accumulation from soil cores. Two peat cores had accumulation rates of 21.9 ± 2.8 and 14.0 ± 37.6 g m^{-2} yr^{-1}. However, estimating the net carbon balance by accumulation studies is limited given they cannot consider carbon losses or the immediate impact of management strategies on peatlands, nor can they distinguish between the uptake or release of different carbon species (Rowson et al., 2010).

Comparison of different methodological approaches to estimating the carbon balance of peatlands can provide a useful constraint on both short-term high resolution monitoring studies and long-term accumulation. Nilsson et al. (2008) found comparable results between the contemporary net ecosystem carbon balance of a minerogenic mire in Sweden and long-term carbon accumulation, estimated from literature values, of the same region. However, Juutinen et al. (2013) found the contemporary budget of a peatland-stream-lake continuum in Finland exceeded that based upon long-term carbon accumulation from peat cores. There were numerous sources of uncertainty in the study of Juutinen et al. (2013): the carbon budget

was dominated by the NEE flux from forests within the catchment, which was only based upon literature values rather than direct observation; the export budget may have underestimated peatland exports as it did not distinguish between forest and fen; and inorganic carbon species were not accounted for, nor were precipitation inputs of carbon and particulate organic carbon (POC). Inclusion of multiple carbon species can be important, as Nilsson et al. (2008) found precipitation carbon, CH_4-C and runoff carbon export (including total organic carbon, dissolved inorganic carbon and CH_4-C) increased the NEE source strength during the net efflux period and decreased the size of the sink during the net-uptake season.

Accounting for the complete fluvial budget is an important requirement of carbon budgets. Hope et al. (2001) demonstrated the necessity of including gaseous evasion of carbon from streams in the overall carbon balance of a given catchment, while Billett et al. (2004) indicated Auchencorth Moss in Scotland was at best carbon neutral, if not a carbon source after including the fluvial carbon flux in the overall carbon mass balance. The study of Billet et al. (2004) was based upon data measured between 1996 – 1998, while Dinsmore et al. (2010) studied a further two years in the Auchencorth Moss catchment with updated methodologies between 2006 – 2008. A large increase in NEE compared to Billet et al. (2004) meant the overall balance was a carbon sink, despite DOC being the largest carbon export. The two studies demonstrated that large inter-annual variability in NEE had the greatest effect upon the net carbon balance (Billett et al., 2010), a finding in agreement with Roulet et al. (2007). Despite the general dominance of the fluvial carbon budget by DOC, disturbed sites such as in the South Pennines that have experienced extensive erosion and degradation show that the production and export of particulate organic carbon (POC) can dominate the fluvial carbon budget (Billett et al., 2010).

Despite the improvement in contemporary carbon balances to include complete budgets, there is a requirement to reduce levels of uncertainty in carbon balances, aided by better measurement and scaling methods (Billett et al., 2010). Furthermore, it is important to

understand not only the short-term function of peatland systems and the impact of management strategies, but also the potential long-term impacts of management strategies upon carbon balances through modelling techniques (Clark et al., 2010a). Clark et al. (2010a) compared the output of nine bioclimatic envelope models (BCEMs) that used statistical relationships with environmental data against the output of three dynamic process-based models. The dynamic models compared two models based upon the partitioning of soil organic carbon pools (ECOSSE and MILLENNIA) against the semi-empirical Durham Carbon Model (DCM) constructed from the carbon balance approach used in contemporary studies.

ECOSSE (Smith et al., 2010a, Smith et al., 2010b) predicted the change in size of five carbon pools and gaseous and fluvial carbon fluxes over time. Decomposition of different soil organic matter pools was based upon first-order rate equations and could be modified for variation in temperature, water content, plant cover and soil pH (Smith et al., 2010a). MILLENNIA (Heinemeyer et al., 2010) assessed carbon storage by modelling the carbon balance between net primary productivity (NPP) inputs and decomposition losses in two peat layers, the acrotelm and catotelm. Decomposition of litter cohorts was divided into soluble, holocellulose and lignin fractions and considered eight major plant functional types (PFTs). Water table depth (WTD), calculated from the difference between precipitation, actual evapotranspiration and runoff, derived coverage of plant functional types and therefore affected NPP. The DCM was based upon the net carbon balance of annual P_G, R_{eco}, CH_4, DOC, POC and dissolved CO_2 (Worrall et al., 2009b). The formation and function of the DCM shall be discussed in further detail below.

The study of Clark et al. (2010a) compared the outputs of the above models across four peat catchments in the UK and found that the BCEMs predicted Auchencorth Mosss and Bleaklow were most likely to be sensitive to shifts from the presence to absence of peat, while the dynamic models suggested Moor House and Conwy were closer to changing from a net carbon sink to source as they were cooler, wetter sites. The greatest differences were between

the dynamic models however: ECOSSE predicted a decline over the next century in the size of the carbon sink leading to a switch to a net carbon source; the DCM predicted a decline in the net carbon sink but no net efflux of carbon; and MILLENNIA predicted a net increase in the carbon sink as unlike ECOSSE and DCM, it was more sensitive to changes in water balance given the dynamic feedback between WTD, PFT and litter quality.

Given the wide variety of results from a range of different carbon budget modelling techniques it is apparent that further work is necessary to continue the development of such models to reduce uncertainty and more accurately capture key processes, such as water table dynamics, and the feedbacks in the carbon cycle associated with them (Clark et al., 2010a). This was the ultimate purpose of capturing variation in carbon fluxes and water table dynamics across the hillslope; to improve the spatial representation of carbon budget models by incorporating hillslope position into the DCM and accounting for the influence it has upon the carbon balance.

The DCM has progressed and developed over time. Worrall et al. (2003b) estimated a complete carbon budget for Moor House in the North Pennines, combining empirical relationships and literature values. When applied across all British peatland catchments, Worrall et al. (2003b) stated that peatlands were a smaller carbon sink than suggested by Cannell et al. (1999), who did not include the fluvial budget in their estimation of the total carbon budget of Britain. Worrall et al. (2007b) published an updated model, using temperature and precipitation to create a water balance model that considered WTD, actual evaporation and runoff as key components affecting different carbon pathways. Although the budget of Worrall et al. (2007b) suggested the Moor House catchment was a net source of carbon, Worrall et al. (2009a) constructed a multi-annual carbon budget calibrated against direct measurement observations and suggested the catchment was a net sink.

The current DCM output was outlined in Worrall et al. (2009b), based upon an updated version of the method used by Worrall et al. (2007b), including changes to the

methods of predicting P_G, DOC and POC. The model (Worrall et al., 2009b) was applied to the Peak District and also assessed the impact of land management including drainage, managed burning and grazing. The Peak District was predicted to be a net carbon sink, but with areas that were net sources of carbon. There was no clear benefit of one particular management strategy in the carbon budget, but the equivalent CO_2 budget suggested vegetation restoration was the best strategy as it reduced the export of POC (Worrall et al., 2009b).

The DCM has therefore been used to assess the impact of land management strategies, including the specific development of a component to account for the presence or absence of sheep grazing (Worrall and Clay, 2012). As such, the DCM has continued to improve over time, incorporating more factors to expand the physical representation of peatland systems. The purpose of this chapter is to include slope position in the DCM and determine whether slope position changes the carbon budget and carbon balance of the DCM. Top-slope, upper mid-slope, lower mid-slope and bottom-slope positions used in Chapter 2 shall be included in the DCM and the effect of slope position on the total carbon budget and individual carbon species assessed. Although not all components of the carbon budget have been studied as part of this thesis, the DCM predicts the flux of CH_4 and dissolved CO_2 by empirical relationships to WTD (Worrall et al., 2009b), thus the impact of slope position can be assessed beyond the fluxes studied in this thesis.

6.2 Aims and objectives

The aim of this chapter is to determine what impact inclusion of slope-position has upon the carbon balance predicted by the DCM given the results of this study. The specific objectives are:

- Assess the individual impacts of top-slope, upper mid-slope, lower mid-slope and bottom-slope on the carbon balance; and
- Assess the impact of each slope position on individual carbon fluxes including R_{eco}, P_G, DOC, CH_4 and dissolved CO_2.

6.3 Methods

6.3.1 Model set-up

Full details of the DCM modelling approach adopted in this chapter can be found in Worrall et al. (2009b), with brief details provided below. Gross photosynthesis was determined using the method of Bubier et al. (1998) that uses a rectangular hyperbola to establish a relationship between P_G and photosynthetically active radiation (PAR). PAR was predicted by correlating PAR and solar radiation using data from Moor House in the North Pennines, meaning solar radiation measurements could be calibrated for Bleaklow Plateau. Ecosystem respiration was predicted using the method of Lloyd and Taylor (1994) and CH_4 flux by an empirical relationship with WTD. Dissolved organic carbon solubility was predicted using an empirical relationship between soil water pH and ionic strength, with DOC flux calculated based upon runoff estimates. Dissolved CO_2 was predicted using the method of Worrall et al. (2005), while POC estimates were derived using an empirical relationship with the percentage of bare peat in the catchment. The model constructs a complete carbon budget composed of:

$$C_{total} = - C_{PG} + C_{Reco} + C_{CH_4} + C_{DOC} + C_{POC} + C_{diss.CO_2} \quad (6.1)$$

Where: C_{total} = total carbon budget of the catchment (tonnes CO_2 eq km^{-2} yr^{-1}); C_{PG} = annual gross photosynthesis (tonnes C km^{-2} yr^{-1}); C_{Reco} = annual ecosystem respiration of CO_2 (tonnes C km^{-2} yr^{-1}) ; C_{CH_4} = annual methane respiration (tonnes C km^{-2} yr^{-1}); C_{DOC} = annual DOC production (tonnes C km^{-2} yr^{-1}); C_{POC} = annual POC production (tonnes C km^{-2} yr^{-1}); and $C_{diss.CO_2}$ = annual dissolved CO_2 flux (tonnes C km^{-2} yr^{-1}). The carbon budget was calculated over a 10 year period from 1997 – 2006, encapsulating inter-annual variation due to changes in weather conditions (Worrall et al., 2009b). As with the convention adopted for CO_2 fluxes throughout this thesis, a negative sign convention indicates a carbon sink.

Of the six components of the carbon budget used in the DCM, only three have been studied. Ecosystem respiration and P_G were derived using gaseous flux measurements while DOC was based upon soil pore water concentrations. Slope position was added to the model as a correction factor, whereby the proportion of WTD, P_G, R_{eco} and DOC input into the model was adjusted for each slope position relative to the top-slope, which was used as a control. The effect of each slope position upon the carbon budget could therefore be assessed individually. Correction factors were based upon the relative data used in Chapter 2 for P_G, R_{eco} and DOC, while WTD was derived as part of this chapter. Thus, slope position was represented based upon data from June 2010 – June 2011 and although the patterns associated with CO_2 flux have been shown to have inter-annual variation based upon results presented in Chapter 4, the purpose of this chapter is to predict the potential impact that slope position may have on the overall carbon balance. Details of the correction factors shall be discussed in more detail in section 6.3.2.

Despite this thesis only considering three components of the carbon budget, incorporating slope position into the DCM further had an additional impact upon CH_4 and POC.

The prediction of CH_4 flux was derived using an empirical relationship to WTD, with higher water tables expected to increase CH_4 flux. WTD in the DCM was derived from a water balance approach between potential evapotranspiration and rainfall, while the DCM also predicts catchment runoff. Consequently, higher water tables produce a greater amount of runoff, which increases the flux of POC from the catchment. Therefore, slope position could have an additional impact beyond the components of the carbon budget monitored as part of the thesis.

6.3.2 Correction factors

As stated in section 6.3.1, the effect of slope position upon the carbon budget of peatlands was assessed using correction factors, which were derived from the 2010 – 2011 dataset presented in Chapter 2. A 1 km^2 grid cell was used as a control to assess the impact of correction factors, which included grazing, burning and vegetation. Thus slope position represents another component of the DCM. The control cell, referred to as PD in Billett et al. (2010), was based on the Bleaklow Plateau in the Peak District. Control cell PD (SK 09054 93154) was situated to the north of the A57, just off the Pennine Way (Figure 6.1), in close proximity to Featherbed Moss and Alport Low and was only 592 m from the bottom-slope position on Featherbed Moss. PD is dominated by *Eriophorum angustifolium* and vegetation in the DCM was set to 100% sedge. The control cell assumed no history of burning or the presence of drainage, but grazing was set to a fixed intensity of 0.12 ewes ha^{-1}. Altitude was fixed at 507 m, the altitude of PD, while peat cover was 100%, with a nominal bare soil contribution of 0.01%.

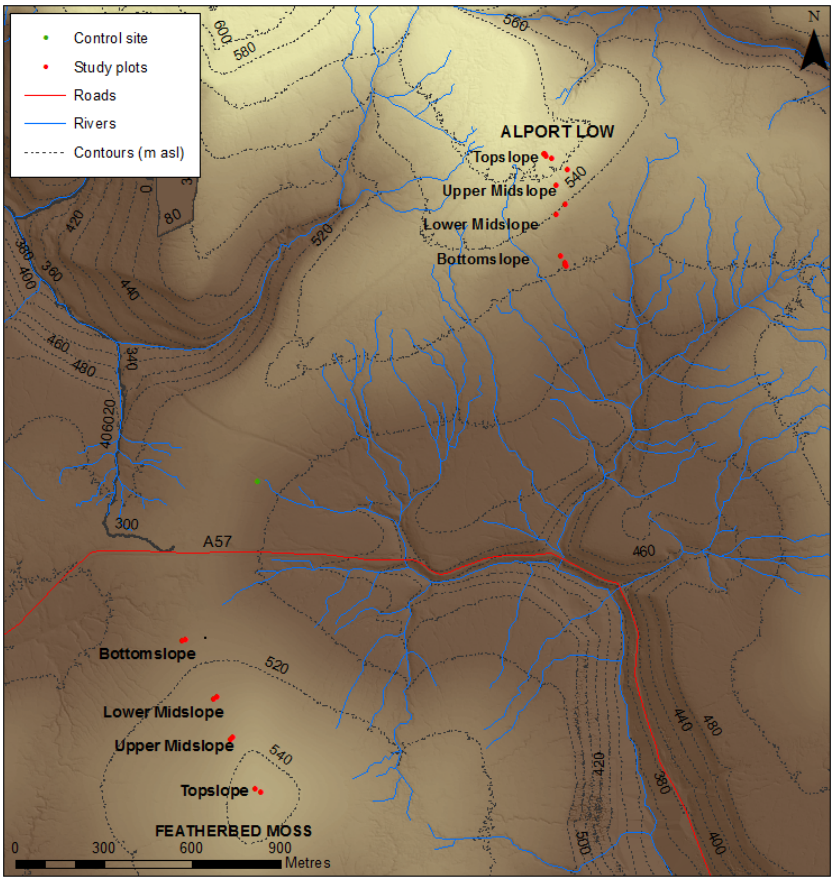

Figure 6.1 Map of study sites in Peak District, Derbyshire, with PD control

The correction factors were determined as the relative proportions of WTD, R_{eco}, P_G and DOC compared to the top-slope. Consequently, all values on the top-slope were fixed to 1.00. The values used were based upon the ANOVA main effects results on relative R_{eco}, P_G and DOC determined in Chapter 2. As such, any possible effects caused by site, sub-slope, month or interaction effects were accounted for in the ANOVA model and the slope positions therefore represent the overall slope effect established for R_{eco}, P_G, and DOC beyond those associated with the other controlling factors.

Section 2.4.2 analysed gaseous fluxes, including relative data for R_{eco} and P_G. A disparity was recognised between the significant differences implied by the ANOVA main effects of the R_{eco} flux data and those of the relative R_{eco} main effects. The bottom-slope was

significantly different from both mid-slope positions in the flux data but not the top-slope, yet while the relative value was significantly higher than the top-slope, the bottom-slope was not significantly different to the mid-slope positions. Though significant differences for P_G were different between the flux and relative datasets, the overall pattern of higher main effects means for the mid-slopes and bottom-slope was reflected in the data. The overall consequence of the different patterns implied by flux and relative data was expected to have a minimal impact upon the model. Though values of relative data for P_G and R_{eco} could be high (Table 6.1), the gaseous carbon budget was derived as the overall net exchange between P_G and R_{eco}. Thus, the overall contribution of slope position to the gaseous budget as correction factors should have been small. For example, though the correction factor for upper mid-slope R_{eco} was 1.64 times higher than the top-slope and P_G was 1.71 times greater, the net difference was in fact a sink of -0.07. Because ANOVA main effects accounted for the influence of other factors and interactions, as well as being based upon the distribution of the data, not all top-slope means were 1.00. Correction factors were re-normalised to make the top-slope value 1.00.

Table 6.1 Relative correction factors input in Durham Carbon Model

Slope position	**Relative correction factors**			
	WTD	**R_{eco}**	**P_G**	**DOC**
Top-slope	1.00	1.00	1.00	1.00
Upper Mid-slope	1.47	1.64	1.71	1.00
Lower Mid-slope	1.11	1.56	1.57	0.85
Bottom-slope	0.64	1.49	1.57	0.71

Water table depth was not analysed in Chapter 2 for relative slope effects because the sign of the data changed depending upon whether the water table was above or below the surface. Because the maximum observed saturation level above the surface was 80 mm, all

water table values had 81 mm added to their WTD, thus making the value closest to the surface -1 mm. Although this modified the true relative values for WTD, the overall main effects nonetheless reflected the deeper water tables on the mid-slope positions and higher WTD on the bottom-slope. As with relative data from Chapter 2, ANOVA was used to determine significant differences and main effects plots. Site ($p < 0.0001$, $\omega^2 = 3.45\%$, Table 6.2), slope ($p < 0.0001$, $\omega^2 = 15.78\%$), sub-slope ($p < 0.0001$, $\omega^2 = 27.39\%$), month ($p = 0.012$, $\omega^2 = 0.87\%$) and site-slope interaction ($p < 0.0001$, $\omega^2 = 4.66\%$) were significant factors. Reflecting the observations of the WTD ANOVA, all slope positions were significantly different from one another.

Table 6.2 Relative WTD ANOVA: ω^2 = percentage variance

LnRelative WTD ANOVA		
Factor	**P**	**ω^2**
Site	<0.0001	3.45%
Slope	<0.0001	15.78%
Sub Slope(Slope)	<0.0001	27.39%
Month	0.012	0.87%
Site*Slope	<0.0001	4.66%
N 704		**R^2 52.17%**

The DCM was run under four scenarios: top-slope correction factors, effectively acting as the slope control – i.e. no slope effect present with WTD, R_{eco}, P_G and DOC fixed to 1.00; upper mid-slope correction factors; lower mid-slope correction factors; bottom-slope correction factors. The outputs of each model scenario were assessed to determine the overall impact each slope position had upon the carbon budget. For instance, inclusion of bottom-slope meant that DOC concentration was adjusted to represent 0.71 times the concentration of DOC for the top-slope. As the DOC correction factor is to concentration, the overall effect on DOC flux is the combination of the change in DOC concentration and the impact on water flow.

Uncertainty in the DCM was determined as outlined in Worrall et al. (2009b), whereby the model was extrapolated to a 25 km^2 subset of data with the model repeated 10 times. As such, error in the final greenhouse gas budget equivalents was ± 6%.

6.4 Results

The DCM predicted higher rates of respiration (Figure 6.2) when mid-slope and bottom-slope positions were incorporated into the model than when the top-slope control was used. Modelled R_{eco} was 31 tonnes C km^{-2} yr^{-1} on the top-slope, compared to 52, 49 and 47 tonnes C km^{-2} yr^{-1} for the upper mid-slope, lower mid-slope and bottom-slope respectively. The R_{eco} flux broadly reflected the results in Chapter 2 (section 2.4.2.1) from the relative R_{eco} data and although this was different from the ANOVA main effects of the flux data, it did reflect the raw data prior to ANOVA analysis, with the top-slope flux being smallest.

Methane was predicted based upon an empirical relationship with WTD. As shown in Table 6.1, WTD on the bottom-slope was closer to the surface than the top-slope, while WTD was deeper than the top-slope on the mid-slopes. It could therefore have been expected that CH_4 flux would vary between slope positions, yet although the top-slope had a flux of 5 tonnes C km^{-2} yr^{-1}, the other three slope positions had a flux of 4 tonnes C km^{-2} yr^{-1}, meaning there was little variation in CH_4 flux between slope positions. Direct monitoring of CH_4 flux may have changed understanding of any slope effect.

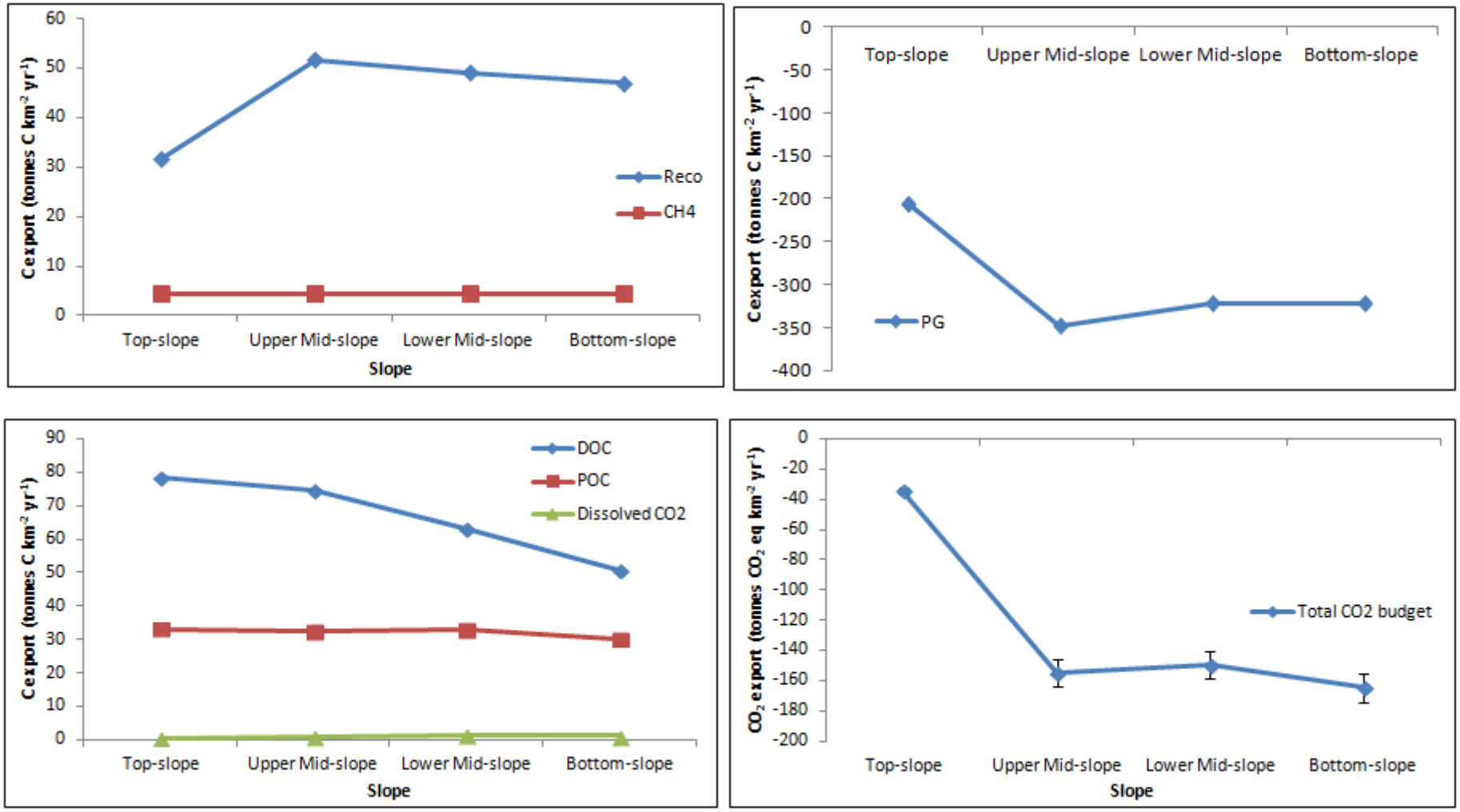

Figure 6.2 Modelled carbon export values for gaseous, fluvial and complete carbon budgets: error bars = ± 6% error

Gross photosynthesis on the top-slope control was -205 tonnes C km^{-2} yr^{-1} (Figure 6.2) but was greatest on the upper mid-slope at -348 tonnes C km^{-2} yr^{-1}, while the lower mid-slope and bottom-slope had totals of -322 tonnes C km^{-2} yr^{-1}. The P_G flux for all slope positions was considerably higher than that of R_{eco}, perhaps suggesting that the DCM did not predict P_G as accurately as R_{eco}. However, if the P_G model output is believed, there was nonetheless a large difference between the top-slope control and all other slope positions, reflecting the relative P_G input values.

For the fluvial carbon budget, DOC was the largest component and was the second largest component of the complete carbon budget after P_G. The top-slope control had the largest DOC flux of 78 tonnes C km^{-2} yr^{-1}. The upper mid-slope DOC flux was close to that of the top-slope at 75 tonnes C km^{-2} yr^{-1} with lower values of 63 and 51 tonnes C km^{-2} yr^{-1} for the lower mid-slope and bottom-slope respectively. Particulate organic carbon export was 33 tonnes C km^{-2} yr^{-1} on the top-slope to lower mid-slope and 30 tonnes C km^{-2} yr^{-1} on the bottom-slope. Despite WTD potentially increasing the flux of POC by a greater water yield when water tables were closer to the surface, this did not appear to affect the POC budget, which remained the same across the slope; it may be that the percentage of bare soil used within the model to predict POC (Worrall et al., 2009b) overrides any influence inferred from WTD. Dissolved CO_2 values were small across all slope positions at 1 tonne C km^{-2} yr^{-1} and consequently dissolved CO_2 was the smallest and least important flux in the carbon budget.

The complete carbon budget was determined in CO_2 equivalents. The fluxes of the upper mid-slope, lower mid-slope and bottom-slope, at -155, -150 and -165 tonnes CO_2 eq km^{-2} yr^{-1} respectively, were within ± 6% error of one another. The carbon budget for the top-slope was much lower at -35 tonnes CO_2 eq km^{-2} yr^{-1}. All slope positions were a carbon sink but incorporation of mid-slope and bottom-slope positions into the DCM would increase the carbon sink capacity of the system which was predominantly determined by P_G. The top-slope

was therefore accumulating carbon at a lower rate than all other slope positions due to the lower rate of P_G.

6.5 Discussion

6.5.1 Limitations

There were a number of limitations to the modelling approach adopted in this chapter. The correction factors applied were based upon one year of data. Considerable variation has been observed in carbon budgets between years, particularly relating to changes in NEE (Roulet et al., 2007, Koehler et al., 2011) and thus the budget amendments presented in this chapter represent a possible carbon budget. Indeed, Chapter 4 observed inter-annual variation between CO_2 fluxes for plots which were between two different study years.

The main drawback of the study related to the correction factors applied. The carbon budget was constructed of P_G, R_{eco}, CH_4, DOC, POC and dissolved CO_2 yet only CO_2 fluxes and relative DOC concentrations for soil pore water were included in the model based upon direct observations in Chapter 2. The modelling approach should have accounted for some of the variation in POC and CH_4 by incorporating WTD as a correction factor and CH_4 was predicted using an empirical relationship with WTD. However, it must be acknowledged that direct monitoring of these fluxes would have improved the utility of slope position as a factor incorporated into the DCM. Furthermore, WTD values had to be adjusted so all values were of the same sign prior to calculation of relative WTD, thus changing the scale of the difference in WTD between slope positions. However, the relative values for WTD did broadly reflect the pattern observed in Chapter 2 across the hillslope. There was an unknown error component caused by using the relative correction factors as input terms for each slope position, though ANOVA does itself incorporate an error term when deriving main effects values.

Incorporation of hillslope positions into carbon budget models across a catchment scale proved difficult. The purpose of this chapter was to assess the impact that each slope position had upon the carbon budget for individual carbon species and the total carbon budget. However, as outlined in Chapter 1 and Chapter 2, the mid-slope was divided into two sub-sections to increase the number of observations along the slope, which was done *in situ* during installation of field equipment. As such, the upper and lower mid-slope positions were not defined on a quantitative basis, meaning that their inclusion and separation when upscaling results to a catchment scale could prove problematic when defining a boundary by which to separate them. Despite individual components of the carbon budget such as P_G and DOC showing variation between the two mid-slope positions, the total carbon budgets were within error of one another, suggesting that when incorporating slope position on a wide-scale, it may be possible to represent the mid-slope as a single landscape unit.

6.5.2 Carbon species and slope position

This study sought to investigate the impact slope position had upon individual carbon species and the total carbon budget when incorporated into the DCM. It was intended that the study catchment would be divided into different slope positions and the impact of slope position on a catchment scale be assessed by including and omitting slope position from the DCM. This was ultimately not possible, but the impact of slope position on individual carbon species was assessed as the top-slope was the equivalent of 'no slope' in the DCM.

The largest individual component of the carbon budget predicted by the DCM was P_G, which was considerably greater across all slope positions than R_{eco}. Top-slope P_G was lower than those of all other slope positions, indicating that accounting for slope position had an important effect upon the gaseous CO_2 budget. Thus while the top-slope control (effectively no

slope position in the model) had a flux of -205 tonnes C km^{-2} yr^{-1}, all other slope positions had a flux >-300 tonnes C km^{-2} yr^{-1}. In a multi-annual carbon budget, Worrall et al. (2009a) reported a maximum P_G of -190 tonnes C km^{-2} yr^{-1} at Moor House in the North Pennines, while the values reported here were also greater than those of Clay et al. (2010b) who assessed the impact of burning and grazing upon carbon budgets. However, Clay et al. (2010b) reported much higher values for R_{eco}, which varied between 136.6 – 258.7 tonnes C km^{-2} yr^{-1} when extrapolating direct measurements for long-term model predictions. The range of values of R_{eco} reported here (31 – 52 tonnes C km^{-2} yr^{-1}) fit more closely to those reported by Worrall et al. (2009a), with all but the top-slope control within the range of 49.1 – 58.2 tonnes C km^{-2} yr^{-1} ± 7.7%. Consequently inclusion of slope position increased both P_G and R_{eco} compared to the top-slope control, with the greatest CO_2 fluxes on the upper mid-slope. The lower mid-slope and bottom-slope had almost identical fluxes.

Net ecosystem exchange has been identified as the most important component of many carbon budgets, though the values of P_G and R_{eco} reported here were greater than those of other studies. Roulet et al. (2007) reported a range in NEE between -2 to -112 tonnes C km^{-2} yr^{-1} with a six year mean of -40.2 ± 40.5 tonnes C km^{-2} yr^{-1}. Nilsson et al. (2008) reported values of -55 ± 1.9 and -48 ± 1.6 tonnes C km^{-2} yr^{-1} for 2004 and 2005 respectively at a poor fen in Sweden and Koehler et al. (2011) similarly reported a six-year mean of -47.8 tonnes C km^{-2} yr^{-1} at an Atlantic blanket bog in Ireland. At Auchencorth Moss in Scotland, Dinsmore et al. (2010) also found NEE to be the most important component of the carbon budget, with values of -136 and -93.5 tonnes C km^{-2} yr^{-1} in 2007 and 2008 respectively; values closer to those suggested by the DCM but still some way off.

Dissolved organic carbon was the second most important carbon flux after P_G, varying between 78 tonnes C km^{-2} yr^{-1} at the top-slope control and 51 tonnes C km^{-2} yr^{-1} on the bottom-slope. The DCM predicted similar values of DOC for the top-slope and upper mid-slope

and showed a continued decrease in DOC down-slope thereafter. Consequently, it would seem prescient to incorporate slope position into the DCM when modelling DOC budgets given the importance of slope to the production and transport of DOC. The range in DOC of 51 – 78 tonnes C km^{-2} yr^{-1} shows that DOC export was larger than predicted at other peatlands, with 19.3 tonnes C km^{-2} yr^{-1} reported for Conwy in Wales (Billett et al., 2010) and 18.6 ± 16.0 and 32.2 ± 18.7 tonnes C km^{-2} yr^{-1} at Auchencorth Moss for 2007 and 2008 respectively (Dinsmore et al., 2010). Dissolved organic carbon export at Auchencorth Moss represented an average 24% of NEE uptake, while Roulet et al. (2007) reported DOC was 37% of NEE uptake at Mer Bleue in Canada.

The higher DOC flux values in this study compared to those of Roulet et al. (2007), Billett et al. (2010) and Dinsmore et al. (2010) can in part be ascribed to the DCM predicting loss at the source rather than the catchment outlet. As such, the DCM does not account for in-stream losses. Indeed, Billett et al. (2010) also reported the DOC flux of acrotelm peat and found ~50% losses during transport from peat soil to the catchment outlet. Despite the higher export values for DOC reported here, DOC was within range of those reported by Clay et al. (2010b) under various land management scenarios of burning and grazing, while all slope positions had a DOC export lower than the maximum reported by Worrall et al. (2011) of 95.6 tonnes C km^{-2} yr^{-1} for a *Vaccinium* control plot unaffected by wildfire. Furthermore, results here showed the importance of DOC to the carbon budget, as it was the second most important component of the carbon budget after P_G.

The importance of DOC to the carbon budget could be particularly relevant to top-slope positions given the higher DOC export reported but much smaller total CO_2 budget of -35 tonnes CO_2 eq km^{-2} yr^{-1}. Roulet et al. (2007) found that of six years studied in constructing a long-term carbon budget, three were net sources, with DOC causing the net loss of carbon when the NEE sink was reduced. Koehler et al. (2011) also found for a budget that considered

NEE, CH_4 and DOC (TOC) that for two out of six years, DOC and CH_4 caused the carbon balance to be a net source, while Nilsson et al. (2008) found CH_4 and runoff carbon had a substantial effect on the carbon budget, increasing the strength of the net source during periods of net loss, or otherwise decreasing the sink during net sink periods. As such, given the size of the contribution of DOC to the DCM and the importance of the slope effect inferred, slope position could have an important impact on the carbon balance via the fluvial pathway as well as the gaseous pathway, suggesting it is important to account for slope position variation in carbon budget models of blanket bogs.

Despite the importance of slope position correction factors in adjusting the carbon export values for P_G, R_{eco} and DOC, there was minimal variation in carbon export between slope positions for the components of the carbon budget with no direct correction factor. Methane varied between 4 - 5 tonnes C km^{-2} yr^{-1} and was thus insensitive to slope position. Similarly, POC varied between 30 - 33 tonnes C km^{-2} yr^{-1} and therefore slope position did not affect the overall POC flux. These results were surprising given the variation in relative WTD reported in Table 6.1. Several studies have noted the important role WTD has upon the production and consumption of CH_4 in peatlands (Clymo and Pearce, 1995, Moore and Dalva, 1997, McNamara et al., 2008), such that micro-topographic variation in CH_4 flux is often defined by the position of the water table. The DCM models CH_4 flux based upon an empirical relationship with WTD (Worrall et al., 2009b) and it would be expected that the higher water tables on the top-slope control and bottom-slope compared to the mid-slopes would result in higher CH_4 values in the carbon budget, yet this was not observed. It was likely that the DCM was insensitive to WTD correction factors for CH_4 because the CH_4 flux was also based upon a range of literature values and incorporating relative WTD into the model did not override the inherent values calculated by the model.

Similarly, though it was anticipated that WTD would have an indirect impact upon POC flux by increasing water yield when water tables were close to the surface, the DCM was not affected by the WTD correction factor. This was because POC flux in the DCM was controlled by fixed factors in the model across all slope positions, including percentage of bare peat that was the most important determinant upon the POC flux. Previous versions of the DCM have shown considerable variation in POC flux (3.4 – 206.3 tonnes C km^{-2} yr^{-1}) when based upon suspended sediment rating curves (Worrall et al., 2011) and therefore a more advanced approach needs to adopted to capture variation in POC associated with slope position. Given the lack of response in the DCM to WTD and consequently CH_4 and POC, direct monitoring of these carbon fluxes is required to fully understand the impact of slope position and the carbon budget implications for these fluxes. Dissolved CO_2 was also fixed across all slope positions at 1 tonne C km^{-2} yr^{-1} but was a minor flux relative to the others in the fluvial carbon budget. Moreover, dissolved CO_2 and gaseous evasion of CO_2 is more relevant to stream export rather than any specific slope effect.

6.5.3 Carbon balance

The overall carbon budget showed considerable variation between the top-slope control and all other slope positions. While the CO_2 equivalents budget varied between -150 and -165 tonnes CO_2 eq km^{-2} yr^{-1} for the mid-slopes and bottom-slope, within ±6% error of each other, the top-slope had a much lower budget of -35 tonnes CO_2 eq km^{-2} yr^{-1}, primarily due to the much lower P_G flux. Despite the difference in carbon budgets between the top-slope and all other slope positions, the carbon balance of every slope position was a net sink. This contrasted with Clay et al. (2010b) in the North Pennines, who observed net sources for all burning and grazing regimes, up to a maximum of 585 tonnes CO_2 eq km^{-2} yr^{-1} under a scenario of no burning or grazing in 2007. However, the CO_2 equivalents budget of the Peak

District, the DCM model on which this study is based (Worrall et al., 2009b), was a net sink across all land management scenarios, ranging between -129 to -216 tonnes CO_2 eq km^{-2} yr^{-1}. It was evident therefore that incorporation of mid-slope and bottom-slope positions into the DCM maintained similar levels of net sink as predicted previously (Worrall et al., 2009b), while the top-slope control suggested it was important to account for different slope positions given the reduced carbon sink.

Given the results inferred by the DCM, it was apparent that the net carbon sink on the top-slope was lower than all other slope positions and that carbon budget models may be underestimating the size of the carbon sink by not including the effect of slope position in the model. In this regard, if the net greenhouse gas sink for each slope position suggested by the DCM equated to long-term carbon accumulation , it would reflect more the process of raised bog formation or expansion rather than blanket bog, as more material could accumulate on the mid-slope relative to the top-slope. Despite this, it was nonetheless evident that accumulation of material in the long-term was greater on the top-slope and bottom-slope given the larger peat deposits compared to the mid-slopes, as shown with peat depths in Table 2.2 and Table 2.3. Peat in blanket bogs can form on slopes up to 18 - 25° (Moore and Bellamy, 1974) but is thinner on steep slopes (Charman, 2002). As such, if the net greenhouse gas sink was reflected in carbon accumulation, the greater level of accumulation on the mid-slopes would indicate accumulation of material in the manner of concentric raised bogs.

6.5.4 Model applicability

The DCM was developed for blanket bogs, while the addition of slope position as a factor to incorporate in carbon budget models is predominantly of importance to upland maritime blanket bogs such as occur in the UK and Ireland. Blanket bogs typically require 1000

mm rainfall annually, with 160 wet days of >1 mm rain and mean temperature of <15 °C for the warmest month and minor seasonal variation in temperature, limiting their presence to hyper-oceanic locations globally (Charman, 2002). Blanket bogs are found across the UK and Ireland as well as the northwestern seaboard of Europe in Atlantic regions (Moore and Bellamy, 1974), but are found in North America as well in cool, wet environments (Charman, 2002) such as Newfoundland (Graniero and Price, 1999). Nonetheless, the research conducted in this thesis was on an upland maritime oligotrophic blanket bog and as such the results of both this modelling chapter and the thesis as a whole are best interpreted in the context of upland blanket bogs that occur across the UK and Ireland, where the cool, wet climate allows the formation of peat deposits on hillslopes at high altitudes.

Given the applicability of the model to upland catchments in the UK and Ireland, further work should be conducted to determine the impact the model has upon catchment scale carbon budgets. Developing a method by which the percentage coverage of each slope position can be determined will allow the overall impact of slope position upon carbon budgets be assessed.

6.6 Conclusions

The purpose of this chapter was to assess how carbon budgets changed when top-slope, upper mid-slope, lower mid-slope and bottom-slope positions were incorporated separately into the DCM. A second aim was to establish how individual components of the carbon budget varied with hillslope position. All slope positions were net carbon sinks, but the top-slope control, which assumed no slope factor present by fixing all relative flux correction factors to a value of 1.00, had a much lower carbon budget of -35 tonnes CO_2 eq km^{-2} yr^{-1} compared to those of the mid-slope and bottom-slope positions that ranged between -150 to -

165 tonnes CO_2 eq km^{-2} yr^{-1} and were within ± 6% error of one another. This was because of the much lower rate of P_G (-205 tonnes C km^{-2} yr^{-1}) compared to other slope positions (-322 to -348 tonnes C km^{-2} yr^{-1}) on the top slope position.

Ecosystem respiration was lower on the top-slope at 31 tonnes C km^{-2} yr^{-1} compared to the mid-slopes and bottom-slope (47 – 52 tonnes C km^{-2} yr^{-1}). In contrast to the gaseous CO_2 trends, DOC was highest on the top-slope (78 tonnes C km^{-2} yr^{-1}), decreasing to 51 tonnes C km^{-2} yr^{-1} on the bottom-slope. Results for gaseous and fluvial carbon budgets indicated that slope position could have an important impact upon individual carbon species and the total carbon budget. Despite the importance of slope position, the use of relative WTD as a slope position correction factor was unsatisfactory for predicting POC and CH_4 budgets. The DCM was insensitive to changes in CH_4 and POC, with fluxes showing minimal variation between slope positions. As such, to fully account for the impact of slope position upon the total carbon budget, it is recommended that additional research is required to directly monitor CH_4 and POC fluxes across the hillslope and further improve the understanding of carbon flux across blanket bogs as well as the accuracy of carbon budget models.

Chapter 7 Conclusions

7.1 Introduction

Peatland carbon cycling is an important issue that should be considered in land use management, with consequences for water quality, water treatment and long-term carbon storage with implications for carbon accumulation or release and subsequent effects upon the carbon balance and health of peatlands. Many different factors that affect carbon flux from peatlands have been studied, such as hydrology, natural erosion and revegetation, differences between vegetation communities, burning and grazing, artificial drainage and climate change. However, an aspect that had not been studied previously in relation to carbon flux from peatlands was the importance of topographic context, particularly in upland blanket bogs where peat develops across the entire landscape, including hillslopes.

While hillslope position has been shown to affect the hydrology of peatland systems, both in terms of water table depth (WTD) and rainfall-runoff response, little work had been done to understand whether hillslope has an impact upon peatland carbon cycling as well as hydrology. Consequently, the purpose of this thesis was to investigate how hillslope position affected the hydrology and carbon flux of blanket bogs in the Peak District with the ultimate goal of improving conceptual and process-based understanding of peatland systems. Furthermore, it was desired that hillslope position should be incorporated as a factor into the Durham Carbon Model (DCM), thus assessing its utility and necessity when incorporated into carbon budget models to improve carbon budget estimates and reduce uncertainty.

7.2 Thesis objectives

There were a number of objectives, both for the broad scope of the thesis as a whole, and individual chapters. The broad aim of the thesis was to establish whether hillslope position was a significant factor affecting the hydrology and carbon flux of peatlands. The secondary purpose of the thesis was to establish what impact incorporating hillslope position into the DCM had upon carbon budgets. The objectives of the individual chapters were:

- Chapter 2 explicitly investigated the impact of hillslope position upon the hydrology and carbon flux of peatlands. Top-slope, upper mid-slope, lower mid-slope and bottom-slope positions were used to assess changes in WTD and runoff response across two hillslopes in the Peak District. Carbon dioxide fluxes were monitored to determine whether gaseous carbon exchange varied with hillslope position, while dissolved organic carbon (DOC) concentrations were assessed in soil pore water and surface runoff water to identify changes in water quality.
- Chapter 3 was a laboratory study assessing the physical and compositional changes of peat, vegetation and litter samples across the two study sites and four hillslope positions established in Chapter 2. Changes in organic matter composition were assessed with reference to hillslope position, sample depth and substrate origin. The final objective was to determine whether physical and compositional measures of organic matter quality helped to explain changes in CO_2 flux and DOC concentration across the hillslope.
- Chapter 4 used a slope transect from the top-slope to riparian zone at the bottom-slope to determine whether the trends identified in Chapter 2 with hydrology, CO_2 flux and DOC composition were consistent with a higher sampling frequency along the slope or whether spatial heterogeneity was more important.

- Chapter 5 assessed how hydrochemistry varied across the hillslope, looking to quantify how changes in water quality established in Chapter 2 and Chapter 4 were linked to hillslope position and evolution of water sources across the hillslope. A secondary objective was to trace water movement along the hillslope and determine the origin of different water sources.
- Chapter 6 incorporated hillslope position into the DCM using results from the initial Chapter 2 study; the purpose was to consider the impact of individual hillslope position factors on both the complete carbon budget and on individual carbon fluxes.

7.3 Principal findings and conclusions

The aim of the thesis was to establish whether hillslope position was a significant factor controlling the hydrology and carbon flux of blanket peatlands, the findings of the research can be summarised as follows:

- Slope position was the most important factor that affected variation in WTD. Water tables were closest to the surface on the bottom-slope, where return flow from subsurface throughflow on the mid-slopes maintained its relatively high position. The top-slope also had high water tables, yet microtopographic variation was also important at this slope position. Slope angle was the most important variable in explaining the influence of slope position, with steeper mid-slopes experiencing water table drawdown. Dry bulk density and WTD were negatively correlated, but the relationship could be explained through site specific slope effects rather than a clear relationship with slope position.
- Slope position influenced CO_2 flux, affecting R_{eco}, P_G and NEE. Mid-slopes had significantly higher rates of R_{eco} than the bottom-slope, while the bottom-slope had

significantly higher rates of P_G than the top-slope. Fluxes of R_{eco} and P_G meant the bottom-slope had a significantly greater daytime NEE sink than the top-slope and mid-slope positions. Organic matter composition, which varied with hillslope position, had a small but significant influence upon CO_2 fluxes. Despite slope position being a significant factor controlling CO_2 fluxes, the influence of slope position was often small compared to other factors. Small-scale heterogeneity and microtopographic variation was more influential in explaining variation in CO_2 fluxes than slope position and the slope effect was not consistent between study years.

- Slope position was key to understanding variation in DOC concentration. Dissolved organic carbon concentration was highest at the top-slope and upper mid-slope and decreased further down-slope, with concentrations lowest on the bottom-slope. Inherently linked to the relationship between slope position and DOC concentration was WTD, with water table drawdown on steep mid-slopes increasing DOC concentration via increased oxidative production and the build-up of humic compounds with increased residence time of deep soil pore water. DOC concentrations towards the surface could nonetheless be high, indicating young, labile DOC was flushed out and diluted further down-slope towards the riparian zone and in surface runoff water. The mass flux and accumulation of a tracer down-slope in the riparian zone contradicted the pattern of decreased DOC on the bottom-slope, but highlighted the extensive water movement through the bottom-slope that maintained not only higher water tables but also the flushing of material from the subsurface.
- Consideration of the above results indicated that slope position was an important variable that needed to be accounted for in carbon budget models. Inclusion of slope position correction factors in the Durham Carbon Model demonstrated that DOC flux was affected by slope-scale variation in DOC concentration, suggesting that results from field monitoring should be transferred into mass balance models of peatland

carbon cycling. However, CO_2 flux had the largest impact upon the carbon budget, showing a considerable decrease in the R_{eco} and particularly P_G flux on the top-slope compared to the mid-slope and bottom-slope. Results demonstrated the importance of CO_2 flux to the overall carbon budget and the necessity of accurately accounting for slope-scale variation. Despite the importance of slope-scale variation in WTD, current modelling techniques were insensitive to changes in slope position and WTD was not an adequate proxy to derive fluxes of particulate organic carbon and CH_4.

7.4 Limitations of the dataset

A number of limitations have been discussed in individual chapters concerning principal issues with the research of those chapters. Some key issues affecting data across this thesis are discussed here:

- When installing plots, disturbance of vegetation and roots was unavoidable, particularly when inserting gas collars. To minimise the impact equipment installation had upon measurements, a minimum of one month was left between installation of study plots and the start of WTD and CO_2 monitoring, as well as water sample collection. This allowed a period of settling and equilibration, while the health of vegetation was observed by the author to be good throughout the study period during visual inspection of collars on a monthly basis.
- Working in upland environments can be challenging, with the functionality of equipment sometimes temperamental. For instance, the infra-red gas analysers (IRGAs) used to measure CO_2 fluxes were prone to power failures, particularly in winter when cold temperatures utilised the power from internal and external batteries at a quicker rate. Consequently, equipment failure sometimes occurred leading to data

gaps. The experimental design of six replicate plots mitigated against this for the experiment in Chapter 2, but increasing the number of sampling points down the hillslope in the transect study meant only three replicate plots were used per slope position. As such, equipment failure did impact the quality of the CO_2 dataset more severely than in the Chapter 2 study.

7.5 Recommendations for future work

Suggestions for further work have been presented in individual chapters based upon the research projects undertaken in each chapter. This section shall discuss possible areas of research when addressing the wider implications when bringing results together from across the thesis. One of the major themes suggested by research in this thesis was the importance of hillslope position to hydrology and DOC production and transport. Dissolved organic carbon concentrations were greatest in soil pore water and 10 cm water, with dilution occurring in surface runoff water. Water table depth was important, with an increase in DOC concentration observed where water tables were lower. Results from absorbance at 400 nm and specific absorbance suggested more humic substances were present in deeper soil pore water samples on the Alport Low mid-slope, which provided an end-member on soil pore water trend lines. Despite this, use of E4:E6 ratios as a compositional measure proved unsatisfactory and despite the importance of different soil pore water and runoff water sources, the composition and residence time of DOC could only be speculated rather than quantified.

There are several methods by which the residence time of water samples and the composition of DOC can be measured. Use of stable isotopes can provide information regarding the residence time of water and whether the water is old or new. Laudon et al. (2004) used $\delta^{18}O$ to analyse soil, stream and groundwater draining a forested catchment in

northern Sweden during snowmelt. Deep groundwater was shown to be isotopically lighter than unsaturated soil water and shallow groundwater, while stream water became lighter following the onset of snowmelt, due to the influx of snowmelt water. Laudon et al. (2004) were also able to show that deep soil water and deep groundwater remained unaffected by infiltrating snowmelt, contributing to baseflow but not to peak discharge. McGlynn and McDonnell (2003) combined use of $\delta^{18}O$ and silica concentrations to separate old water in the catchment prior to a storm event and new water associated with rainfall during a storm event; combining silica with $\delta^{18}O$ enabled a further distinction between old hillslope and old riparian water as well as new water. As such, isotope data can be used to distinguish different water sources and the origin of water samples relative to event water.

Use of oxygen isotopes has also been combined with DOC data to enhance the interpretation of DOC concentration and flux patterns (Laudon et al., 2011). Laudon et al. (2011) found that precipitation affected isotopic composition in a wetland area in surface runoff and at two metres depth. Dissolved organic carbon concentrations were also shown to be high in wetland-dominated streams during baseflow conditions and declined during peak discharge, related to dilution from event water as overland flow and from two metres depth through preferential flowpaths, as indicated by the distinct isotopic trends at those sample depths (Laudon et al., 2011). The use of $\delta^{18}O$ has been questioned as insensitive when residence times extend beyond four years (Stewart et al., 2010) but mean residence time (MRT) decreases with increasing percentage of responsive soils such as with peat-dominated soils (Soulsby and Tetzlaff, 2008), which further reduces uncertainty as well. Indeed, Soulsby and Tetzlaff (2008) found MRT in catchments dominated by responsive soils was 2 – 4 months, while more free-draining soils had MRTs of 10 – 14 months. Thus use of isotopic data can be successfully applied to relate rainfall, runoff and DOC patterns together and would further enhance understanding of hydrological processes and biogeochemical cycling on the hillslope.

It is important to not only interpret the relationship between DOC and water cycling to hydrology but also the origin and composition of DOC. Palmer et al. (2001) used $\delta^{13}C$ and ^{14}C ages to show that stream water DOC in Brocky Burn, north east Scotland, was related to terrestrial sources while the younger age of ^{14}C in soil pore water relative to soil organic matter suggested a supply of young DOC from near surface soil pore water to Brocky Burn. Other methods such as fluorescence spectroscopy can prove useful as well; Strohmeier et al. (2013) used excitation-emission matrices from fluorescence to compare DOC quality in various source compartments to that of runoff. Riparian wetland soil water DOC and runoff DOC was separated from that of groundwater and upstream runoff sources, suggesting riparian wetland soils were the main source of DOC in runoff during both high and low flow (Strohmeier et al., 2013).

Fluorescence techniques have also been used to: assess the quality of DOC and derive humification indices (Höll et al., 2009); to establish peaks with fulvic and humic acids, tryptophan-like substances and levels of aromaticity (Baker et al., 2008); and relate humification and aromatic structures to substrate quality and its effect on CO_2 efflux (Glatzel et al., 2003). Using fluorescence spectroscopy would prove useful in determining changes in the composition of DOC across the hillslope, to determine how it changes with WTD such as on the Alport Low mid-slope where soil pore water samples came from much deeper depths, but also to compare how DOC composition changes between soil pore water and runoff water. E4:E6 ratio proved a poor compositional measure and fluorescence spectroscopy would prove valuable in determining what the differences between soil pore water, runoff and stream water are. A study assessing how DOC age varies along the hillslope and how DOC is broken down and undergoes compositional changes over short time-scales would improve understanding of DOC production and cycling.

This thesis has focused upon carbon cycling when assessing peatland water quality, determining DOC concentrations in soil pore water, runoff water and stream water samples. However, there are a variety of water quality issues from streams draining peatland catchments, particularly in upland areas such as the South Pennines where atmospheric deposition has resulted in considerable levels of pollution in the peat profile, such as with heavy metals (Rothwell et al., 2007, Rothwell et al., 2008). Indeed, given that slope position is important to DOC concentrations, metal concentrations may also vary across the slope as As, Pb, Al and Fe positively correlate to DOC (Rothwell et al., 2009, Knorr, 2013). Aluminium (Muller and Tankéré-Muller, 2012) and Pb (Rothwell et al., 2007) have been shown to display strong sorption to DOC. As such, although stream export and, in areas such as the Peak District reservoirs for drinking-water supplies, are of ultimate importance to water quality, understanding cycling of various water quality parameters could be improved by quantifying variation across the hillslope for different water source types such as soil pore water, surface runoff water and its delivery to the riparian zone and stream.

Appendices

The appendices are provided on a CD. A brief outline of each appendix is provided below:

Appendix A

Appendix A contains data files used in Chapter 2:

- 2010-11 All data: This file contains four spreadsheets: Water table depth (WTD) & Environmental data; CO_2 flux data; soil pore water chemistry; and runoff water chemistry. Each spreadsheet includes site, slope position, sub-slope, plot and month designations. Covariates are also included. Each spreadsheet contains: raw untransformed data; untransformed data with values outside three standard deviations removed; natural-log transformed data; and natural-log transformed data with values outside three standard deviations removed. For the CO_2 flux and soil pore water chemistry spreadsheets, the untransformed or natural-log transformed environmental variables used in analysis of covariance (ANCOVA) are also included.
- 2010-11 Data by slope: This file contains four spreadsheets, one for each slope position (top-slope, upper mid-slope, lower mid-slope, bottom-slope). The data contains the WTD, CO_2 flux and soil pore water variables used in multiple linear regression.
- Chi squared: This file contains the raw runoff water observation data and the chi squared statistics and *post hoc* test results.
- 2010-11 vegetation surveys: Separate files for Alport Low and Featherbed Moss vegetation surveys, including individual spreadsheets for all slope positions and a summary spreadsheet. Each spreadsheet includes a legend with a key of denotations.

Appendix B

Appendix B contains data files used in Chapter 3:

- Compositional data: Contains soil core and substrate spreadsheets. Includes raw data, data minus outlying values and natural-log transformed data.
- TGA dataset: Includes all TGA weight loss data between 10 degree weight loss steps from 180 – 190 °C onwards and a spreadsheet of the variables used in principal components analysis (PCA) and the principal components (PCs) derived from analysis.
- Composition multivariate PCA: Contains the dataset used in multivariate PCA, including z-transformed data and PCs. Only the final dataset used is shown – all rows of data without a complete multivariate dataset have been removed. The file includes matrix plots of TG PC2 and TG PC3 and the significant variables in regression analysis.
- Organic matter covariates: This file contains the average values for top 20 cm soil core data and litter data used as covariates in Chapter 2 ANOVA. Data is identified by site, slope position and sub-slope, so they can be added to the datasets in Appendix A for each sub-slope on Featherbed Moss and Alport Low.

Appendix C

Appendix C contains data files used in Chapter 4:

- 2011-12 All data: Contains the raw WTD, CO_2 flux, environmental, soil pore water, runoff water, stream water and water type (used in water type ANOVA) data. The file also included natural-log transformed data and data minus outlying values used in ANOVA.

- Year 1 & 2 CO_2 data: Contains the raw data, natural-log transformed data and data minus outlying values used in ANOVA of CO_2 fluxes for slope positions 1-E, 1-H and 4 that were used in both Chapter 2 and Chapter 4.
- 2011-12 Transect vegetation survey: Vegetation survey from November 2012, from which the percentage *Eriophorum spp.* covariate was derived. This file has spreadsheets for the 12 slope positions and a summary spreadsheet.
- 2011-12 Chi squared: Contains two files, one for runoff water and one for 10 cm water. Contains raw observation data by slope position and the chi squared results.

Appendix D

Appendix D contains the files used in Chapter 5:

- Water chemistry PCA: Spreadsheets for 2010-11 and 2011-12 PCA that include z-transformed data and PCs. Only the final datasets used are provided - all data gaps have been removed. 2011-12 10 cm water raw water chemistry is also included.
- Tracer study anion data: This file contains the raw anion data used in the tracer study.
- Tracer study chi squared: This file contains the raw data for runoff water and 10 cm water observations and the chi squared results for both.

Appendix E

Appendix E contains the data file used in Chapter 6:

- Relative WTD: Contains Chapter 2 WTD, converted into relative data after making all values negative. Data was used in Durham Carbon Model correction factors. Natural-log transformed data used and ANOVA main effects re-normalised prior to use in DCM.

References

ADAMSON, J. K., SCOTT, W. A., ROWLAND, A. P. & BEARD, G. R. 2001. Ionic concentrations in a blanket peat bog in northern England and correlations with deposition and climate variables. *European Journal of Soil Science,* 52**,** 69-79.

AITKENHEAD, J. A. & MCDOWELL, W. H. 2000. Soil C : N ratio as a predictor of annual riverine DOC flux at local and global scales. *Global Biogeochemical Cycles,* 14**,** 127-138.

AITKENHEAD-PETERSON, J. A., SMART, R. P., AITKENHEAD, M. J., CRESSER, M. S. & MCDOWELL, W. H. 2007. Spatial and temporal variation of dissolved organic carbon export from gauged and ungauged watersheds of Dee Valley, Scotland: Effect of land cover and C : N. *Water Resources Research,* 43.

ALLOTT, T. E. H., EVANS, M. G., LINDSAY, J. B., AGNEW, C. T., FREER, J. E., JONES, A. & PARNELL, M. 2009. Water table in Peak District blanket peatlands: Moors for the Future Report No 17.

ALM, J., SCHULMAN, L., WALDEN, J., NYKANEN, H., MARTIKAINEN, P. J. & SILVOLA, J. 1999. Carbon balance of a boreal bog during a year with an exceptionally dry summer. *Ecology,* 80**,** 161-174.

ALM, J., TALANOV, A., SAARNIO, S., SILVOLA, J., IKKONEN, E., AALTONEN, H., NYKANEN, H. & MARTIKAINEN, P. J. 1997. Reconstruction of the carbon balance for microsites in a boreal oligotrophic pine fen, Finland. *Oecologia,* 110**,** 423-431.

ALMENDROS, G., KNICKER, H. & GONZALEZ-VILA, F. J. 2003. Rearrangement of carbon and nitrogen forms in peat after progressive thermal oxidation as determined by solid-state C-13 and N-15-NMR spectroscopy. *Organic Geochemistry,* 34**,** 1559-1568.

ALMENDROS, G., POLO, A. & VIZCAYNO, C. 1982. APPLICATION OF THERMAL-ANALYSIS TO THE STUDY OF SEVERAL SPANISH PEATS. *Journal of Thermal Analysis,* 24**,** 175-182.

ANDERSON, A. E., WEILER, M., ALILA, Y. & HUDSON, R. O. 2009. Subsurface flow velocities in a hillslope with lateral preferential flow. *Water Resources Research,* 45**,** 15.

ANDERSON, D. E. 2002. Carbon accumulation and C/N ratios of peat bogs in North-West Scotland. *Scottish Geographical Journal,* 118**,** 323-341.

ANDERSON, M. G. & BURT, T. P. 1978. ROLE OF TOPOGRAPHY IN CONTROLLING THROUGHFLOW GENERATION. *Earth Surface Processes and Landforms,* 3**,** 331-344.

ANDERSSON, R. A., MEYERS, P., HORNIBROOK, E., KUHRY, P. & MORTH, C.-M. 2012. Elemental and isotopic carbon and nitrogen records of organic matter accumulation in a Holocene permafrost peat sequence in the East European Russian Arctic. *Journal of Quaternary Science,* 27**,** 545-552.

BAHN, M., REICHSTEIN, M., DAVIDSON, E. A., GRUNZWEIG, J., JUNG, M., CARBONE, M. S., EPRON, D., MISSON, L., NOUVELLON, Y., ROUPSARD, O., SAVAGE, K., TRUMBORE, S. E., GIMENO, C., YUSTE, J. C., TANG, J., VARGAS, R. & JANSSENS, I. A. 2010. Soil respiration at mean annual temperature predicts annual total across vegetation types and biomes. *Biogeosciences,* 7**,** 2147-2157.

BAIRD, A., BECKWITH, C. & HEATHWAITE, L. 1997. Water management in undamaged blanket peats. *In:* TALLIS, J. H., MEADE, R. & HULME, P. D. (eds.) *Blanket mire degradation: causes, consequences and challenges: proceedings: University of Manchester 9 -11 April 1997.* Aberdeen: The Macaulay Land Use Research Institute.

BAIRD, A. J., EADES, P. A. & SURRIDGE, B. W. J. 2008. The hydraulic structure of a raised bog and its implications for ecohydrological modelling of bog development. *Ecohydrology,* 1**,** 289-298.

BAIRD, A. J. & GAFFNEY, S. W. 2000. Solute movement in drained fen peat: a field tracer study in a Somerset (UK) wetland. *Hydrological Processes,* 14**,** 2489-2503.

BAKER, A., TIPPING, E., THACKER, S. A. & GONDAR, D. 2008. Relating dissolved organic matter fluorescence and functional properties. *Chemosphere,* 73**,** 1765-1772.

BALDOCK, J. A., MASIELLO, C. A., GELINAS, Y. & HEDGES, J. I. 2004. Cycling and composition of organic matter in terrestrial and marine ecosystems. *Marine Chemistry,* 92**,** 39-64.

BARROS, N., SALGADO, J. & FEIJOO, S. 2007. Calorimetry and soil. *Thermochimica Acta,* 458**,** 11-17.

BARTLETT, R. J. & ROSS, D. S. 1988. COLORIMETRIC DETERMINATION OF OXIDIZABLE CARBON IN ACID SOIL SOLUTIONS. *Soil Science Society of America Journal,* 52**,** 1191-1192.

BECKWITH, C. W., BAIRD, A. J. & HEATHWAITE, A. L. 2003. Anisotropy and depth-related heterogeneity of hydraulic conductivity in a bog peat. I: laboratory measurements. *Hydrological Processes,* 17**,** 89-101.

BERGLUND, O. & BERGLUND, K. 2011. Influence of water table level and soil properties on emissions of greenhouse gases from cultivated peat soil. *Soil Biology & Biochemistry,* 43**,** 923-931.

BERGNER, K. & ALBANO, C. 1993. THERMAL-ANALYSIS OF PEAT. *Analytical Chemistry,* 65**,** 204-208.

BILLETT, M. F., CHARMAN, D. J., CLARK, J. M., EVANS, C. D., EVANS, M. G., OSTLE, N. J., WORRALL, F., BURDEN, A., DINSMORE, K. J., JONES, T., MCNAMARA, N. P., PARRY, L., ROWSON, J. G. & ROSE, R. 2010. Carbon balance of UK peatlands: current state of knowledge and future research challenges. *Climate Research,* 45**,** 13-29.

BILLETT, M. F., DEACON, C. M., PALMER, S. M., DAWSON, J. J. C. & HOPE, D. 2006. Connecting organic carbon in stream water and soils in a peatland catchment. *Journal of Geophysical Research-Biogeosciences,* 111.

BILLETT, M. F., DINSMORE, K. J., SMART, R. P., GARNETT, M. H., HOLDEN, J., CHAPMAN, P., BAIRD, A. J., GRAYSON, R. & STOTT, A. W. 2012. Variable source and age of different forms of carbon released from natural peatland pipes. *Journal of Geophysical Research-Biogeosciences,* 117**,** 16.

BILLETT, M. F., PALMER, S. M., HOPE, D., DEACON, C., STORETON-WEST, R., HARGREAVES, K. J., FLECHARD, C. & FOWLER, D. 2004. Linking land-atmosphere-stream carbon fluxes in a lowland peatland system. *Global Biogeochemical Cycles,* 18**,** 12.

BLODAU, C. & SIEMS, M. 2012. Drainage-induced forest growth alters belowground carbon biogeochemistry in the Mer Bleue bog, Canada. *Biogeochemistry,* 107**,** 107-123.

BOND-LAMBERTY, B., WANG, C. K. & GOWER, S. T. 2004. A global relationship between the heterotrophic and autotrophic components of soil respiration? *Global Change Biology,* 10**,** 1756-1766.

BORTOLUZZI, E., EPRON, D., SIEGENTHALER, A., GILBERT, D. & BUTTLER, A. 2006. Carbon balance of a European mountain bog at contrasting stages of regeneration. *New Phytologist,* 172**,** 708-718.

BOWER, M. M. 1961. THE DISTRIBUTION OF EROSION IN BLANKET PEAT BOGS IN THE PENNINES. *Transactions of the Institute of British Geographers***,** 17-30.

BOYER, E. W., HORNBERGER, G. M., BENCALA, K. E. & MCKNIGHT, D. M. 1997. Response characteristics of DOC flushing in an alpine catchment. *Hydrological Processes,* 11**,** 1635-1647.

BRAGAZZA, L., FREEMAN, C., JONES, T., RYDIN, H., LIMPENS, J., FENNER, N., ELLIS, T., GERDOL, R., HAJEK, M., HAJEK, T., LACUMIN, P., KUTNAR, L., TAHVANAINEN, T. & TOBERMAN, H. 2006. Atmospheric nitrogen deposition promotes carbon loss from peat bogs. *Proceedings of the National Academy of Sciences of the United States of America,* 103**,** 19386-19389.

BRAGG, O. M. 2002. Hydrology of peat-forming wetlands in Scotland. *Science of the Total Environment,* 294**,** 111-129.

BUBIER, J. L., BHATIA, G., MOORE, T. R., ROULET, N. T. & LAFLEUR, P. M. 2003. Spatial and temporal variability in growing-season net ecosystem carbon dioxide exchange at a large peatland in Ontario, Canada. *Ecosystems,* 6**,** 353-367.

BUBIER, J. L., CRILL, P. M., MOORE, T. R., SAVAGE, K. & VARNER, R. K. 1998. Seasonal patterns and controls on net ecosystem CO2 exchange in a boreal peatland complex. *Global Biogeochemical Cycles,* 12**,** 703-714.

BURROWS, E. H., BUBIER, J. L., MOSEDALE, A., COBB, G. W. & CRILL, P. M. 2005. Net ecosystem exchange of carbon dioxide in a temperate poor fen: a comparison of automated and manual chamber techniques. *Biogeochemistry,* 76**,** 21-45.

BURT, T., LABADZ, J. & BUTCHER, D. 1997. The hydrology and fluvial geomorphology of blanket peat: implications for integrated catchment management. *In:* TALLIS, J. H., MEADE, R. & HULME, P. D. (eds.) *Blanket mire degradation: causes, consequences and challenges: proceedings, University of Manchester 9 -11 April 1997.* Aberdeen: The Macaulay Land Use Research Institute.

BURT, T. P. & PINAY, G. 2005. Linking hydrology and biogeochemistry in complex landscapes. *Progress in Physical Geography,* 29**,** 297-316.

CANNELL, M. G. R., MILNE, R., HARGREAVES, K. J., BROWN, T. A. W., CRUICKSHANK, M. M., BRADLEY, R. I., SPENCER, T., HOPE, D., BILLETT, M. F., ADGER, W. N. & SUBAK, S. 1999. National inventories of terrestrial carbon sources and sinks: The UK experience. *Climatic Change,* 42**,** 505-530.

CAPELL, R., TETZLAFF, D., MALCOLM, I. A., HARTLEY, A. J. & SOULSBY, C. 2011. Using hydrochemical tracers to conceptualise hydrological function in a larger scale catchment draining contrasting geologic provinces. *Journal of Hydrology,* 408**,** 164-177.

CAPREZ, R., NIKLAUS, P. A. & KORNER, C. 2012. Forest soil respiration reflects plant productivity across a temperature gradient in the Alps. *Oecologia,* 170**,** 1143-1154.

CASTELLANO, M. J., LEWIS, D. B. & KAYE, J. P. 2013. Response of soil nitrogen retention to the interactive effects of soil texture, hydrology, and organic matter. *Journal of Geophysical Research-Biogeosciences,* 118**,** 280-290.

CHAPMAN, P. J., PALMER, S. M., IRVINE, B. J., MITCHELL, G. & MCDONALD, A. T. 2012. A response to 'Changes in water colour between 1986 and 2006 in the headwaters of the River Nidd, Yorkshire, UK: a critique of methodological approaches and measurement of burning management' by Yallop et al. *Biogeochemistry,* 111**,** 105-109.

CHARMAN, D. J. 2002. *Peatlands and environmental change,* Chichester, Wiley.

CHEN, H., ZHAO, W. & LIU, N. 2011. Thermal Analysis and Decomposition Kinetics of Chinese Forest Peat under Nitrogen and Air Atmospheres. *Energy & Fuels,* 25**,** 797-803.

CLAIR, T. A., POLLOCK, T. L. & EHRMAN, J. M. 1994. EXPORTS OF CARBON AND NITROGEN FROM RIVER BASINS IN CANADAS ATLANTIC PROVINCES. *Global Biogeochemical Cycles,* 8**,** 441-450.

CLARK, J. M., ASHLEY, D., WAGNER, M., CHAPMAN, P. J., LANE, S. N., EVANS, C. D. & HEATHWAITE, A. L. 2009. Increased temperature sensitivity of net DOC production from ombrotrophic peat due to water table draw-down. *Global Change Biology,* 15**,** 794-807.

CLARK, J. M., BILLETT, M. F., COYLE, M., CROFT, S., DANIELS, S., EVANS, C. D., EVANS, M., FREEMAN, C., GALLEGO-SALA, A. V., HEINEMEYER, A., HOUSE, J. I., MONTEITH, D. T., NAYAK, D., ORR, H. G., PRENTICE, I. C., ROSE, R., ROWSON, J., SMITH, J. U., SMITH, P., TUN, Y. M., VANGUELOVA, E., WETTERHALL, F. & WORRALL, F. 2010a. Model inter-comparison between statistical and dynamic model assessments of the long-term stability of blanket peat in Great Britain (1940-2099). *Climate Research,* 45**,** 227-U281.

CLARK, J. M., BOTTRELL, S. H., EVANS, C. D., MONTEITH, D. T., BARTLETT, R., ROSE, R., NEWTON, R. J. & CHAPMAN, P. J. 2010b. The importance of the relationship between scale and process in understanding long-term DOC dynamics. *Science of the Total Environment,* 408**,** 2768-2775.

CLARK, J. M., CHAPMAN, P. J., ADAMSON, J. K. & LANE, S. N. 2005. Influence of drought-induced acidification on the mobility of dissolved organic carbon in peat soils. *Global Change Biology,* 11**,** 791-809.

CLARK, J. M., GALLEGO-SALA, A. V., ALLOTT, T. E. H., CHAPMAN, S. J., FAREWELL, T., FREEMAN, C., HOUSE, J. I., ORR, H. G., PRENTICE, I. C. & SMITH, P. 2010c. Assessing the vulnerability of blanket peat to climate change using an ensemble of statistical bioclimatic envelope models. *Climate Research,* 45**,** 131-U462.

CLARK, J. M., HEINEMEYER, A., MARTIN, P. & BOTTRELL, S. H. 2012. Processes controlling DOC in pore water during simulated drought cycles in six different UK peats. *Biogeochemistry,* 109**,** 253-270.

CLARK, J. M., LANE, S. N., CHAPMAN, P. J. & ADAMSON, J. K. 2008. Link between DOC in near surface peat and stream water in an upland catchment. *Science of the Total Environment,* 404**,** 308-315.

CLAY, G. D., DIXON, S., EVANS, M. G., ROWSON, J. G. & WORRALL, F. 2012. Carbon dioxide fluxes and DOC concentrations of eroding blanket peat gullies. *Earth Surface Processes and Landforms,* 37**,** 562-571.

CLAY, G. D. & WORRALL, F. 2011. Charcoal production in a UK moorland wildfire - How important is it? *Journal of Environmental Management,* 92**,** 676-682.

CLAY, G. D., WORRALL, F., CLARK, E. & FRASER, E. D. G. 2009a. Hydrological responses to managed burning and grazing in an upland blanket bog. *Journal of Hydrology,* 376**,** 486-495.

CLAY, G. D., WORRALL, F. & FRASER, E. D. G. 2009b. Effects of managed burning upon dissolved organic carbon (DOC) in soil water and runoff water following a managed burn of a UK blanket bog. *Journal of Hydrology,* 367**,** 41-51.

CLAY, G. D., WORRALL, F. & FRASER, E. D. G. 2010a. Compositional changes in soil water and runoff water following managed burning on a UK upland blanket bog. *Journal of Hydrology,* 380**,** 135-145.

CLAY, G. D., WORRALL, F. & ROSE, R. 2010b. Carbon budgets of an upland blanket bog managed by prescribed fire. *Journal of Geophysical Research-Biogeosciences,* 115**,** 14.

CLUTTERBUCK, B. & YALLOP, A. R. 2010. Land management as a factor controlling dissolved organic carbon release from upland peat soils 2 Changes in DOC productivity over four decades. *Science of the Total Environment,* 408**,** 6179-6191.

CLYMO, R. S. 1992. Models of peat growth. *Suo (Helsinki),* 43**,** 127-136.

CLYMO, R. S. 2004. Hydraulic conductivity of peat at Ellergower Moss, Scotland. *Hydrological Processes,* 18**,** 261-274.

CLYMO, R. S. & PEARCE, D. M. E. 1995. METHANE AND CARBON-DIOXIDE PRODUCTION IN, TRANSPORT THROUGH, AND EFFLUX FROM A PEATLAND. *Philosophical Transactions of the Royal Society a-Mathematical Physical and Engineering Sciences,* 351**,** 249-259.

COGGINS, A. M., JENNINGS, S. G. & EBINGHAUS, R. 2006. Accumulation rates of the heavy metals lead, mercury and cadmium in ombrotrophic peatlands in the west of Ireland. *Atmospheric Environment,* 40**,** 260-278.

CONACHER, A. J. & DALRYMPLE, J. B. 1977. 9 UNIT LAND-SURFACE MODEL - APPROACH TO PEDOGEOMORPHIC RESEARCH. *Geoderma,* 18**,** 1-154.

CORY, N., LAUDON, H., KOEHLER, S., SEIBERT, J. & BISHOP, K. 2007. Evolution of soil solution aluminum during transport along a forested boreal hillslope. *Journal of Geophysical Research-Biogeosciences,* 112.

COULSON, J. P., BOTTRELL, S. H. & LEE, J. A. 2005. Recreating atmospheric sulphur deposition histories from peat stratigraphy: Diagenetic conditions required for signal preservation and reconstruction of past sulphur deposition in the Derbyshire Peak District, UK. *Chemical Geology,* 218**,** 223-248.

CREED, I. F., WEBSTER, K. L., BRAUN, G. L., BOURBONNIERE, R. A. & BEALL, F. D. 2013. Topographically regulated traps of dissolved organic carbon create hotspots of soil carbon dioxide efflux in forests. *Biogeochemistry,* 112**,** 149-164.

CROW, S. E. & WIEDER, R. K. 2005. Sources of Co-2 emission from a northern peatland: Root respiration, exudation, and decomposition. *Ecology,* 86**,** 1825-1834.

DALVA, M., MOORE, T. R., ARP, P. & CLAIR, T. A. 2001. Methane and soil and plant community respiration from wetlands, Kejimkujik National Park, Nova Scotia: Measurements, predictions, and climatic change. *Journal of Geophysical Research-Atmospheres,* 106**,** 2955-2962.

DANIELS, S. M., AGNEW, C. T., ALLOTT, T. E. H. & EVANS, M. G. 2008a. Water table variability and runoff generation in an eroded peatland, South Pennines, UK. *Journal of Hydrology,* 361**,** 214-226.

DANIELS, S. M., EVANS, M. G., AGNEW, C. T. & ALLOTT, T. E. H. 2008b. Sulphur leaching from headwater catchments in an eroded peatland, South Pennines, U.K. *Science of the Total Environment,* 407**,** 481-496.

DANIELS, S. M., EVANS, M. G., AGNEW, C. T. & ALLOTT, T. E. H. 2012. Ammonium release from a blanket peatland into headwater stream systems. *Environmental Pollution,* 163**,** 261-272.

DE LA ROSA ARRANZ, J. M., GONZALEZ-VILA, F. J., LOPEZ-CAPEL, E., MANNING, D. A. C., KNICKER, H. & ANTONIO GONZALEZ-PEREZ, J. 2009. Structural properties of non-combustion-derived refractory organic matter which interfere with BC quantification. *Journal of Analytical and Applied Pyrolysis,* 85**,** 399-407.

DEFRA 2013. UKEAP River Etherow 2010 - 2012 precipitation water chemistry. © Crown 2013 copyright Defra via uk-air.defra.gov.uk, licenced under the http://www.nationalarchives.gov.uk/doc/open-government-licence/version/2/.

DINSMORE, K. J., BILLETT, M. F. & DYSON, K. E. 2013. Temperature and precipitation drive temporal variability in aquatic carbon and GHG concentrations and fluxes in a peatland catchment. *Global Change Biology,* 19**,** 2133-2148.

DINSMORE, K. J., BILLETT, M. F., SKIBA, U. M., REES, R. M., DREWER, J. & HELFTER, C. 2010. Role of the aquatic pathway in the carbon and greenhouse gas budgets of a peatland catchment. *Global Change Biology,* 16**,** 2750-2762.

DIXON, S. D. 2012. *Controls on carbon cycling in upland blanket peat soils.* PhD Thesis, Durham University Library.

DOMISCH, T., FINER, L., LAINE, J. & LAIHO, R. 2006. Decomposition and nitrogen dynamics of litter in peat soils from two climatic regions under different temperature regimes. *European Journal of Soil Biology,* 42**,** 74-81.

DORREPAAL, E., TOET, S., VAN LOGTESTIJN, R. S. P., SWART, E., VAN DE WEG, M. J., CALLAGHAN, T. V. & AERTS, R. 2009. Carbon respiration from subsurface peat accelerated by climate warming in the subarctic. *Nature,* 460**,** 616-U79.

DUNN, A. L., WOFSY, S. C. & BRIGHT, A. V. 2009. Landscape heterogeneity, soil climate, and carbon exchange in a boreal black spruce forest. *Ecological Applications,* 19**,** 495-504.

EVANS, C. D., JONES, T. G., BURDEN, A., OSTLE, N., ZIELINSKI, P., COOPER, M. D. A., PEACOCK, M., CLARK, J. M., OULEHLE, F., COOPER, D. & FREEMAN, C. 2012. Acidity controls on dissolved organic carbon mobility in organic soils. *Global Change Biology,* 18**,** 3317-3331.

EVANS, M. & LINDSAY, J. 2010a. High resolution quantification of gully erosion in upland peatlands at the landscape scale. *Earth Surface Processes and Landforms,* 35**,** 876-886.

EVANS, M. & LINDSAY, J. 2010b. Impact of gully erosion on carbon sequestration in blanket peatlands. *Climate Research,* 45**,** 31-41.

EVANS, M. G., BURT, T. P., HOLDEN, J. & ADAMSON, J. K. 1999. Runoff generation and water table fluctuations in blanket peat: evidence from UK data spanning the dry summer of 1995. *Journal of Hydrology,* 221**,** 141-160.

FENNER, N., OSTLE, N., FREEMAN, C., SLEEP, D. & REYNOLDS, B. 2004. Peatland carbon afflux partitioning reveals that Sphagnum photosynthate contributes to the DOC pool. *Plant and Soil,* 259**,** 345-354.

FLEISS, J. L., LEVIN, B. & PAIK, M. C. 2003. Statistical Methods for Rates and Proportions. Third ed. New Jersey: John Wiley & Sons.

FONTAINE, S., BAROT, S., BARRE, P., BDIOUI, N., MARY, B. & RUMPEL, C. 2007. Stability of organic carbon in deep soil layers controlled by fresh carbon supply. *Nature,* 450**,** 277-U10.

FREEMAN, C., EVANS, C. D., MONTEITH, D. T., REYNOLDS, B. & FENNER, N. 2001a. Export of organic carbon from peat soils. *Nature,* 412**,** 785-785.

FREEMAN, C., OSTLE, N. & KANG, H. 2001b. An enzymic 'latch' on a global carbon store - A shortage of oxygen locks up carbon in peatlands by restraining a single enzyme. *Nature,* 409**,** 149-149.

FREEMAN, T. G. 1991. CALCULATING CATCHMENT-AREA WITH DIVERGENT FLOW BASED ON A REGULAR GRID. *Computers & Geosciences,* 17**,** 413-422.

GARY, C., FROSSARD, J. S. & CHENEVARD, D. 1995. HEAT OF COMBUSTION, DEGREE OF REDUCTION AND CARBON CONTENT .3. INTERRELATED METHODS OF ESTIMATING THE CONSTRUCTION COST OF PLANT-TISSUES. *Agronomie,* 15**,** 59-69.

GAZOVIC, M., FORBRICH, I., JAGER, D. F., KUTZBACH, L., WILLE, C. & WILMKING, M. 2013. Hydrology-driven ecosystem respiration determines the carbon balance of a boreal peatland. *The Science of the total environment,* 463-464**,** 675-82.

GEBAUER, R. L. E., REYNOLDS, J. F. & TENHUNEN, J. D. 1998. Diurnal patterns of CO2 and H2O exchange of the Arctic sedges Eriophorum angustifolium and E-vaginatum (Cyperaceae). *American Journal of Botany,* 85**,** 592-599.

GIBSON, H. S., WORRALL, F., BURT, T. P. & ADAMSON, J. K. 2009. DOC budgets of drained peat catchments: implications for DOC production in peat soils. *Hydrological Processes,* 23**,** 1901-1911.

GILLEY, J. E., FINKNER, S. C., DORAN, J. W. & KOTTWITZ, E. R. 1990. Adsorption of bromide tracers onto sediment. *Applied Engineering in Agriculture,* 6**,** 35-38.

GLATZEL, S., KALBITZ, K., DALVA, M. & MOORE, T. 2003. Dissolved organic matter properties and their relationship to carbon dioxide efflux from restored peat bogs. *Geoderma,* 113**,** 397-411.

GONDAR, D., LOPEZ, R., FIOL, S., ANTELO, J. M. & ARCE, F. 2005. Characterization and acid-base properties of fulvic and humic acids isolated from two horizons of an ombrotrophic peat bog. *Geoderma,* 126**,** 367-374.

GRANIERO, P. A. & PRICE, J. S. 1999. Distribution of bog and heath in a Newfoundland blanket bog complex: topographic limits on the hydrological processes governing blanket bog development. *Hydrology and Earth System Sciences,* 3**,** 223-231.

HARDIE, S. M. L., GARNETT, M. H., FALLICK, A. E., ROWLAND, A. P., OSTLE, N. J. & FLOWERS, T. H. 2011. Abiotic drivers and their interactive effect on the flux and carbon isotope (C-14 and delta C-13) composition of peat-respired CO2. *Soil Biology & Biochemistry,* 43**,** 2432-2440.

HEATHWAITE, A. L. 1993. DISAPPEARING PEAT REGENERATING PEAT - THE IMPACT OF CLIMATE-CHANGE ON BRITISH PEATLANDS. *Geographical Journal,* 159**,** 203-208.

HEDIN, L. O., VON FISCHER, J. C., OSTROM, N. E., KENNEDY, B. P., BROWN, M. G. & ROBERTSON, G. P. 1998. Thermodynamic constraints on nitrogen transformations and other biogeochemical processes at soil-stream interfaces. *Ecology,* 79**,** 684-703.

HEINEMEYER, A., CROFT, S., GARNETT, M. H., GLOOR, E., HOLDEN, J., LOMAS, M. R. & INESON, P. 2010. The MILLENNIA peat cohort model: predicting past, present and future soil carbon budgets and fluxes under changing climates in peatlands. *Climate Research,* 45**,** 207-226.

HELLER, C. & ZEITZ, J. 2012. Stability of soil organic matter in two northeastern German fen soils: the influence of site and soil development. *Journal of Soils and Sediments,* 12**,** 1231-1240.

HINTON, M. J., SCHIFF, S. L. & ENGLISH, M. C. 1998. Sources and flowpaths of dissolved organic carbon during storms in two forested watersheds of the Precambrian Shield. *Biogeochemistry,* 41**,** 175-197.

HOAG, R. S. & PRICE, J. S. 1995. A FIELD-SCALE, NATURAL GRADIENT SOLUTE TRANSPORT EXPERIMENT IN PEAT AT A NEWFOUNDLAND BLANKET BOG. *Journal of Hydrology,* 172**,** 171-184.

HOCKADAY, W. C., MASIELLO, C. A., RANDERSON, J. T., SMERNIK, R. J., BALDOCK, J. A., CHADWICK, O. A. & HARDEN, J. W. 2009. Measurement of soil carbon oxidation state and oxidative ratio by C-13 nuclear magnetic resonance. *Journal of Geophysical Research-Biogeosciences,* 114.

HOLDEN, J. 2005a. Controls of soil pipe frequency in upland blanket peat. *Journal of Geophysical Research-Earth Surface,* 110**,** 11.

HOLDEN, J. 2005b. Peatland hydrology and carbon release: why small-scale process matters. *Philosophical Transactions of the Royal Society a-Mathematical Physical and Engineering Sciences,* 363**,** 2891-2913.

HOLDEN, J. 2009. Topographic controls upon soil macropore flow. *Earth Surface Processes and Landforms,* 34**,** 345-351.

HOLDEN, J. & BURT, T. P. 2002a. Infiltration, runoff and sediment production in blanket peat catchments: implications of field rainfall simulation experiments. *Hydrological Processes,* 16**,** 2537-2557.

HOLDEN, J. & BURT, T. P. 2002b. Laboratory experiments on drought and runoff in blanket peat. *European Journal of Soil Science,* 53**,** 675-689.

HOLDEN, J. & BURT, T. P. 2002c. Piping and pipeflow in a deep peat catchment. *Catena,* 48**,** 163-199.

HOLDEN, J. & BURT, T. P. 2003. Hydrological studies on blanket peat: the significance of the acrotelm-catotelm model. *Journal of Ecology,* 91**,** 86-102.

HOLDEN, J., SMART, R. P., DINSMORE, K. J., BAIRD, A. J., BILLETT, M. F. & CHAPMAN, P. J. 2012. Natural pipes in blanket peatlands: major point sources for the release of carbon to the aquatic system. *Global Change Biology,* 18**,** 3568-3580.

HOLDEN, J., WALLAGE, Z. E., LANE, S. N. & MCDONALD, A. T. 2011. Water table dynamics in undisturbed, drained and restored blanket peat. *Journal of Hydrology,* 402**,** 103-114.

HOPE, D., PALMER, S. M., BILLETT, M. F. & DAWSON, J. J. C. 2001. Carbon dioxide and methane evasion from a temperate peatland stream. *Limnology and Oceanography,* 46**,** 847-857.

HUGGETT, R. J. 1975. SOIL LANDSCAPE SYSTEMS - MODEL OF SOIL GENESIS. *Geoderma,* 13**,** 1-22.

HÖLL, B. S., FIEDLER, S., JUNGKUNST, H. F., KALBITZ, K., FREIBAUER, A., DROSLER, M. & STAHR, K. 2009. Characteristics of dissolved organic matter following 20 years of peatland restoration. *Science of the Total Environment,* 408**,** 78-83.

INGRAM, H. A. P. 1978. SOIL LAYERS IN MIRES - FUNCTION AND TERMINOLOGY. *Journal of Soil Science,* 29**,** 224-227.

IRVIN, B. J., VENTURA, S. J. & SLATER, B. K. 1997. Fuzzy and isodata classification of landform elements from digital terrain data in Pleasant Valley, Wisconsin. *Geoderma,* 77**,** 137-154.

JACKSON-BLAKE, L., HELLIWELL, R. C., BRITTON, A. J., GIBBS, S., COULL, M. C. & DAWSON, L. 2012. Controls on soil solution nitrogen along an altitudinal gradient in the Scottish uplands. *Science of the Total Environment,* 431**,** 100-108.

JANSSENS, I. A., LANKREIJER, H., MATTEUCCI, G., KOWALSKI, A. S., BUCHMANN, N., EPRON, D., PILEGAARD, K., KUTSCH, W., LONGDOZ, B., GRUNWALD, T., MONTAGNANI, L., DORE, S., REBMANN, C., MOORS, E. J., GRELLE, A., RANNIK, U., MORGENSTERN, K., OLTCHEV, S., CLEMENT, R., GUDMUNDSSON, J., MINERBI, S., BERBIGIER, P., IBROM, A., MONCRIEFF, J., AUBINET, M., BERNHOFER, C., JENSEN, N. O., VESALA, T., GRANIER, A., SCHULZE, E. D., LINDROTH, A., DOLMAN, A. J., JARVIS, P. G., CEULEMANS, R. & VALENTINI, R. 2001. Productivity overshadows temperature in determining soil and ecosystem respiration across European forests. *Global Change Biology,* 7**,** 269-278.

JOOSTEN, H. 2009. The Global Peatland CO2 Picture: Peatland status and drainage related emissions in all countries of the world. *UN-FCCC.* Copenhagen: Wetlands International, Ede.

JUUTINEN, S., VALIRANTA, M., KUUTTI, V., LAINE, A. M., VIRTANEN, T., SEPPA, H., WECKSTROM, J. & TUITTILA, E. S. 2013. Short-term and long-term carbon dynamics in a northern peatland-stream-lake continuum: A catchment approach. *Journal of Geophysical Research-Biogeosciences,* 118**,** 171-183.

KECHAVARZI, C., DAWSON, Q. & LEEDS-HARRISON, P. B. 2010. Physical properties of low-lying agricultural peat soils in England. *Geoderma,* 154**,** 196-202.

KENNEY, B. C. 1982. BEWARE OF SPURIOUS SELF-CORRELATIONS. *Water Resources Research,* 18**,** 1041-1048.

KINDLER, R., SIEMENS, J., KAISER, K., WALMSLEY, D. C., BERNHOFER, C., BUCHMANN, N., CELLIER, P., EUGSTER, W., GLEIXNER, G., GRUNWALD, T., HEIM, A., IBROM, A., JONES, S. K., JONES, M., KLUMPP, K., KUTSCH, W., LARSEN, K. S., LEHUGER, S., LOUBET, B., MCKENZIE, R., MOORS, E., OSBORNE, B., PILEGAARD, K., REBMANN, C., SAUNDERS, M., SCHMIDT, M. W. I., SCHRUMPF, M., SEYFFERTH, J., SKIBA, U., SOUSSANA, J. F., SUTTON, M. A., TEFS, C., VOWINCKEL, B., ZEEMAN, M. J. & KAUPENJOHANN, M. 2011. Dissolved carbon leaching from soil is a crucial component of the net ecosystem carbon balance. *Global Change Biology,* 17**,** 1167-1185.

KLAVINS, M., SIRE, J., PURMALIS, O. & MELECIS, V. 2008. Approaches to estimating humification indicators for peat. *Mires and Peat,* 3**,** Article 7.

KNORR, K. H. 2013. DOC-dynamics in a small headwater catchment as driven by redox fluctuations and hydrological flow paths - are DOC exports mediated by iron reduction/oxidation cycles? *Biogeosciences,* 10**,** 891-904.

KOEHLER, A. K., SOTTOCORNOLA, M. & KIELY, G. 2011. How strong is the current carbon sequestration of an Atlantic blanket bog? *Global Change Biology,* 17**,** 309-319.

KOMULAINEN, V. M., TUITTILA, E. S., VASANDER, H. & LAINE, J. 1999. Restoration of drained peatlands in southern Finland: initial effects on vegetation change and CO2 balance. *Journal of Applied Ecology,* 36**,** 634-648.

KRACHT, O. & GLEIXNER, G. 2000. Isotope analysis of pyrolysis products from Sphagnum peat and dissolved organic matter from bog water. *Organic Geochemistry,* 31**,** 645-654.

KUHRY, P. & VITT, D. H. 1996. Fossil carbon/nitrogen ratios as a measure of peat decomposition. *Ecology,* 77**,** 271-275.

KVÆRNER, J. & KLØVE, B. 2006. Tracing sources of summer streamflow in boreal headwaters using isotopic signatures and water geochemical components. *Journal of Hydrology,* 331**,** 186-204.

LAFLEUR, P. M., MOORE, T. R., ROULET, N. T. & FROLKING, S. 2005. Ecosystem respiration in a cool temperate bog depends on peat temperature but not water table. *Ecosystems,* 8**,** 619-629.

LAHDESMAKI, P. & PIISPANEN, R. 1988. DEGRADATION PRODUCTS AND THE HYDROLYTIC ENZYME-ACTIVITIES IN THE SOIL HUMIFICATION PROCESSES. *Soil Biology & Biochemistry,* 20**,** 287-292.

LAIHO, R., PENTTILA, T. & LAINE, J. 2004. Variation in soil nutrient concentrations and bulk density within peatland forest sites. *Silva Fennica,* 38**,** 29-41.

LAIHO, R., SALLANTAUS, T. & LAINE, J. 1999. The effect of forestry drainage on vertical distributions of major plant nutrients in peat soils. *Plant and Soil,* 207**,** 169-181.

LAINE, A., RIUTTA, T., JUUTINEN, S., VALIRANTA, M. & TUITTILA, E.-S. 2009. Acknowledging the spatial heterogeneity in modelling/reconstructing carbon dioxide exchange in a northern aapa mire. *Ecological Modelling,* 220**,** 2646-2655.

LAINE, A., SOTTOCORNOLA, M., KIELY, G., BYRNE, K. A., WILSON, D. & TUITTILA, E. S. 2006. Estimating net ecosystem exchange in a patterned ecosystem: Example from blanket bog. *Agricultural and Forest Meteorology,* 138**,** 231-243.

LANE, S. N. & MILLEDGE, D. G. 2013. Impacts of upland open drains upon runoff generation: a numerical assessment of catchment-scale impacts. *Hydrological Processes,* 27**,** 1701-1726.

LAROWE, D. E. & VAN CAPPELLEN, P. 2011. Degradation of natural organic matter: A thermodynamic analysis. *Geochimica Et Cosmochimica Acta,* 75**,** 2030-2042.

LARSEN, K. S., IBROM, A., BEIER, C., JONASSON, S. & MICHELSEN, A. 2007. Ecosystem respiration depends strongly on photosynthesis in a temperate heath. *Biogeochemistry,* 85**,** 201-213.

LASSLOP, G., REICHSTEIN, M., DETTO, M., RICHARDSON, A. D. & BALDOCCHI, D. D. 2010a. Comment on Vickers et al.: Self-correlation between assimilation and respiration resulting from flux partitioning of eddy-covariance CO2 fluxes. *Agricultural and Forest Meteorology,* 150**,** 312-314.

LASSLOP, G., REICHSTEIN, M., PAPALE, D., RICHARDSON, A. D., ARNETH, A., BARR, A., STOY, P. & WOHLFAHRT, G. 2010b. Separation of net ecosystem exchange into assimilation and respiration using a light response curve approach: critical issues and global evaluation. *Global Change Biology,* 16**,** 187-208.

LAUDON, H., BERGGREN, M., AGREN, A., BUFFAM, I., BISHOP, K., GRABS, T., JANSSON, M. & KOHLER, S. 2011. Patterns and Dynamics of Dissolved Organic Carbon (DOC) in Boreal Streams: The Role of Processes, Connectivity, and Scaling. *Ecosystems,* 14**,** 880-893.

LAUDON, H., SEIBERT, J., KOHLER, S. & BISHOP, K. 2004. Hydrological flow paths during snowmelt: Congruence between hydrometric measurements and oxygen 18 in meltwater, soil water, and runoff. *Water Resources Research,* 40**,** 9.

LEIFELD, J., STEFFENS, M. & GALEGO-SALA, A. 2012. Sensitivity of peatland carbon loss to organic matter quality. *Geophysical Research Letters,* 39**,** 6.

LEINWEBER, P., SCHULTEN, H. R., KALBITZ, K., MEISSNER, R. & JANCKE, H. 2001. Fulvic acid composition in degraded fenlands. *Journal of Plant Nutrition and Soil Science,* 164**,** 371-379.

LEWIS, C., ALBERTSON, J., XU, X. L. & KIELY, G. 2012. Spatial variability of hydraulic conductivity and bulk density along a blanket peatland hillslope. *Hydrological Processes,* 26**,** 1527-1537.

LIMPENS, J., BERENDSE, F., BLODAU, C., CANADELL, J. G., FREEMAN, C., HOLDEN, J., ROULET, N., RYDIN, H. & SCHAEPMAN-STRUB, G. 2008. Peatlands and the carbon cycle: from local processes to global implications - a synthesis. *Biogeosciences,* 5**,** 1475-1491.

LINDSAY, J. B. 2005. The Terrain Analysis System: a toot for hydro-geomorphic applications. *Hydrological Processes,* 19**,** 1123-1130.

LINDSAY, J. B. & CREED, I. F. 2005. Removal of artifact depressions from digital elevation models: towards a minimum impact approach. *Hydrological Processes,* 19**,** 3113-3126.

LINDSAY, R. A. 1995. *Bogs: the Ecology, Classification and Conservation of Ombrotrophic Mires,* Perth, Scottish Natural Heritage.

LINDSAY, R. A., CHARMAN, D. J., EVERINGHAM, F., O'REILLY, R. M., PALMER, M. A., ROWELL, T. A. & STROUD, D. A. 1988. *The Flow Country: the Peatlands of Caithness and Sutherland,* Peterborough, NCC.

LINDSAY, R. M. 2010. Peatbogs and carbon: a critical synthesis to inform policy development in oceanic peat bog conservation and restoration in the context of climate change. London.

LLOYD, J. & TAYLOR, J. A. 1994. ON THE TEMPERATURE-DEPENDENCE OF SOIL RESPIRATION. *Functional Ecology,* 8**,** 315-323.

LOPEZ-CAPEL, E., KRULL, E. S., BOL, R. & MANNING, D. A. C. 2008. Influence of recent vegetation on labile and recalcitrant carbon soil pools in central Queensland, Australia: evidence from thermal analysis-quadrupole mass spectrometry-isotope ratio mass spectrometry. *Rapid Communications in Mass Spectrometry,* 22**,** 1751-1758.

LOPEZ-CAPEL, E., SOHI, S. P., GAUNT, J. L. & MANNING, D. A. C. 2005. Use of thermogravimetry-differential scanning calorimetry to characterize modelable soil organic matter fractions. *Soil Science Society of America Journal,* 69**,** 136-140.

MANNING, D. A. C., LOPEZ-CAPEL, E. & BARKER, S. 2005. Seeing soil carbon: use of thermal analysis in the characterization of soil C reservoirs of differing stability. *Mineralogical Magazine,* 69**,** 425-435.

MARINIER, M., GLATZEL, S. & MOORE, T. R. 2004. The role of cotton-grass (Eriophorum vaginatum) in the exchange of CO2 and CH4 at two restored peatlands, eastern Canada. *Ecoscience,* 11**,** 141-149.

MARTIKAINEN, P. J., NYKANEN, H., ALM, J. & SILVOLA, J. 1995. CHANGE IN FLUXES OF CARBON-DIOXIDE, METHANE AND NITROUS-OXIDE DUE TO FOREST DRAINAGE OF MIRE SITES OF DIFFERENT TROPHY. *Plant and Soil,* 168**,** 571-577.

MASIELLO, C. A., GALLAGHER, M. E., RANDERSON, J. T., DECO, R. M. & CHADWICK, O. A. 2008. Evaluating two experimental approaches for measuring ecosystem carbon oxidation state and oxidative ratio. *Journal of Geophysical Research-Biogeosciences,* 113.

MCCARTHY, D. R. & BROWN, K. J. 2006. Soil respiration responses to topography, canopy cover, and prescribed burning in an oak-hickory forest in southeastern Ohio. *Forest Ecology and Management,* 237**,** 94-102.

MCGLYNN, B. L. & MCDONNELL, J. J. 2003. Quantifying the relative contributions of riparian and hillslope zones to catchment runoff. *Water Resources Research,* 39**,** 20.

MCNAMARA, N. P., PLANT, T., OAKLEY, S., WARD, S., WOOD, C. & OSTLE, N. 2008. Gully hotspot contribution to landscape methane (CH4) and carbon dioxide (CO2) fluxes in a northern peatland. *Science of the Total Environment,* 404**,** 354-360.

MEI, Y., HORNBERGER, G. M., KAPLAN, L. A., NEWBOLD, J. D. & AUFDENKAMPE, A. K. 2012. Estimation of dissolved organic carbon contribution from hillslope soils to a headwater stream. *Water Resources Research,* 48**,** 17.

MICHEL, K. & MATZNER, E. 1999. Release of dissolved organic carbon and nitrogen from forest floors in relation to solid phase properties, respiration and N-mineralization. *Journal of Plant Nutrition and Soil Science-Zeitschrift Fur Pflanzenernahrung Und Bodenkunde,* 162**,** 645-652.

MIGLIAVACCA, M., REICHSTEIN, M., RICHARDSON, A. D., COLOMBO, R., SUTTON, M. A., LASSLOP, G., TOMELLERI, E., WOHLFAHRT, G., CARVALHAIS, N., CESCATTI, A., MAHECHA, M. D., MONTAGNANI, L., PAPALE, D., ZAEHLE, S., ARAIN, A., ARNETH, A., BLACK, T. A., CARRARA, A., DORE, S., GIANELLE, D., HELFTER, C., HOLLINGER, D., KUTSCH, W. L., LAFLEUR, P. M., NOUVELLON, Y., REBMANN, C., DA ROCHA, H. R.,

RODEGHIERO, M., ROUPSARD, O., SEBASTIA, M. T., SEUFERT, G., SOUSSANA, J. F. & VAN DER MOLEN, M. K. 2011. Semiempirical modeling of abiotic and biotic factors controlling ecosystem respiration across eddy covariance sites. *Global Change Biology,* 17**,** 390-409.

MINKKINEN, K. & LAINE, J. 1998. Effect of forest drainage on the peat bulk density of pine mires in Finland. *Canadian Journal of Forest Research-Revue Canadienne De Recherche Forestiere,* 28**,** 178-186.

MITCHELL, G. & MCDONALD, A. T. 1995. CATCHMENT CHARACTERIZATION AS A TOOL FOR UPLAND WATER-QUALITY MANAGEMENT. *Journal of Environmental Management,* 44**,** 83-95.

MONTANARELLA, L., JONES, R. J. A. & HIEDERER, R. 2006. The distribution of peatland in Europe. *Mires and Peat,* 1**,** Article 1.

MOORE, P. D. 1989. THE ECOLOGY OF PEAT-FORMING PROCESSES - A REVIEW. *International Journal of Coal Geology,* 12**,** 89-103.

MOORE, P. D. & BELLAMY, D. J. 1974. *Peatlands,* London, Elek Science.

MOORE, T. R., BUBIER, J. L., FROLKING, S. E., LAFLEUR, P. M. & ROULET, N. T. 2002. Plant biomass and production and CO2 exchange in an ombrotrophic bog. *Journal of Ecology,* 90**,** 25-36.

MOORE, T. R. & DALVA, M. 1997. Methane and carbon dioxide exchange potentials of peat soils in aerobic and anaerobic laboratory incubations. *Soil Biology & Biochemistry,* 29**,** 1157-1164.

MOORE, T. R., PARE, D. & BOUTIN, R. 2008. Production of dissolved organic carbon in Canadian forest soils. *Ecosystems,* 11**,** 740-751.

MOREL, B., DURAND, P., JAFFREZIC, A., GRUAU, G. & MOLENAT, J. 2009. Sources of dissolved organic carbon during stormflow in a headwater agricultural catchment. *Hydrological Processes,* 23**,** 2888-2901.

MORRIS, P. J. & WADDINGTON, J. M. 2011. Groundwater residence time distributions in peatlands: Implications for peat decomposition and accumulation. *Water Resources Research,* 47**,** 12.

MULLER, F. L. L. & TANKÉRÉ-MULLER, S. P. C. 2012. Seasonal variations in surface water chemistry at disturbed and pristine peatland sites in the Flow Country of northern Scotland. *Science of the Total Environment,* 435**,** 351-362.

MURSITO, A. T., HIRAJIMA, T. & SASAKI, K. 2010. Upgrading and dewatering of raw tropical peat by hydrothermal treatment. *Fuel,* 89**,** 635-641.

NIEVEEN, J. P., JACOBS, C. M. J. & JACOBS, A. F. G. 1998. Diurnal and seasonal variation of carbon dioxide exchange from a former true raised bog. *Global Change Biology,* 4**,** 823-833.

NILSSON, M., SAGERFORS, J., BUFFAM, I., LAUDON, H., ERIKSSON, T., GRELLE, A., KLEMEDTSSON, L., WESLIEN, P. & LINDROTH, A. 2008. Contemporary carbon accumulation in a boreal oligotrophic minerogenic mire - a significant sink after accounting for all C-fluxes. *Global Change Biology,* 14**,** 2317-2332.

OJANEN, P., MINKKINEN, K., ALM, J. & PENTTILA, T. 2010. Soil-atmosphere CO2, CH4 and N2O fluxes in boreal forestry-drained peatlands. *Forest Ecology and Management,* 260**,** 411-421.

OLEJNIK, S. & ALGINA, J. 2003. Generalized eta and omega squared statistics: Measures of effect size for some common research designs. *Psychological Methods,* 8**,** 434-447.

ORTIZ, J. E., TORRES, T., DELGADO, A., JULIA, R., LUCINI, M., LLAMAS, F. J., REYES, E., SOLER, V. & VALLE, M. 2004. The palaeoenvironmental and palaeohydrological evolution of Padul Peat Bog (Granada, Spain) over one million years, from elemental, isotopic and molecular organic geochemical proxies. *Organic Geochemistry,* 35**,** 1243-1260.

PACIFIC, V. J., MCGLYNN, B. L., RIVEROS-IREGUI, D. A., WELSCH, D. L. & EPSTEIN, H. E. 2011. Landscape structure, groundwater dynamics, and soil water content influence soil respiration across riparian-hillslope transitions in the Tenderfoot Creek Experimental Forest, Montana. *Hydrological Processes,* 25**,** 811-827.

PALMER, S. M., HOPE, D., BILLETT, M. F., DAWSON, J. J. C. & BRYANT, C. L. 2001. Sources of organic and inorganic carbon in a headwater stream: Evidence from carbon isotope studies. *Biogeochemistry,* 52**,** 321-338.

PARK, S. J. & VAN DE GIESEN, N. 2004. Soil-landscape delineation to define spatial sampling domains for hillslope hydrology. *Journal of Hydrology,* 295**,** 28-46.

PARSONS, D. F., HAYASHI, M. & VAN DER KAMP, G. 2004. Infiltration and solute transport under a seasonal wetland: bromide tracer experiments in Saskatoon, Canada. *Hydrological Processes,* 18**,** 2011-2027.

PASTOR, J., SOLIN, J., BRIDGHAM, S. D., UPDEGRAFF, K., HARTH, C., WEISHAMPEL, P. & DEWEY, B. 2003. Global warming and the export of dissolved organic carbon from boreal peatlands. *Oikos,* 100**,** 380-386.

PELLETIER, L., GARNEAU, M. & MOORE, T. R. 2011. Variation in CO2 exchange over three summers at microform scale in a boreal bog, Eastmain region, Quebec, Canada. *Journal of Geophysical Research-Biogeosciences,* 116**,** 11.

PENNOCK, D. J., ZEBARTH, B. J. & DEJONG, E. 1987. LANDFORM CLASSIFICATION AND SOIL DISTRIBUTION IN HUMMOCKY TERRAIN, SASKATCHEWAN, CANADA. *Geoderma,* 40**,** 297-315.

PEREIRA, R. C., KAAL, J., ARBESTAIN, M. C., PARDO LORENZO, R., AITKENHEAD, W., HEDLEY, M., MACIAS, F., HINDMARSH, J. & MACIA-AGULLO, J. A. 2011. Contribution to characterisation of biochar to estimate the labile fraction of carbon. *Organic Geochemistry,* 42**,** 1331-1342.

PERSSON, J. A., JOHANSSON, E. & ALBANO, C. 1986. QUANTITATIVE THERMOGRAVIMETRY ON PEAT - A MULTIVARIATE APPROACH. *Analytical Chemistry,* 58**,** 1173-1178.

PLANTE, A. F., FERNANDEZ, J. M. & LEIFELD, J. 2009. Application of thermal analysis techniques in soil science. *Geoderma,* 153**,** 1-10.

PRAIRIE, Y. T. & BIRD, D. F. 1989. SOME MISCONCEPTIONS ABOUT THE SPURIOUS CORRELATION-PROBLEM IN THE ECOLOGICAL LITERATURE. *Oecologia,* 81**,** 285-288.

PRICE, J. 1997. Soil moisture, water tension, and water table relationships in a managed cutover bog. *Journal of Hydrology,* 202**,** 21-32.

PRICE, J. S. 1992. BLANKET BOG IN NEWFOUNDLAND .2. HYDROLOGICAL PROCESSES. *Journal of Hydrology,* 135**,** 103-119.

PROCTOR, M. C. F. 2008. WATER ANALYSES FROM SOME IRISH BOGS AND FENS, WITH THOUGHTS ON 'THE SCHOENUS PROBLEM'. *Biology and Environment-Proceedings of the Royal Irish Academy,* 108B**,** 81-95.

PRÉVOST, M., PLAMONDON, A. P. & BELLEAU, P. 1999. Effects of drainage of a forested peatland on water quality and quantity. *Journal of Hydrology,* 214**,** 130-143.

RAICH, J. W. & SCHLESINGER, W. H. 1992. THE GLOBAL CARBON-DIOXIDE FLUX IN SOIL RESPIRATION AND ITS RELATIONSHIP TO VEGETATION AND CLIMATE. *Tellus Series B-Chemical and Physical Meteorology,* 44**,** 81-99.

RANDERSON, J. T., MASIELLO, C. A., STILL, C. J., RAHN, T., POORTER, H. & FIELD, C. B. 2006. Is carbon within the global terrestrial biosphere becoming more oxidized? Implications for trends in atmospheric O-2. *Global Change Biology,* 12**,** 260-271.

REICHE, M., GLEIXNER, G. & KUSEL, K. 2010. Effect of peat quality on microbial greenhouse gas formation in an acidic fen. *Biogeosciences,* 7**,** 187-198.

REINERS, W. A. & REINERS, N. M. 1970. ENERGY AND NUTRIENT DYNAMICS OF FOREST FLOORS IN 3 MINNESOTA FORESTS. *Journal of Ecology,* 58**,** 497-&.

RIVEROS-IREGUI, D. A., MCGLYNN, B. L., MARSHALL, L. A., WELSCH, D. L., EMANUEL, R. E. & EPSTEIN, H. E. 2011. A watershed-scale assessment of a process soil CO2 production and efflux model. *Water Resources Research,* 47**,** 12.

ROBINSON, S. D. & MOORE, T. R. 1999. Carbon and peat accumulation over the past 1200 years in a landscape with discontinuous permafrost, northwestern Canada. *Global Biogeochemical Cycles,* 13**,** 591-601.

ROBROEK, B. J. M., SMART, R. P. & HOLDEN, J. 2010. Sensitivity of blanket peat vegetation and hydrochemistry to local disturbances. *Science of the Total Environment,* 408**,** 5028-5034.

ROTHWELL, J. J., EVANS, M. G., DANIELS, S. A. & ALLOTT, T. E. H. 2008. Peat soils as a source of lead contamination to upland fluvial systems. *Environmental Pollution,* 153**,** 582-589.

ROTHWELL, J. J., EVANS, M. G., DANIELS, S. M. & ALLOTT, T. E. H. 2007. Baseflow and stormflow metal concentrations in streams draining contaminated peat moorlands in the Peak District National Park (UK). *Journal of Hydrology,* 341**,** 90-104.

ROTHWELL, J. J., TAYLOR, K. G., ANDER, E. L., EVANS, M. G., DANIELS, S. M. & ALLOTT, T. E. H. 2009. Arsenic retention and release in ombrotrophic peatlands. *Science of the Total Environment,* 407**,** 1405-1417.

ROULET, N. T., LAFLEUR, P. M., RICHARD, P. J. H., MOORE, T. R., HUMPHREYS, E. R. & BUBIER, J. 2007. Contemporary carbon balance and late Holocene carbon accumulation in a northern peatland. *Global Change Biology,* 13**,** 397-411.

ROWSON, J. 2008. *Carbon emissions from managed upland peat.* PhD Thesis, Durham University.

ROWSON, J. G., GIBSON, H. S., WORRALL, F., OSTLE, N., BURT, T. P. & ADAMSON, J. K. 2010. The complete carbon budget of a drained peat catchment. *Soil Use and Management,* 26**,** 261-273.

ROWSON, J. G., WORRALL, F. & EVANS, M. G. 2013. Predicting soil respiration from peatlands. *The Science of the total environment,* 442**,** 397-404.

RUBINO, M., LUBRITTO, C., D'ONOFRIO, A., TERRASI, F., GLEIXNER, G. & COTRUFO, M. F. 2007. An isotopic method for testing the influence of leaf litter quality on carbon fluxes during decomposition. *Oecologia,* 154**,** 155-166.

RUHE, R. V. Elemenets of the soil landscape. Trans. 7th Int. Congr. Soil Sci., 1960 Madison, Wisc., 165-170.

RUHE, R. V. & WALKER, P. H. Hillslope models and soil formation, II. Open systems. Transactions of the 9th International Soil Science Society, 1968 Adelaide, Australia. 551-560.

RUTHERFORD, A. 2001. *Introducing ANOVA and ANCOVA a GLM Approach,* London, SAGE.

SCHLOTZHAUER, S. M. & PRICE, J. S. 1999. Soil water flow dynamics in a managed cutover peat field, Quebec: Field and laboratory investigations. *Water Resources Research,* 35**,** 3675-3683.

SCHMIDER, E., ZIEGLER, M., DANAY, E., BEYER, L. & BUHNER, M. 2010. Is It Really Robust? Reinvestigating the Robustness of ANOVA Against Violations of the Normal Distribution Assumption. *Methodology-European Journal of Research Methods for the Behavioral and Social Sciences,* 6**,** 147-151.

SCHRIER-UIJL, A. P., KROON, P. S., HENSEN, A., LEFFELAAR, P. A., BERENDSE, F. & VEENENDAAL, E. M. 2010. Comparison of chamber and eddy covariance-based CO2 and CH4 emission estimates in a heterogeneous grass ecosystem on peat. *Agricultural and Forest Meteorology,* 150**,** 825-831.

SCOTT, M. J., JONES, M. N., WOOF, C. & TIPPING, E. 1998. Concentrations and fluxes of dissolved organic carbon in drainage water from an upland peat system. *Environment International,* 24**,** 537-546.

SHABAGA, J. A. & HILL, A. R. 2010. Groundwater-fed surface flow path hydrodynamics and nitrate removal in three riparian zones in southern Ontario, Canada. *Journal of Hydrology,* 388**,** 52-64.

SHURPALI, N. J., VERMA, S. B., KIM, J. & ARKEBAUER, T. J. 1995. CARBON-DIOXIDE EXCHANGE IN A PEATLAND ECOSYSTEM. *Journal of Geophysical Research-Atmospheres,* 100**,** 14319-14326.

SILVOLA, J., ALM, J., AHLHOLM, U., NYKANEN, H. & MARTIKAINEN, P. J. 1996a. CO2 fluxes from peat in boreal mires under varying temperature and moisture conditions. *Journal of Ecology,* 84**,** 219-228.

SILVOLA, J., ALM, J., AHLHOLM, U., NYKANEN, H. & MARTIKAINEN, P. J. 1996b. The contribution of plant roots to CO2 fluxes from organic soils. *Biology and Fertility of Soils,* 23**,** 126-131.

SMART, R. P., HOLDEN, J., DINSMORE, K. J., BAIRD, A. J., BILLETT, M. F., CHAPMAN, P. J. & GRAYSON, R. 2013. The dynamics of natural pipe hydrological behaviour in blanket peat. *Hydrological Processes,* 27**,** 1523-1534.

SMITH, J., GOTTSCHALK, P., BELLARBY, J., CHAPMAN, S., LILLY, A., TOWERS, W., BELL, J., COLEMAN, K., NAYAK, D., RICHARDS, M., HILLIER, J., FLYNN, H., WATTENBACH, M., AITKENHEAD, M., YELURIPATI, J., FARMER, J., MILNE, R., THOMSON, A., EVANS, C., WHITMORE, A., FALLOON, P. & SMITH, P. 2010a. Estimating changes in Scottish soil carbon stocks using ECOSSE. I. Model description and uncertainties. *Climate Research,* 45**,** 179-192.

SMITH, J., GOTTSCHALK, P., BELLARBY, J., CHAPMAN, S., LILLY, A., TOWERS, W., BELL, J., COLEMAN, K., NAYAK, D., RICHARDS, M., HILLIER, J., FLYNN, H., WATTENBACH, M., AITKENHEAD, M., YELURIPATI, J., FARMER, J., MILNE, R., THOMSON, A., EVANS, C., WHITMORE, A., FALLOON, P. & SMITH, P. 2010b. Estimating changes in Scottish soil carbon stocks using ECOSSE. II. Application. *Climate Research,* 45**,** 193-205.

SOMMERKORN, M. 2008. Micro-topographic patterns unravel controls of soil water and temperature on soil respiration in three Siberian tundra systems. *Soil Biology & Biochemistry,* 40**,** 1792-1802.

SOULSBY, C., RODGERS, P., SMART, R., DAWSON, J. & DUNN, S. 2003. A tracer-based assessment of hydrological pathways at different spatial scales in a mesoscale Scottish catchment. *Hydrological Processes,* 17**,** 759-777.

SOULSBY, C. & TETZLAFF, D. 2008. Towards simple approaches for mean residence time estimation in ungauged basins using tracers and soil distributions. *Journal of Hydrology,* 363**,** 60-74.

STEWART, A. J. A. & LANCE, A. N. 1991. EFFECTS OF MOOR-DRAINING ON THE HYDROLOGY AND VEGETATION OF NORTHERN PENNINE BLANKET BOG. *Journal of Applied Ecology,* 28**,** 1105-1117.

STEWART, M. K., MORGENSTERN, U. & MCDONNELL, J. J. 2010. Truncation of stream residence time: how the use of stable isotopes has skewed our concept of streamwater age and origin. *Hydrological Processes,* 24**,** 1646-1659.

STROHMEIER, S., KNORR, K. H., REICHERT, M., FREI, S., FLECKENSTEIN, J. H., PEIFFER, S. & MATZNER, E. 2013. Concentrations and fluxes of dissolved organic carbon in runoff from a forested catchment: insights from high frequency measurements. *Biogeosciences,* 10**,** 905-916.

STUTTER, M. I., DUNN, S. M. & LUMSDON, D. G. 2012. Dissolved organic carbon dynamics in a UK podzolic moorland catchment: linking storm hydrochemistry, flow path analysis and sorption experiments. *Biogeosciences,* 9**,** 2159-2175.

SULMAN, B. N., DESAI, A. R., SCHROEDER, N. M., RICCIUTO, D., BARR, A., RICHARDSON, A. D., FLANAGAN, L. B., LAFLEUR, P. M., TIAN, H. Q., CHEN, G. S., GRANT, R. F., POULTER, B., VERBEECK, H., CIAIS, P., RINGEVAL, B., BAKER, I. T., SCHAEFER, K., LUO, Y. Q. & WENG,

E. S. 2012. Impact of hydrological variations on modeling of peatland CO2 fluxes: Results from the North American Carbon Program site synthesis. *Journal of Geophysical Research-Biogeosciences,* 117**,** 21.

SUTCU, H. 2007. Pyrolysis by thermogravimetric analysis of blends of peat with coals of different characteristics and biomass. *Journal of the Chinese Institute of Chemical Engineers,* 38**,** 245-249.

TALBOT, M. R. & LIVINGSTONE, D. A. 1989. HYDROGEN INDEX AND CARBON ISOTOPES OF LACUSTRINE ORGANIC-MATTER AS LAKE LEVEL INDICATORS. *Palaeogeography Palaeoclimatology Palaeoecology,* 70**,** 121-137.

TALLIS, J. H. 1973. STUDIES ON SOUTHERN PENNINE PEATS .5. DIRECT OBSERVATIONS ON PEAT EROSION AND PEAT HYDROLOGY AT FEATHERBED MOSS, DERBYSHIRE. *Journal of Ecology,* 61**,** 1-22.

TALLIS, J. H. 1985. MASS MOVEMENT AND EROSION OF A SOUTHERN PENNINE BLANKET PEAT. *Journal of Ecology,* 73**,** 283-315.

TANG, R., CLARK, J. M., BOND, T., GRAHAM, N., HUGHES, D. & FREEMAN, C. 2013. Assessment of potential climate change impacts on peatland dissolved organic carbon release and drinking water treatment from laboratory experiments. *Environmental Pollution,* 173**,** 270-277.

THOMAS, K. L., BENSTEAD, J., DAVIES, K. L. & LLOYD, D. 1996. Role of wetland plants in the diurnal control of CH4 and CO2 fluxes in peat. *Soil Biology & Biochemistry,* 28**,** 17-23.

THORMANN, M. N. & BAYLEY, S. E. 1997. Aboveground plant production and nutrient content of the vegetation in six peatlands in Alberta, Canada. *Plant Ecology,* 131**,** 1-16.

THURMAN, E. M. 1985. *Organic geochemistry of natural waters,* Dordrecht ; Boston

Hingham, MA, USA, M. Nijhoff ;

Distributors for the U.S. and Canada, Kluwer Academic.

TOMLINSON, R. W. 2005. Soil carbon stocks and changes in the Republic of Ireland. *Journal of Environmental Management,* 76**,** 77-93.

TROEH, F. R. 1964. Landform parameters correlated to soil drainage. *Soil Science Society of America Journal,* 28**,** 808-812.

TROFIMOV, S. Y. & EMELYANENKO, V. I. 2000. Study of thermodynamic functions of soil organic matter in the course of its decomposition. *Journal of Thermal Analysis and Calorimetry,* 62**,** 69-74.

TUITTILA, E.-S., VASANDER, H. & LAINE, J. 2000. Impact of rewetting on the vegetation of a cut-away peatland. *Applied Vegetation Science,* 3**,** 205-212.

TUITTILA, E. S., VASANDER, H. & LAINE, J. 2004. Sensitivity of C sequestration in reintroduced Sphagnum to water-level variation in a cutaway peatland. *Restoration Ecology,* 12**,** 483-493.

VAN DEN BERG, L. J. L., SHOTBOLT, L. & ASHMORE, M. R. 2012. Dissolved organic carbon (DOC) concentrations in UK soils and the influence of soil, vegetation type and seasonality. *Science of the Total Environment,* 427**,** 269-276.

VICKERS, D., THOMAS, C. K., MARTIN, J. G. & LAW, B. 2009. Self-correlation between assimilation and respiration resulting from flux partitioning of eddy-covariance CO2 fluxes. *Agricultural and Forest Meteorology,* 149**,** 1552-1555.

VOGT, R. D. & MUNIZ, I. P. 1997. Soil and stream water chemistry in a pristine and boggy site in mid-Norway. *Hydrobiologia,* 348**,** 19-38.

WALLAGE, Z. E. & HOLDEN, J. 2010. Spatial and temporal variability in the relationship between water colour and dissolved organic carbon in blanket peat pore waters. *Science of the Total Environment,* 408**,** 6235-6242.

WALLAGE, Z. E., HOLDEN, J. & MCDONALD, A. T. 2006. Drain blocking: An effective treatment for reducing dissolved organic carbon loss and water discolouration in a drained peatland. *Science of the Total Environment,* 367**,** 811-821.

WARD, S. E., BARDGETT, R. D., MCNAMARA, N. P. & OSTLE, N. J. 2009. Plant functional group identity influences short-term peatland ecosystem carbon flux: evidence from a plant removal experiment. *Functional Ecology,* 23**,** 454-462.

WARD, S. E., OSTLE, N. J., MCNAMARA, N. P. & BARDGETT, R. D. 2010. Litter evenness influences short-term peatland decomposition processes. *Oecologia,* 164**,** 511-520.

WEBSTER, K. L., CREED, I. F., BOURBONNIERE, R. A. & BEALL, F. D. 2008. Controls on the heterogeneity of soil respiration in a tolerant hardwood forest. *Journal of Geophysical Research-Biogeosciences,* 113**,** 15.

WHITE, C. C., DAWOD, A. M. & CRESSER, M. S. 1996. Nitrogen accumulation in surface horizons of moorland podzols: Evidence from a Scottish survey. *Science of the Total Environment,* 184**,** 229-237.

WILSON, J. P. 2012. Digital terrain modeling. *Geomorphology,* 137**,** 107-121.

WILSON, L., WILSON, J., HOLDEN, J., JOHNSTONE, I., ARMSTRONG, A. & MORRIS, M. 2010. Recovery of water tables in Welsh blanket bog after drain blocking: Discharge rates, time scales and the influence of local conditions. *Journal of Hydrology,* 391**,** 377-386.

WILSON, L., WILSON, J., HOLDEN, J., JOHNSTONE, I., ARMSTRONG, A. & MORRIS, M. 2011. Ditch blocking, water chemistry and organic carbon flux: Evidence that blanket bog restoration reduces erosion and fluvial carbon loss. *Science of the Total Environment,* 409**,** 2010-2018.

WORRALL, F. & ADAMSON, J. K. 2008. The effect of burning and sheep grazing on soil water composition in a blanket bog: evidence for soil structural changes? *Hydrological Processes,* 22**,** 2531-2541.

WORRALL, F., ARMSTRONG, A. & ADAMSON, J. K. 2007a. The effects of burning and sheep-grazing on water table depth and soil water quality in a upland peat. *Journal of Hydrology,* 339**,** 1-14.

WORRALL, F., BURT, T. & ADAMSON, J. 2003a. Controls on the chemistry of runoff from an upland peat catchment. *Hydrological Processes,* 17**,** 2063-2083.

WORRALL, F., BURT, T. & ADAMSON, J. 2005. Fluxes of dissolved carbon dioxide and inorganic carbon from an upland peat catchment: implications for soil respiration. *Biogeochemistry,* 73**,** 515-539.

WORRALL, F., BURT, T. & ADAMSON, J. 2006a. Long-term changes in hydrological pathways in an upland peat catchment - recovery from severe drought? *Journal of Hydrology,* 321**,** 5-20.

WORRALL, F., BURT, T., ADAMSON, J., REED, M., WARBURTON, J., ARMSTRONG, A. & EVANS, M. 2007b. Predicting the future carbon budget of an upland peat catchment. *Climatic Change,* 85**,** 139-158.

WORRALL, F., BURT, T. P. & ADAMSON, J. 2006b. The rate of and controls upon DOC loss in a peat catchment. *Journal of Hydrology,* 321**,** 311-325.

WORRALL, F., BURT, T. P., JAEBAN, R. Y., WARBURTON, J. & SHEDDEN, R. 2002. Release of dissolved organic carbon from upland peat. *Hydrological Processes,* 16**,** 3487-3504.

WORRALL, F., BURT, T. P., ROWSON, J. G., WARBURTON, J. & ADAMSON, J. K. 2009a. The multi-annual carbon budget of a peat-covered catchment. *Sci Total Environ,* 407**,** 4084-94.

WORRALL, F. & CLAY, G. D. 2012. The impact of sheep grazing on the carbon balance of a peatland. *Science of the Total Environment,* 438**,** 426-434.

WORRALL, F., CLAY, G. D., BURT, T. P. & ROSE, R. 2012a. The multi-annual nitrogen budget of a peat-covered catchment - Changing from sink to source? *Science of the Total Environment,* 433**,** 178-188.

WORRALL, F., DAVIES, H., BHOGAL, A., LILLY, A., EVANS, M., TURNER, K., BURT, T., BARRACLOUGH, D., SMITH, P. & MERRINGTON, G. 2012b. The flux of DOC from the UK - Predicting the role of soils, land use and net watershed losses. *Journal of Hydrology,* 448**,** 149-160.

WORRALL, F., EVANS, M. G., BONN, A., REED, M. S., CHAPMAN, D. & HOLDEN, J. 2009b. Can carbon offsetting pay for upland ecological restoration? *Science of the Total Environment,* 408**,** 26-36.

WORRALL, F., GIBSON, H. S. & BURT, T. P. 2008. Production vs. solubility in controlling runoff of DOC from peat soils - The use of an event analysis. *Journal of Hydrology,* 358**,** 84-95.

WORRALL, F., HARRIMAN, R., EVANS, C. D., WATTS, C. D., ADAMSON, J., NEAL, C., TIPPING, E., BURT, T., GRIEVE, I., MONTEITH, D., NADEN, P. S., NISBET, T., REYNOLDS, B. & STEVENS, P. 2004. Trends in dissolved organic carbon in UK rivers and lakes. *Biogeochemistry,* 70**,** 369-402.

WORRALL, F., REED, M. S., WARBURTON, J. & BURT, T. 2003b. Carbon budget for a British upland peat catchment. *Science of the Total Environment,* 312**,** 133-146.

WORRALL, F., ROWSON, J. G., EVANS, M. G., PAWSON, R., DANIELS, S. & BONN, A. 2011. Carbon fluxes from eroding peatlands - the carbon benefit of revegetation following wildfire. *Earth Surface Processes and Landforms,* 36**,** 1487-1498.

WU, J. H., ROULET, N. T., MOORE, T. R., LAFLEUR, P. & HUMPHREYS, E. 2011. Dealing with microtopography of an ombrotrophic bog for simulating ecosystem-level CO2 exchanges. *Ecological Modelling,* 222**,** 1038-1047.

YALLOP, A. R. & CLUTTERBUCK, B. 2009. Land management as a factor controlling dissolved organic carbon release from upland peat soils 1: Spatial variation in DOC productivity. *Science of the Total Environment,* 407**,** 3803-3813.

YALLOP, A. R., CLUTTERBUCK, B. & THACKER, J. 2010. Increases in humic dissolved organic carbon export from upland peat catchments: the role of temperature, declining sulphur deposition and changes in land management. *Climate Research,* 45**,** 43-56.

YU, Z. C. 2012. Northern peatland carbon stocks and dynamics: a review. *Biogeosciences,* 9**,** 4071-4085.

YUAN, W. P., LUO, Y. Q., LI, X. L., LIU, S. G., YU, G. R., ZHOU, T., BAHN, M., BLACK, A., DESAI, A. R., CESCATTI, A., MARCOLLA, B., JACOBS, C., CHEN, J. Q., AURELA, M., BERNHOFER, C., GIELEN, B., BOHRER, G., COOK, D. R., DRAGONI, D., DUNN, A. L., GIANELLE, D., GRUNWALD, T., IBROM, A., LECLERC, M. Y., LINDROTH, A., LIU, H. P., MARCHESINI, L. B., MONTAGNANI, L., PITA, G., RODEGHIERO, M., RODRIGUES, A., STARR, G. & STOY, P. C. 2011. Redefinition and global estimation of basal ecosystem respiration rate. *Global Biogeochemical Cycles,* 25**,** 14.

ZACCONE, C., SAID-PULLICINO, D., GIGLIOTTI, G. & MIANO, T. M. 2008. Diagenetic trends in the phenolic constituents of Sphagnum-dominated peat and its corresponding humic acid fraction. *Organic Geochemistry,* 39**,** 830-838.